

Henrique Matheus Gauy

(5+1)-Dimensional Braneworld Models and the Charged Lepton Spectrum

Brasil

19 de dezembro de 2023

Henrique Matheus Gauy

(5+1)-Dimensional Braneworld Models and the Charged Lepton Spectrum

Tese apresentada ao Programa de Pós-Graduação em Física da Universidade Federal de São Carlos, para obtenção do título de doutor em Física.

Universidade Federal de São Carlos – UFSCar
Centro de Ciências Exatas e de Tecnologia – CCET
Programa de Pós-Graduação em Física – PPGF

Supervisor: Alex Eduardo de Bernardini

Brasil
19 de dezembro de 2023

Henrique Matheus Gauy

(5+1)-Dimensional Braneworld Models and the Charged Lepton Spectrum/ Henrique Matheus Gauy. – Brasil, 19 de dezembro de 2023 –

151 p. : il. (algumas color.) ; 30 cm.

Supervisor: Alex Eduardo de Bernardini

Tese – Universidade Federal de São Carlos – UFSCar

Centro de Ciências Exatas e de Tecnologia – CCET

Programa de Pós-Graduação em Física – PPGF, 19 de dezembro de 2023.

1. Higher Dimensions 2. Braneworlds 3. Lepton Masses I. Alex Eduardo de Bernardini II. Universidade Federal de São Carlos. III. Programa de Pós-Graduação em Física. IV. (5+1)-Dimensional Braneworld Models and the Charged Lepton Spectrum



UNIVERSIDADE FEDERAL DE SÃO CARLOS

Centro de Ciências Exatas e de Tecnologia
Programa de Pós-Graduação em Física

Folha de Aprovação

Defesa de Tese de Doutorado do candidato Henrique Matheus Gauy, realizada em 27/10/2023.

Comissão Julgadora:

Prof. Dr. Alex Eduardo de Bernardini (UFSCar)

Prof. Dr. Javier Fernando Ramos Caro (UFSCar)

Prof. Dr. Fernando David Marmolejo Schmitt (UFSCar)

Prof. Dr. Daniel Augusto Turolla Vanzela (USP)

Prof. Dr. Roldão da Rocha Junior (UFABC)

Acknowledgements

Gostaria de agradecer a minha família pelo incentivo e apoio incondicional; ao meu orientador Alex Eduardo de Bernardini pela orientação, correções e incentivos; a todos que direta ou indiretamente fizeram parte da minha formação. Por fim, agradeço ao CNPq pelo apoio financeiro.

Abstract

This manuscript is concerned with a mechanism for explaining the mass spectrum of the charged leptons within $(5 + 1)$ -dimensional braneworlds. As a preliminary objective, new two co-dimensional thick braneworlds ought to be proposed and investigated. By considering a twofold-warp factor constructed from two intersecting warp factors and scalar fields that generates the extra dimension defect, an alternative bulk configuration is examined. With the brane localization thus driven by two crossing scalar fields, the possible solvable models obtained from such a two co-dimensional setup are systematically discussed. The obtained solutions are classified into two subsets, string and intersecting-like. The intersecting-like models are sorted in six different models organized into two subsets for which some of their physical properties are evaluated. For models *I* and *II*, in the first subset, Einstein equation solutions are rigidly defined, up to some arbitrary constant. For models *III*, *IV*, *V* and *VI*, in the second subset, an additional degree of freedom not constrained by Einstein equations is admitted. For all intersecting-like models, gravity and standard matter fields are shown to be localized in the vicinity of the brane. Finally, by studying the zero modes of leptons, which are localized by the inclusion of a non-trivial gauge field, over asymmetric versions of the classified braneworlds, one is able to model the masses of the electron, muon and tauon based on two parameters: the gauge field strength and the ratio between the sizes of the co-dimensions.

Palavras-chave: Higher Dimensions, Braneworlds, Lepton Masses.

List of Figures

Figure 1 – (a) A string-like defect example for the warp factor. (b) A non-string-like example for the warp factor.	31
Figure 2 – Stress energy tensor $T_{\mu\nu}^{\zeta^{III*}} = -r^2 T_{\mu\nu}^{\zeta^{III}} / 3M^4 n^2 \eta_{\mu\nu}$ as a function of φ , for $n = 1$ (black line), $n = 2$ (black dashed line), $n = 3$ (red line) and $n = 4$ (red dashed line).	38
Figure 3 – Warp factor $e^{-2\hat{A}^{IV}}$ of model IV as a function of φ , for $n = 1$ (black line), $n = 2$ (black dashed line), $n = 3$ (red line) and $n = 4$ (red dashed line).	42
Figure 4 – (a) The warp factor $e^{-2\hat{A}^V}$ of model V_0 as a function of φ . (b) The stress energy tensor $T_{\mu\nu}^{\zeta^*} = -T_{\mu\nu}^{\zeta} 3r^2 / 4M^4 n^2 \omega_{\mu\nu}^-$ of model V as a function of φ . The plots are for $n = 1$ (solid black line), $n = 2$ (black dashed line), $n = 3$ (solid red line) and $n = 4$ (red dashed line).	44
Figure 5 – The Planck scale, $\sqrt[4]{C} M_{\text{pl}}^{\text{VI}} / M^2 \sqrt{\int e^{-3\hat{A}} e^{-\hat{f}} du}$, as a function of the cosmological constant, Λ/C	46
Figure 6 – Potential $\mathcal{V}_\zeta^* = \mathcal{V}_\zeta / 32M^4 a^2$ as a function of the scalar field $\phi_\zeta^* = \phi_\zeta / 4M^2$. The plots are for $C = 0$ (solid black line), $C = a^2/4$ (dotted black line), $C = a^2$ (dashed black line), $C = 2a^2$ (solid red line), $C = 3a^2$ (dotted red line), $C = 7a^2/2$ (dashed red line).	49
Figure 7 – (a) Scalar field $\phi_\epsilon^* = \phi_\epsilon / 4M^2$ as a function of $\theta = a(u + u_0)$. (b) Potential $\mathcal{V}_\epsilon^* = (1 - \kappa) \mathcal{V}_\epsilon / 2CM^4 (5 - 4\kappa)$ as a function of $\phi_\epsilon^* = \phi_\epsilon / 4M^2 \sqrt{1 - \kappa}$. The plots are for $\kappa = 0.1$ (solid black line), $\kappa = 0.2$ (dashed black line), $\kappa = 0.4$ (dotted black line), $\kappa = 0.6$ (solid blue line), $\kappa = 0.8$ (dashed blue line), $\kappa = 0.9$ (dotted blue line), $\kappa = 0.99$ (solid red line) and $\kappa = 0.999$ (dashed red line).	50
Figure 8 – (a) Warp factor $e^{-2\hat{A}}$ as a function of $y^* = \sqrt{C}y/2$. (b) Scalar field $\phi_\epsilon^* = \phi_\epsilon / 4M^2$ as a function of $y^* = \sqrt{C}y/2$. The plots are for $\kappa = 0.1$ (solid black line), $\kappa = 0.2$ (dashed black line), $\kappa = 0.4$ (dotted black line), $\kappa = 0.6$ (solid blue line), $\kappa = 0.8$ (dashed blue line), $\kappa = 0.9$ (dotted blue line), $\kappa = 0.99$ (solid red line) and $\kappa = 0.999$ (dashed red line).	52

Figure 9 – (a) Scalar field $\phi^* = \phi/4\sqrt{1 - C/4}$ (thick black line), warp factor \tilde{A} (thick black dashed line) and potential $\mathcal{V}^* = \mathcal{V}/4$. (b) The θ dependence of the stress energy tensor $T^\phi_{\mu\nu}$, $T^{\phi^*}_{\mu\nu} = -\sin^2\theta T^{\phi^\mu}_\nu/8$. The plots are for $C = 0$ (thin black line), $C = 1/16$ (thin black dotted line), $C = 1/4$ (thin black dashed line), $C = 9/16$ (thin black dot-dashed line), $C = 1$ (thin red line), $C = 25/16$ (thin red dotted line), $C = 9/4$ (thin red dashed line), $C = 49/16$ (thin red dot-dashed line) and $C = 4$ (thick black solid line), with $M = r = 1$	54
Figure 10 – Warp factor e^{-2A} of model <i>III</i> in a spherical plot, with $r = \Lambda = 1$. The top figures are for $n = 0, 1, 2, 3$ and 4 (from left to right) and the bottom ones are for $n = 5, 6, 7$ and 8 (from left to right).	55
Figure 11 – Warp factor e^{-2A} of model <i>IV</i> for $n = 1$ (left figure) and $n = 2$ (right figure) in a spherical plot, with $r = \Lambda = 1$	55
Figure 12 – Warp factor e^{-2A} of model <i>III</i> in stereographic coordinates. The top figures are for $n = 0, 1, 2, 3$ and 4 (from left to right) and the bottom ones are for $n = 5, 6, 7$ and 8 (from left to right).	56
Figure 13 – Warp factor e^{-2A} of model <i>IV</i> for $n = 1$ (left figure) and $n = 2$ (right figure), in stereographic coordinates.	57
Figure 14 – (a) Scalar field $\phi^* = \phi/4M^2$ as a function of θ . (b) The θ dependence of the stress energy tensor $T^\phi_{\mu\nu}$, $T^{\phi^*}_{\mu\nu} = -\sin^2\theta T^{\phi^\mu}_\nu(1 - \kappa)/8(5 - 3\kappa)$. The plots are for $\kappa = 0.1$ (solid black line), $\kappa = 0.2$ (dashed black line), $\kappa = 0.4$ (dotted black line), $\kappa = 0.6$ (solid blue line), $\kappa = 0.8$ (dashed blue line), $\kappa = 0.9$ (dotted blue line), $\kappa = 0.99$ (solid red line) and $\kappa = 0.999$ (dashed red line).	58
Figure 15 – (a) Scalar field $\phi^* = \phi/4M^2$ as a function of θ . (b) The θ dependence of the stress energy tensor $T^\phi_{\mu\nu}$, $T^{\phi^*}_{\mu\nu} = -\sin^2\theta T^{\phi^\mu}_\nu(1 - \kappa)/8(5 - 3\kappa)$. The plots are for $\kappa = 0.1$ (solid black line), $\kappa = 0.2$ (dashed black line), $\kappa = 0.4$ (dotted black line), $\kappa = 0.6$ (solid blue line), $\kappa = 0.8$ (dashed blue line), $\kappa = 0.9$ (dotted blue line), $\kappa = 0.99$ (solid red line) and $\kappa = 0.999$ (dashed red line).	59
Figure 16 – The Planck scale $M_{pl}^* = 2M_{pl}\sqrt{c_u c_v}/M^2\sqrt{\pi}$ as a function of p . The plots are for model <i>I</i> (red line) and <i>II</i> (black line).	76
Figure 17 – The degeneracies of the zero mode of model <i>III</i> as functions of $\varphi = 2\sqrt{C}v$ for $j = 0$ (full line), $j = 1$ (dashed line), $j = 2$ (dotted line) and $j = 3$ (dot-dashed line).	77
Figure 18 – Normalized gravitational wave functions $\hat{\chi}^{IV}$ for model <i>IV</i> as functions of $z = v\sqrt{C}/2$, for $k^2/C = 7/16$ (black lines), $k^2/C = 0$ (blue lines), $k^2/C = -9/16$ (red lines) and $k^2/C = -33/16$ (brown lines). The full, dashed and dot-dashed lines represent $j = 0, l = 0$ and $j = 1$, respectively.	80

- Figure 19 – Normalized gravitational wave functions $\hat{\chi}^V$ for model V as functions of $y = v\sqrt{3|\Lambda|}$, for $j = 0$ (black lines), $j = 1$ (blue lines), $j = 2$ (red lines), $j = 3$ (brown lines) and $j = 4$ (purple lines). The full, dashed and dot-dashed lines represent $j = 0, l = 0$ and $j = 1$, respectively. 81
- Figure 20 – Normalized gravitational wave functions $\tilde{\chi}_k^\zeta$ for the sphere models, for $k = 0$ (full black line) and $k = -3/r^2$ (black dashed line). 82
- Figure 21 – (a) The quantum mechanical potential associated with right-handed spinors, U_R , for $\lambda = 4$ (solid lines), $\lambda = 3$ (dashed lines) and $\lambda = 2$ (dotted lines). (b) The quantum mechanical potential associated with left-handed spinors, U_L , for $\lambda = 4$ (solid lines), $\lambda = 3$ (dashed lines), $\lambda = 2$ (dot-dashed lines) and $\lambda = 1$ (dotted lines). The plots are for $k = 0$ (blue lines), $k = 1$ (black lines) and $k = -1$ (red lines), with $s = 2$. 98
- Figure 22 – (a) The quantum mechanical potential associated with right-handed spinors, U_R , for $\mathbf{a} = 4$ (solid lines), $\mathbf{a} = 3$ (dashed lines) and $\mathbf{a} = 2$ (dotted lines). (b) The quantum mechanical potential associated with left-handed spinors, U_L , for $\mathbf{a} = 4$ (solid lines), $\mathbf{a} = 3$ (dashed lines), $\mathbf{a} = 2$ (dot-dashed lines) and $\mathbf{a} = 1$ (dotted lines). The plots are for $k = 0$ (blue lines), $k = 1$ (black lines) and $k = -1$ (red lines), with $\mathbf{b} = 4$. 100
- Figure 23 – The normalized zero modes with $\mathbf{a} = \mathbf{b} = 4$, for $k = 0$ (solid blue line), $k = 1$ (solid red line), $k = 2$ (solid black line), $k = 3$ (solid brown line), $k = -1$ (dashed red line), $k = -2$ (dashed black line) and $k = -3$ (dashed brown line). 103
- Figure 24 – (a) The normalized right-handed bound states. (b) The normalized left-handed bound states. The plots are for $k = 0$ (solid blue line), $k = 1$ (solid red line), $k = 2$ (solid black line), $k = 3$ (solid brown line), $k = -1$ (dashed red line), $k = -2$ (dashed black line) and $k = -3$ (dashed brown line), with $\mathbf{a} = \mathbf{b} = 4$ and $j = 0$ 104
- Figure 25 – (a) The normalized right-handed bound states. (b) The normalized left-handed bound states. The plots are for $k = 0$ (solid blue line), $k = 1$ (solid red line), $k = 2$ (solid black line), $k = 3$ (solid brown line), $k = -1$ (dashed red line), $k = -2$ (dashed black line) and $k = -3$ (dashed brown line), with $\mathbf{a} = \mathbf{b} = 4$ and $j = 1$ 104
- Figure 26 – (a) The normalized right-handed bound states. (b) The normalized left-handed bound states. The plots are for $k = 0$ (solid blue line), $k = 1$ (solid red line), $k = 2$ (solid black line), $k = 3$ (solid brown line), $k = -1$ (dashed red line), $k = -2$ (dashed black line) and $k = -3$ (dashed brown line), with $\mathbf{a} = \mathbf{b} = 4$ and $j = 2$ 105

Figure 27 – (a) The left/right-handed chiral approach. The solid red and black lines represent the left, right-handed wave functions, while the dashed black line represents the overlap between them. (b) The non-trivial bulk Higgs approach.	110
Figure 28 – The non-trivial curvature approach. The solid black line represents the warp factor A (here $A \equiv B$). The solid red, blue and brown represent the normalized wave functions of the tauon, muon and electron, respectively. The dashed red, blue and brown lines represent the overlap between the wave functions of tauon, muon and electron with the warp factor, respectively.	110
Figure 29 – (a) The charged lepton mass spectrum associated with the metric (5.40) for $l - o = 1$. (b) The charged lepton mass spectrum associated with the metric (5.40) for $l - o = 2$. The solid black, solid red and dashed black lines represent the equations $m_\mu/m_e = 206.768$, $m_\tau/m_\mu = 16.817$ and $\mathcal{K} = 2/3$, respectively. Results are for triple intersecting points at $l = 6, 7, 8$, and 9	118
Figure 30 – (a) The charged lepton mass spectrum associated with the metric (5.40) for $a = 1$. (b) The charged lepton mass spectrum associated with the metric (5.40) for $a = 2$. The solid black, solid red and dashed black lines represent the equations $m_\mu/m_e = 206.768$, $m_\tau/m_\mu = 16.817$ and $\mathcal{K} = 2/3$, respectively. Results are for triple intersecting points at $l = 3, 4, 5$, and 6	119
Figure 31 – (a) Warp factor $e^{-2\hat{A}}$ of model I as a function of φ , for $n = 1$ (solid black line), $n = 2$ (dashed black line), $n = 3$ (solid red line) and $n = 4$ (dashed red line). (b) Conformal factor e^{-2B^I} of model I as a function of φ , for $p = 3$ (black), $p = 4$ (red) and $p = 5$ (blue), the solid and dashed lines correspond to $n = 1$ and $n = 2$, respectively.	146
Figure 32 – The scalar fields of model I : (a) $\phi^{*I} = \phi^I/\sqrt{2p-5} M^2$; (b) $\zeta^{*I} = \zeta^I/\sqrt{3+2p} M^2$. The plots are for $n = 1$ (solid black line), $n = 2$ (dashed black line), $n = 3$ (solid red line) and $n = 4$ (dashed red line).	147
Figure 33 – Scalar fields of model II for $p = 1/2$ (black) and $p = 2$ (red): (a) $\phi^{*II} = \phi^{II}/M^2$ as a function of θ ; (b) $\zeta^{*II} = \zeta^{II}/M^2$ as a function of φ . The plots are for $n = l = 1$ (solid lines), $n = 2, l = 1$ (dashed lines) and $n = l = 2$ (dotted lines).	148
Figure 34 – Potential \mathcal{V}^{II} of model II as a function of (θ, φ) , for $p = 1/2$ (a) and $p = 2$ (b).	148
Figure 35 – Energy density $-T_{\mu\nu}^{II}\sqrt{-g}$ of model II as a function of (θ, φ) , for $p = 1/2$ (a) and $p = 2$ (b).	149

Contents

1	INTRODUCTION	17
2	SIX-DIMENSIONAL BRANEWORLDS	21
2.1	Six-Dimensional Braneworlds from Scalar fields	22
2.1.1	The Geometry of the Brane	26
2.1.2	The Geometry of The Internal Space	27
2.2	The Newtonian Gravitational Constant	29
2.3	Classification of Separable Solutions	30
2.4	Intersecting Braneworlds	32
2.4.1	The Flat Brane Case ($\Lambda = 0$)	33
2.4.1.1	The $p \neq 0$ (or $p \neq 1$) Case (Models <i>I</i> and <i>II</i>)	33
2.4.1.2	The $p = 0$ (or $p = 1$) Case (Model <i>III</i>)	36
2.4.2	The Bent Brane Case ($p = 0, \Lambda \neq 0$)	39
2.4.2.1	The Single Scalar Field Case (Model <i>IV</i>)	40
2.4.2.2	The $C=0$ Case (Model <i>V</i>)	43
2.4.2.3	The General Bent Brane (Model <i>VI</i>)	44
2.4.3	Setups From Predetermined Internal Spaces	47
2.4.4	Solving Eqs. (2.84) and (2.85)	48
2.4.5	The Geometry of \mathbb{S}^2	51
2.4.6	The Sphere Models	53
2.4.7	The Spheroid Models	57
3	GRAVITY LOCALIZATION	61
3.1	Gravitational Fluctuations	62
3.1.1	The Decoupling Between Scalar and Tensorial Perturbations	65
3.1.2	The Perturbed Action	67
3.1.3	The Quantum Mechanical Analogy	70
3.1.4	On the Stability of the Scalar Fields	70
3.1.5	The Effective Action and Localization	71
3.1.6	The Newtonian Limit	72
3.2	The Quantum Analogue Problem for Separable Solutions	74
3.2.1	Intersecting-like Models	75
3.2.1.1	Intesecting Branes: Models <i>I</i> and <i>II</i>	75
3.2.1.2	Intesecting Branes: Model <i>III</i>	76
3.2.1.3	Intesecting Branes: Model <i>IV</i>	78
3.2.1.4	Intesecting Branes: Model <i>V</i>	79

3.2.1.5	Intesecting Branes: Model <i>VI</i>	80
3.2.2	The \mathbb{S}^2 Models	81
3.2.2.1	Model <i>III</i> ($C = 0$)	82
3.2.2.2	Model <i>IV</i>	83
4	MATTER LOCALIZATION	85
4.1	Scalar Fields	86
4.2	Gauge Fields	87
4.2.1	The Zero Mode	87
4.2.2	The Massive Modes	88
4.3	Fermionic Fields	90
4.3.1	Six-Dimensional Weyl Spinors	91
4.3.2	Six-Dimensional Charged Weyl Spinors	95
4.3.2.1	Trivial-like Models	97
4.3.2.2	Intersecting-like Models: Model <i>IV</i>	99
5	ASYMMETRICAL BRANES AND THE CHARGED LEPTON SPEC-	
	TRUM	107
5.1	The Asymmetrical Mechanism	111
5.1.1	The Mechanism for a $U(1)$ Model	111
5.1.2	The Complete Lepton Sector	114
5.1.3	The Asymmetry Parametrized	117
5.1.4	Beyond The Standard Model	118
5.1.4.1	Massive Modes: The Charged Leptons	119
5.1.4.2	Massive Modes: The Higgs Field	121
5.1.5	Neutrino Masses	122
5.2	For Other Sets of the Classification	123
6	CONCLUSION	127
6.1	On the Six-dimensional Braneworld Models	127
6.2	On the Lepton Masses	130
	BIBLIOGRAPHY	133
	APPENDIX	143
	APPENDIX A – DETAILS OF MODELS <i>I</i> AND <i>II</i>	145
A.1	Model <i>I</i>	146
A.2	Model <i>II</i>	147

APPENDIX B – ON THE SMOOTHNESS OF HYPERGEOMETRIC FUNCTIONS	151
--	-----

1 Introduction

In the last decades, inspired by the modern attempts of unifying all interactions, the idea of extra dimensions has been currently scrutinized [1]. Admitting the possibility of extra dimensions playing some role in physics requires a deeper understanding of the evinced observation of three space dimensions [1]. A naive explanation for the $(3 + 1)$ -dimensional universe is based on the idea that extra dimensions can be compactified with a tiny radius of the order of the Planck length ($\approx 10^{-33}$ cm) [1]. In this scenario, all the effects due to additional dimensions would be hidden to experimental measurements [1]. In such a context, Arkani-Hamed–Dimopoulos–Dvali (ADD) [2] and Randall–Sundrum (RS) [3, 4] seminal papers diffused the possibility of implementing large extra dimensions into realistic phenomenological contexts [1]. In particular, as suggested by the ADD model [2], one of the most inspiring motivations for pursuing large extra dimensions in physics is the possibility of resolving the hierarchy problem [2] in quantum field theories [1]. While the ADD model was performed on a flat space, Randall-Sundrum (RS) models [3, 4] assume that the brane should gravitate, being spatially localized by an extra dimension warping effect so as to explain the field hierarchy [1].

In order to motivate further studies in higher-dimensional braneworld models, it is relevant to provide a minimal review of the RS models, that exemplifies some of braneworlds main ideas. The RS models can be broken down into two contrasting models, by the different topologies one can couple to a one-dimensional co-space, \mathbb{R} or \mathbb{S}^1 . For the first RS model [3] the metric is assumed to satisfy the ansatz

$$\mathbf{g} = e^{-2A(\varphi)} \eta_{\mu\nu} dx^\mu \otimes dx^\nu + r^2 d\varphi \otimes d\varphi, \quad (1.1)$$

where $\varphi \in \mathbb{S}^1$, r is the radius of \mathbb{S}^1 and A is the so called warp factor, and to obey the action

$$S_{RS} = \int dx^5 \sqrt{-g} (2M^3 R - \Lambda) - \int dx^5 \sqrt{-g} [-\delta(\varphi) \Lambda + \delta(\varphi - \pi) \Lambda], \quad (1.2)$$

where it is understood that one has two branes; one with energy $-\Lambda$ at $\varphi = 0$, called the hidden brane, and the other with energy Λ at $\varphi = \pi$, called the TeV brane. All Standard Model (SM) fields are thus assumed to be confined to the TeV brane.

Varying Eq. (1.2) with respect to \mathbf{g} and solving for the warp factor, A , gives

$$A = \pm r \sqrt{-\frac{\Lambda}{12M^3}} \varphi = \pm r k \varphi. \quad (1.3)$$

Imposing mirror symmetry, $\varphi \in \mathbb{S}^1/\mathbb{Z}_2$, the metric of space-time is thus

$$\mathbf{g} = e^{-2rk|\varphi|} \eta_{\mu\nu} dx^\mu dx^\nu + r^2 d\varphi^2. \quad (1.4)$$

With the RS setup at hand, one can finally investigate the physical scales of matter fields that are confined on the TeV brane. Relevant to the hierarchy problem, consider the action of the Higgs field,

$$\begin{aligned} S_H &= \int dx^4 \sqrt{-g_{TeV}} \left[g_{TeV}^{\mu\nu} H_{,\mu}^\dagger H_{,\nu} + \mu^2 H^\dagger H - \lambda (H^\dagger H)^2 \right] \\ &= \int dx^4 \left[e^{-2rk\pi} \eta^{\mu\nu} H_{,\mu}^\dagger H_{,\nu} + \mu^2 e^{-4rk\pi} H^\dagger H - \lambda e^{-4rk\pi} (H^\dagger H)^2 \right]. \end{aligned} \quad (1.5)$$

After canonical normalization, $H = e^{rk\pi} \tilde{H}$, one finds

$$S_H = \int dx^4 \left[\eta^{\mu\nu} \tilde{H}_{,\mu}^\dagger \tilde{H}_{,\nu} + \mu^2 e^{-2rk\pi} \tilde{H}^\dagger \tilde{H} - \lambda (\tilde{H}^\dagger \tilde{H})^2 \right], \quad (1.6)$$

which is the action of an ordinary Higgs field, but with a vacuum expectation value (v.e.v.) that is exponentially suppressed,

$$v_{eff} = \frac{\mu e^{-rk\pi}}{\sqrt{\lambda}} = e^{-rk\pi} v. \quad (1.7)$$

Since all the mass parameters of the SM are set by the v.e.v. of the Higgs field, then every mass scale admits an exponential suppression on the TeV brane.

On the other hand, the gravitational scale of gravity is calculated differently. Gravity is not bound to the branes, thus its gravitational scale is calculated by the integration on the new dimensions. Consider that a particle of mass M is included in the configuration, this will induce perturbations to the gravitational background and one will be able to read the gravitational strength from the perturbed action. The gravitational portion of the perturbed action thus takes the form

$$\begin{aligned} S_g &= 2M^3 \int_{-\pi}^{\pi} d\varphi e^{-2rk|\varphi|} \int dx^4 \sqrt{-g^{(4)}} R^{(4)} \\ &= 2 \frac{M^3}{k} (1 - e^{-2rk\pi}) \int dx^4 \sqrt{-g^{(4)}} R^{(4)}, \end{aligned} \quad (1.8)$$

which corresponds to the four-dimensional action, with an effective gravitational scale given by

$$M_{pl}^2 = \frac{M^3}{k} (1 - e^{-2rk\pi}). \quad (1.9)$$

The gravitational scale is weakly dependent on the size of the new dimension, if r is very large.

Every mass scale is exponentially suppressed by large values of r , while the gravity scale is mostly independent of it. Therefore if the bare value of the Higgs mass is of the order of the fundamental Planck scale, then the four-dimensional effective Higgs mass is exponentially suppressed to the weak scale. While the effective value of the gravitational scale is almost unaffected by the size of the new dimensions and should be close in value to the Planck scale. As a consequence, the RS model warped metric admits an elegant

alternative explanation to the hierarchy problem, in contrast to the ADD compactification [3].

The second RS model can be build from the the first one. Resuming from Eqs. (1.2) and (1.4), but taking the TeV brane to infinity, implies in a single brane setup with an infinitely extended extra dimension, and the metric

$$\mathbf{g} = e^{-2rk|y|}\eta_{\mu\nu}dx^\mu dx^\nu + dy^2, \quad (1.10)$$

where $y \in \mathbb{R}$. In such a scenario, the curvature of space engenders a localization mechanism which admits a suppression of the higher-dimensional terms, thus recovering, within certain limits, the Newton's gravitation theory in the brane even when the additional dimensions are of infinity extent. This is in direct contrast to the ADD models, which requires the additional dimensions to be compactified in a torus.

Higher dimensional theories by themselves have also supported braneworld scenarios driven by topological defects [5] where the fields of the SM are hypothetically confined by brane-like regions of space [2, 5, 6, 7, 8, 9, 10, 11, 12, 13, 14, 1]. Given that RS models rely on thin branes, and the standard model fields are confined in a thin slice of space, a more realistic framework suggests that the matter fields ought to be smeared over extra dimensions. The novel paradigm thus led to several spin-off models, including the now so-called thick braneworlds, where the thin brane is replaced by a topological defect, an equivalent structure to those ones introduced for describing domain walls [5, 1]. The thick brane framework has thus been considered as an engendering tool for obtaining the configuration to the RS model, by admitting some lump-like (non-topological) defect solution for the warp factor [1]. In this case, the non-topological nature of curvature begets the same localization mechanism of the RS models for gravitational and matter fields in the brane, which may host some internal structure [15, 16, 17, 18, 19, 20, 21, 22, 23, 1].

Besides working as a platform for the resolution of the hierarchy problem, thick braneworlds in $(4 + 1)$ -dimensions [15, 16, 17, 18, 19, 20, 21, 22, 23, 24, 25, 26, 27, 28, 29, 30, 31, 32, 33, 34, 1] have include the dark scalar field dynamics into their formulation. Notwithstanding the ferment in this field, theoretical and phenomenological connections with cosmology and astroparticle physics have also been evaluated [35, 36, 37, 38, 39, 40, 41, 42, 43, 44, 45, 46, 47, 48, 49, 50, 51, 52, 53, 54, 55, 56, 57, 58, 59, 60, 1]. More recently, in the strict theoretical front, the possibility of traversable wormholes in RS models [61] has also been suggested [1].

Regardless of the lack of experimental verification, the study of higher-dimensional theories is a promising theoretical front, because this framework allows the connection between two phenomena, that initially seem to be uncorrelated. Apart from having played a prominent role in our understanding of the hierarchy problem, higher dimensions have also been proposed as a means to unifying gravity and electromagnetism by the seminal

Kaluza-Klein models [62]. Our ultimate goal with this manuscript is to include another one of this correlations. Based on the existence of a six-dimensional thick braneworld model, a mechanism for explaining the charged lepton mass spectrum is proposed, and, as a consequence, the existence of three lepton generations is justified.

As a preliminary objective, six-dimensional thick braneworlds ought to be constructed, classified and investigated. Particularly, the separable solutions of thick braneworlds are classified into two contrasting set of models, the string and intersecting-like. String-like have already been widely investigated [63, 64, 65, 66, 67, 68]. On the other hand, the intersecting-like consists on a novel kind of solution and can be broken into six analytical models, for which the physical and localization properties shall be evaluated.

This manuscript is thus organized as follows. Ch. 2 presents the elementary introduction to the $(5+1)$ -dimensional setup and provides a classification of separable solutions that will serve as a background for every construction in following chapters. Ch. 3 addresses the localization of the gravitational and the stability of the configurations, providing the conditions for each one of the models of Ch. 2 to be physically acceptable. Ch. 4 is devoted to the localization of matter fields, establishing the foundations of six-dimensional fermionic matter. Ch. 5 presents the main result of the manuscript: a higher-dimensional mechanism for explaining the masses of the leptons. Our conclusions are drawn in Ch. 6 pointing out the most relevant features of the proposed models.

It is important to emphasize that: the content of Ch. 2 is a strict reproduction of the content of the manuscript “*(5+1)-Dimensional Analytical Brane-World Models: Intersecting Thick Branes*” [1], the content of Ch. 3 is a strict reproduction of the content of the manuscript “*Gravity Localization on Intersecting Thick Braneworlds*” [69], and the content of Ch. 5 is a strict reproduction of the content of the manuscript “*Asymmetrical braneworlds and the charged lepton mass spectrum*” [70], all from the author, all of them with some sufficient literary adaptations in order to establish a cohesive timeline for this thesis content.

2 Six-Dimensional Braneworlds

With the ultimate proposal of enlarging the phenomenology alternatives for thick brane scenarios, the present chapter intends to investigate six-dimensional braneworlds, an idea already explored through different facets which include, for instance, thin branes and string-like defects [63, 64, 65, 66, 67, 68, 71, 72, 73, 74, 75, 76, 77, 1]. However, instead of considering string-like defects as they are typically engendered from thick brane 1-dim warping mechanisms, the possibility of a larger classification of solution is here admitted. By considering a twofold-warp factor which is separable into two intersecting warp factors respectively driven by two intersecting scalar fields, several novel solutions for thick braneworld models are obtained and the possible construction are classified [1]. In fact, with respect to the featured compact internal structure, some of the resulting constructions here admitted shall contrast with the second RS model. Otherwise, the involved scalar fields and self-gravity mechanisms shall consistently resemble the well-succeeded thick braneworld models in admitting lump-like defect solutions for the warp factors [1]. Considering the eventual complexity of some $(5 + 1)$ -dimensional metrics, this chapter is constrained to finding and classifying classical solutions that define the corresponding braneworld scenarios so as to prepare the clean framework for describing the localization of gravitational and matter fields in following chapters [1].

By placing braneworlds over some novel topological spaces append the possibility of some new physics. While five-dimensional setups have only two manifolds, \mathbb{R} and \mathbb{S}^1 , for the topology of the internal one-dimensional space, six-dimensional braneworlds may exhibit a wide range of topologies from the two-dimensional space [1]. Due to the compact features of \mathbb{S}^2 , our straightforward proposal lies in constructing the total space from a priori internal space \mathbb{S}^2 , where, in particular, it is not regarded as the sphere, but as a set with a space topology homeomorphic to the sphere [1]. Considering a departing topological manifold with a defined metric, and that \mathbb{S}^2 , as a coupled structure, intrinsically carries several different metrics, models over two distinct geometries of \mathbb{S}^2 , the sphere and the spheroid, can be solved and evaluated [1].

A more specialized summary of the above procedure is provided by a departure metric given by $\sigma = e^{-2f} du \otimes du + e^{-2h} dv \otimes dv$, which is nothing but the conformally flat metric [78] $\sigma = e^{-2B} (du \otimes du + dv \otimes dv)$ for any (pseudo-) Riemannian space of two dimensions, (\mathbb{B}^2, σ) , although it is written in terms of different coordinates [1]. Despite dealing with braneworld models with two co-dimensions, the choice of the coordinates implying into the conformally flat form of the metric is too restrictive. For the purpose of finding Einstein equation solutions for the warp factor A , the conformally flat approach would be intractable. When considering separable solutions one assumes a twofold-warp

factor A , $A = \tilde{A}(u) + \hat{A}(v)$, and separable metric components, i.e. $f = \tilde{f}(u) + \hat{f}(v)$ and $h = \tilde{h}(u) + \hat{h}(v)$, where \tilde{A} and \hat{A} depend on two different variables with independent warping characteristics [1]. The setup for the corresponding brane is provided by two scalar fields, ϕ and ζ , which also depend on the same two different variables, evidently with $\phi_{,v} = \zeta_{,u} = 0$ [1]. The separable solutions can thus be classified in two different sets; the set of string-like solutions that are driven by a single scalar field ζ ($\phi = 0$), and the set of intersecting-like solutions that are driven by two intersecting scalar fields, ϕ and ζ . The intersecting-like result into two subset of sorted analytical solutions composing of six different models: from I to VI , for which the physical properties and the reducibility to $(4 + 1)$ scenarios shall be evaluated. At the intersection of the sets of string and intersecting-like one finds trivial-like solutions that will also be evaluated.

The chapter is thus organized as follows. Sec. 2.1 presents the elementary introduction to the $(5 + 1)$ -dimensional setup driven by two scalar fields and sets the equations to be solved. Sec. 2.3 is devoted to separable solutions and its classification. In particular, the case of intersecting-like thick branes is discussed, to which the solutions for the so-called models from I to VI are obtained. Considering that only for models I and II , in the above-mentioned first subset, Einstein equation solutions are rigidly defined, and that, for models III , IV , V and VI , in the above-mentioned second subset, an additional degree of freedom, related to the coupled fields that are not constrained by Einstein equations, is admitted, and fixing the geometry of the internal space is mandatory for definitely determining all the fields. Such aspects and their complete understanding are thus evaluated in Sec. 2.4.3. Finally, In Sec. 2.2, a simple initial consistency check for the Newtonian gravitational constant is provided.

2.1 Six-Dimensional Braneworlds from Scalar fields

The space-time is postulated to be a six-dimensional manifold $(\mathbb{E}^6, \mathbf{g})$ that is, as a set, equivalent to the product space $\mathbb{M}^4 \times \mathbb{B}^2$, where $(\mathbb{M}^4, \boldsymbol{\omega})$ is some four-dimensional pseudo-Riemannian manifold and $(\mathbb{B}^2, \boldsymbol{\sigma})$ is some two-dimensional Riemannian manifold. The geometry of \mathbb{E}^6 is represented by the metric,

$$\mathbf{g} = e^{-2A} \omega_{\mu\nu} dx^\nu \otimes dx^\mu + \sigma_{ij} dx^i \otimes dx^j, \quad (2.1)$$

where A is the warp factor, $\boldsymbol{\omega}$ is the metric of the space-time \mathbb{M}^4 ($\boldsymbol{\omega} : \mathbb{M}^4 \rightarrow \mathcal{T}^{(0,2)}\mathbb{M}^4$) and $\boldsymbol{\sigma}$ is the metric of the internal space \mathbb{B}^2 ($\boldsymbol{\sigma} : \mathbb{B}^2 \rightarrow \mathcal{T}^{(0,2)}\mathbb{B}^2$). Here $A : \mathbb{B}^2 \rightarrow \mathbb{R}$, which means that $A = A(u, v)$, with $u = x^4$ and $v = x^5$; $\omega_{\mu\nu} : \mathbb{M}^4 \rightarrow \mathbb{R}$; and $\sigma_{ij} : \mathbb{B}^2 \rightarrow \mathbb{R}$. Clarifying the notation, Greek indices (μ, ν, \dots) are valued in the set $\{0, 1, 2, 3\}$, uppercase Latin indices (M, N, \dots) are valued in $\{0, 1, 2, 3, 4, 5\}$, lowercase Latin indices (m, n, i, j, \dots) are valued in $\{4, 5\}$ (and represent the bulk co-dimensions) and the labels $x^4 = u$ and $x^5 = v$, represent the choice of coordinates for the co-dimensions (\mathbb{B}^2); the use of notation

$T_{45} \equiv T_{uv}$ whenever suited, indicates that "4" = "u" and "5" = "v"; derivatives, whenever suited, will be represented by a *comma*, i.e. $f_{,\mu} := \partial f / \partial x^\mu$; finally, tensors when being referred to its (abstract) entirety will be in boldface, as \mathbf{g} , but its components will be cast in regular font, as $g_{\mu\nu}$.

Suppose that matter in this space are of scalar nature and it corresponds to two canonical real scalar fields minimally coupled to gravity [1]. The action for gravity is the usual Einstein-Hilbert action in six dimensions so as to have

$$S = S_{\text{EH}} + S_\phi, \quad (2.2)$$

$$S_{\text{EH}} = \int d^6x \sqrt{-g} 2M^4 R, \quad (2.3)$$

and

$$S_\phi = - \int d^6x \sqrt{-g} \left(\frac{g^{MN}}{2} \phi_{,M} \phi_{,N} + \frac{g^{MN}}{2} \zeta_{,M} \zeta_{,N} + \mathcal{V} \right), \quad (2.4)$$

where $\phi : \mathbb{B}^2 \rightarrow \mathbb{R}$ ($\phi \equiv \phi(u, v)$), $\zeta : \mathbb{B}^2 \rightarrow \mathbb{R}$ ($\zeta \equiv \zeta(u, v)$), \mathcal{V} is some function of ϕ and ζ , and $g = \det(g_{MN})$. Varying S_{EH} and S_ϕ with respect to the metric, \mathbf{g} , one finds

$$\delta S_{\text{EH}} = 2M^4 \int d^6x \delta(g_{MN}) \sqrt{-g} \left(\frac{g^{MN}}{2} R - R^{MN} \right), \quad (2.5)$$

and

$$\delta S_\phi = \int d^6x \delta g_{MN} \sqrt{-g} \left[\frac{g^{MP} g^{NK}}{2} (\phi_{,K} \phi_{,P} + \zeta_{,K} \zeta_{,P}) - \frac{g^{MN}}{2} \left(\frac{\phi^{,K} \phi_{,K}}{2} + \frac{\zeta^{,K} \zeta_{,K}}{2} + \mathcal{V} \right) \right], \quad (2.6)$$

which results into the usual Einstein equations,

$$G_{MN} = R_{MN} - \frac{1}{2} g_{MN} R = \frac{T_{MN}}{4M^4}, \quad (2.7)$$

where one defined

$$T_{MN} := \phi_{,M} \phi_{,N} + \zeta_{,M} \zeta_{,N} - g_{MN} \left(\frac{\phi^{,K} \phi_{,K}}{2} + \frac{\zeta^{,K} \zeta_{,K}}{2} + \mathcal{V} \right). \quad (2.8)$$

On the other hand, the equations of motion of the scalar fields can be determined by varying S_ϕ with respect to both scalar fields,

$$\delta S_\phi|_\phi = \int d^6x \delta\phi \left[\left(\sqrt{-g} g^{MN} \phi_{,M} \right)_{,N} - \sqrt{-g} \mathcal{V}_{,\phi} \right], \quad (2.9)$$

$$\delta S_\phi|_\zeta = \int d^6x \delta\zeta \left[\left(\sqrt{-g} g^{MN} \zeta_{,M} \right)_{,N} - \sqrt{-g} \mathcal{V}_{,\zeta} \right], \quad (2.10)$$

which implies in

$$\square\phi = \frac{1}{\sqrt{-g}} \left[\sqrt{-g} g^{MN} \phi_{,N} \right]_{,M} = \mathcal{V}_{,\phi}, \quad (2.11)$$

$$\square\zeta = \frac{1}{\sqrt{-g}} \left[\sqrt{-g} g^{MN} \zeta_{,N} \right]_{,M} = \mathcal{V}_{,\zeta}, \quad (2.12)$$

For the configurations considered here, eqs. (2.11) and (2.12) will be completely redundant, since the solutions of (2.7) will already determine the scalar fields ϕ and ζ [1]. This can be straightforwardly proven by first noting that the conservation of the stress energy tensor implies

$$(\nabla_M T)^{MN} = 0 \iff (\nabla_M G)^{MN} = 0, \quad (2.13)$$

which, for the two scalar fields, results into

$$(\nabla_M T)^{MN} = \phi^{,N} (\square\phi - \mathcal{V}_{,\phi}) + \zeta^{,N} (\square\zeta - \mathcal{V}_{,\zeta}) = 0. \quad (2.14)$$

In the following sections, the accomplishment of the intersecting thick brane scenario shall admit scalar fields, $\phi = \phi(u)$ and $\zeta = \zeta(v)$, regarded as independent quantities one from each other, with $\phi_{,v} = \zeta_{,u} = 0$ [1]. From such an assumption one has

$$(\nabla_M G)^{MN} = 0 \iff \begin{cases} \square\phi - \mathcal{V}_{,\phi} = 0, \\ \square\zeta - \mathcal{V}_{,\zeta} = 0. \end{cases} \quad (2.15)$$

This means that any solution of Eq. (2.7) also satisfies Eqs. (2.11) and (2.12) for the scalar fields. Nevertheless, this is only true for very particular configurations, which include the case $\phi_{,v} = \zeta_{,u} = 0$. Therefore, in this case, the redundancy of the scalar field Eqs. (2.11) and (2.12) are clear¹ [1].

More generically, to realize the field equations one first writes down the components of the Einstein tensor through a straightforward – even if long and tedious – process. To simplify the following steps, a rescaling of the metric given by $\mathbf{g} = e^{-2A}\hat{\mathbf{g}}$ can be used to remove the conformal factor, where one defines

$$\hat{\mathbf{g}} = \omega_{\mu\nu} dx^\mu \otimes dx^\nu + \hat{\sigma}_{ij} dx^i \otimes dx^j, \quad (2.16)$$

and $\hat{\sigma} = e^{2A}\sigma$. Notice that the metric $\hat{\mathbf{g}}$ is factorable since $\omega_{\mu\nu} : \mathbb{M}^4 \rightarrow \mathbb{R}$ and $\hat{\sigma}_{ij} : \mathbb{B}^2 \rightarrow \mathbb{R}$, and the calculations that follow can be easily extended to any dimension [1].

One can now write the relation between the operators compatible with \mathbf{g} and $\hat{\mathbf{g}}$: the connection, the Riemann and the Einstein tensors compatible with \mathbf{g} , calling it ∇ , $R^M{}_{NPQ}$ and G_{MN} , respectively, and those ones compatible with $\hat{\mathbf{g}}$, calling it $\hat{\nabla}$, $\hat{R}^M{}_{NPQ}$ and \hat{G}_{MN} , respectively.

The Levi-Civita connections, Ricci tensors and Ricci scalars compatible with metrics \mathbf{g} and $\hat{\mathbf{g}}$ are related by the equations

$$\Gamma_{MN}^P = \hat{\Gamma}_{MN}^P - A_{,N}\delta_M^P - A_{,M}\delta_N^P + A_{,S}\hat{g}^{PS}\hat{g}_{MN}, \quad (2.17)$$

¹ The analytical solutions must not only define the metric, but also the scalar fields as functions of u and v , which does not necessarily implies into identifying \mathcal{V} explicitly in terms of the scalar fields, i.e. $\mathcal{V} = \mathcal{V}(\phi, \zeta)$.

$$R_{MN} = \hat{R}_{MN} + 4\hat{\nabla}_M \hat{\nabla}_N A + \hat{g}_{MN} \hat{\square} A + 4\hat{\nabla}_M A \hat{\nabla}_N A - 4\hat{g}_{MN} \hat{\nabla}^P A \hat{\nabla}_P A, \quad (2.18)$$

and

$$R = e^{2A} \left[\hat{R} + 25\hat{\square} A - 20\hat{\nabla}^P A \hat{\nabla}_P A \right], \quad (2.19)$$

respectively.

The Einstein equations are thus re-defined in terms of the metric \hat{g} rather than g . Meanwhile, the Einstein tensor of the metric g can be recast in terms of the metric \hat{g} and A , in the form of

$$G_{MN} = \hat{G}_{MN} + 4\hat{\nabla}_M \hat{\nabla}_N A + 4\hat{\nabla}_M A \hat{\nabla}_N A - 4\hat{g}_{MN} \hat{\square} A + 6\hat{g}_{MN} \hat{\nabla}^P A \hat{\nabla}_P A. \quad (2.20)$$

To compute \hat{G}_{MN} in order to obtain the equations of motion, one firstly notices that the Riemann tensor $\hat{\mathbf{R}}$ is factorable,

$$\begin{aligned} \hat{\mathbf{R}} &= \hat{R}^\rho_{\alpha\mu\nu}(x^\kappa) \frac{\partial}{\partial x^\rho} \otimes dx^\alpha \otimes dx^\nu \otimes dx^\nu + \hat{R}^j_{klc}(x^s) \frac{\partial}{\partial x^j} \otimes dx^k \otimes dx^l \otimes dx^c \\ &= \mathcal{R}^\rho_{\alpha\mu\nu}(x^\kappa) \frac{\partial}{\partial x^\rho} \otimes dx^\alpha \otimes dx^\nu \otimes dx^\nu + \hat{\Sigma}^j_{klc}(x^s) \frac{\partial}{\partial x^j} \otimes dx^k \otimes dx^l \otimes dx^c, \end{aligned} \quad (2.21)$$

where $\hat{R}^\rho_{\alpha\mu\nu}$ encodes de curvature of (\mathbb{M}^4, ω) , and which has been labeled by $\mathcal{R}^\rho_{\alpha\mu\nu}$, and \hat{R}^j_{klc} encodes de curvature of $(\mathbb{B}^2, \hat{\sigma})$, which has been labeled by $\hat{\Sigma}^j_{klc}$ [1]. From here on \mathcal{R} and Δ are the curvature and covariant derivative compatible with ω . Analogously, $\hat{\Sigma}$ and $\hat{\Delta}$ are compatible with $\hat{\sigma}$, with $\hat{\Sigma}$ being compatible with $\hat{\sigma}$. Also, a shortened notation given in terms of $\hat{\Delta} := \omega^{\mu\nu} \Delta_\mu \Delta_\nu$ and $\hat{\Delta}^2 := \sigma^{ij} \Delta_i \Delta_j$ shall be useful in the following steps [1].

From the Riemann tensor, the set of expressions for Ricci tensors and Riccis scalar are given by

$$\hat{R}_{\mu\nu} = \hat{R}^M_{\mu M\nu} = \hat{R}^\kappa_{\mu\kappa\nu} = \mathcal{R}^\kappa_{\mu\kappa\nu}(x^\rho) = \mathcal{R}_{\mu\nu}(x^\rho), \quad (2.22)$$

$$\hat{R}_{ij} = \hat{R}^M_{iMj} = \hat{R}^m_{imj} = \hat{\Sigma}^m_{imj}(x^l) = \hat{\Sigma}_{ij}(x^l), \quad (2.23)$$

and

$$\hat{R} = \hat{g}^{MN} \hat{R}_{MN} = \omega^{\mu\nu} \mathcal{R}_{\mu\nu} + \hat{\sigma}^{ij} \hat{\Sigma}_{ij} = \mathcal{R} + \hat{\Sigma}, \quad (2.24)$$

which can be re-introduced into Eq. (2.20) so as to return

$$G_{\mu\nu} = \mathcal{R}_{\mu\nu} - \frac{1}{2}\omega_{\mu\nu} \mathcal{R} - \frac{1}{2}\omega_{\mu\nu} \hat{\Sigma} - 4\omega_{\mu\nu} \hat{\Delta}^2 A + 6\omega_{\mu\nu} \hat{\sigma}^{ij} A_{,i} A_{,j}, \quad (2.25)$$

and

$$G_{ij} = \hat{\Sigma}_{ij} - \frac{1}{2}\hat{\sigma}_{ij} \hat{\Sigma} - \frac{1}{2}\hat{\sigma}_{ij} \mathcal{R} + 4\hat{\Delta}_i \hat{\Delta}_j A + 4A_{,i} A_{,j} - 4\hat{\sigma}_{ij} \hat{\Delta}^2 A + 6\hat{\sigma}_{ij} \hat{\sigma}^{mn} A_{,n} A_{,m}. \quad (2.26)$$

Finally, by substituting the above expressions into Einstein field equations decoupled from Eq. (2.7), one finds

$$\mathcal{R}_{\mu\nu} - \frac{1}{2}\omega_{\mu\nu}\mathcal{R} = \omega_{\mu\nu} \left[\frac{1}{2}\hat{\Sigma} + 4\hat{\Delta}^2 A - 6\hat{\sigma}^{ij}A_{,i}A_{,j} - \frac{e^{-2A}}{4M^4} \left(\frac{\phi^{,K}\phi_{,K}}{2} + \frac{\zeta^{,K}\zeta_{,K}}{2} + \mathcal{V} \right) \right], \quad (2.27)$$

and

$$\begin{aligned} & \hat{\Sigma}_{ij} - \frac{1}{2}\hat{\sigma}_{ij}(\mathcal{R} + \hat{\Sigma}) + 4\hat{\Delta}_i\hat{\Delta}_j A + 4A_{,i}A_{,j} - 4\hat{\sigma}_{ij}\hat{\Delta}^2 A \\ & + 6\hat{\sigma}_{ij}\hat{\sigma}^{mn}A_{,n}A_{,m} = \frac{1}{4M^4} \left[\phi_{,i}\phi_{,j} + \zeta_{,i}\zeta_{,j} - e^{-2A}\hat{\sigma}_{ij} \left(\frac{\phi^{,K}\phi_{,K}}{2} + \frac{\zeta^{,K}\zeta_{,K}}{2} + \mathcal{V} \right) \right]. \end{aligned} \quad (2.28)$$

Since $\mathcal{R}_{\mu\nu}$ and \mathcal{R} are functions of space-time, \mathbb{M}^4 , and $\hat{\Sigma}_{ij}$ and $\hat{\Sigma}$ are functions of the internal space, \mathbb{B}^2 , then one may separate variables at Eqs. (2.27) and (2.28). Through a more familiar notation, one chooses a separation constant which can be interpreted as the so-called cosmological constant Λ [1]. After some mathematical manipulations, one thus obtains

$$\mathcal{R}_{\mu\nu} = \Lambda\omega_{\mu\nu}, \quad (2.29)$$

$$\frac{1}{2}\hat{\Sigma} + 4\hat{\Delta}^2 A - 6\hat{\sigma}^{ij}A_{,i}A_{,j} - \frac{e^{-2A}}{4M^4} \left(\frac{\phi^{,l}\phi_{,l}}{2} + \frac{\zeta^{,l}\zeta_{,l}}{2} + \mathcal{V} \right) = -\Lambda, \quad (2.30)$$

and

$$\begin{aligned} & \hat{\Sigma}_{ij} - \frac{1}{2}\hat{\sigma}_{ij}(4\Lambda + \hat{\Sigma}) + 4\hat{\Delta}_i\hat{\Delta}_j A + 4A_{,i}A_{,j} - 4\hat{\sigma}_{ij}\hat{\Delta}^2 A \\ & + 6\hat{\sigma}_{ij}\hat{\sigma}^{mn}A_{,n}A_{,m} = \frac{1}{4M^4} \left[\phi_{,i}\phi_{,j} + \zeta_{,i}\zeta_{,j} - e^{-2A}\hat{\sigma}_{ij} \left(\frac{\phi^{,l}\phi_{,l}}{2} + \frac{\zeta^{,l}\zeta_{,l}}{2} + \mathcal{V} \right) \right]. \end{aligned} \quad (2.31)$$

From a geometrical perspective, Eqs. (2.30) and (2.31) clearly illustrate why the two co-dimensional problem is circumstantially more complicated than one co-dimensional analysis [1]. The existence of curvature for the internal space \mathbb{B}^2 increases the complexity of the equations to be solved. For a one co-dimension problem, the equations are, up to some constants, equivalent, but the curvature is null. In addition, the complexity that arises solely from topological considerations is evinced: while for one co-dimension there are only two possible topologies, \mathbb{R}^1 or \mathbb{S}^1 , for two co-dimensions a vaster scenario can be explored [1].

2.1.1 The Geometry of the Brane

From the above results, Eq. (2.29) defines the geometry of space-time (\mathbb{M}^4, ω), and one can readily obtain some solutions summarized by [1]

1. if $\Lambda = 0$, a solution is a Minkowski space, $\omega = \eta$;

2. if $\Lambda > 0$, a solution is a de Sitter space of four dimensions (dS^4), $\omega = \omega^+$;
3. if $\Lambda < 0$, a solution is an anti-de Sitter space of four dimensions (AdS^4); $\omega = \omega^-$;
4. there are also FRW space-times solutions of these equations for all values of Λ [36].

Therefore one may fit each of these $(3 + 1)$ solutions in the model construction that follows. Again, to simplify the notation, whenever one is dealing with a space-time \mathbb{M}^4 where $\Lambda = 0$, its metric will be labeled η , while either for $\Lambda > 0$ or for $\Lambda < 0$, it will be labeled either by ω^+ or by ω^- , respectively. Eq. (2.29) does not completely determine the curvature of space-time, since the Riemann tensor is not completely specified. In later chapters, one will restrict the brane to be of constant curvature, i.e. the Riemann tensor

$$\mathcal{R}_{\delta\mu\rho\nu} = \frac{\Lambda}{3} (\omega_{\delta\rho}\omega_{\mu\nu} - \omega_{\delta\nu}\omega_{\mu\rho}), \quad (2.32)$$

this will lead to significant simplifications to the equations, specially when dealing with gravitational perturbations.

2.1.2 The Geometry of The Internal Space

Hence the subsequent steps can be resumed by obtaining the solutions for Eqs. (2.30) and (2.31), which define the geometry of the internal space ($\mathbb{B}^2, \hat{\sigma}$) [1]. However, since they are still expressed in terms of $\hat{\sigma}$, it should be simpler to work with the started geometry preliminarily resumed by σ . Turning back to such a departure metric, one firstly writes

$$\hat{\Xi}_{ij}^l = \Xi_{ij}^l + A_{,j}\delta_i^l + A_{,i}\delta_j^l - A_{,s}\sigma^{ls}\sigma_{ij}, \quad (2.33)$$

$$\hat{\Sigma}_{ij} = \Sigma_{ij} - \sigma_{ij}\Delta^2 A, \quad (2.34)$$

$$\hat{\Sigma} = e^{-2A} [\Sigma - 2\Delta^2 A], \quad (2.35)$$

and

$$\hat{\Delta}_i\hat{\Delta}_j A = \Delta_i\Delta_j A - 2A_{,i}A_{,j} + \sigma^{ls}\sigma_{ij}A_{,l}A_{,s}, \quad (2.36)$$

which, once substituted into Eqs. (2.30) and (2.31), after some straightforward manipulations, leads to

$$\frac{\mathcal{V}}{4M^4} = 2\Lambda e^{2A} + 2\Delta^2 A - 8A^{,m}A_{,m}, \quad (2.37)$$

and

$$\Sigma_{ij} - \sigma_{ij}\Lambda e^{2A} + 4\Delta_i\Delta_j A - \sigma_{ij}\Delta^2 A + 4\sigma_{ij}A^{,m}A_{,m} - 4A_{,i}A_{,j} = \frac{\phi_{,i}\phi_{,j} + \zeta_{,i}\zeta_{,j}}{4M^4}, \quad (2.38)$$

from which one can notice that some coordinate degree of freedom is still present [1]. Eqs. (2.37) and (2.38) encode the needed information to determine the geometry of space (\mathbb{B}^2, σ), the warp factor, A , and the scalar fields, ϕ and ζ . Turning back to the systematic procedure for solving Eqs. (2.37) and (2.38), one can state the following theorem [78],

Theorem 1 *Every two-dimensional (pseudo-) Riemannian space (\mathbb{B}^2, σ) is conformally flat.*

This means that, without loss of generality, one can consider the metric of the space of co-dimensions to be conformally flat, i.e.

$$\sigma = e^{-2B(u,v)} (du \otimes du + dv \otimes dv). \quad (2.39)$$

As previously argued, one has made a previous choice for the coordinates so as to be able to write the resulting expression for the metric. However, since Eq. (2.38) may not be analytically solvable, it would be counterproductive to keep that expressed in terms of conformal coordinates [1]. A more treatable set coordinates for solving the resulting differential equations, that do not result in a conformally flat metric, can be identified by rewriting the system in terms of the following metric,

$$\sigma = e^{-2f(u,v)} du \otimes du + e^{-2h(u,v)} dv \otimes dv. \quad (2.40)$$

This is not the most general metric choice², but it does allow for some leeway when solving the equations [1]. Naturally, this is equivalent to the conformally flat form, since one has just used a different set of coordinates. By substituting the metric choice from (2.40) into the field Eqs. (2.37) and (2.38), it is straightforward to write

$$\begin{aligned} \frac{\mathcal{V}}{8M^4} = & \Lambda e^{2A} + e^{2f} (A_{,uu} + A_{,u}f_{,u} - A_{,u}h_{,u} - 4A_{,u}{}^2) \\ & + e^{2h} (A_{,vv} + A_{,v}h_{,v} - A_{,v}f_{,v} - 4A_{,v}{}^2), \end{aligned} \quad (2.41)$$

$$\begin{aligned} \frac{\phi_{,u}{}^2 + \zeta_{,u}{}^2}{4M^4} = & e^{2h-2f} (f_{,vv} + f_{,v}h_{,v} - f_{,v}{}^2 + 4A_{,v}{}^2 - 3f_{,v}A_{,v} - A_{,vv} - A_{,v}h_{,v}) \\ & + h_{,uu} + f_{,u}h_{,u} - h_{,u}{}^2 + 3A_{,uu} + 3f_{,u}A_{,u} + A_{,u}h_{,u} - \Lambda e^{2A-2f}, \end{aligned} \quad (2.42)$$

$$\begin{aligned} \frac{\phi_{,v}{}^2 + \zeta_{,v}{}^2}{4M^4} = & e^{2f-2h} (h_{,uu} + f_{,u}h_{,u} - h_{,u}{}^2 + 4A_{,u}{}^2 - 3h_{,u}A_{,u} - A_{,uu} - A_{,u}f_{,u}) \\ & + f_{,vv} + f_{,v}h_{,v} - f_{,v}{}^2 + 3A_{,vv} + 3h_{,v}A_{,v} + A_{,v}f_{,v} - \Lambda e^{2A-2h}, \end{aligned} \quad (2.43)$$

and

$$\frac{\phi_{,u}\phi_{,v} + \zeta_{,u}\zeta_{,v}}{4M^4} = 4A_{,uv} + 4f_{,v}A_{,u} + 4h_{,u}A_{,v} - 4A_{,u}A_{,v}. \quad (2.44)$$

From Eqs. (2.41)-(2.44) one can determine the warp factor and scalar fields, and consequently obtaining the defect that generates the thick brane. From this point, different techniques must be employed for solving Eqs. (2.41)-(2.44) analytically [1]. One may separate the techniques into two opposite categories:

² The most general one would allow non-diagonal terms.

1. Starting from a predetermined internal space (\mathbb{B}^2, σ) , which in some other words correspond to the preliminary knowledge of f and h , one can thus calculate the warp factor A ;
2. Starting with no knowledge of the geometry of the internal space (\mathbb{B}^2, σ) , i.e. of f and h , one thus assume some simplifying hypothesis so as to solve the equations in order to find A , f and h .

Our focus will be on the second technique, which can be later connected to the first one by using their solutions to fit them into predetermined geometries. Looking at the second technique, the equations will necessarily determine the metric, but the topology of \mathbb{B}^2 will still remain undetermined. This fact is true, since the metric does not have, in general, enough information to define the topological properties of space, with the exception of some of the compact characteristics of the latter, which is only possible because of the bulk geometry³ [1]. Besides this special topological invariant, not many topological statements can be extracted about the spaces here within, unless it is imposed *a priori*. Such an indeterminacy will be advantageous to the model building, since the same solution may fit different topologies and thus configure distinctive space-times [1].

2.2 The Newtonian Gravitational Constant

For any braneworld model to be physically acceptable it must recover a finite four-dimensional gravitational coupling strength, which can be calculated directly from the one in the bulk by applying a simple procedure. Substituting the ansatz for the bulk metric, Eq. (2.1), into the gravitational action and isolating the terms that specify the curvature of the brane,

$$S_g = \int_{\mathbb{E}^6} d^4x dy^2 \sqrt{-g} 2M^4 R \sim 2M^4 \int_{\mathbb{B}^2} dy^2 \sqrt{\sigma} e^{-2A} \int_{\mathbb{M}^4} d^4x \sqrt{-\omega} \mathcal{R} + \dots, \quad (2.45)$$

from which one can read the gravitational field strength (or Planck Scale) for the brane,

$$M_{pl}^2 = M^4 \int_{\mathbb{B}^2} dy^2 \sqrt{\sigma} e^{-2A}, \quad (2.46)$$

where $G_N \sim M_{pl}^{-2}$. Eq. (2.46) establishes the first condition for a braneworld model to be physically acceptable, and also serves as the first consistency check for the linear approach: if the Planck scale calculated from this procedure does not coincide with the one associated with the linear approach, then the model in question is inconsistent. Fortunately, for any braneworld model the Planck scale coincides in every approach, as shall be presented in Ch. 3. For the present chapter, this will be the only condition imposed for physical acceptable solutions. However, in Ch. 3, the stability and effective Newtonian theory will also be imposed and addressed for each one of the intersecting-like models.

³ According to Refs. [79, 80], one can extract out of Einstein equations whether or not the space \mathbb{B}^2 is non-compact.

2.3 Classification of Separable Solutions

Solving Eqs. (2.42)-(2.44) in general is not a straightforward task, but there is a particularly interesting way in which the separable solutions of Eqs. (2.41)-(2.44) can be classified. By separable solutions we mean the ones that satisfy

$$\phi = \phi(u), \zeta = \zeta(v), A = \hat{A}(v) + \tilde{A}(u), f = \hat{f}(v) + \tilde{f}(u) \text{ and } h = \hat{h}(v) + \tilde{h}(u), \quad (2.47)$$

which allows one to apply a separation of variables technique to Eqs. (2.41)-(2.44). Exceptionally, Eq. (2.44) implies into

$$\hat{f}_{,v}\tilde{A}_{,u} + \tilde{h}_{,u}\hat{A}_{,v} - \tilde{A}_{,u}\hat{A}_{,v} = 0, \quad (2.48)$$

which can be solved under two independent hypothesis [1].

Firstly, when either $\hat{A}_{,v}$ or $\tilde{A}_{,u}$ are set equal to zero, thus one has either $\hat{f}_{,v} = 0$, if $\hat{A}_{,v} = 0$, or $\tilde{h}_{,u} = 0$, if $\tilde{A}_{,u} = 0$, – consequently, the most simplified scenario [1]. For instance, with $\hat{A} = 0$, and arbitrarily setting $\hat{h} = 0$, the resulting metric would be cast in the form of

$$\mathbf{g} = e^{-2\tilde{A}}\omega_{\mu\nu}dx^\mu \otimes dx^\nu + e^{-2\tilde{f}}du \otimes du + e^{-2\tilde{h}}dv \otimes dv, \quad (2.49)$$

which leads to a string-like defect for the warp factor [1]. If the coordinates are chosen such that $\tilde{f} = \tilde{h}$, then the warp factor and scalar fields satisfy the field equations,

$$\frac{\mathcal{V}}{8M^4} = \Lambda e^{2\tilde{A}} + e^{2\tilde{h}} (\tilde{A}_{,uu} - 4\tilde{A}_{,u}^2), \quad (2.50)$$

$$\frac{\phi_{,u}^2}{4M^4} = \tilde{h}_{,uu} + 3\tilde{A}_{,uu} + 4\tilde{h}_{,u}\tilde{A}_{,u} - \Lambda e^{2\tilde{A}-2\tilde{h}}, \quad (2.51)$$

and

$$\frac{\zeta_{,v}^2}{4M^4} = \tilde{h}_{,uu} + 4\tilde{A}_{,u}^2 - 4\tilde{h}_{,u}\tilde{A}_{,u} - \tilde{A}_{,uu} - \Lambda e^{2\tilde{A}-2\tilde{h}} = C, \quad (2.52)$$

where C is some constant. Generically $C = 0$ and $\zeta = 0$, otherwise $\zeta = Cv$, which is not allowed by the boundary conditions, since the solutions have to fit topologies⁴ like the ones shown in Figs. 1a and 1b.

These set of solutions have already been widely investigated [63, 64, 65, 66, 67, 68] even when they are not driven by scalar fields. Considering our more general interest, such constructions will not be further pursued. However, it is worth to mention that several models that shall be more deeply understood also have, as limiting cases, string-like solutions for the warp factor.

Furthermore, solutions like Eq. (2.49) do not necessarily entail in string-like defects, since the latter requires specific topological impositions. Generally, solutions like the

⁴ Note that the variable v will generally be interpreted as an angular variable in this set of solutions, otherwise there be no other way of localizing standard fields in this configurations.

previous can fit many kinds of topologies, particularly \mathbb{R}^2 leads to string-like defects, like Fig. 1a. But solutions like Eq. (2.49) over $\mathbb{R} \times \mathbb{S}$ (Fig. 1b), \mathbb{T}^2 and \mathbb{S}^2 are also possible, yet they do not engender string-like defects because they constrain either u or v to be compactified. Regardless, throughout this work, every metric like Eq. (2.49) shall be labeled a string-like solution.

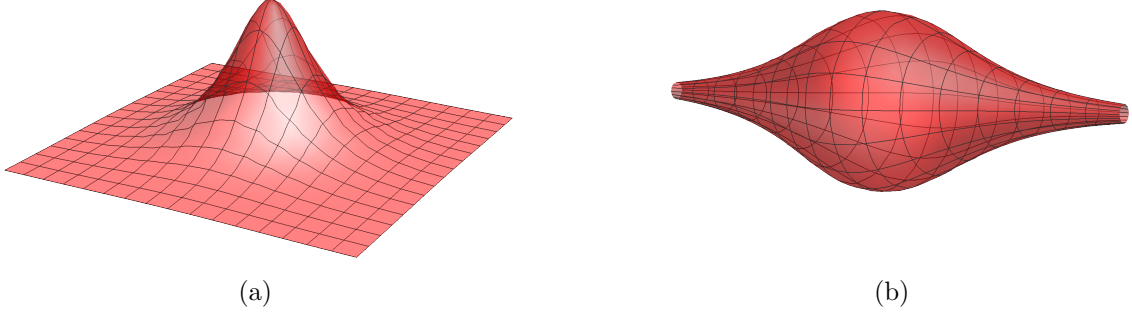


Figure 1 – (a) A string-like defect example for the warp factor. (b) A non-string-like example for the warp factor.

Within the string-like solutions there is a particular subset that will be of interest later. These are constructed by enforcing $\tilde{h} = \tilde{A}$, leading to the metric

$$\mathbf{g} = e^{-2\tilde{A}} (\omega_{\mu\nu} dx^\mu \otimes dx^\nu + dv \otimes dv + du \otimes du), \quad (2.53)$$

where the warp factor and scalar fields satisfy the field equations:

$$\frac{\mathcal{V}}{8M^4} = \Lambda e^{2\tilde{A}} + e^{2\tilde{A}} (\tilde{A}_{,uu} - 4\tilde{A}_{,u}^2), \quad (2.54)$$

$$\frac{\phi_{,u}^2}{4M^4} = 4\tilde{A}_{,uu} + 4\tilde{A}_{,u}^2 - \Lambda, \quad (2.55)$$

and

$$\frac{\zeta_{,v}^2}{4M^4} = -\Lambda, \quad (2.56)$$

which lead to equivalent, up to some constants, models to the seminal five-dimensional braneworld models constructed previously in the literature. Thus, in this work, any metric like Eq. (2.53) shall be labeled trivial-like, because they are trivially deduced from five-dimensional models. Generically, the scalar field ζ and the cosmological constant have to be null, otherwise the scalar would not fit the topology of spaces like Figs. 1a and 1b.

Secondly, the most promising scenario emerges from considering non-vanishing values for both components, $\tilde{A}_{,u}$ and $\hat{A}_{,v}$ [1]. Following a simplified stratagem, from Eq. (2.48), one may write $\hat{f} = p\hat{A}$ and $\tilde{h} = (1-p)\tilde{A}$, where $p \in \mathbb{R}$, while \hat{h} and \tilde{f} are mapped by an aleatory correspondence with the coordinates u and v [1]. In this case, the metric is recast in the form of

$$\mathbf{g} = e^{-2\hat{A}} e^{-2\tilde{A}} \omega_{\mu\nu} dx^\mu \otimes dx^\nu + e^{-2p\hat{A}} e^{-2\tilde{f}} du \otimes du + e^{-2\hat{h}} e^{-2(1-p)\tilde{A}} dv \otimes dv, \quad (2.57)$$

which leads to a novel class of solutions which indeed is not covered by the metric from (2.49) [1]. From now on, solutions like Eq. (2.57) shall be labelled intersecting-like, because the different components of the two-fold warp factor, \hat{A} and \tilde{A} , are associated with the intersecting defects of the scalar fields ϕ and ζ , respectively.

The separable solutions can thus be classified into two distinct sets:

1. The set of string-like solutions, $\mathbb{S}\mathfrak{t}$, defined by Eq. (2.49);
2. The set of intersecting-like solutions, $\mathbb{I}\mathfrak{n}$, defined by Eq. (2.57).

At the intersection of $\mathbb{S}\mathfrak{t}$ with $\mathbb{I}\mathfrak{n}$ one finds the set of trivial-like solutions $\mathbb{T}\mathfrak{r}$, defined by metric Eq. (2.53), i.e. $\mathbb{I}\mathfrak{n} \cap \mathbb{S}\mathfrak{t} = \mathbb{T}\mathfrak{r}$.

2.4 Intersecting Braneworlds

As argued before both the metrics of string and trivial-like solutions, Eqs. (2.49) and (2.53), are a consequence of a defect generated by a single scalar field, ϕ , since ζ is, generically, null. On the other hand, for branes regarded as the intersection between the defects generated by ϕ , such that $\phi_{,v} = 0$, and by ζ , such that $\zeta_{,u} = 0$, which are achieved through an appropriate choice of coordinates, u and v , one can follow the strong supposition that the warp factor A and the functions f and h will all be separable functions of u and v [1], i.e. they satisfy Eq. (2.47).

As implicitly mentioned, from the metric Eq. (2.57), one can realize that the exchange of coordinates $u \leftrightarrow v$ (as well as $f \leftrightarrow h$), does not modify the space-time, which is just re-labeled in terms of $u \leftrightarrow v$. This means that a model with $p = p_1$ is equivalent to a model with $p = 1 - p_1$, which can be mathematically expressed in terms of the equivalence relation, $\forall p \in \mathbb{R} : p \sim 1 - p$, i.e. for any p value there is an equivalent model with p replaced by $1 - p$ [1]. Thus, the algorithm for solving the equations of motion can be constrained by choosing, for instance,

$$p \in \mathbb{R}/\sim = \{p \in \mathbb{R} \mid p \geq 1/2\},$$

such that the equations to be solved, (2.41)-(2.43), can be resumed by

$$\begin{aligned} \frac{\mathcal{V}}{8M^4} = & e^{2p\hat{A}} e^{2\tilde{f}} \left[(p-5) \tilde{A}_{,u}^2 + \tilde{f}_{,u} \tilde{A}_{,u} + \tilde{A}_{,uu} \right] \\ & + e^{2\hat{h}} e^{2(1-p)\tilde{A}} \left[\hat{h}_{,v} \hat{A}_{,v} - (p+4) \hat{A}_{,v}^2 + \hat{A}_{,vv} \right] + \Lambda e^{2\tilde{A}} e^{2\hat{A}}, \end{aligned} \quad (2.58)$$

$$\begin{aligned} \frac{e^{2(p-1)\tilde{A}} e^{2\tilde{f}} \phi_{,u}^2}{4M^4} = & e^{2(p-1)\tilde{A}} e^{2\tilde{f}} \left[p(1-p) \tilde{A}_{,u}^2 + (4-p) \tilde{f}_{,u} \tilde{A}_{,u} + (4-p) \tilde{A}_{,uu} \right] - \Lambda e^{2p\tilde{A}} e^{2(1-p)\hat{A}} \\ & + e^{-2p\hat{A}} e^{2\hat{h}} \left[(4-3p-p^2) \hat{A}_{,v}^2 + (p-1) \hat{h}_{,v} \hat{A}_{,v} + (p-1) \hat{A}_{,vv} \right], \end{aligned} \quad (2.59)$$

and

$$\begin{aligned} \frac{e^{-2p\hat{A}}e^{2\hat{h}}}{4M^4}\zeta_{,v}^2 = & e^{-2(1-p)\tilde{A}}e^{2\tilde{f}} \left[p(5-p)\tilde{A}_{,u}^2 - p\tilde{f}_{,u}\tilde{A}_{,u} - p\tilde{A}_{,uu} \right] - \Lambda e^{2p\tilde{A}}e^{2(1-p)\hat{A}} \\ & + e^{-2p\hat{A}}e^{2\hat{h}} \left[p(1-p)\hat{A}_{,v}^2 + (3+p)\hat{h}_{,v}\hat{A}_{,v} + (3+p)\hat{A}_{,vv} \right]. \end{aligned} \quad (2.60)$$

Notice that Eq. (2.58) just defines the potential as a function of u and v [1]. Unless one imposes to the potential \mathcal{V} its analytical dependence on ϕ and/or ζ , which would suppress some degrees of freedom from Eqs. (2.59) and (2.60), Eq. (2.58) is redundant to the solutions from Eqs. (2.59) and (2.60) when they are used to obtain \mathcal{V} . Otherwise, the analytical solutions for Eqs. (2.59) and (2.60) can be obtained under the following constraints [1].

1. When $\Lambda = 0$, thus the brane is flat;
2. When $\Lambda \neq 0$, but $p = 0$ (or $p = 1$).

This happens because the term with the cosmological constant will necessarily contribute to a function that depends on both variables, unless $p = 0$ (or $p = 1$) or the brane is flat ($\Lambda = 0$).

2.4.1 The Flat Brane Case ($\Lambda = 0$)

After applying the separation of variables technique, Eqs. (2.59) and (2.60) are written as

$$(4+p)\hat{A}_{,v}^2 - \hat{h}_{,v}\hat{A}_{,v} - \hat{A}_{,vv} = \frac{C_1}{1-p}e^{2p\hat{A}}e^{-2\hat{h}}, \quad (2.61)$$

$$\frac{\phi_{,u}^2}{4M^4} - (4-p)\tilde{f}_{,u}\tilde{A}_{,u} - p(1-p)\tilde{A}_{,u}^2 - (4-p)\tilde{A}_{,uu} = C_1e^{-2\tilde{f}}e^{2(1-p)\tilde{A}}, \quad (2.62)$$

$$(5-p)\tilde{A}_{,u}^2 - \tilde{f}_{,u}\tilde{A}_{,u} - \tilde{A}_{,uu} = \frac{C_2}{p}e^{-2\tilde{f}}e^{2(1-p)\tilde{A}}, \quad (2.63)$$

and

$$\frac{\zeta_{,v}^2}{4M^4} - (3+p)\hat{h}_{,v}\hat{A}_{,v} - p(1-p)\hat{A}_{,v}^2 - (3+p)\hat{A}_{,vv} = C_2e^{-2p\hat{A}}e^{2\hat{h}}, \quad (2.64)$$

where $C_i \in \mathbb{R}$, $i \in \{1, 2\}$, are the separation constants. To find solutions of Eqs. (2.61)-(2.64) one needs to separate the $p = 0$ (or $p = 1$) case from the $p \neq 0$ (or $p \neq 1$).

2.4.1.1 The $p \neq 0$ (or $p \neq 1$) Case (Models I and II)

Essentially, the above introduced sequence of steps for preparing the equations of motion to be solved corresponds to some kind of suppression of unnecessary degrees of freedom [1]. Looking at Eqs. (2.61)-(2.64), the coordinate freedom are represented by \hat{h}

and \tilde{f} . Again, the coordinate constraints, $\hat{h} = p\hat{A}$ and $\tilde{f} = (1-p)\tilde{A}$, are chosen in order to simplify the equation manipulability. With the metric in the form of

$$\mathbf{g} = e^{-2\tilde{A}}e^{-2\hat{A}}\eta_{\mu\nu}dx^\mu \otimes dx^\nu + e^{-2(1-p)\tilde{A}}e^{-2p\hat{A}}(du \otimes du + dv \otimes dv) \quad (2.65)$$

corresponds to the singular configuration for which a conformally flat approach simplifies the equation resolutions. From Eqs. (2.61) and (2.63), the solutions obtained are expressed by

$$\hat{A} = \hat{A}_0 - \frac{1}{4} \ln \left\{ \cosh \left[2c_v(v + v_0) \right] \right\}, \quad (2.66)$$

and

$$\tilde{A} = \tilde{A}_0 - \frac{1}{4} \ln \left\{ \cosh \left[2c_u(u + u_0) \right] \right\}, \quad (2.67)$$

where, without loss of generality, one set the boundary conditions as given by $\hat{A}_0 = \tilde{A}_0 = 0$, with

$$c_v^2 = -\frac{C_1}{p-1} \text{ and } c_u^2 = \frac{C_2}{p}, \quad (2.68)$$

where $c_v, c_u \in \mathbb{C}$, but either $Im(c_i) = 0$ or $Re(c_i) = 0$, since C_1, C_2 and p are real constants.

To develop models which can “localize” fields on the brane, one may break this solution into two different configurations, one for $p > 2$ and $Im(c_u) = 0$, and another for $p \leq 2$ and $Re(c_u) = 0$. They correspond to the models that shall be further explored in appendix A.

Starting with $p > 2$ ($Im(c_u) = 0$), which is now labeled model *I*, one finds the metric ($u_0 = v_0 = 0$),

$$\mathbf{g}^I = \sqrt{\cosh(2c_u u) \left| \cos\left(\frac{n\varphi}{2}\right) \right|} \eta_{\mu\nu} dx^\mu \otimes dx^\nu + \sqrt{\frac{\left| \cos\left(\frac{n\varphi}{2}\right) \right|^p}{\cosh^{p-1}(2c_u u)}} (du \otimes du + r^2 d\varphi \otimes d\varphi). \quad (2.69)$$

Scalar fields and potential are resumed by

$$\mathcal{V}^I = -8M^4 \operatorname{sech}^{(1-p)/2}(2c_u u) \operatorname{sec}^{p/2}\left(\frac{n\varphi}{2}\right) \left(c_u^2 - \frac{n^2}{16r^2}\right), \quad (2.70)$$

$$\phi^I = \pm 2M^2 \sqrt{a_\phi} \left\{ u \sqrt{1+b_\phi} - \frac{\sqrt{b_\phi}}{2c_u} \operatorname{arcsinh} \left[\sqrt{b_\phi} \tanh(2c_u u) \right] - \frac{\sqrt{1+b_\phi}}{4c_u} \ln \left[\frac{\sqrt{1+b_\phi} \sqrt{1+b_\phi \tanh^2(2c_u u)} + 1 - b_\phi \tanh(2c_u u)}{\sqrt{1+b_\phi} \sqrt{1+b_\phi \tanh^2(2c_u u)} + 1 + b_\phi \tanh(2c_u u)} \right] \right\}, \quad (2.71)$$

and

$$\zeta^I = \pm M^2 \cos\left(\frac{n\varphi}{2}\right) \frac{4r\sqrt{2a_\zeta}\sqrt{1-b_\zeta \tan^2\left(\frac{n\varphi}{2}\right)}}{n\sqrt{1-b_\zeta+(1+b_\zeta)\cos(n\varphi)}} \left\{ \sqrt{1+b_\zeta} \arcsin\left[\sqrt{1+b_\zeta}\sin\left(\frac{n\varphi}{2}\right)\right] + \sqrt{-b_\zeta} \operatorname{arctanh}\left[\frac{\sqrt{2}\sqrt{-b_\zeta}\sin\left(\frac{n\varphi}{2}\right)}{\sqrt{(b_\zeta+1)\cos(n\varphi)-b_\zeta+1}}\right] \right\}, \quad (2.72)$$

where the following constants have been defined,

$$a_\phi = -(1-p)\frac{n^2}{16r^2} + (p-4)c_u^2, \quad b_\phi = \frac{(5-2p)c_u^2}{a_\phi}, \quad (2.73)$$

$$a_\zeta = pc_u^2 + (3+p)\frac{n^2}{16r^2} \quad \text{and} \quad b_\zeta = -\frac{(3+2p)n^2}{16r^2a_\zeta}, \quad (2.74)$$

through which the constraints $a_\phi \geq 0$, $b_\phi \geq -1$, $a_\zeta \geq 0$ and $b_\zeta \leq 0$ are sufficient and necessary conditions for obtaining real scalar fields, ϕ and ζ (cf. Eqs. (2.71) and (2.72)).

Besides the singularities exhibited by the scalar field ζ^I , the behavior of the variable u suggests that an infinite amount of energy to achieve model I configuration is required (see appendix A) [1]. The Planck scale for model I is

$$M_{pl}^{I^2} = \frac{M^4 r \pi \Gamma\left(\frac{p+3}{4}\right) \Gamma\left(\frac{p-2}{4}\right)}{c_u \Gamma\left(\frac{p+5}{4}\right) \Gamma\left(\frac{p}{4}\right)}, \quad (2.75)$$

and model I presents the structure capable of localizing the gravitational field.

To avoid such a shortcoming, the model II , with $p \leq 4$ and $Re(c_u) = 0$, can be introduced. In this case, the metric can be stated as ($u_0 = v_0 = 0$),

$$g^{II} = \sqrt{\left|\cos\left(\frac{l\theta}{2}\right)\cos\left(\frac{n\varphi}{2}\right)\right|} \eta_{\mu\nu} dx^\mu \otimes dx^\nu + \sqrt{\frac{|\cos\left(\frac{n\varphi}{2}\right)|^p}{|\cos\left(\frac{l\theta}{2}\right)|^{p-1}}} (\rho^2 d\theta \otimes d\theta + r^2 d\varphi \otimes d\varphi). \quad (2.76)$$

The Planck scale associated with metric Eq. (2.76) will be singular if $p \geq 4$, as can be seen in Sec. 2.2. The scalar fields and potential for such a configuration are as follows,

$$\mathcal{V}^{II} = M^4 \sec^{(1-p)/2}\left(\frac{l\theta}{2}\right) \sec^{p/2}\left(\frac{n\varphi}{2}\right) \left(\frac{l^2}{2\rho^2} + \frac{n^2}{2r^2}\right), \quad (2.77)$$

$$\phi^{II} = \pm M^2 \cos\left(\frac{l\theta}{2}\right) \frac{4\rho\sqrt{2a_\phi}\sqrt{1-b_\phi \tan^2\left(\frac{l\theta}{2}\right)}}{l\sqrt{1-b_\phi+(1+b_\phi)\cos(l\theta)}} \left\{ \sqrt{1+b_\phi} \arcsin\left[\sqrt{1+b_\phi}\sin\left(\frac{l\theta}{2}\right)\right] + \sqrt{-b_\phi} \operatorname{arctanh}\left[\frac{\sqrt{2}\sqrt{-b_\phi}\sin\left(\frac{l\theta}{2}\right)}{\sqrt{(b_\phi+1)\cos(l\theta)-b_\phi+1}}\right] \right\}, \quad (2.78)$$

and

$$\zeta^{II} = \pm M^2 \cos\left(\frac{n\varphi}{2}\right) \frac{4r\sqrt{2a_\zeta}\sqrt{1-b_\zeta \tan^2\left(\frac{n\varphi}{2}\right)}}{n\sqrt{1-b_\zeta+(1+b_\zeta)\cos(n\varphi)}} \left\{ \sqrt{1+b_\zeta} \arcsin\left[\sqrt{1+b_\zeta}\sin\left(\frac{n\varphi}{2}\right)\right] + \sqrt{-b_\zeta} \operatorname{arctanh}\left[\frac{\sqrt{2}\sqrt{-b_\zeta}\sin\left(\frac{n\varphi}{2}\right)}{\sqrt{(b_\zeta+1)\cos(n\varphi)-b_\zeta+1}}\right] \right\}, \quad (2.79)$$

where one identifies the following constants,

$$a_\phi = -(1-p)\frac{n^2}{16r^2} - (p-4)\frac{l^2}{16\rho^2}, \quad b_\phi = -\frac{(5-2p)l^2}{16\rho^2 a_\phi}, \quad (2.80)$$

$$a_\zeta = -p\frac{l^2}{16\rho^2} + (3+p)\frac{n^2}{16r^2} \quad \text{and} \quad b_\zeta = -\frac{(3+2p)n^2}{16r^2 a_\zeta}. \quad (2.81)$$

In this case, $a_\phi \geq 0$, $b_\phi \leq 0$, $a_\zeta \geq 0$ and $b_\zeta \leq 0$ are the sufficient and necessary conditions for assuring real scalar fields. The Planck scale for model *II* is

$$M_{pl}^{II^2} = 4M^4 \rho r \pi \frac{\Gamma\left(\frac{3+p}{4}\right)\Gamma\left(\frac{4-p}{4}\right)}{\Gamma\left(\frac{5+p}{4}\right)\Gamma\left(\frac{6-p}{4}\right)}, \quad (2.82)$$

and model *II* presents the structure capable of localizing the gravitational field.

The scalar fields exhibit several singularities, depending on the values for n and l . These singularities explains the number of cusps in the warp factor. In order to realize physically consistent solutions, the required energy to achieve their internal structure must be finite [1]. Even though model *II* exhibits several singularities as depicted by the scalar fields, the total energy necessary to accomplish model *II* is finite (see appendix A). This is an evinced advantage with respect to the model *I* [1]. Although model *II* has finite total energy, one may still argue against its physical significance, due to its recurrent singularities, a shortcoming that must be considered in the following model issues [1].

2.4.1.2 The $p = 0$ (or $p = 1$) Case (Model *III*)

The third option of analytical models with flat branes, with two scalar fields and $p = 0$, starts from setting $\hat{f} = 0$ and $\tilde{h} = \tilde{A}$, which leads to the subsequent metric,

$$\mathbf{g} = e^{-2\hat{A}} e^{-2\tilde{A}} \omega_{\mu\nu} dx^\mu \otimes dx^\nu + e^{-2\tilde{f}} du \otimes du + e^{-2\hat{h}} e^{-2\tilde{A}} dv \otimes dv. \quad (2.83)$$

Again, from Eqs. (2.58)-(2.60), after separation of variables and some straightforward manipulations, one finds the following system of equations,

$$\frac{\mathcal{V}}{8M^4} = e^{2\tilde{f}} \left(-5\tilde{A}_{,u}^2 + \tilde{f}_{,u}\tilde{A}_{,u} + \tilde{A}_{,uu} \right) + C e^{2\tilde{A}}, \quad (2.84)$$

$$\frac{\phi_{,u}^2}{4M^4} = 4\tilde{f}_{,u}\tilde{A}_{,u} + 4\tilde{A}_{,uu} - C e^{2\tilde{A}} e^{-2\tilde{f}}, \quad (2.85)$$

$$C = -e^{2\hat{h}} \left(4\hat{A}_{,v}^2 - \hat{A}_{,v}\hat{h}_{,v} - \hat{A}_{,vv} \right), \quad (2.86)$$

and

$$\frac{\zeta_{,v}^2}{4M^4} = 3\hat{h}_{,v}\hat{A}_{,v} + 3\hat{A}_{,vv}, \quad (2.87)$$

where $C \in \mathbb{R}$ is some separation constant. Here one can interpret Eqs. (2.84) and (2.85) as defining the potential and the scalar field ϕ , respectively, and one can actually solve Eqs. (2.86) and (2.87). By choosing $\hat{h} = 0$ straightforwardly implies into the solution

$$\hat{A}^{III} = \hat{A}_0 - \frac{1}{4} \ln \left| \cos \left[2\sqrt{C} (v + v_0) \right] \right|, \quad (2.88)$$

and

$$\zeta^{III} = \pm 2\sqrt{3}M^2 \operatorname{arctanh} \left\{ \sin \left[2\sqrt{C} (v + v_0) \right] \right\}, \quad (2.89)$$

which, from now on, shall be called model *III* and for which, without loss of generality, one can set $\hat{A}_0 = 0$ and $v_0 = 0$ [1].

Given the periodicity of \hat{A}^{III} , one departs from the choice of $v = r\varphi$, where $\varphi \in \mathbb{S}^1$ and r is the radius of \mathbb{S}^1 . Since the metric must be continuous in \mathbb{S}^1 one must have that $e^{-2\hat{A}}$ must also be continuous in \mathbb{S}^1 , which means that

$$\left| \cos \left(2\sqrt{C}r2\pi \right) \right| = |\cos(0)| = 1 \implies C = \frac{n^2}{16r^2}, \quad n \in \mathbb{N}.$$

Therefore one may write the metric, with $\hat{A}_0 = 0$ and $v_0 = 0$, as

$$\mathbf{g}^{III} = \sqrt{\left| \cos \left(\frac{n\varphi}{2} \right) \right|} e^{-2\hat{A}} \eta_{\mu\nu} dx^\mu \otimes dx^\nu + e^{-2\tilde{f}} du \otimes du + r^2 e^{-2\hat{A}} d\varphi \otimes d\varphi, \quad (2.90)$$

which expresses a setup with a Minkowski brane ($\Lambda = 0$) with two scalar fields [1]. Both the scalar field ζ^{III} and warp factor \hat{A}^{III} are, up to some constant, equivalent in form to those ones from model *I*, as depicted in Figs. 31a and 32b. Considering the possible values of n , only $n = 1$ configuration does not require the modulus in $\sqrt{\left| \cos(n\varphi/2) \right|}$, since $\cos(\varphi/2)$ is strictly positive in this region [1]. The Planck scale for model *III* is

$$M_{pl}^{III^2} = 2\sqrt{\pi}M^4 r \frac{\Gamma\left(\frac{3}{4}\right)}{\Gamma\left(\frac{5}{4}\right)} \int du e^{-\tilde{f}} e^{-3\hat{A}}, \quad (2.91)$$

and model *III* presents the structure capable of localizing the gravitational field.

In this case, one may be tempted to interpret each of the cusps of the warp factor as forming different branes [1]. However, since the unique localizing parameter in this model is the radius r of \mathbb{S}^1 , it is better to interpret such a configuration as a single brane with some internal structure as the same is true for models *I* and *II* [1].

In this case, before evaluating metric g^{III} , scalar field ϕ and potential configurations, one should turn the attention to the associated stress energy tensor [1]. For $p = 0$ models, from Eqs. (2.84) and (2.85), the total stress energy tensor can be separated as follows,

$$T_{MN} = T_{MN}^{\zeta} + T_{MN}^{\phi}, \quad (2.92)$$

$$T_{MN}^{\zeta} = \zeta_{,M}\zeta_{,N} - g_{MN} \frac{\zeta^{,K}\zeta_{,K}}{2}, \quad (2.93)$$

and

$$T_{MN}^{\phi} = \phi_{,M}\phi_{,N} - g_{MN} \left(\frac{\phi^{,K}\phi_{,K}}{2} + \mathcal{V} \right). \quad (2.94)$$

which allows one to focus on the stress energy tensor driven by the scalar field ζ (2.93),

$$T_{\mu\nu}^{\zeta^{III}} = -\frac{3M^4 n^2 \eta_{\mu\nu}}{2r^2} \left| \sec\left(\frac{n\varphi}{2}\right) \right|^{3/2}. \quad (2.95)$$

which is depicted Fig. 2. Of course, Fig. 2 evinces that the $T_{\mu\nu}^{\zeta^{III}}$ singularities shall support a

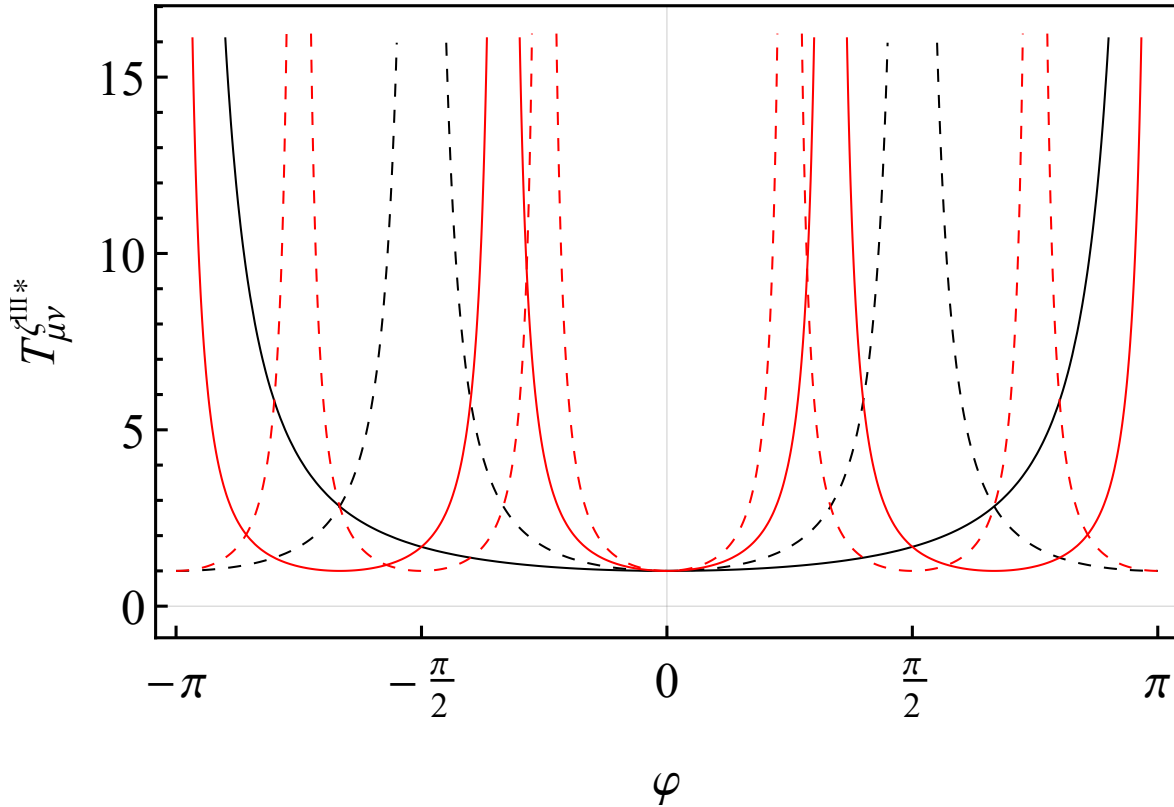


Figure 2 – Stress energy tensor $T_{\mu\nu}^{\zeta^{III}*} = -r^2 T_{\mu\nu}^{\zeta^{III}} / 3M^4 n^2 \eta_{\mu\nu}$ as a function of φ , for $n = 1$ (black line), $n = 2$ (black dashed line), $n = 3$ (red line) and $n = 4$ (red dashed line).

number of cusps in the warp factor. From the perspective of the bulk, the energy necessary to achieve such a configuration can be computed in terms of

$$E_{\mu\nu}^{\zeta^{III}} = \int_{\mathbb{E}^6} T_{\mu\nu}^{\zeta^{III}} \sqrt{-g} d^6x \propto \int_{-\pi}^{\pi} \left| \sec\left(\frac{n\varphi}{2}\right) \right|^{1/2} d\varphi,$$

where the last integral converges for all values of n [1]. Therefore, the energy of these models, as far as ζ is concerned, is finite. Although the energy needed for this configuration is finite, one may still argue against the physical significance of this model, due to the number of singularities in the stress energy tensor [1].

To complete the model one now only lacks the dependence of the warp factor to the u coordinate related to \tilde{A} , to the scalar field ϕ , as well as to the potential \mathcal{V} [1]. For model *III* these fields must satisfy Eqs. (2.84) and (2.85). Notice here that while \mathcal{V} , ϕ and \tilde{A} are still undetermined, \tilde{f} is a mere choice of coordinates. Therefore one has complete freedom for choosing one of such fields, as long as further analytical integration is allowed for the other two fields. This means that a multitude of solutions can be found as to fit such a building procedure. As will be presented later a similar set of equations for \tilde{A} , ϕ and \mathcal{V} will be found for different solutions of \hat{A} and ζ , this is to be expected since the equations are separated in the variables u and v . Later a couple of examples will be proposed, all of which start by assuming \tilde{A} . This is simply to achieve an intended geometry for $(\mathbb{B}^2, \boldsymbol{\sigma})$, which shall lead to a common solution set for \tilde{A} , ϕ and \mathcal{V} for all the models with $p = 0$ [1].

To resume, model *III* also contains a trivial extension of well known models of $(4 + 1)$ -dimensional braneworlds. Looking at Eqs. (2.84) and (2.85), one should notice that, for $\tilde{f} = n = 0$ (which is nothing but a choice of coordinates and $C = 0$), exactly the same equations, up to some constants, are obtained from such a five-dimensional case [15, 16, 17, 18, 19, 20, 21, 22, 23, 24, 25, 26, 27, 28]. These models contain, which is nothing surprising, trivial extensions of the five-dimensional braneworld models so deeply considered in the previously quoted works. One may call it trivial because the metric takes the form,

$$\mathbf{g} = e^{-2\tilde{A}} \left(\eta_{\mu\nu} dx^\mu \otimes dx^\nu + r^2 d\varphi \otimes d\varphi \right) + du \otimes du, \quad (2.96)$$

which is nothing but the same metric of five-dimensional setup with an additional co-dimensional compactified structure as \mathbb{S}^1 , and with the defect generated by the scalar field ϕ and potential \mathcal{V} ($\zeta = 0$) [1].

2.4.2 The Bent Brane Case ($p = 0$, $\Lambda \neq 0$)

Considering the bent brane case, Eqs. (2.58)-(2.60) with $\Lambda \neq 0$ and $p = 0$, no preliminary assumption about the curvature of \mathbb{M}^4 (i.e. about $\Lambda \neq 0$) is required [1]. Departing from the metric Eq. (2.83), and after some straightforward manipulations involving Eqs. (2.58)-(2.60) (for $p = 0$), they can be cast in the form of

$$C = \Lambda e^{2\hat{A}} - e^{2\hat{h}} \left(4\hat{A}_{,v}^2 - \hat{A}_{,v}\hat{h}_{,v} - \hat{A}_{,vv} \right), \quad (2.97)$$

and

$$\frac{\zeta_{,v}^2}{4M^4} = 3\hat{h}_{,v}\hat{A}_{,v} + 3\hat{A}_{,vv} - \Lambda e^{2\hat{A}} e^{-2\hat{h}}, \quad (2.98)$$

where $C \in \mathbb{R}$ is the separation constant. Again, the expressions defining the potential \mathcal{V} and the scalar field ϕ are given by Eqs. (2.84) and (2.85), which correspond to the flat brane model with $p = 0$. To solve Eq. (2.97), one can set: *i*) either $\zeta_{,v} = 0$ ($\zeta = 0$); *ii*) or $C = 0$, but $\zeta_{,v} \neq 0$ [1].

It means that only when two scalar fields are present and the brane is not flat that some additional supposition ($C = 0$) about the solution must be made, in all other cases one can generally solve these equations [1]. The last possible construction, i.e. $C \neq 0$ and $\zeta_{,v} \neq 0$, leads to a highly enhanced equation that is not of straightforward analytical solution. Regardless, an implicit method can be applied to generally solve the equations, but the solutions will not be of straightforward interpretation.

In particular, the first case, with $\zeta = 0$, is the most interesting one [1]. It corresponds to a model with a single scalar field which drives a smooth behavior with no singularities in the stress energy tensor, which are ingrained in the other configurations (*I*, *II* and *III*) [1].

2.4.2.1 The Single Scalar Field Case (Model *IV*)

Starting from the constraint imposed by $\zeta = 0$, model *IV* is resumed by the behavior of a single scalar field [1]. To solve Eqs. (2.97) and (2.98) one can set $\hat{h} = 0$ in order to obtain some simplifications. Thus, combining Eqs. (2.97) and (2.98), one can write

$$\frac{\Lambda}{3} e^{2\hat{A}} - \hat{A}_{,v}^2 = \frac{C}{4} \iff \int \frac{d\hat{A}}{\sqrt{\frac{\Lambda}{3} e^{2\hat{A}} - \frac{C}{4}}} = \pm (v + v_0), \quad (2.99)$$

which exhibits three different solution which depends on the values of Λ and C , i.e.

$$\hat{A} = \ln \left(\frac{\sqrt{3}}{\sqrt{\Lambda} |v + v_0|} \right), \text{ if } C = 0 \text{ and } \Lambda > 0, \quad (2.100)$$

$$\hat{A} = -\ln \left\{ 2\sqrt{\frac{|\Lambda|}{3|C|}} \cosh \left[\frac{\sqrt{|C|}}{2} (v + v_0) \right] \right\}, \text{ if } C, \Lambda < 0, \quad (2.101)$$

and

$$\hat{A}^{IV} = -\ln \left\{ 2\sqrt{\frac{\Lambda}{3C}} \left| \cos \left[\frac{\sqrt{C}}{2} (v + v_0) \right] \right| \right\}, \text{ if } C, \Lambda > 0, \quad (2.102)$$

which are all consistent with Eqs. (2.97) and (2.98) [1].

Clearly, the solutions from (2.100) and (2.101) do not depict RS-like features: gravity is not localized along the corresponding extra dimension, unless one could force v to be periodic [1]. Nevertheless, the warp factors (2.100) and (2.101) are not periodic and no thin brane can supply the required boundary conditions. Gravity can be localized only by setting $C = \Lambda = 0$, which leads to constraining $\hat{A}(v) = \hat{A}_0$ ($\hat{A}_0 \in \mathbb{R}$), and by supposing

$v = r\varphi$, with $\varphi \in \mathbb{S}^1$. In this case, one has the same trivial case from Eq. (2.96), which corresponds to a trivial extension of five-dimensional braneworlds [1].

On the other hand, looking at solution (2.102), which is periodic, i.e. with $v = r\varphi$, where $\varphi \in \mathbb{S}^1$, one does find more appealing localization features, which emerge from its compact characteristic [1]. Since one expects the metric to be continuous, then the warp factor $e^{-2\tilde{A}}$ shall also be periodic and continuous in \mathbb{S}^1 , i.e. (for $v_0 = 0$),

$$\cos^2\left(\frac{\sqrt{C}}{2}r2\pi\right) = \cos^2(0) = 1 \implies C = \frac{n^2}{r^2}, n \in \mathbb{N}^+, \quad (2.103)$$

where one should notice that $n \neq 0$, since the warp factor is ill defined for $n = 0$ [1].

Since the peculiarities related to the solutions from Eqs. (2.100) and (2.101) have already been discussed, one should pay more attention to the solution from Eq. (2.102) [1].

In this case, the related metric, with $v_0 = 0$, is written as

$$\mathbf{g}^{IV} = \frac{4r^2\Lambda}{3n^2} \cos^2\left(\frac{n\varphi}{2}\right) e^{-2\tilde{A}} \omega_{\mu\nu}^+ dx^\mu \otimes dx^\nu + e^{-2\tilde{f}} du \otimes du + r^2 e^{-2\tilde{A}} d\varphi \otimes d\varphi, \quad (2.104)$$

which corresponds to the most appealing solutions once some physical conditions are imposed [1]. In particular, it only works either for a de Sitter brane ($\Lambda > 0$) or, at least, for a space with positive constant curvature. Clearly, since no scalar field ζ is effective, the energy to achieve such a configuration is finite. Fig. 3 depicts the form of the warp factor $e^{-2\tilde{A}^{IV}}$, which explains why this model should be more relevant than models *I*, *II* and *III*: there are no cusps in the warp factor. This corresponds to a straightforward consequence of no singularities in the stress energy tensor [1]. The Planck scale for model *IV* is

$$M_{pl}^{IV^2} = M^4 \frac{4r^3\Lambda}{3n^2} \pi \int du e^{-\tilde{f}} e^{-3\tilde{A}}, \quad (2.105)$$

and model *IV* presents the structure capable of localizing the gravitational field.

Even with singularities eliminated from the stress energy tensor, this model still exhibits curvature singularities. Whenever $\cos^2(n\varphi/2) = 0$ the warp factor is null and the metric would have vanishing components. This could be an effect of a badly defined choice of coordinates, and represent some form of horizon [1]. In this context, the Kretschmann scalar for model *IV* reads,

$$\begin{aligned} K &= R^{MNPQ} R_{MNPQ} \\ &= e^{4\tilde{A}} \left\{ \frac{3n^2}{r^2} \sec^2\left(\frac{n\varphi}{2}\right) \left[\frac{n^2}{r^2} \tan^2\left(\frac{n\varphi}{2}\right) + 4\tilde{A}_{,u}^2 \right] + \frac{5n^4}{2r^4} \right. \\ &\quad \left. + e^{-4\tilde{A}} \mathfrak{K}(u) + 16\tilde{A}_{,uu}^2 + 40\tilde{A}_{,u}^4 - \tilde{A}_{,u}^2 \right\}, \quad (2.107) \end{aligned}$$

which results into curvature singularities, since this scalar invariant is singular whenever $\cos^2(n\varphi/2) = 0$ [1].

Another interesting property of model *IV* is the constant $4\Lambda/3C$ that multiplies the warp factor. This constant can not be removed from the warp factor, otherwise it will not be a solution of Eqs. (2.97) and (2.98). Yet if one increases the value of C , the warp factor becomes not only more localized, but also exhibits a decreasing amplitude [1]. In fact, one could expect the maximum value of the warp factor to be one, thus one could impose $4\Lambda/3C = 1$. For Λ assuming tiny values, one should have tiny values for C . Therefore, the warp factor would not be exceptionally localized. Here, no concerns to such relation between C and Λ will be made, then C will be regarded as a completely independent value [1].

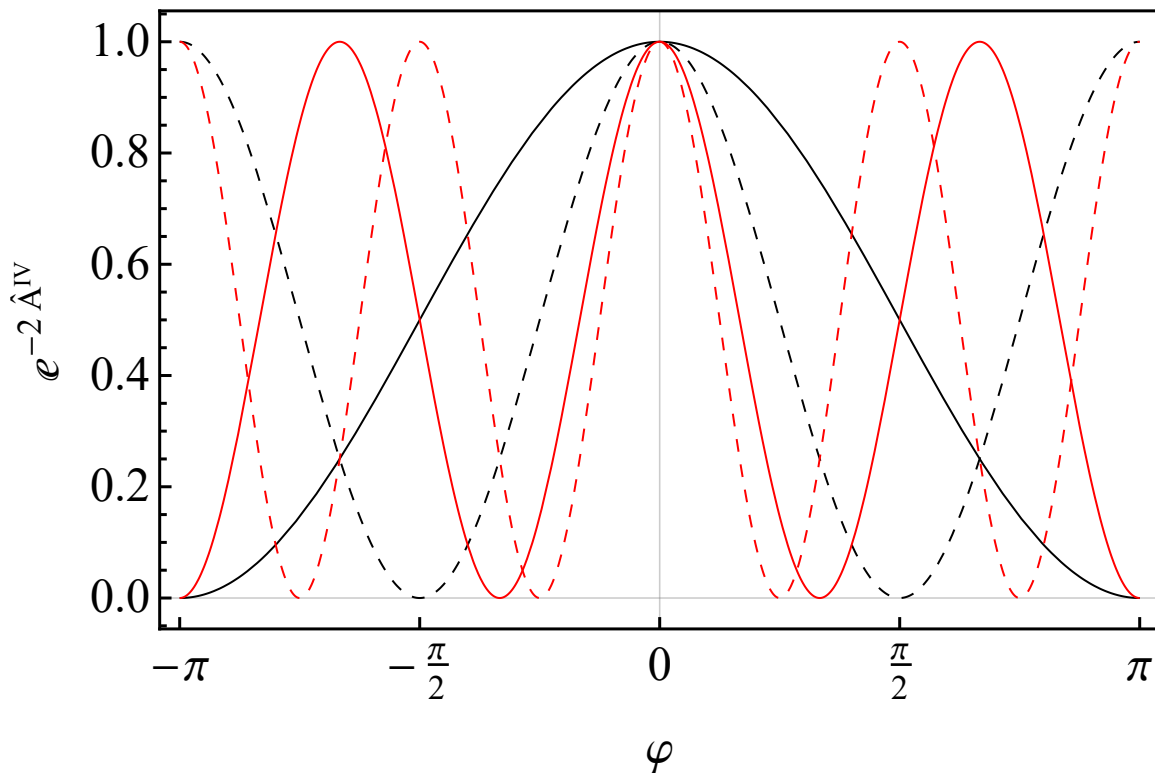


Figure 3 – Warp factor $e^{-2\hat{A}^{IV}}$ of model *IV* as a function of φ , for $n = 1$ (black line), $n = 2$ (black dashed line), $n = 3$ (red line) and $n = 4$ (red dashed line).

One again only lacks the dependence of the warp factor on the u coordinate related to \tilde{A} , to the scalar field ϕ , as well as to the potential \mathcal{V} . In this case, the involved fields must satisfy Eqs. (2.84) and (2.85), with $C = n^2/r^2$ for model *IV*. Therefore, the dependence of these quantities on u is equivalent to that obtained for the flat brane model *III*, with metric (2.76), and with the distinction being only due to the value of C : for model *III*, the constant $C = n^2/16r^2$, $n \in \mathbb{N}$, while for model *IV*, the constant $C = n^2/r^2$, $n \in \mathbb{N}^+$. Eqs. (2.84) and (2.85) will be solved in a redundant way, for models *III*, *IV* and *V* in section 2.4.3.

2.4.2.2 The $C=0$ Case (Model V)

So far one has built models over a flat and de Sitter branes, the whole spectrum of possible values of Λ can be filled by anti-de Sitter brane solutions [1].

To realize analytical solutions of Eq. (2.97) when two scalar fields are present and the brane is bent, i.e. the space-time curvature of \mathbb{M}^4 is non null, one must constrain C to 0. Other values of C do not allow strict analytical calculations [1]. A simplified scenario is accomplished by setting $\hat{h} = \hat{A}$ so as to reduce Eqs. (2.97) and (2.98) for the warp factor \hat{A} and ζ , respectively, to the now called model V , for which

$$\hat{A}^V = \hat{A}_0 - \frac{1}{3} \ln \left| \cos \left[\sqrt{3|\Lambda|} (v + v_0) \right] \right|, \quad (2.108)$$

and

$$\zeta^V = \pm \frac{4M^2}{\sqrt{3}} \operatorname{arctanh} \left\{ \sin \left[\sqrt{3|\Lambda|} (v + v_0) \right] \right\}, \quad (2.109)$$

with $\Lambda < 0$. The solution \hat{A} for positive values of Λ does not exhibit RS-like features [1]. Due to the periodicity of \hat{A}^V , one is able to choose $v = r\varphi$, where $\varphi \in \mathbb{S}^1$. Since the metric must be continuous, one must also have $e^{-2\hat{A}}$ continuous in \mathbb{S}^1 , therefore

$$\left[\cos \left(\sqrt{3|\Lambda|} r 2\pi \right) \right]^{2/3} = 1 \implies r = \frac{n}{2\sqrt{3|\Lambda|}}, \quad n \in \mathbb{N}^+, \quad (2.110)$$

where simplified expressions are yielded from choosing $\hat{A}_0 = 0$ and $v_0 = 0$. For such a completely contrasting result, obviously there is no relation between C and the radius r of \mathbb{S}^1 , as well as Λ is a free parameter. In fact, the radius r of \mathbb{S}^1 is constrained by the value of the cosmological constant Λ one chooses for the space-time \mathbb{M}^4 , and the metric is written as

$$\mathbf{g}^V = \cos^{2/3} \left(\frac{n\varphi}{2} \right) e^{-2\tilde{A}} \omega_{\mu\nu}^- dx^\mu \otimes dx^\nu + e^{-2\tilde{f}} du \otimes du + r^2 \cos^{2/3} \left(\frac{n\varphi}{2} \right) e^{-2\tilde{A}} d\varphi \otimes d\varphi, \quad (2.111)$$

which expresses a compactified setup for an anti-de Sitter brane ($\Lambda < 0$) scenario at \mathbb{M}^4 , with constant negative curvature and two scalar fields. In Fig. 4a the form of the warp factor is exhibited for different values of n . The form of the scalar field is exactly the same as the one depicted in Fig. 32b [1]. But the scalar field now depends on the φ coordinate, which is different from that one considered in model I . The Planck scale for model V is

$$M_{pl}^{V2} = 4rM^4 \int du e^{-\tilde{f}} e^{-3\tilde{A}}, \quad (2.112)$$

and model V presents the structure capable of localizing the gravitational field.

Fig. (4b) depicts the stress energy tensor, $T_{\mu\nu}^\zeta$, for the scalar field ζ ,

$$T_{\mu\nu}^{\zeta^V} = -\frac{4M^4 n^2 \omega_{\mu\nu}^-}{3r^2} \sec^2 \left(\frac{n\varphi}{2} \right), \quad (2.113)$$

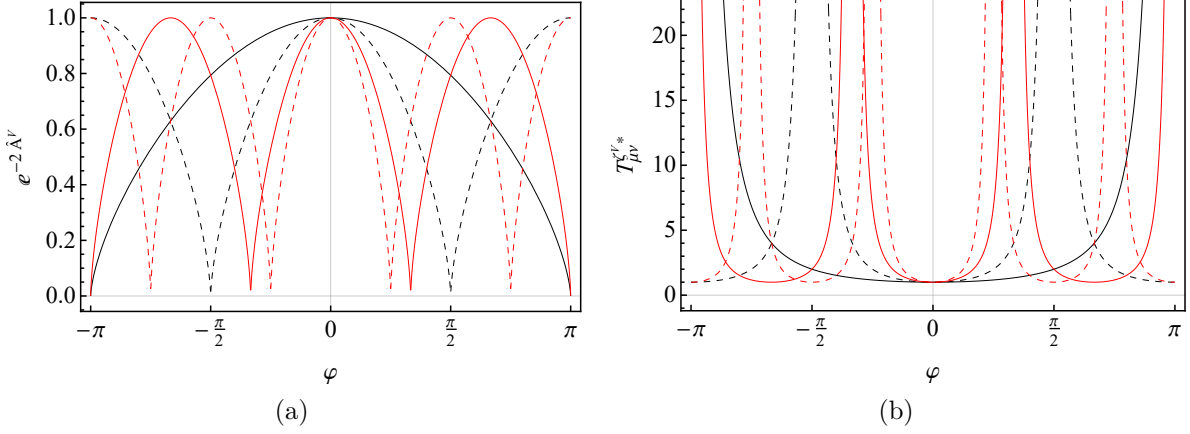


Figure 4 – (a) The warp factor $e^{-2\hat{A}^V}$ of model V_0 as a function of φ . (b) The stress energy tensor $T_{\mu\nu}^{\zeta^*} = -T_{\mu\nu}^{\zeta} 3r^2/4M^4 n^2 \omega_{\mu\nu}^-$ of model V as a function of φ . The plots are for $n = 1$ (solid black line), $n = 2$ (black dashed line), $n = 3$ (solid red line) and $n = 4$ (red dashed line).

which evidently exhibit singularities correlated to the number of cusps exhibited by the warp factor. Again, from the perspective of the bulk, one has the finite formation energy given by

$$E_{\mu\nu}^{\zeta^V} = \int_{\mathbb{E}^6} T_{\mu\nu}^{\zeta^V} \sqrt{-g} d^6x \propto \int_{-\pi}^{\pi} \sec^{1/3} \left(\frac{n\varphi}{2} \right) d\varphi. \quad (2.114)$$

To complete the model, one notices that the fields must satisfy Eqs. (2.84) and (2.85) with $C = 0$, such that

$$\frac{\mathcal{V}}{8M^4} = e^{2\tilde{f}} \left(-5\tilde{A}_{,u}^2 + \tilde{f}_{,u}\tilde{A}_{,u} + \tilde{A}_{,uu} \right), \quad (2.115)$$

and

$$\frac{\phi_{,u}^2}{4M^4} = 4\tilde{f}_{,u}\tilde{A}_{,u} + 4\tilde{A}_{,uu}. \quad (2.116)$$

By choosing coordinates such that $\tilde{f} = 0$, one recovers the same equations, up to some constants, as in the five-dimensional thick braneworlds with a single scalar field. It means that, one more time one has a non-trivial extension of the usual five-dimensional braneworld models, which can be ratified by setting $\tilde{f} = n = 0$ into Eqs. (2.111), (2.108) and (2.109) [1].

2.4.2.3 The General Bent Brane (Model VI)

Eqs. (2.97) and (2.98) can be generally solved by proposing an implicit method; we assume coordinates such that \hat{A} is a linear function and solve Eqs. (2.97) and (2.98) for \hat{h} , instead of \hat{A} . This assumption can be understood by the metric

$$\mathbf{g} = e^{-2\hat{A}} e^{-2\hat{A}} \omega_{\mu\nu} dx^\mu dx^\nu + e^{-2\hat{A}} e^{-2\hat{h}} d\hat{A}^2 + e^{-2\tilde{f}} du^2 \quad (2.117)$$

where coordinates have been chosen such that the coordinate v , in metric (2.57), coincides with \hat{A} . Eqs. (2.97) and (2.98) can then be written as

$$C = \Lambda e^{2\hat{A}} - 4e^{2\hat{h}} + e^{2\hat{h}} \hat{h}_{,\hat{A}}, \quad (2.118)$$

and

$$\frac{\zeta_{,\hat{A}}^2}{4M^4} = 3\hat{h}_{,\hat{A}} - \Lambda e^{2\hat{A}} e^{-2\hat{h}}. \quad (2.119)$$

Eq. (2.118) is integrable and has the solution

$$\hat{h} = \frac{1}{2} \ln \left[C b e^{8\hat{A}} + \frac{\Lambda e^{2\hat{A}}}{3} - \frac{C}{4} \right], \quad (2.120)$$

Therefore, the metric of space-time takes the implicit form

$$\mathbf{g} = e^{-2\hat{A}} e^{-2\tilde{A}} \omega_{\mu\nu} dx^\mu dx^\nu + e^{-2\tilde{A}} \frac{d\hat{A}^2}{C b e^{8\hat{A}} + \frac{\Lambda e^{2\hat{A}}}{3} - \frac{C}{4}} + e^{-2\tilde{f}} du^2, \quad (2.121)$$

which is the analytical solution of Eqs. (2.97) and (2.98), but it is given in an implicit form, since the components of the metric are functions of the warp factor. On the other hand, the scalar field is a solution of

$$\frac{\zeta_{,\hat{A}}^2}{4M^4} = \frac{12b e^{8\hat{A}}}{b e^{8\hat{A}} + \frac{\Lambda e^{2\hat{A}}}{3C} - \frac{1}{4}}, \quad (2.122)$$

which is real valued as long as $b \geq 0$.

It is still possible to evaluate the localization features of metric (2.121), but, ideally, it would be interesting to find the solution for coordinates such that⁵ $\hat{h} = 0$, i.e. are flat with relation to v .

In flat coordinates v , the warp factor \hat{A} is a solution of the equation

$$\frac{d\hat{A}^2}{C b e^{8\hat{A}} + \frac{\Lambda e^{2\hat{A}}}{3} - \frac{C}{4}} = dv^2 \iff \hat{A}_{,v} = \pm \sqrt{C b e^{8\hat{A}} + \frac{\Lambda e^{2\hat{A}}}{3} - \frac{C}{4}}, \quad (2.123)$$

Thus the implicit method has reduced Eq. (2.97), which is a second order non-linear differential equation, to Eq. (2.123), which is a first order non-linear equation. Although some simplification was achieved, Eq. (2.123) is still not integrable, unless $b = 0$, which simply leads to model *IV*⁶. Even if one is not able to solve Eq. (2.123) one can now evaluate the localization properties of this space-time, which was not possible with only Eq. (2.97).

The solutions of Eq. (2.123) can present RS features if and only if they present a finite effective volume. This is generally achieved if the warp factor asymptotes to zero and

⁵ In this coordinates the metric would take the form $\mathbf{g} = e^{-2\hat{A}} e^{-2\tilde{A}} \omega_{\mu\nu} dx^\mu dx^\nu + e^{-2\tilde{A}} dv^2 + e^{-2\tilde{f}} du^2$.

⁶ The same is true when $C = 0$, but, to integrate, coordinates have to be chosen in order to achieve the metric component as $e^{-2\hat{A}} dv^2$.

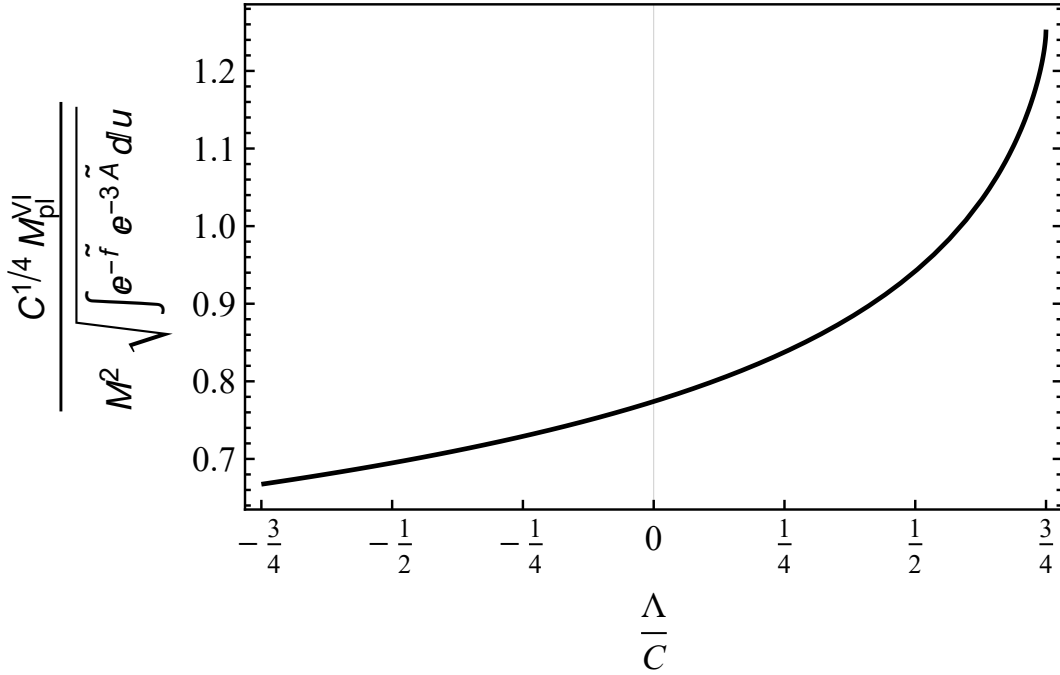


Figure 5 – The Planck scale, $\sqrt[4]{C} M_{\text{pl}}^{\text{VI}} / M^2 \sqrt{\int e^{-\tilde{f}} e^{-3\tilde{A}} du}$, as a function of the cosmological constant, Λ/C .

presents a global maximum. If the global maximum is located at $v = 0$, then a necessary condition for RS features is

$$\hat{A}_{,v}|_{v=0} = 0 \text{ and } \hat{A}|_{v=0} = 0 \iff b = \frac{1}{4} - \frac{\Lambda}{3C} \geq 0, \quad (2.124)$$

which is a necessary condition for localizing gravity and other fields. The Planck scale for model *VI* is

$$M_{\text{pl}}^{\text{VI}2} = M^4 \int_0^\infty \frac{e^{-2\hat{A}} d\hat{A}}{\sqrt{\left(\frac{C}{4} - \frac{\Lambda}{3}\right) e^{8\hat{A}} + \frac{\Lambda}{3} e^{2\hat{A}} - \frac{C}{4}}} \int du e^{-\tilde{f}} e^{-3\tilde{A}}. \quad (2.125)$$

The profile of $M_{\text{pl}}^{\text{VI}2}$ is described as a function of Λ in Fig. 5, from which one can conclude that model *VI* presents the structure capable of localizing the gravitational field.

The equation for the scalar field ζ can also be evaluated in this flat coordinate system,

$$\zeta_{,v} = \pm 2M^2 \sqrt{12Cb} e^{4\hat{A}}, \quad (2.126)$$

which is likely singular at the boundary, since $e^{\hat{A}}$ diverges at $v \rightarrow \infty$. This singular behavior is clearly avoidable if $b = 0$, but the model reduces to model *IV*. Even if the scalar field is divergent, the resulting energy density is well behaved for the entire configuration.

To realize that the effective volume of metric (2.121) is finite, and, therefore, presents RS features, it is simpler to assume a system of coordinates such that

$$\hat{A} = \ln [\cosh (y)], \quad (2.127)$$

which implies in the metric

$$\mathbf{g} = e^{-2\tilde{A}} \left[\text{sech}^2(y) \omega_{\mu\nu} dx^\mu dx^\nu + \frac{\tanh^2(y) dy^2}{\frac{C}{4} [\cosh^8(y) - 1] + \frac{\Lambda}{3} \cosh^2(y) [1 - \cosh^6(y)]} \right] + e^{-2\tilde{f}} du^2. \quad (2.128)$$

It is straightforward to notice that metric (2.128) is well behaved at the center of the configuration and presents a finite effective volume. Yet the curvature will most likely be singular at the boundary, this will not be explored further. On the other hand, the scalar field is then a solution of

$$\frac{\zeta_{,y}^2}{4M^4} = \frac{12b \tanh^2(y)}{b + \frac{\Lambda \text{sech}^6(y)}{3C} - \frac{\text{sech}^8(y)}{4}}. \quad (2.129)$$

Eq. (2.129) is clearly not easy to integrate, but one can find its asymptotic behavior,

$$\frac{\zeta_{,y}}{2M^2} \rightarrow \pm \sqrt{12} \tanh(y) \implies \zeta \rightarrow \pm 2\sqrt{12} M^2 \log[\cosh(y)], \quad (2.130)$$

which necessarily diverges at $y \rightarrow \infty$, therefore singularities at the boundary for the scalar fields are unavoidable in this model. But, as mentioned before, the energy density will be well behaved at the entirety of the configuration.

2.4.3 Setups From Predetermined Internal Spaces

In the previous sections, a first subset of models *I* and *II* for intersecting thick branes was obtained and discussed in terms of the model degenerate dependence on a single co-dimensional coordinate $v \leftrightarrow u$. A second subset, for models *III*, *IV*, *V* and *VI*, which include a split dependence between v and u and admit some additional freedom in the choice of the field parameters \tilde{A} , ϕ , and \mathcal{V} , has also been evaluated [1]. In this section, the hypothesis of constraining such additional degree of freedom by imposing a geometry for (\mathbb{B}^2, σ) shall be considered [1].

As previously argued, Eqs. (2.84) and (2.85) form a common set of equations for all the $p = 0$ models. These two equations involve three field parameters \tilde{A} , ϕ , and \mathcal{V} . Due to the remnant degree of freedom, Eqs. (2.84) and (2.85) can be recast in to a first order configuration (see [81]) to be solved [1]. Given that $p = 0$, one finds that the metric of the internal space \mathbb{B}^2 takes the form of

$$\sigma = e^{-2\tilde{f}} du \otimes du + e^{-2\tilde{A}} e^{-2\hat{h}} dv \otimes dv. \quad (2.131)$$

Thus the choice of \tilde{A} and \tilde{f} fixes the geometry of \mathbb{B}^2 , since \hat{h} is nothing but a choice of coordinates which has been previously specified for each model. That makes choosing the field \tilde{A} a better option than fixing either ϕ or \mathcal{V} , in manner that one can achieve an intended geometry [1]. For this reason, these spaces have a predetermined geometry, since one does not determine it from the field equations, but chooses \tilde{A} and \tilde{f} such that an

expected geometry is achieved. As long as one is able to cast the metric of the internal space as (2.131), the geometrical interpretation that follows is straightforward [1]. The tricky thing here is finding a combination of \tilde{A} and \tilde{f} that allows for the integration at Eq. (2.85). In the following subsections, solutions to these equations will be provided by a choice of the metric of the internal space \mathbb{B}^2 that allows for the respective analytical integration of Eq. (2.85).

In particular, when $\hat{h} = 0$ and the coordinate v is compactified as \mathbb{S}^1 (models *III* and *IV*) one is able to cast the metric (2.131) in a particular fashion so that the internal space could be a sphere or spheroid (subsecs. 2.4.6 and 2.4.7). Since models *III* and *IV* have the same common geometry and topology for the internal space, the solutions that follow are common to both of them [1]. Model *V* can also share these specific solutions for \tilde{A} , ϕ and \mathcal{V} , but the applied geometrical interpretation shall not be valid in the latter cases [1].

2.4.4 Solving Eqs. (2.84) and (2.85)

When one chooses coordinates such that $\tilde{f} = 0$, Eqs. (2.84) and (2.85) are similar in structure to the equations that define five-dimensional bent braneworlds [81, 82, 83], reminded that there are some constraints imposed by the separation constants, Λ and C . Therefore, a departure solution as, for instance, due to Ref. [82],

$$\tilde{A} = -\ln \left| \cos \left[a(u + u_0) \right] \right|, \quad (2.132)$$

can be considered. Notice that one is able to choose $a(u + u_0) = \theta$, with $\theta \in [-\pi/2, \pi/2]$, as long as one allows for the singularities at $\pm\pi/2$ for the scalar field. Thus one is able to consider u to be compactified as \mathbb{S}^1 , just imposing $a = 1/2r$, where r is the radius of \mathbb{S}^1 . It allows one to run θ from $-\pi$ to π . As an example, for the sphere models that follow, one regards $a = 1/r$, $u_0 = -r\pi/2$, and thus $u \in [0, r\pi]$ [1].

From Eqs. (2.84) and (2.85), scalar field, ϕ , and potential, \mathcal{V} , are cast as

$$\phi_\zeta = \pm 2M^2 \sqrt{4 - \frac{C}{a^2}} \operatorname{arctanh} \left\{ \sin \left[a(u + u_0) \right] \right\}, \quad (2.133)$$

and

$$\mathcal{V}_\zeta = 8M^4 a^2 \left\{ 5 - \left(4 - \frac{C}{a^2} \right) \sec^2 \left[a(u + u_0) \right] \right\}. \quad (2.134)$$

which, in this case, allows for an explicit correspondence given by

$$\mathcal{V}_\zeta = 8M^4 a^2 \left\{ 5 - \left(4 - \frac{C}{a^2} \right) \cosh^2 \left[\frac{a\phi}{2M^2 \sqrt{4a^2 - C}} \right] \right\}. \quad (2.135)$$

When $C = 4a^2$ the scalar field ϕ_ζ is null and the potential \mathcal{V}_ζ is a constant, thus one either has either a single scalar field ζ , as for models *III* and *V*, or no scalar field, as

for model *IV*. For model *IV*, since no scalar field is present, $\zeta = \phi = 0$, the potential is a constant. Once returning to Einstein equations, one then finds $G_{MN} = -5Cg_{MN}/2$, and thus \mathbb{E}^6 is nothing but a de Sitter space of six dimensions (dS^6) written in some unusual system of coordinates. The form of the scalar field ϕ_ζ can be seen in Fig. 32b, while the potential \mathcal{V}_ζ is depicted in Fig. 6.

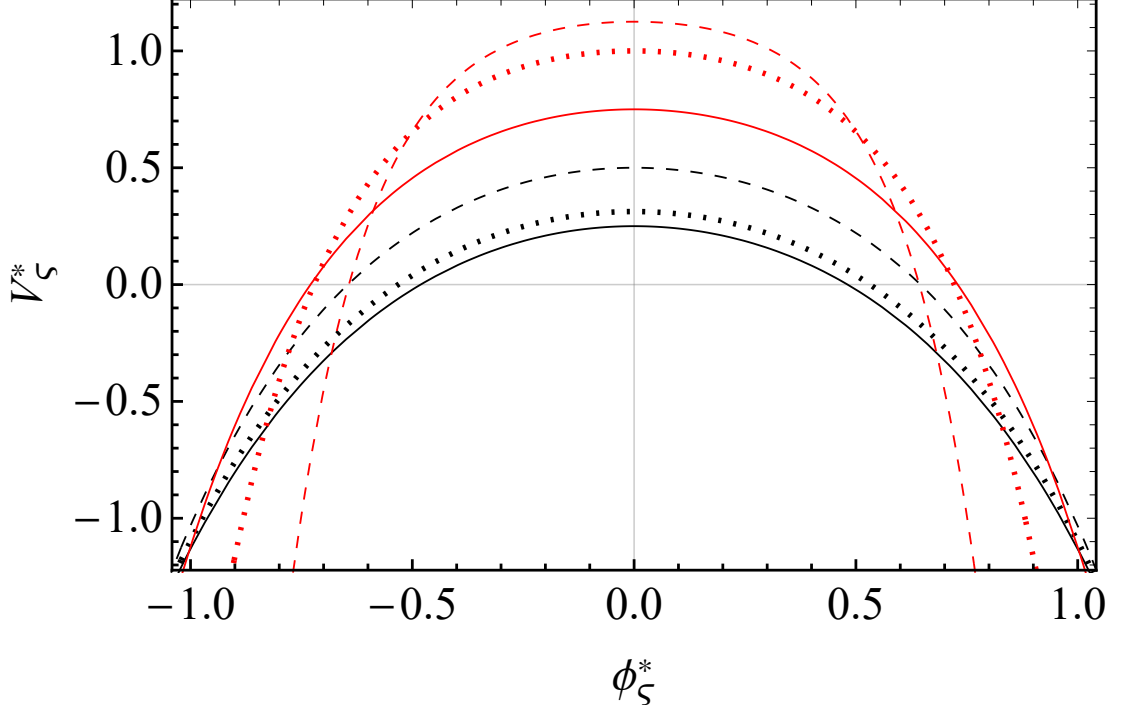


Figure 6 – Potential $\mathcal{V}_\zeta^* = \mathcal{V}_\zeta/32M^4a^2$ as a function of the scalar field $\phi_\zeta^* = \phi_\zeta/4M^2$. The plots are for $C = 0$ (solid black line), $C = a^2/4$ (dotted black line), $C = a^2$ (dashed black line), $C = 2a^2$ (solid red line), $C = 3a^2$ (dotted red line), $C = 7a^2/2$ (dashed red line).

The corresponding metric of such configuration is given by

$$\mathbf{g}_\zeta^J = \cos^2 [a(u + u_0)] e^{-2\hat{A}^J} \omega_{\mu\nu} dx^\mu \otimes dx^\nu + \cos^2 [a(u + u_0)] e^{-2\hat{h}^J} dv \otimes dv + du \otimes du. \quad (2.136)$$

where the index J in \mathbf{g}_ζ^J , \hat{A}^J and \hat{h}^J refers to one of the models *III*, *IV* or *V* (i.e. $J = III$, $\hat{A}^J = \hat{A}^{III}$, refers to the warp factor of model *III*). See that the warp factor from Eq. (2.136) exhibit the same pattern as for model *IV* (2.104) cf. Fig. 3 [1].

Other configurations can also be achieved by choosing \tilde{f} to be non-null, thus even if the warp factor given by Eq. (2.132), the configuration would be different. As an example, one may consider the following choice of \tilde{f} ,

$$\tilde{f} = -\frac{1}{2} \ln \left\{ 1 - \kappa \cos^2 [a(u + u_0)] \right\}, \quad (2.137)$$

where κ is a constant such that $\kappa \in (0, 1)$. For $\kappa = 0$, one recovers the metric from (2.136). As it shall be clarified in the following subsection, this choice corresponds to a

reduction of the spheroid model, for which

$$\mathbf{g}_\epsilon^J = \cos^2 [a(u + u_0)] \left(e^{-2\hat{A}^J} \omega_{\mu\nu} dx^\mu dx^\nu + e^{-2\hat{h}^J} dv^2 \right) + \left\{ 1 - \kappa \cos^2 [a(u + u_0)] \right\} du^2, \quad (2.138)$$

where \hat{A}^J and \hat{h}^J could be any of the functions determined in models *III*, *IV* or *V*.

Analytical solution for Eq. (2.85) are constrained by the choice of $C = 4a^2$, i.e. with $J = III$ and *IV* at (2.138). In this cases, upon an integration of Eq. (2.85), one has

$$\frac{\phi_\epsilon}{4M^2} = \mp \sqrt{1 - \kappa} \operatorname{arctanh} \left(\frac{\sqrt{\kappa} \sin \left[\frac{\sqrt{C}(u+u_0)}{2} \right]}{\sqrt{1 - \kappa \cos^2 \left[\frac{\sqrt{C}(u+u_0)}{2} \right]}} \right), \quad (2.139)$$

and

$$\frac{\mathcal{V}_\epsilon}{2CM^4} = \frac{5(1 - \kappa) - 4\kappa(1 - \kappa) \cos^2 \left[\frac{\sqrt{C}(u+u_0)}{2} \right]}{\left\{ 1 - \kappa \cos^2 \left[\frac{\sqrt{C}(u+u_0)}{2} \right] \right\}^2}, \quad (2.140)$$

and no longer does the scalar field shall exhibit singularities at $\pm\pi/2$. It is straightforward

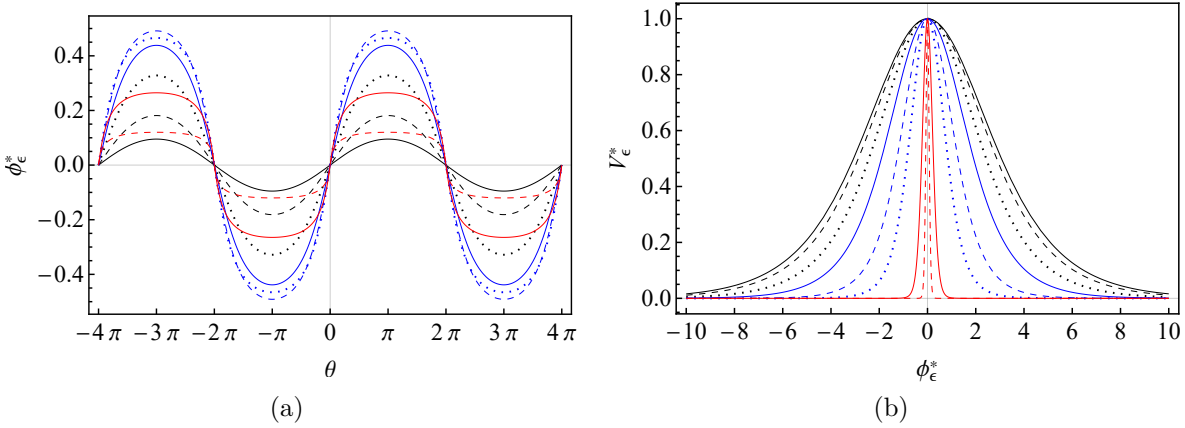


Figure 7 – (a) Scalar field $\phi_\epsilon^* = \phi_\epsilon/4M^2$ as a function of $\theta = a(u + u_0)$. (b) Potential $\mathcal{V}_\epsilon^* = (1 - \kappa) \mathcal{V}_\epsilon/2CM^4(5 - 4\kappa)$ as a function of $\phi_\epsilon^* = \phi_\epsilon/4M^2\sqrt{1 - \kappa}$. The plots are for $\kappa = 0.1$ (solid black line), $\kappa = 0.2$ (dashed black line), $\kappa = 0.4$ (dotted black line), $\kappa = 0.6$ (solid blue line), $\kappa = 0.8$ (dashed blue line), $\kappa = 0.9$ (dotted blue line), $\kappa = 0.99$ (solid red line) and $\kappa = 0.999$ (dashed red line).

to invert the expression for ϕ so as to write the potential \mathcal{V} as a function of ϕ . After some forthright manipulations one finds,

$$\mathcal{V}_\epsilon = 2CM^4 \left[\frac{1 + 4(1 - \kappa) \cosh^2 \left(\frac{\phi_\epsilon}{4M^2\sqrt{1 - \kappa}} \right)}{(1 - \kappa) \cosh^4 \left(\frac{\phi_\epsilon}{4M^2\sqrt{1 - \kappa}} \right)} \right], \quad (2.141)$$

from which scalar field and potential forms are depicted in Fig. 7.

The warp factor for the metric (2.138) is exactly the same as in (2.136), but due to the contribution from g_{uu} , the u coordinate has a different meaning. Thus it would be interesting to change coordinates to be able to better compare how the metric (2.138) fares against the one from (2.136). To this end, one chooses a new coordinate y , with such luck that

$$dy = \sqrt{1 - \kappa \cos^2 \left[\frac{\sqrt{C}}{2} (u + u_0) \right]} du, \quad (2.142)$$

upon which, after an integration, one finds

$$y = \frac{2\sqrt{1-\kappa}}{\sqrt{C}} E \left(\frac{\sqrt{C}}{2} (u + u_0) \middle| \frac{\kappa}{\kappa - 1} \right), \quad (2.143)$$

where $E(x|m)$ is the elliptic integral of second kind. The inverted expression results into

$$\frac{\sqrt{C}}{2} (u + u_0) = E^{-1} \left(\frac{\sqrt{C}y}{2\sqrt{1-\kappa}} \middle| \frac{\kappa}{\kappa - 1} \right), \quad (2.144)$$

where E^{-1} is the inverse function of the elliptic integral of second kind. Then one may write the metric (2.138) in the term of the coordinate y as

$$\mathbf{g}_\epsilon^J = \cos^2 \left[E^{-1} \left(\frac{\sqrt{C}y}{2\sqrt{1-\kappa}} \middle| \frac{\kappa}{\kappa - 1} \right) \right] \left(e^{-2\hat{A}^J} \omega_{\mu\nu} dx^\mu dx^\nu + e^{-2\hat{h}^J} dv^2 \right) + dy^2. \quad (2.145)$$

Finally, the warp factor $e^{-2\hat{A}}$ and the scalar field ϕ as functions of y can be seen in Fig. 8. Clearly, from Fig. 8, as κ gets closer to 1, the warp factor becomes more localized, and in the limit of κ going to 1, a thin brane is recovered [1]. Hence κ is the localizing parameter in this model: as it gets closer to 1, the brane should be closer to a thin brane and the matter distribution in this model should look more like a cusped function, which can only be realized by looking at metric (2.145). Otherwise, one generally prefers to work with (2.138) since a straightforward geometrical interpretation is achieved when one applies this geometry to \mathbb{S}^2 .

Note that the setup from Eq. (2.138) could also be considered in the five-dimensional context, since the equations are, up to some constant, equivalent. From the previous choice of \tilde{f} , one can thus construct some novel models of bent branes in five dimensions, since the metric is just given by

$$\mathbf{g} = \cos^2 \left[\frac{\sqrt{|\Lambda|}}{2} (u + u_0) \right] \omega_{\mu\nu} dx^\mu dx^\nu + \left\{ 1 - \kappa \cos^2 \left[\frac{\sqrt{|\Lambda|}}{2} (u + u_0) \right] \right\} du^2, \quad (2.146)$$

where Λ is the curvature of space-time (\mathbb{M}^4, ω) .

2.4.5 The Geometry of \mathbb{S}^2

This section is dedicated to demonstrating some of the possible geometry one can couple to \mathbb{S}^2 . One starts by first considering a general geometry for \mathbb{S}^2 , namely an ellipsoid.

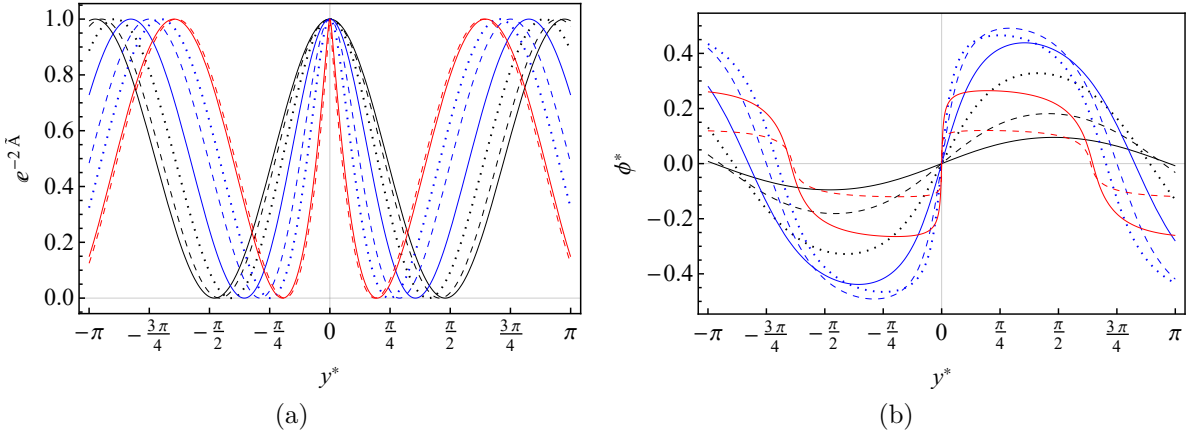


Figure 8 – (a) Warp factor $e^{-2\bar{A}}$ as a function of $y^* = \sqrt{C}y/2$. (b) Scalar field $\phi_\epsilon^* = \phi_\epsilon/4M^2$ as a function of $y^* = \sqrt{C}y/2$. The plots are for $\kappa = 0.1$ (solid black line), $\kappa = 0.2$ (dashed black line), $\kappa = 0.4$ (dotted black line), $\kappa = 0.6$ (solid blue line), $\kappa = 0.8$ (dashed blue line), $\kappa = 0.9$ (dotted blue line), $\kappa = 0.99$ (solid red line) and $\kappa = 0.999$ (dashed red line).

In this context an ellipsoid is \mathbb{S}^2 , but with a particularly distorted metric. This metric can be determined from its immersion⁷ in (\mathbb{R}^3, γ) , where γ is the usual Euclidean metric. For a triaxial ellipsoid, the immersion⁸ is a map $\Phi : \mathbb{S}^2 \rightarrow \mathbb{R}^3$, where it is defined by

$$(\theta, \varphi) \mapsto \Phi(\theta, \varphi) := (a \cos(\varphi) \sin(\theta), b \sin(\varphi) \sin(\theta), c \cos(\theta)), \quad (2.147)$$

with a , b and c being the three radii that define ellipsoid. Then, from Φ , it is possible to define a pull-back Φ^* of $T^{(0,2)}\mathbb{R}^3$:

$$\Phi^* : T^{(0,2)}\mathbb{R}^3 \rightarrow T^{(0,2)}\mathbb{S}^2, \quad (2.148)$$

according to

$$\gamma \mapsto \varepsilon(X, Y) := (\Phi^*\gamma)(X, Y) \equiv \gamma(\Phi_*X, \Phi_*Y), \quad (2.149)$$

where Φ_* is the push-forward on TM induced by Φ , which is defined by

$$(\Phi_*X)^i = X^a \frac{\partial(x^i \circ \Phi)}{\partial y^a}, \quad (2.150)$$

where, finally, x and y are the coordinate chart maps for \mathbb{R}^3 and \mathbb{S}^2 , respectively, also with $i \in \{1, 2, 3\}$ and $a \in \{1, 2\}$. Substituting the above expressions back, one finds the components of the metric ε of \mathbb{S}^2 ,

$$\varepsilon_{ab} = \gamma_{ij} \frac{\partial(x^i \circ \Phi)}{\partial y^a} \frac{\partial(x^j \circ \Phi)}{\partial y^b}, \quad (2.151)$$

which leads to the metric,

$$\begin{aligned} \varepsilon = & \left[a^2 \cos^2(\varphi) \cos^2(\theta) + b^2 \sin^2(\varphi) \cos^2(\theta) + c^2 \sin^2(\theta) \right] d\theta^2 \\ & + \frac{a-b}{2} \sin(2\varphi) \sin(2\theta) d\varphi d\theta + \left[a^2 \sin^2(\varphi) + b^2 \cos^2(\varphi) \right] \sin^2(\theta) d\varphi^2. \end{aligned} \quad (2.152)$$

⁷ The map is considered to be an immersion since the first derivatives of the map must be injective.

⁸ An immersion of a compact space, such as \mathbb{S}^2 , is also an embedding.

This is a triaxial set-up. It is a bit complicated, and even if one could find coordinates such that the off diagonal terms are null, which is always possible, one would end up with an extremely enhanced metric which can be simplified by making assumptions about the radii a and b into a spheroid configuration or a diaxial ellipsoid, i.e. $a = b = r$ and $c = \rho$, which would return the metric

$$\epsilon = \left[r^2 \cos^2(\theta) + \rho^2 \sin^2(\theta) \right] d\theta \otimes d\theta + r^2 \sin^2(\theta) d\varphi \otimes d\varphi. \quad (2.153)$$

This result removes the off-diagonal terms, which turn the procedure into simpler analytical calculations, which should be still simpler for $r = \rho$, as it returns

$$\zeta = r^2 d\theta \otimes d\theta + r^2 \sin^2(\theta) d\varphi \otimes d\varphi. \quad (2.154)$$

Metrics from (2.153) and (2.154) are exactly the metrics used in sec. 2.4.3.

2.4.6 The Sphere Models

An interesting application of the models constructed in previous sections is concerned with the possibility of constructing braneworlds over \mathbb{S}^2 .

The sphere models, for instance, starts with the assumption that the internal space (\mathbb{B}^2, σ) is a sphere, or in other words, $(\mathbb{B}^2, \sigma) \equiv (\mathbb{S}^2, \zeta)$, where ζ is given by Eq. (2.154). In this case, one has chosen $u \equiv r\theta$, $\tilde{f} \equiv 0$ and $\tilde{A} \equiv -\ln[\sin(\theta)]$, as well as $\varphi \in [-\pi, \pi]$ and $\theta \in [0, \pi]$ [1]. This choice corresponds to exactly the same as the one from Eq. (2.132), where now one choses $u_0 = \pi/2r$, $a = 1/r$ and u only takes values at the subinterval $[0, r\pi]$. See that this choice for \tilde{f} and \tilde{A} is also allowed for model V , which however does not have the internal space metric as from Eq. (2.154) [1]. For this reason, model V will be disregarded in this section.

Turning to the point from Eq. (2.154), Eqs. (2.84) and (2.85) are easily solved so as to return the quantities

$$\mathcal{V} = \frac{8M^4}{r^2} \left[5 - 4 \left(1 - \frac{Cr^2}{4} \right) \csc^2 \theta \right], \quad (2.155)$$

and

$$\phi = \pm 4M^2 \sqrt{1 - \frac{Cr^2}{4}} \ln \left[\tan \left(\frac{\theta}{2} \right) \right], \quad (2.156)$$

such that the potential as a function of ϕ is given by

$$\mathcal{V} = \frac{8M^4}{r^2} \left\{ 5 - (4 - Cr^2) \cosh^2 \left[\frac{\phi}{4M^2 \sqrt{1 - \frac{Cr^2}{4}}} \right] \right\}. \quad (2.157)$$

For ϕ read as a real scalar field, one has

$$1 - \frac{Cr^2}{4} \geq 0 \iff C \leq \frac{4}{r^2}, \quad (2.158)$$

from which, for models *III* and *IV*, the constraints over C restrict the number of possible models to its dependence on the value of n ,

1. $C^{III} = n^2/16r^2 \implies n \in \{0, 1, 2, 3, 4, 5, 6, 7, 8\}$;
2. $C^{IV} = n^2/r^2 \implies n \in \{1, 2\}$.

Thus one can have, for model *III*, nine different configurations for the scalar field and potential, each for different values of n . Meanwhile, for model *IV*, there are only two different configurations [1].

When $C = 4/r^2$ ($n = 8$ for model *III* or $n = 2$ for model *IV*) one finds a vacuum: the scalar field ϕ is null and the potential \mathcal{V} is a constant. For model *IV*, this configuration turns out to be dS⁶. In Fig. 9a the scalar, warp factor and potential, for different values of C , are presented. The potential as a function of ϕ can be seen in Fig. 7b. For models

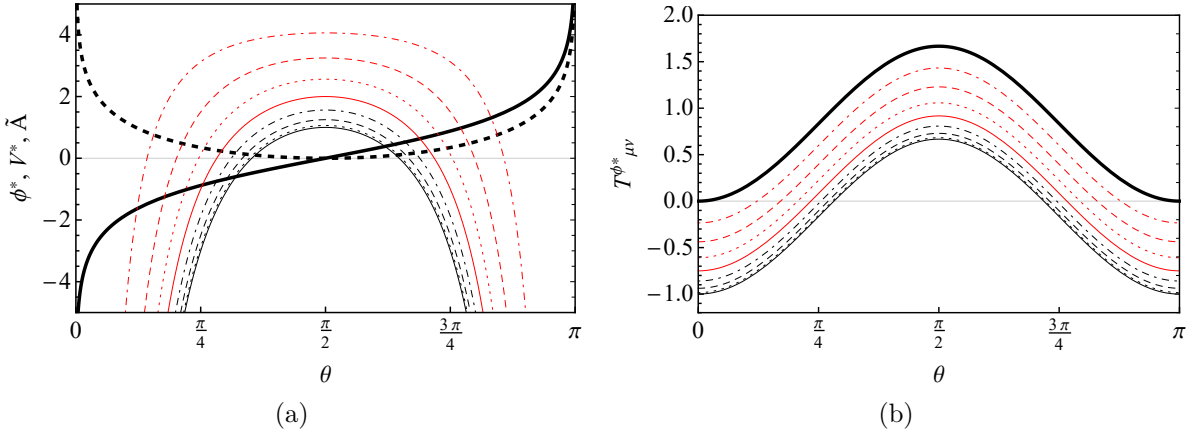


Figure 9 – (a) Scalar field $\phi^* = \phi/4\sqrt{1 - C/4}$ (thick black line), warp factor \tilde{A} (thick black dashed line) and potential $\mathcal{V}^* = \mathcal{V}/4$. (b) The θ dependence of the stress energy tensor $T^{\phi^*}_{\mu\nu}$, $T^{\phi^*}_{\mu\nu} = -\sin^2\theta T^{\phi^\mu}_{\nu}/8$. The plots are for $C = 0$ (thin black line), $C = 1/16$ (thin black dotted line), $C = 1/4$ (thin black dashed line), $C = 9/16$ (thin black dot-dashed line), $C = 1$ (thin red line), $C = 25/16$ (thin red dotted line), $C = 9/4$ (thin red dashed line), $C = 49/16$ (thin red dot-dashed line) and $C = 4$ (thick black solid line), with $M = r = 1$.

III and *IV* the complete metric can be written in the form,

$$\mathbf{g}^{III} = \sqrt{\left|\cos\left(\frac{n\varphi}{2}\right)\right|} \sin^2\theta \eta_{\mu\nu} dx^\mu \otimes dx^\nu + r^2 d\theta \otimes d\theta + r^2 \sin^2(\theta) d\varphi \otimes d\varphi, \quad (2.159)$$

$$\mathbf{g}^{IV} = \frac{4r^2\Lambda}{3n^2} \cos^2\left(\frac{n\varphi}{2}\right) \sin^2\theta \omega_{\mu\nu}^+ dx^\mu \otimes dx^\nu + r^2 d\theta \otimes d\theta + r^2 \sin^2(\theta) d\varphi \otimes d\varphi. \quad (2.160)$$

Figs. 10 and 11 depict the warp factor e^{-2A} of models *III* and *IV* for various values of n . Finally, using the definition from Eq. (2.94), the stress energy tensor of the scalar field ϕ can be obtained for different models. Redundantly, the explicit form of $T^{\phi^\mu}_{\nu}$ is common to all models (*III* and *IV*) and is only a function of θ ,

$$T^{\phi^\mu}_{\nu} = \frac{8M^4}{r^2} \delta^\mu_{\nu} \left[3 \left(1 - \frac{Cr^2}{4} \right) \csc^2(\theta) - 5 \right]. \quad (2.161)$$

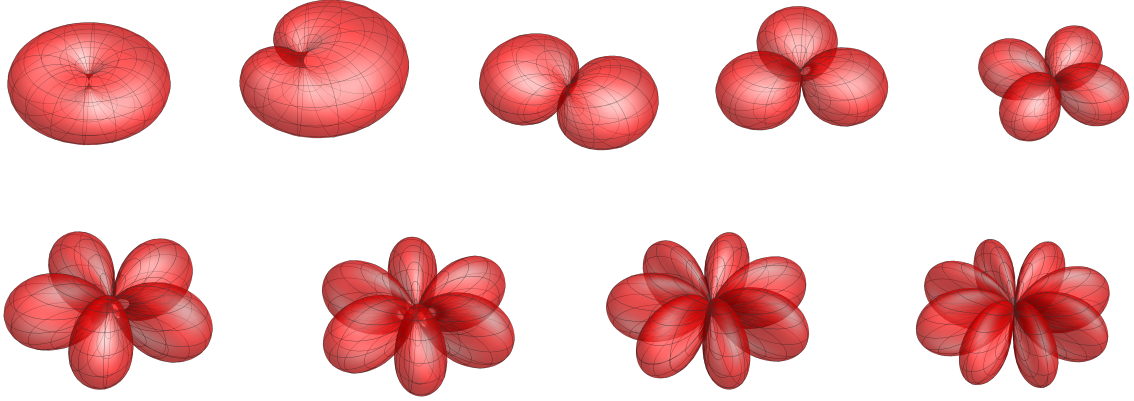


Figure 10 – Warp factor e^{-2A} of model *III* in a spherical plot, with $r = \Lambda = 1$. The top figures are for $n = 0, 1, 2, 3$ and 4 (from left to right) and the bottom ones are for $n = 5, 6, 7$ and 8 (from left to right).



Figure 11 – Warp factor e^{-2A} of model *IV* for $n = 1$ (left figure) and $n = 2$ (right figure) in a spherical plot, with $r = \Lambda = 1$.

Despite exhibiting some singularities, $T^{\phi}_{\mu\nu}$ is localized and non-singular, since once it is multiplied by the warp factor it becomes well behaved [1]. In Fig. 9b, the θ dependence of $T^{\phi}_{\mu\nu}$ is depicted for several values of C . Clearly the total energy in these models, as far as ϕ is concerned, is finite, given that the stress energy tensor is localized. In fact, for all these scenarios, the total stress energy tensor is given by

$$T^{\text{III}}_{\mu\nu} = -\frac{24M^4\eta_{\mu\nu}}{r^2} \sqrt{\left|\cos\left(\frac{n\varphi}{2}\right)\right|} \left[\frac{n^2}{8} \sec^2\left(\frac{n\varphi}{2}\right) + \left(\frac{5}{3} \sin^2\theta - 1 + \frac{n^2}{64}\right) \right], \quad (2.162)$$

$$T^{\text{IV}}_{\mu\nu} = \frac{32M^4\Lambda}{n^2} \omega^+_{\mu\nu} \cos^2\left(\frac{n\varphi}{2}\right) \left[1 - \frac{n^2}{4} - \frac{5}{3} \sin^2(\theta) \right]. \quad (2.163)$$

So far these models have been presented in spherical coordinates, the introduction of stereographic coordinates, i.e.

$$u = r \cot\left(\frac{\theta}{2}\right) \cos(\varphi), \quad (2.164)$$

and

$$v = r \cot\left(\frac{\theta}{2}\right) \sin(\varphi), \quad (2.165)$$

allows one to rewrite the metrics of models *III* and *IV* as

$$\mathbf{g}^{III} = \frac{4r^2(u^2 + v^2)}{(r^2 + u^2 + v^2)^2} \left\{ \sqrt{\left| \cos\left[\frac{n}{2} \arccos\left(\frac{u}{\sqrt{u^2 + v^2}}\right)\right] \right|} \eta_{\mu\nu} dx^\mu dx^\nu + du^2 + dv^2 \right\}, \quad (2.166)$$

and

$$\mathbf{g}^{IV} = \frac{4r^2(u^2 + v^2)}{(r^2 + u^2 + v^2)^2} \left\{ \frac{4r^2\Lambda}{3n^2} \cos^2\left[\frac{n}{2} \arccos\left(\frac{u}{\sqrt{u^2 + v^2}}\right)\right] \omega_{\mu\nu}^+ dx^\mu dx^\nu + du^2 + dv^2 \right\}, \quad (2.167)$$

respectively.

One can thus notice the advantage of choosing the initial metric of \mathbb{B}^2 as from Eq. (2.40) if, on the other hand, one had started with a conformally flat form. As can be seen from expressions (2.166) and (2.167), it would not be straightforward finding these solutions, since the warp factor is, most notably, not separable in u and v [1]. Moreover, one could express all the warp factors without the use of arccos and so on. In this case, the warp factor of models *III* and *IV* for all the allowed values of n can be depicted as they appear in Figs. 12 and 13.

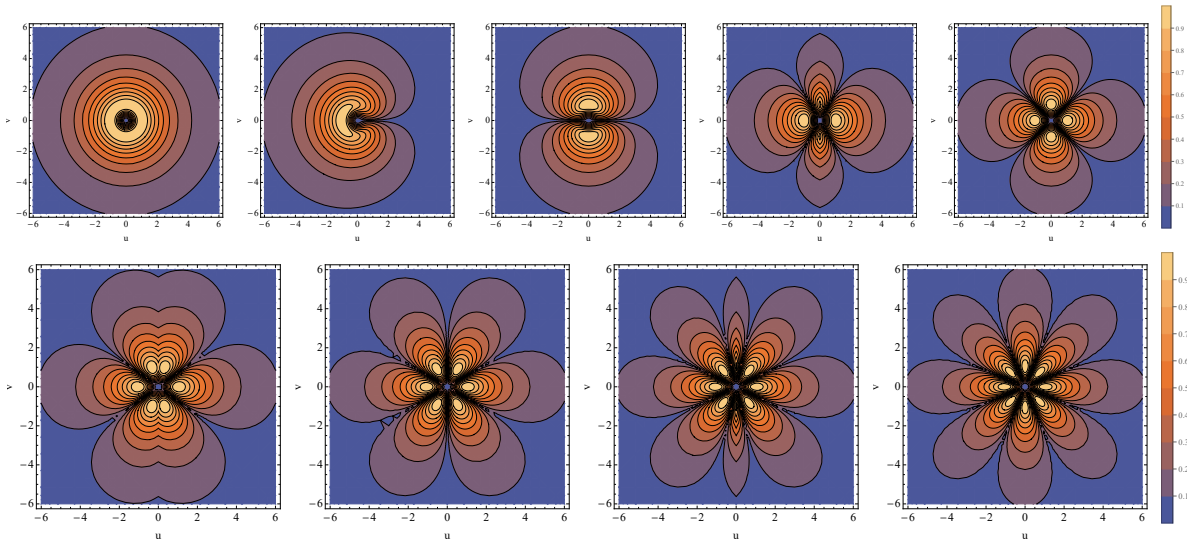


Figure 12 – Warp factor e^{-2A} of model *III* in stereographic coordinates. The top figures are for $n = 0, 1, 2, 3$ and 4 (from left to right) and the bottom ones are for $n = 5, 6, 7$ and 8 (from left to right).

From Figs. 12 and 13 it is clear the localization of the warp factor, even when the space goes to infinity. Therefore these models give rise to thick branes over the sphere where the only adjustable localization parameter is the radius r of the sphere. This corresponds to a detriment to the model since it would be interesting to have a parameter to make the brane thinner while maintaining the radius of the sphere fixed [1].

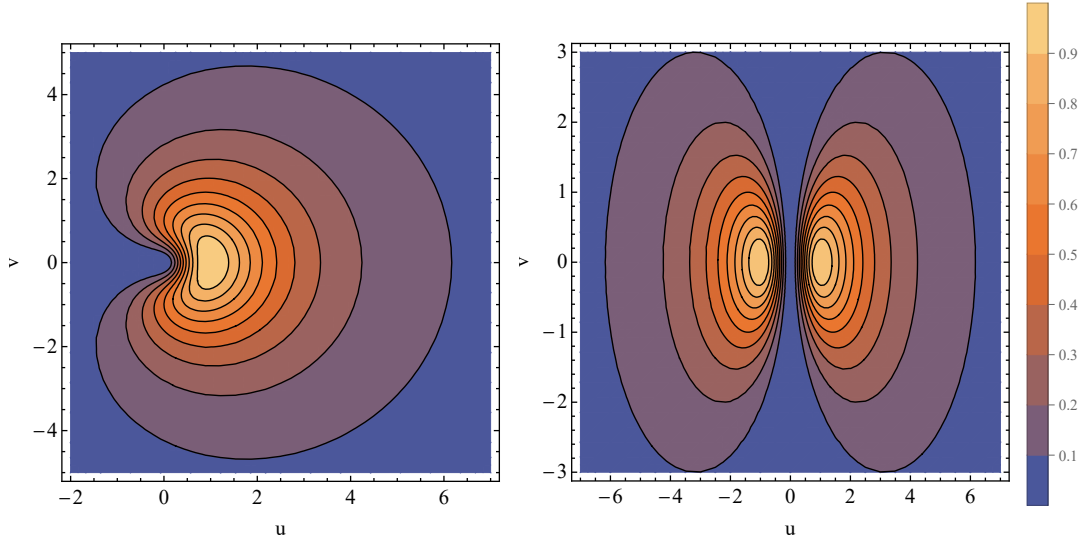


Figure 13 – Warp factor e^{-2A} of model IV for $n = 1$ (left figure) and $n = 2$ (right figure), in stereographic coordinates.

2.4.7 The Spheroid Models

Departing from the model over the sphere, one may consider that the ground space (\mathbb{B}^2, σ) is a spheroid. In some other words, $(\mathbb{B}^2, \sigma) \equiv (\mathbb{S}^2, \epsilon)$, where ϵ is given by Eq. (2.153). The difference between sphere and spheroid models is simply due to the geometry represented by the metric ϵ . The spheroid built here is a di-axial ellipsoid, with radii r and ρ . In this case, the setup variables are

$$u = r\theta, \quad (2.168)$$

$$\tilde{f} = -\frac{1}{2} \ln \left\{ \left[1 - \kappa \sin^2(\theta) \right] \right\}, \quad (2.169)$$

and

$$\tilde{A} \equiv -\ln [\sin(\theta)], \quad (2.170)$$

where $\kappa = 1 - \rho^2/r^2$. Setting $\kappa = 0$, one recovers the model over the sphere. See that this is mapped by the metric from Eq. (2.138) where one just imposes $u_0 = \pi/2r$, $a = 1/r$. Thus, through Eqs. (2.84) and (2.85), one can determine the potential and scalar field as

$$\frac{\mathcal{V}}{4M^4} = \frac{2}{r^2 [1 - \kappa \sin^2(\theta)]} \left[\frac{1 - \kappa}{1 - \kappa \sin^2(\theta)} - 4 \cot^2(\theta) \right] + 2C \csc^2(\theta), \quad (2.171)$$

and

$$\frac{\phi_{,\theta}^2}{4M^4} = \frac{4(1 - \kappa)}{1 - \kappa \sin^2(\theta)} + (4 - Cr^2) \cot^2(\theta) - (1 - \kappa) Cr^2, \quad (2.172)$$

In this case, if $C > 4/r^2$ then the left side of equation (2.172) is not necessarily positive for all θ values. Notice that as θ approaches $\pi/2$ the term with $\cot(\theta)$ goes to infinity, while the other terms remain finite [1]. This means that ϕ would necessarily be imaginary

for some value of θ , which is not allowed. Therefore, one has $C \leq 4/r^2$. In fact, one can not solve (2.172) in general. It can only be solved analytically when $C = 4/r^2$, which is translated into choosing $n = 8$ for model III or $n = 2$ for model IV [1]. Henceforward up to the end only this cases will be considered. For $C = 4/r^2$, the scalar field Eq. (2.172) is easily integrated,

$$\phi = \mp 4M^2 \sqrt{1 - \kappa} \operatorname{arctanh} \left[\frac{\sqrt{\kappa} \sin(\theta)}{\sqrt{1 - \kappa \cos^2(\theta)}} \right], \quad (2.173)$$

and, if $\kappa = 1$ or $\kappa = 0$, one finds a vacuum solution. From Fig. 14a the profile of the scalar

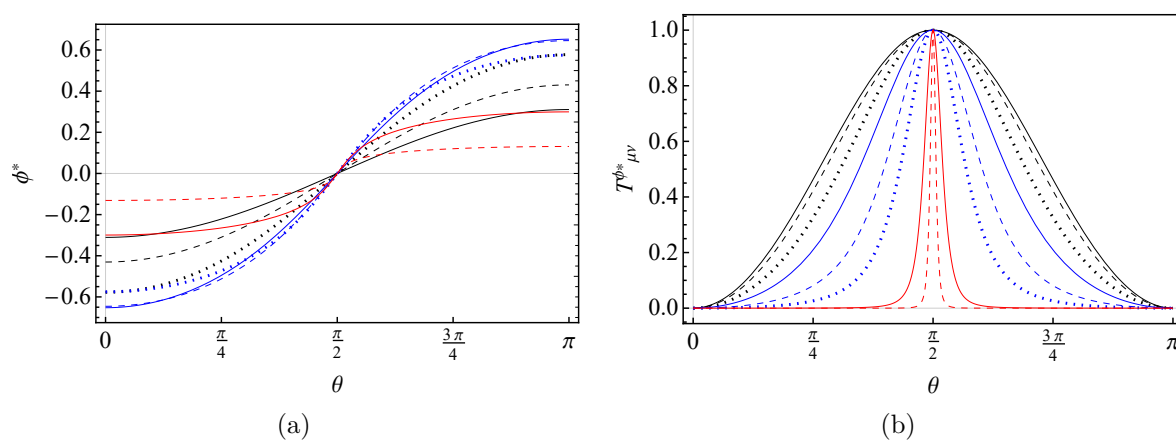


Figure 14 – (a) Scalar field $\phi^* = \phi/4M^2$ as a function of θ . (b) The θ dependence of the stress energy tensor $T^{\phi}_{\mu\nu}$, $T^{\phi^*}_{\mu\nu} = -\sin^2 \theta T^{\phi}_{\mu\nu} (1 - \kappa) / 8(5 - 3\kappa)$. The plots are for $\kappa = 0.1$ (solid black line), $\kappa = 0.2$ (dashed black line), $\kappa = 0.4$ (dotted black line), $\kappa = 0.6$ (solid blue line), $\kappa = 0.8$ (dashed blue line), $\kappa = 0.9$ (dotted blue line), $\kappa = 0.99$ (solid red line) and $\kappa = 0.999$ (dashed red line).

field can be read as a topological or kink-like defect. The potential \mathcal{V} in terms of ϕ is exactly as given by Eq. (2.141) (cf. Fig. 7b), and the stress energy tensor of ϕ , which is common to all models, is given by

$$T^{\phi}_{\mu\nu} = -\delta^{\mu}_{\nu} \frac{8M^4 (1 - \kappa) [5 - 3\kappa \sin^2(\theta)]}{r^2 [1 - \kappa^2 \sin^2(\theta)]^2}. \quad (2.174)$$

Differently from the sphere models, these models possess another localizing parameter other than the radius r . As κ approaches 1 the stress energy tensor becomes more and more localized, from Fig. 14b one can notice such a behavior. Consequently, these models give rise to thick branes that are even more interesting than the spherical ones, as one chooses κ closer to 1 the thinner the distribution of matter becomes [1].

To more appropriately present the localizing effect that κ has on the model, it is convenient to show how it can affect the warp factor. To do this, the change of coordinates as given by (2.143) is preminent. By writing

$$dy = \sqrt{1 - \kappa \sin^2(\theta)} d\theta, \quad (2.175)$$

thus one must choose $y = E(\theta|\kappa)$, where $E(\theta|\kappa)$ is the elliptic integral of second kind. The inverse is simply expressed abstractly by $\theta = E^{-1}(y|\kappa)$, where $E^{-1}(y|\kappa)$ is the inverse function of the elliptic integral of second kind. Then one is able to express the metric and the scalar field in terms of the coordinate y by

$$\mathbf{g}^J = e^{-2\hat{A}^J} \sin^2 [E^{-1}(y|\kappa)] \omega_{\mu\nu} dx^\mu dx^\nu + r^2 \sin^2 [E^{-1}(y|\kappa)] d\varphi^2 + r^2 dy^2, \quad (2.176)$$

and

$$\phi = \mp 4M^2 \sqrt{1-\kappa} \operatorname{arctanh} \left\{ \frac{\sqrt{\kappa} \sin [E^{-1}(y|\kappa)]}{\sqrt{1-\kappa \cos^2 [E^{-1}(y|\kappa)]}} \right\}, \quad (2.177)$$

where both quantities are valued in the domain $[E(0|\kappa) = 0, E(\pi|\kappa)]$, i.e. $y \in [0, E(\pi|\kappa)]$. The warp factor $e^{-2\hat{A}}$ and the scalar field ϕ , in terms of y , are depicted in Fig. (15). From Fig. (15) one can notice that the closer κ gets to 1 the more the thick brane looks like a thin brane, thus the more localized is the model. One had already depured it from the stress energy tensor pattern, but the above analysis paints a better picture of the localization of the model. Of course, express the same quantities in terms of θ instead of y , turns back the expected analytical form.

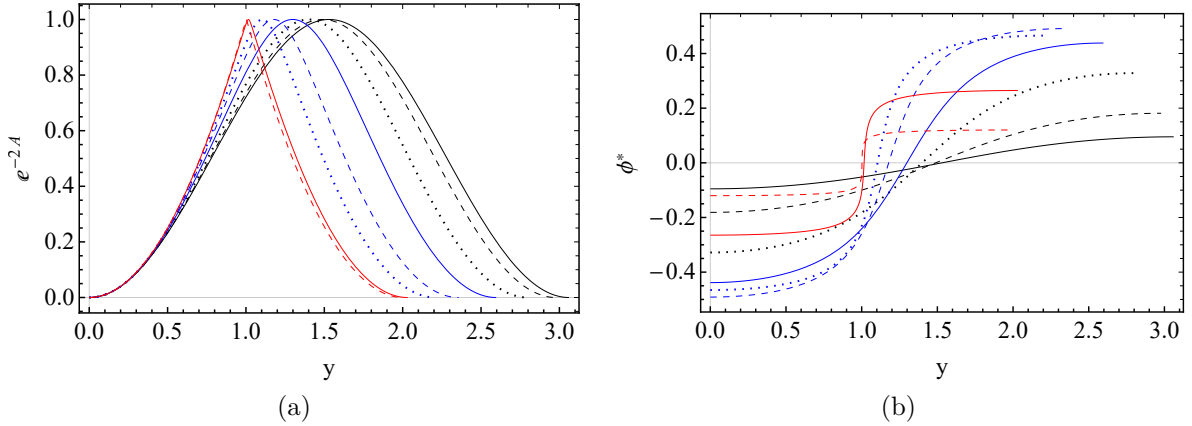


Figure 15 – (a) Scalar field $\phi^* = \phi/4M^2$ as a function of θ . (b) The θ dependence of the stress energy tensor $T^{\phi}_{\mu\nu}$, $T^{\phi^*}_{\mu\nu} = -\sin^2 \theta T^{\phi}_{\nu}(1-\kappa)/8(5-3\kappa)$. The plots are for $\kappa = 0.1$ (solid black line), $\kappa = 0.2$ (dashed black line), $\kappa = 0.4$ (dotted black line), $\kappa = 0.6$ (solid blue line), $\kappa = 0.8$ (dashed blue line), $\kappa = 0.9$ (dotted blue line), $\kappa = 0.99$ (solid red line) and $\kappa = 0.999$ (dashed red line).

Finally one can express the metric for models *III* and *IV* by

$$\mathbf{g}^{III} = \sqrt{|\cos(4\varphi)|} \sin^2(\theta) \omega_{\mu\nu} dx^\mu dx^\nu + r^2 [1 - \kappa \sin^2(\theta)] d\theta^2 + r^2 \sin^2(\theta) d\varphi^2, \quad (2.178)$$

$$\mathbf{g}^{IV} = \frac{r^2 \Lambda}{3} \cos^2(\varphi) \sin^2(\theta) \omega_{\mu\nu} dx^\mu dx^\nu + r^2 [1 - \kappa \sin^2(\theta)] d\theta^2 + r^2 \sin^2(\theta) d\varphi^2, \quad (2.179)$$

with the warp factor being essentially the same as in the $C = 4/r^2$ spherical model, as depicted in Figs. 10 and 11. In this fashion one can realize that the spherical models with

$C = 4/r^2$ represent a braneworld model in a vacuum for ϕ , while the spheroid models represent a topological defect that alternate between two vacuums like depicted in Fig. 14a (or 15b).

Unfortunately, it is not so simple to find stereographic coordinates for the spheroids as it was for the sphere. It is feasible to analytical calculations, but the expressions are too complicated for a meaningful analysis. Here no appeal to a different set of coordinates will be made to discuss the properties of these models.

3 Gravity Localization

Additional dimensions introduces a novel problem: Why have the co-dimensions not been measured before? Here we point to the simple fact that we observe the universe through light, then there should be no way of knowing if new dimensions do exist if light is confined to the brane (or at least at the vicinity of the brane). The new dimensions could be “invisible” to electromagnetism for all we know. But this is not the case for gravity. Gravity is space-time itself, therefore it should perceive the new dimensions and corrections to its interactions should follow. But experiments severely restricts the gravitational interaction to be very similar, up to a sensible limit, to the Newtonian one. Therefore any realistic brane model must be required to satisfy:

1. The brane is stable;
2. Four-dimensional Newtonian gravity is recovered.

Both are checked by perturbing the bulk metric, by adding a test particle of mass \mathcal{M} inside the brane, that perturbs the gravitational interaction, one hopes that it resembles Newtonian gravity to a certain degree.

Considering that any braneworld model should recover standard four-dimensional physics, at least within reasonable limits [7], and assuming that all physical fields must be localized in a brane-like region of space, it is natural to suppose that the braneworld solutions classified in the previous chapter admit the localization of gravity for all configurations [69]. Besides the inherent classical aspects, from systematic metric perturbations over the braneworld [3, 4], which renders a linearized formulation that encompass non-linear aspects of gravity, the equations for the metric fluctuations can be reduced to time independent Schrödinger-like equations [3, 4, 22, 71, 82], which are then subjected to some separation of variables technique that results into the quantum mechanical analogue problem [69].

The quantum mechanical aspects will then be further extended to the interpretation of the associated wave functions, solutions of such Schrödinger-like equation, which are not only relevant for the localization on the brane, but also for identifying the Newtonian limit [69]. Recovering the Newtonian gravity in the brane, up to a sensitive limit, is indeed an important test for braneworld models. One may determine the Newtonian limit by assuming that perturbations of the metric are generated by a particle of mass \mathcal{M} [69]. As a first approach, the effective coupling between the massive particle with gravity becomes dependent on the normalization of the graviton modes and on its value at the position of the particle (which is generically placed at the maximum of the wave functions of the

zero mode) [69]. However, a more realistic description would consider any particle to be smeared over the co-dimensions [71, 84], in contrast to a Dirac delta localization. In this case, the gravitational constant would no longer depend on the value of the graviton modes at the position of the particle, but would be determined by an average value of the matter distribution with the graviton modes [69]. For the proposal considered here, the simplified stratagem of a Dirac delta distribution is enough, since one can at least determine the correct gravitational constant, even if failing to ascertain the correct gravitational interaction¹ [69].

Broadly speaking, the pertinence of considering six-dimensional braneworlds resides in obtaining Schrödinger-like linearized equations for a two (and not only one) dimensional curved background [69]. For string and trivial-like solutions the inherited Schrödinger-like equations always allows for a further separation of the co-dimensional variables. On one hand, intersecting-like branes allow for a further separation of the co-dimensional variables for a subset of our models (from *III* to *VI*). On the other hand, for another subset (models *I* and *II*), the variables are not separable unless the graviton mass is null [69]. Furthermore, for one of the intersecting-like models, *IV*, the Schrödinger-like equations solutions are analytically defined for the entire spectrum of gravitons [69]. In particular, this provides a wide range for the mass spectrum. For models *I*, *II*, *III* and *VI*, however, only zero modes can be analytically extracted, while from model *V* one can extract some of the massive modes. Regardless, some remarkable features are still accomplished from the Newtonian limit for all these models, from *I* to *VI*, as they shall be scrutinized along this chapter [69].

The chapter is thus organized as follows. Sec. 3.1 is devoted to determine the equations for the gravitational perturbations and the effective for a general background. One also defines the condition for localization. Subsecs. 3.1.3 and 3.1.5 presents the straightforward mapping of the perturbed equations to the quantum mechanical analogue problem that describes the localization and spectrum of the graviton modes for the proposed classification. Finally, in Sec. 3.2, the Schrödinger equation for each of intersecting-like braneworld model is yielded and their corresponding spectrum of gravitons as well as their Newtonian limits are obtained.

3.1 Gravitational Fluctuations

A basic requirement of any braneworld model is that it reproduces, up to a sensible limit, Newtonian gravity [3, 4, 22, 71, 82, 69]. The Newtonian limit of any braneworld model can be studied within the framework of linearized gravity, where it is assumed

¹ Generically, the Newtonian limit of some braneworld should append some modifications to the gravitational interaction. To avoid contradictions with experimental data one expects the corrections to be insignificant above some scale, thus recovering Newtonian gravity.

that the spacetime can be described by small fluctuations about a given background [69]. Following similar arguments as outlined by [71]², tensorial perturbations of (2.1) are written as

$$\bar{\mathbf{g}} = e^{-2A} (\hat{g}_{MN} + \varpi_{MN}) dx^M dx^N = e^{-2A} [\omega_{\mu\nu} + \varpi_{\mu\nu}] dx^\mu dx^\nu + \sigma_{ij} dy^i dy^j, \quad (3.1)$$

where $\varpi_{\mu\nu}$ are functions such that $\varpi_{\mu\nu} : \mathbb{M}^4 \times \mathbb{B}^2 \rightarrow \mathbb{R}$ (i.e. $\varpi_{\mu\nu}(x^\rho, u, v)$), and $\varpi_{ij} = 0$ [69]. Several objects are now necessary to determine the perturbations of the Einstein tensor, including the inverse metric and the connections compatible with $\bar{\mathbf{g}}$ [69]. The inverse metric can be assumed to be

$$\bar{\mathbf{g}}^{-1} = e^{2A} \left[\hat{g}^{MN} + (\varpi^{-1})^{MN} \right] \partial_M \otimes \partial_N, \quad (3.2)$$

where $(\varpi^{-1})^{MN}$ refers to the inverse of ϖ , while ϖ^{MN} refers to ϖ_{MN} with indexes raised by $\hat{\mathbf{g}}$. Since ϖ_{MN} and $(\varpi^{-1})^{MN}$ are small perturbations then one finds

$$\delta^A_B = \bar{g}^{AN} \bar{g}_{NB} = \delta^A_B + \hat{g}^{AN} \varpi_{NB} + (\varpi^{-1})^{AN} \hat{g}_{NB} + O(\varpi^2), \quad (3.3)$$

which implies in

$$(\varpi^{-1})^{MN} = -\varpi^{MN} = -\varpi_{AB} \hat{g}^{AM} \hat{g}^{BN}, \quad (3.4)$$

and the inverse metric can be written as

$$\bar{\mathbf{g}}^{-1} = e^{2A(u,v)} (\omega^{\mu\nu} - \varpi^{\mu\nu}) \partial_\mu \otimes \partial_\nu + \sigma^{ij} \partial_i \otimes \partial_j, \quad (3.5)$$

On the other hand, the connections compatible with $\bar{\mathbf{g}}$ can be expressed in terms of the connections compatible with $\hat{\mathbf{g}}$, to first order in ϖ , as

$$\bar{\Gamma}_{MN}^P = \hat{\Gamma}_{MN}^P - A_{,N} \delta_M^P - A_{,M} \delta_N^P + A_{,S} \hat{g}^{PS} \hat{g}_{MN} + A_{,S} \hat{g}^{PS} \varpi_{MN} - A_{,S} \varpi^{PS} \hat{g}_{MN} + (\delta\Gamma)_{MN}^P, \quad (3.6)$$

where $(\delta\Gamma)_{MN}^P$ is a true tensor, since it is the difference between two connections. The components $(\delta\Gamma)_{MN}^P$ can be determined by noting that

$$\bar{\nabla}_P \bar{g}_{MN} \equiv 0 \iff \hat{\nabla}_P \varpi_{MN} = \hat{g}_{MK} \delta\Gamma_{NP}^K + \hat{g}_{NK} \delta\Gamma_{MP}^K, \quad (3.7)$$

permuting some of the indexes and summing in a particular order implies³ in

$$\delta\Gamma_{MN}^P = \frac{1}{2} \hat{g}^{PK} \left(\hat{\nabla}_N \varpi_{MK} + \hat{\nabla}_M \varpi_{KN} - \hat{\nabla}_K \varpi_{MN} \right). \quad (3.8)$$

² Extending this line of reasoning in order to account for a curved four-dimensional space [85].

³ Actually, the following result is true for any difference between two connections (not only for small perturbations) that is compatible with some metric.

With this results in hand the Einstein tensor (\bar{G}_{MN}) compatible with \bar{g} is then expressed, up to the first order in $\varpi_{\mu\nu}$, by

$$\begin{aligned}\bar{G}_{MN} &= G_{MN} + \delta G_{MN} \\ &= G_{MN} + \frac{1}{2}\hat{g}^{PK}\hat{\nabla}_P\hat{\nabla}_N\varpi_{MK} + \frac{1}{2}\hat{g}^{PK}\hat{\nabla}_P\hat{\nabla}_M\varpi_{KN} - \frac{1}{2}\hat{\square}\varpi_{MN} - \frac{1}{2}\hat{g}^{PK}\hat{\nabla}_M\hat{\nabla}_N\varpi_{PK} \\ &\quad - \frac{1}{2}\varpi_{MN}\hat{R} + \frac{1}{2}\hat{g}_{MN}\varpi_{PK}\hat{R}^{PK} - \frac{1}{2}\hat{g}_{MN}\hat{g}^{SD}\hat{g}^{PK}\hat{\nabla}_P\hat{\nabla}_S\varpi_{KD} + \frac{1}{2}\hat{g}_{MN}\hat{g}^{SD}\hat{\square}\varpi_{SD} \\ &\quad - 2\hat{g}^{PK}\left(\hat{\nabla}_N\varpi_{MK} + \hat{\nabla}_M\varpi_{KN} - \hat{\nabla}_K\varpi_{MN}\right)A_{,P} + 6\varpi_{MN}\hat{g}^{PS}A_{,S}A_{,P} \\ &\quad + 2\hat{g}_{MN}\hat{g}^{PK}\hat{g}^{SD}\left(\hat{\nabla}_K\varpi_{PD} + \hat{\nabla}_P\varpi_{KD} - \hat{\nabla}_D\varpi_{PK}\right)A_{,S} - 4\varpi_{MN}\hat{\square}A \\ &\quad - 6\hat{g}_{MN}\hat{g}^{PD}\hat{g}^{SJ}\varpi_{DJ}A_{,S}A_{,P} + 4\hat{g}_{MN}\hat{g}^{PS}\hat{g}^{KD}\varpi_{SD}\hat{\nabla}_P\hat{\nabla}_KA, \quad (3.9)\end{aligned}$$

where $\hat{g}_{MN} = e^{2A}g_{MN}$ and $\hat{\nabla}$ is a covariant derivative compatible with \hat{g} . Introducing the assumed constraints, $\varpi_{Mi} = A_{,\mu} = 0$, fixing the gauge $\hat{\nabla}^M\varpi_{MN} = \hat{g}^{MN}\varpi_{MN} = 0$, noticing the commutation properties of the covariant derivatives⁴ and considering that⁵ $\varpi_{\rho\kappa}\hat{R}^{\rho\kappa} = 0$, one obtains the first order perturbed Einstein tensor in the form of

$$\begin{aligned}\delta G_{MN} &= \frac{1}{2}\hat{g}^{\zeta\delta}\varpi_{\zeta(M}\hat{R}_{N)\delta} - \varpi^{\delta\rho}\hat{R}_{\delta M\rho N} - \frac{1}{2}\hat{\square}\varpi_{MN} \\ &\quad + 2\hat{\sigma}^{ij}A_{,i}\hat{\nabla}_j\varpi_{MN} + \varpi_{MN}\left(6\hat{\sigma}^{ij}A_{,i}A_{,j} - 4\hat{\square}A - \frac{1}{2}\hat{R}\right), \quad (3.10)\end{aligned}$$

where $t_{(MN)} = t_{MN} + t_{NM}$.

One would also expect perturbations in the configuration of the scalar fields (A , ϕ and ζ), but the scalar and tensorial perturbations are completely decoupled one from each other when linear perturbations are considered [71] (see Sec. 3.1.1 for further details) [69]. For this reason, when dealing with the dynamics of the gravitational field, one can disregard the perturbations of the scalar fields [69].

The perturbation of the scalar fields are completely dissociated from the tensorial perturbations, yet the stress energy tensor will still be perturbed in this configurations, since the metric fluctuations induce perturbations in the stress energy tensor [69]. In particular, in the context of our analysis, only stress energy tensors constructed out of scalar fields shall be considered. The stress energy tensor calculated out of metric \bar{g} is then given by

$$\bar{T}_{MN} = T_{MN} - e^{-2A}\varpi_{MN}\left(\frac{g^{KS}\phi_{,S}\phi_{,K}}{2} + \frac{g^{KS}\zeta_{,S}\zeta_{,K}}{2} + V\right). \quad (3.11)$$

Following the same stratagem from Ref. [71], one finds that

$$\varpi_{MP}T^P{}_N = -\varpi_{MN}\left(\frac{g^{KS}\phi_{,S}\phi_{,K}}{2} + \frac{g^{KS}\zeta_{,S}\zeta_{,K}}{2} + V\right), \quad (3.12)$$

⁴ $\hat{g}^{PK}\hat{\nabla}_P\hat{\nabla}_N\varpi_{MK} = \hat{g}^{PK}\hat{\nabla}_N\hat{\nabla}_P\varpi_{MK} - \hat{g}^{SD}\hat{g}^{PK}\varpi_{SK}\hat{R}_{DMPN} + \hat{g}^{SD}\varpi_{MS}\hat{R}_{DN}$.

⁵ Which is true whenever one assumes the gauge condition $\hat{g}^{MN}\varpi_{MN} = 0$.

which can be used to derive the perturbations of the stress energy tensor,

$$\delta T_{MN} = 4M^4 \hat{g}^{\rho\zeta} \varpi_{M\rho} \hat{R}_{\zeta N} + 4M^4 \varpi_{MN} \left(6\hat{g}^{ij} A_{,i} A_{,j} - 4\hat{\square}A - \frac{1}{2}\hat{R} \right). \quad (3.13)$$

Finally, equalizing the first order contributions, δG_{MN} and δT_{MN} , from Eqs. (3.10) and (3.13), through the Einstein equation, one finds

$$-\frac{1}{2}\hat{\square}\varpi_{MN} + 2\hat{\sigma}^{ij} A_{,i} \hat{\nabla}_j \varpi_{MN} = \frac{1}{2}\hat{g}^{\zeta\delta} \varpi_{\zeta[M} \hat{R}_{N]\delta} + \varpi^{\delta\rho} \hat{R}_{\delta M\rho N}, \quad (3.14)$$

where $t_{[MN]} = t_{MN} - t_{NM}$. The above result be simplified by noticing that $\hat{\nabla}_j \varpi_{MN} = \varpi_{MN,j}$, since $\hat{\Gamma}_{jM}^N = 0$ and that \hat{g} is factorable. One thus has

$$\hat{R} = \mathcal{R}^\rho_{\alpha\mu\nu}(x^\kappa) \frac{\partial}{\partial x^\rho} \otimes dx^\alpha \otimes dx^\nu \otimes dx^\nu + \hat{\Sigma}^j_{klc}(x^s) \frac{\partial}{\partial x^j} \otimes dx^k \otimes dx^l \otimes dx^c, \quad (3.15)$$

with $\mathcal{R}^\rho_{\alpha\mu\nu}$ and $\hat{\Sigma}^j_{klc}$ encoding the curvature of (\mathbb{M}^4, ω) and $(\mathbb{B}^2, \hat{\sigma})$, respectively (cf. [1]). To summarize, one can still write the equation for the perturbation of the gravitational field for general bent branes,

$$\hat{\square}\varpi_{\mu\nu} - 4\hat{\sigma}^{ij} A_{,i} \varpi_{\mu\nu,j} = \omega^{\zeta\delta} \varpi_{\zeta[\nu} \mathcal{R}_{\mu]\delta} - 2\varpi^{\delta\rho} \mathcal{R}_{\delta\mu\rho\nu}, \quad (3.16)$$

and notice that, for solutions (2.69), (2.76), (2.90), (2.104), (2.111) and (2.121), only the Ricci tensor is written as $\mathcal{R}_{\mu\nu} = \Lambda\omega_{\mu\nu}$. For further simplifications, a maximally symmetric spacetime (\mathbb{M}^4, ω) can be assumed, i.e. $\mathcal{R}_{\delta\mu\rho\nu} = (\omega_{\delta\rho}\omega_{\mu\nu} - \omega_{\delta\nu}\omega_{\mu\rho})\Lambda/3$, such that Eq. (3.16) is thus simplified into the form of

$$\hat{\square}\varpi_{\mu\nu} - 4\hat{\sigma}^{ij} A_{,i} \varpi_{\mu\nu,j} = \frac{2\Lambda}{3}\varpi_{\mu\nu}, \quad (3.17)$$

which describes the tensorial perturbation in the bulk [69].

3.1.1 The Decoupling Between Scalar and Tensorial Perturbations

In Sec. 3.1, the perturbations were cast form of Eq. (3.1). Just as a preliminary consideration, the general form from Eq. (3.1) should involve perturbations of the warp factor, yet this can be disregarded because the latter can always be encompassed by $\varpi_{\mu\nu}$, as follows,

$$\begin{aligned} \bar{g} &= e^{-2\bar{A}} (\omega_{\mu\nu} + \varpi_{\mu\nu}) dx^\mu dx^\nu + \sigma_{ij} dy^i dy^j \\ &= e^{-2A} (\omega_{\mu\nu} + \varpi_{\mu\nu} - 2\delta A \omega_{\mu\nu}) dx^\mu dx^\nu + \sigma_{ij} dy^i dy^j, \end{aligned} \quad (3.18)$$

where $\bar{A} = A + \delta A$ and δA is the perturbation of the warp factor [69]. In which concerns the scalar perturbation related to δA , every calculation of Sec. 3.1 follows straightforwardly from defining $\tilde{\varpi}_{\mu\nu} = \varpi_{\mu\nu} - 2\delta A \omega_{\mu\nu}$.

Of course, to clear up the above statement, from a more explicit approach, once that one assumes the metric to be (3.18), the gravitational portion of the action, if expanded up to the second order in the perturbative parameters, can be written as

$$\begin{aligned}
\bar{S}_g &= 2M^4 \int d^6x \sqrt{-\bar{g}} \bar{R} \\
&= 2M^4 \int d^6x e^{-2\bar{A}} \sqrt{-\omega\sigma} \left[\mathcal{R} + e^{-2\bar{A}} \left(\Sigma - 2\Delta^2 \bar{A} - 20\bar{A}^i \bar{A}_{,i} \right) + 10\hat{\square}\bar{A} \right. \\
&\quad \left. - 20\bar{A}^{\mu} \bar{A}_{,\mu} - \varpi_{\mu\nu} \mathcal{R}^{\mu\nu} - 20\varpi^{\mu\nu} A_{,\mu} \bar{A}_{,\nu} \right] \\
&\quad + 2M^4 \int d^6x e^{-2A} \sqrt{-\omega\sigma} \left[\hat{\nabla}_S \left(\hat{g}^{SN} \varpi^{\mu\nu} \hat{\nabla}_N \varpi_{\mu\nu} - \hat{g}^{S\eta} \varpi^{\mu\nu} \hat{\nabla}_\nu \varpi_{\mu\eta} \right) \right. \\
&\quad - 20\varpi^\mu{}_\kappa \varpi^{\kappa\nu} A_{,\mu} A_{,\nu} - \frac{1}{4} \varpi^{\mu\nu} \varpi_{\mu\nu} \hat{R} + 10\varpi^\mu{}_\kappa \varpi^{\kappa\nu} \hat{\nabla}_\mu \hat{\nabla}_\nu A \\
&\quad - \frac{1}{4} \hat{\nabla}^K \varpi^{\mu\nu} \hat{\nabla}_K \varpi_{\mu\nu} - \frac{5}{2} \varpi^{\mu\nu} \varpi_{\mu\nu} \hat{\square} A + 5\varpi^{\mu\nu} \varpi_{\mu\nu} A^P A_{,P} \\
&\quad \left. + \frac{1}{2} \hat{\nabla}^\nu \varpi^{\mu\kappa} \hat{\nabla}_\kappa \varpi_{\mu\nu} + \varpi^\mu{}_\kappa \varpi^{\kappa\nu} \mathcal{R}_{\mu\nu} + 5\hat{g}^{SJ} \varpi^{\mu\nu} \left(2\hat{\nabla}_\nu \varpi_{\mu J} - \hat{\nabla}_J \varpi_{\mu\nu} \right) A_{,S} \right]. \quad (3.19)
\end{aligned}$$

The only terms that can exhibit some coupling between the tensorial, $\varpi_{\mu\nu}$, and warp factor, δA , perturbations are⁶ $e^{-2\bar{A}} \varpi_{\mu\nu} \mathcal{R}^{\mu\nu}$ and $e^{-2\bar{A}} \varpi^{\mu\nu} A_{,\mu} \bar{A}_{,\nu}$. By construction, these terms are null, since $A_{,\mu} = \phi_{,\mu} = \zeta_{,\mu} = 0$. Therefore, there is no coupling between $\varpi_{\mu\nu}$ and δA , such that neither $\varpi_{\mu\nu}$ nor δA do affect one each other.

Likewise, the effects of the scalar fields (ϕ and ζ) on the localization of gravitational fields can also be evaluated. For the metric described by Eq. (3.1), the action of the scalar fields is written as

$$\begin{aligned}
\bar{S}_{\bar{\phi}, \bar{\zeta}} &= - \int dx^6 \sqrt{-\bar{g}} \left[\frac{\bar{g}^{MN}}{2} \bar{\phi}_{,M} \bar{\phi}_{,N} + \frac{\bar{g}^{MN}}{2} \bar{\zeta}_{,M} \bar{\zeta}_{,N} + \mathcal{V}(\bar{\phi}, \bar{\zeta}) \right] \\
&= - \int dx^6 \sqrt{-g} \left(1 - \frac{1}{4} \varpi^{MN} \varpi_{MN} \right) \left[\frac{\bar{g}^{MN}}{2} \bar{\phi}_{,M} \bar{\phi}_{,N} + \frac{\bar{g}^{MN}}{2} \bar{\zeta}_{,M} \bar{\zeta}_{,N} + \mathcal{V}(\bar{\phi}, \bar{\zeta}) \right] \\
&= \frac{1}{4} \int dx^6 \sqrt{-g} \varpi^{MN} \varpi_{MN} \left[\frac{g^{MN}}{2} \phi_{,M} \phi_{,N} + \frac{g^{MN}}{2} \zeta_{,M} \zeta_{,N} + \mathcal{V}(\phi, \zeta) \right] \\
&\quad - \int dx^6 \sqrt{-g} \left[\frac{g^{MN}}{2} \bar{\phi}_{,M} \bar{\phi}_{,N} + \frac{g^{MN}}{2} \bar{\zeta}_{,M} \bar{\zeta}_{,N} \right. \\
&\quad \left. + \frac{\varpi^{MN}}{2} \bar{\phi}_{,M} \bar{\phi}_{,N} + \frac{\varpi^{MN}}{2} \bar{\zeta}_{,M} \bar{\zeta}_{,N} + \mathcal{V}(\bar{\phi}, \bar{\zeta}) \right], \quad (3.20)
\end{aligned}$$

⁶ There are also $\varpi^{MN} \hat{\nabla}_M \hat{\nabla}_N \delta A$ and $\varpi_{MN} \hat{g}^{MN} \hat{g}^{AB} \hat{\nabla}_A \hat{\nabla}_B \delta A$, which are either null ($\varpi_{MN} \hat{g}^{MN} \hat{g}^{AB} \hat{\nabla}_A \hat{\nabla}_B \delta A = 0$) or contribute only as a boundary term ($\varpi^{MN} \hat{\nabla}_M \hat{\nabla}_N \delta A = \hat{\nabla}_M (\varpi^{MN} \hat{\nabla}_N \delta A)$) in the transverse traceless gauge ($\hat{\nabla}^M \varpi_{MN} = \hat{g}^{MN} \varpi_{MN} = 0$) [69]. Therefore, one has a vanishing contribution from $(\partial_\mu \partial_\nu - \frac{1}{4} \omega_{\mu\nu} \omega^{\alpha\beta} \partial_\alpha \partial_\beta) \delta A$, i.e. the fluctuations of the scalar contributions are completely decoupled from the transverse traceless gravitational fluctuations, which is consistent with preliminary results in six-dimensional models [71].

where $\bar{\phi} = \phi + \delta\phi$ and $\bar{\zeta} = \zeta + \delta\zeta$. The only relevant terms for the coupling between tensorial and scalar perturbations are $\varpi^{MN}\bar{\phi}_{,M}\bar{\phi}_{,N}$ and $\varpi^{MN}\bar{\zeta}_{,M}\bar{\zeta}_{,N}$, which once again are evidently null since $\varpi^{MN}\phi_{,M} = \varpi^{MN}\zeta_{,M} = 0$.

Hence, to summarize, the tensorial fluctuations, $\varpi_{\mu\nu}$, are completely decoupled from the scalar perturbations, i.e. δA , $\delta\phi$ and $\delta\zeta$, and the action that drives the dynamics of $\varpi_{\mu\nu}$ can be cast in the form of (3.40), as pointed out in Ref. [71]. In the above context, one can disregard the perturbations of the scalar fields when dealing with the dynamics of gravity [69]. Note that the decoupling of scalar perturbations only happen because we assumed ϖ^{ij} to vanish, in general tensorial perturbations can only couple with scalar perturbations by terms alike $\varpi^{ij}\bar{\phi}_{,i}\bar{\phi}_{,j}$.

3.1.2 The Perturbed Action

In Sec. 2.2, the action for gravity was presented to the zero-th order in ϖ . But to determine the dynamical portion of the perturbations one needs to determine the action to the second order in ϖ . The gravitational portion of the action is given by

$$\bar{S}_g = 2M^4 \int \bar{R}\sqrt{-\bar{g}}d^6x, \quad (3.21)$$

where $\bar{g} = \det(g)$. Thus one is required to calculate the Ricci scalar, \bar{R} , and the metric determinant, \bar{g} , both to second order in ϖ . To achieve one must determine the inverse of the metric and the connections to second order. The inverse metric can be written as

$$\bar{g}^{-1} = e^{2A} \left(\hat{g}^{MN} - \varpi^{MN} + \delta^2 g^{MN} \right) \frac{\partial}{\partial x^M} \otimes \frac{\partial}{\partial x^N}, \quad (3.22)$$

which satisfies

$$\bar{g}_{MD}\bar{g}^{DN} = (\hat{g}_{MD} + \varpi_{MD}) \left(\hat{g}^{DN} - \varpi^{DN} + \delta^2 g^{DN} \right) = \delta_M^N, \quad (3.23)$$

therefore one must have that

$$\delta^2 g^{MN} = \varpi^M{}_D \varpi^{DN} \quad (3.24)$$

The connections on the other hand is given by

$$\begin{aligned} \bar{\Gamma}_{MN}^P = & \hat{\Gamma}_{MN}^P - A_{,N}\delta_M^P - A_{,M}\delta_N^P + A_{,S}\hat{g}^{PS}\hat{g}_{MN} \\ & + A_{,S}\hat{g}^{PS}\varpi_{MN} - A_{,S}\varpi^{PS}\hat{g}_{MN} + (\delta\Gamma)_{MN}^P + \delta^2\Gamma_{MN}^P, \end{aligned} \quad (3.25)$$

where $\delta\Gamma$ are $\delta^2\Gamma$ are tensor fields. The condition of compatibility between the metric and the covariant derivative then implies

$$\bar{\nabla}_P\bar{g}_{MN} = 0 \implies \begin{cases} \hat{\nabla}_P\varpi_{MN} = \hat{g}_{MK}\delta\Gamma_{NP}^K + \hat{g}_{NK}\delta\Gamma_{MP}^K, \\ \hat{g}_{MK}\delta^2\Gamma_{NP}^K + \hat{g}_{NK}\delta^2\Gamma_{MP}^K = -\varpi_{MK}\delta\Gamma_{NP}^K - \varpi_{NK}\delta\Gamma_{MP}^K. \end{cases} \quad (3.26)$$

The first equation is exactly (3.7), and from it we have already isolated $\delta\Gamma_{MN}^P$,

$$\delta\Gamma_{MN}^P = \frac{1}{2}\hat{g}^{PK} \left(\hat{\nabla}_N \varpi_{MK} + \hat{\nabla}_M \varpi_{KN} - \hat{\nabla}_K \varpi_{MN} \right). \quad (3.27)$$

From equation (3.26), one now isolates $\delta^2\Gamma_{MN}^P$ by summing the permutations in a particular order to find

$$\delta^2\Gamma_{MN}^P = \frac{1}{2} \left(\varpi^{-1} \right)^{SK} \left(\hat{\nabla}_N \varpi_{MD} + \hat{\nabla}_M \varpi_{DN} - \hat{\nabla}_D \varpi_{MN} \right). \quad (3.28)$$

All the previous can be substituted in the expression of the Ricci scalar, to find it to second order in ϖ ,

$$\begin{aligned} \bar{R} = e^{2A} \left\{ \hat{R} - \varpi_{PK} \hat{R}^{PK} + \varpi^M{}_D \varpi^{DN} \hat{R}_{MN} + \hat{\nabla}_S \left[\hat{\nabla}_M \varpi^{SM} - \hat{g}^{MN} \hat{\nabla}^S \varpi_{MN} \right. \right. \\ \left. \left. - \hat{g}^{MN} \varpi^{SD} \hat{\nabla}_N \varpi_{MD} + \hat{g}^{SN} \varpi^{PD} \hat{\nabla}_N \varpi_{PD} - \hat{g}^{SN} \varpi^{PD} \hat{\nabla}_D \varpi_{PN} + \hat{g}^{MN} \varpi^{SD} \hat{\nabla}_D \varpi_{MN} \right] \right. \\ \left. - \frac{1}{4} \hat{g}^{MN} \hat{g}^{PS} \hat{\nabla}^K \varpi_{PS} \hat{\nabla}_K \varpi_{MN} + \frac{1}{2} \hat{\nabla}^K \varpi^{MN} \hat{\nabla}_N \varpi_{MK} - \frac{1}{4} \hat{\nabla}^K \varpi^{MN} \hat{\nabla}_K \varpi_{MN} \right. \\ \left. + 10 \left[\hat{\square} A - \frac{1}{2} \hat{g}^{SJ} \hat{g}^{PK} \left(2 \hat{\nabla}_K \varpi_{PJ} - \hat{\nabla}_J \varpi_{PK} \right) A_{,S} - \varpi^{PK} \hat{\nabla}_P \hat{\nabla}_K A + \varpi^P{}_J \varpi^{JK} \hat{\nabla}_P \hat{\nabla}_K A \right. \right. \\ \left. \left. + \frac{1}{2} \hat{g}^{SJ} \varpi^{PK} \left(2 \hat{\nabla}_K \varpi_{PJ} - \hat{\nabla}_J \varpi_{PK} \right) A_{,S} + \frac{1}{2} \hat{g}^{PK} \varpi^{SJ} \left(2 \hat{\nabla}_K \varpi_{PJ} - \hat{\nabla}_J \varpi_{PK} \right) A_{,S} \right] \right. \\ \left. - 20 \left[\hat{g}^{PK} A_{,P} A_{,K} - \varpi^{PK} A_{,P} A_{,K} + \varpi^P{}_J \varpi^{JK} A_{,P} A_{,K} \right] \right\}, \quad (3.29) \end{aligned}$$

On the other hand, the determinant of the metric is given by

$$\begin{aligned} \sqrt{-\bar{g}} &= e^{-6A} \sqrt{-\det[\hat{g}_{MN} + \varpi_{MN}]} = e^{-6A} \sqrt{-\det[\hat{g}_{SN}] \det[\delta_M^S + \hat{g}^{SP} \varpi_{PM}]} \\ &= e^{-6A} \sqrt{-\hat{g}} \sqrt{1 + \varpi^M{}_M - \frac{1}{2} \varpi^{MN} \varpi_{MN} + \frac{1}{2} \varpi^M{}_M \varpi^N{}_N} \\ &= e^{-6A} \sqrt{-\hat{g}} \left(1 + \frac{1}{2} \varpi^M{}_M - \frac{1}{4} \varpi^{MN} \varpi_{MN} + \frac{1}{8} \varpi^M{}_M \varpi^N{}_N \right) \end{aligned} \quad (3.30)$$

Substituting Eqs. (3.29) and (3.30) in action (3.21), then introducing the assumed constraints, $\varpi_{Mi} = A_{,\mu} = 0$, fixing the gauge $\hat{\nabla}^M \varpi_{MN} = \hat{g}^{MN} \varpi_{MN} = 0$ and discarding boundary terms, leads to the gravitational perturbed action

$$S_g = 2M^4 \int d^6x \sqrt{-g} R, \quad (3.31)$$

and

$$\begin{aligned} \delta S_g = 2M^4 \int d^6x e^{-4A} \sqrt{-\hat{g}} \left\{ -\frac{1}{4} \hat{\nabla}^K \varpi^{\mu\nu} \hat{\nabla}_K \varpi_{\mu\nu} - \frac{1}{4} \varpi^{\mu\nu} \varpi_{\mu\nu} \hat{R} - \frac{5}{2} \varpi^{\mu\nu} \varpi_{\mu\nu} \hat{\square} A \right. \\ \left. + 5 \varpi^{\mu\nu} \varpi_{\mu\nu} A^i{}_{,i} + \frac{1}{2} \hat{\nabla}^\kappa \varpi^{\mu\nu} \hat{\nabla}_\nu \varpi_{\mu\kappa} + \varpi^\mu{}_\delta \varpi^{\delta\nu} \hat{R}_{\mu\nu} - \hat{g}^{ij} \varpi^{\mu\nu} \hat{\nabla}_j \varpi_{\mu\nu} A_{,i} \right\}, \quad (3.32) \end{aligned}$$

where S_g represents the zero-th order term, and from it the Planck scale was determined in Sec. 2.2. It is δS_g that contains the dynamical portion of the perturbations. But to

realize the complete formalism one still needs to determine the action for the matter fields, to second order in ϖ , which is given by

$$\begin{aligned}
\bar{S}_M &= \int d^6x \sqrt{-\bar{g}} \left(-\frac{\bar{g}^{MN}}{2} \phi_{,M} \phi_{,N} - \frac{\bar{g}^{MN}}{2} \zeta_{,M} \zeta_{,N} - V \right) \\
&= \int d^6x e^{-6A} \sqrt{-\hat{g}} \left(1 - \frac{1}{4} \varpi^{MN} \varpi_{MN} \right) \left[-\frac{e^{2A} (\hat{g}^{MN} - \varpi^{MN} + \varpi^{MD} \varpi^N_D)}{2} \phi_{,M} \phi_{,N} \right. \\
&\quad \left. - \frac{e^{2A} (\hat{g}^{MN} - \varpi^{MN} + \varpi^{MD} \varpi^N_D)}{2} \zeta_{,M} \zeta_{,N} - V \right] \\
&= \int d^6x e^{-6A} \sqrt{-\hat{g}} \left(1 - \frac{1}{4} \varpi^{MN} \varpi_{MN} \right) \left[-\frac{g^{MN}}{2} \phi_{,M} \phi_{,N} - \frac{g^{MN}}{2} \zeta_{,M} \zeta_{,N} - V \right] \\
&= S_M + \delta S_M,
\end{aligned} \tag{3.33}$$

where one defines

$$S_M = \int d^6x \sqrt{-g} \left[-\frac{g^{MN}}{2} \phi_{,M} \phi_{,N} - \frac{g^{MN}}{2} \zeta_{,M} \zeta_{,N} - V \right], \tag{3.34}$$

and

$$\delta S_M = \int d^6x e^{-6A} \sqrt{-\hat{g}} \frac{1}{4} \varpi^{MN} \varpi_{MN} \left[\frac{g^{MN}}{2} \phi_{,M} \phi_{,N} + \frac{g^{MN}}{2} \zeta_{,M} \zeta_{,N} + V \right]. \tag{3.35}$$

The perturbed portion of the matter action can be better expressed if one employs that

$$\varpi^{MJ} \varpi^D_M T_{JD} = -e^{-2A} \varpi^{MN} \varpi_{NM} \left(\frac{\phi^{,K} \phi_{,K}}{2} + \frac{\zeta^{,K} \zeta_{,K}}{2} + V \right), \tag{3.36}$$

and

$$\varpi^{MJ} \varpi^D_M \frac{T_{JD}}{4M^4} = \varpi^{\mu\kappa} \varpi^\delta_\mu \hat{G}_{\kappa\delta} - 4\varpi^{\mu\nu} \varpi_{\mu\nu} \hat{\square} A + 6\varpi^{\mu\nu} \varpi_{\mu\nu} \hat{g}^{ij} A_{,i} A_{,j}. \tag{3.37}$$

Substituting in the perturbed matter action leads to

$$\delta S_M = -M^4 \int d^6x e^{-4A} \sqrt{-\hat{g}} \left(\varpi^{\mu\kappa} \varpi^\delta_\mu \hat{G}_{\kappa\delta} - 4\varpi^{\mu\nu} \varpi_{\mu\nu} \hat{\square} A + 6\varpi^{\mu\nu} \varpi_{\mu\nu} \hat{g}^{ij} A_{,i} A_{,j} \right). \tag{3.38}$$

Resuming from the total action,

$$\bar{S} = \bar{S}_g + \bar{S}_M = S_g + S_M + \delta S_g + \delta S_M = S + \delta S, \tag{3.39}$$

substituting Eqs. (3.32) and (3.38), imposing a constant curvature space⁷, and discarding boundary terms, one finds the total perturbed action as

$$\begin{aligned}
\delta S &= 2M^4 \int d^6x e^{-4A} \sqrt{-\hat{g}} \left[-\frac{1}{4} \hat{\nabla}^K \varpi^{\mu\nu} \hat{\nabla}_K \varpi_{\mu\nu} - \hat{g}^{ij} \varpi^{\mu\nu} \hat{\nabla}_j \varpi_{\mu\nu} A_{,i} \right. \\
&\quad \left. + \varpi^{\mu\nu} \varpi_{\mu\nu} \left(2A^{,i} A_{,i} - \frac{\Lambda}{6} - \frac{1}{2} \hat{\square} A \right) \right],
\end{aligned} \tag{3.40}$$

which will later select the localized solutions of Eq. (3.17), which namely describe the four-dimensional gravity. Varying action (3.40) with respect to ϖ^{MN} reduces to Eq. (3.17), as expected.

⁷ $\mathcal{R}_{\epsilon\mu\nu\kappa} = \frac{\Lambda}{3} (\omega_{\epsilon\nu} \omega_{\mu\kappa} - \omega_{\epsilon\kappa} \omega_{\mu\nu})$.

3.1.3 The Quantum Mechanical Analogy

Eq. (3.17) can be readily refined by assuming a separation of variables algorithm,

$$\varpi_{\mu\nu} = \sum_{m \in \mathbb{I}} \Phi_m(u, v) \widetilde{\varpi}_{\mu\nu}^m(x^\rho), \quad (3.41)$$

which implies into two equations,

$$(\Delta - m^2) \widetilde{\varpi}_{\mu\nu}^m = 0, \quad (3.42)$$

and

$$\hat{\Delta}^2 \Phi_m - 4\hat{\sigma}^{ij} A_{,i} \Phi_{m,j} = \left(\frac{2\Lambda}{3} - m^2 \right) \Phi_m, \quad (3.43)$$

where $\Delta = \omega^{\alpha\beta} \hat{\nabla}_\alpha \hat{\nabla}_\beta$, $\hat{\Delta}^2 = \hat{\sigma}^{ij} \hat{\nabla}_i \hat{\nabla}_j$ and m^2 is a separation constant.

A simpler form of Eq. (3.43) can be achieved by rescaling the field $\Phi_m = e^{2A} \chi_m$, so as to give

$$-\hat{\Delta}^2 \chi_m + 2 \left(2\hat{\sigma}^{ij} A_{,i} A_{,j} - \hat{\Delta}^2 A \right) \chi_m = \left(m^2 - \frac{2\Lambda}{3} \right) \chi_m, \quad (3.44)$$

which shall be identified with a time independent Schrödinger-like equation in curved space $(\mathbb{B}^2, \hat{\sigma})$, with the energy $E_{QM} = m^2 - 2\Lambda/3$ and the “quantum mechanical” potential

$$V_{QM}(u, v) = 2 \left(2A^i A_{,i} - \hat{\Delta}^2 A \right) = 2 \left[2\hat{\sigma}^{ij} A_{,i} A_{,j} - \frac{1}{\sqrt{\hat{\sigma}}} \left(\sqrt{\hat{\sigma}} \hat{\sigma}^{ij} A_{,i} \right)_{,j} \right]. \quad (3.45)$$

A “flat” Schrödinger-like equation is indeed solely justified for a conformally flat metric ($\bar{f} = \bar{h} = 0 \iff \hat{\sigma} = \gamma$), with $\gamma = \text{diag}(1, 1)$ [69]. Otherwise the curvature of $(\mathbb{B}^2, \hat{\sigma})$ is completely arbitrary, and the curvature intricacies introduce the possibility of some additional localization aspect [69].

The set \mathbb{I} is populated by the eigenvalues of Eq. (3.44), which give the masses of the gravitational fluctuations [69]. If \mathbb{I} does not contain any tachyonic states, i.e. states with imaginary masses ($m^2 < 0$), then the brane model is stable by tensorial perturbations. Otherwise, the configuration may present instabilities.

3.1.4 On the Stability of the Scalar Fields

As identified in previous sections, the scalar field perturbation is completely decoupled from tensorial ones, thus it be addressed separately. If the potential for the scalar fields do not present a local minima, occurrence of instabilities is not discarded [69]. However, the dynamics of the scalar field is not only governed by the potential, but also by the curvature of space, i.e. A , h and f . Thus, even if there not being local minima from \mathcal{V} , stable configurations are possible under particular conditions [69]. As an example, consider models III, IV and V [1]. The scalar field ϕ follows a similar structure to the ones found

in five-dimensional models [81, 82, 83, 1], thus should be stable by extension. Since model *IV* only presents one scalar field (ϕ) it should be stable [69]. On the other hand, scalar field ζ could exhibit instabilities in models *III* and *V*, since potential \mathcal{V} is independent on ζ [69]. But the existence of curvature implies in the constraint equation,

$$\square(\zeta + \delta\zeta) = 0 \implies \hat{\square}(\delta\zeta) - 4\hat{\sigma}^{ij}A_{,i}(\delta\zeta)_{,j} = 0. \quad (3.46)$$

Therefore, the scalar field ζ satisfies the same stability equation (with $\Lambda = 0$) as the gravitational field (cf. Eq. (3.17)), and should be stable if the gravitational field is⁸ [69]. The stability of braneworld models is thus completely determined by the tensorial perturbations [69].

3.1.5 The Effective Action and Localization

The quantum mechanical analogy can be further extended by determining the effective action and analyzing its properties [69]. Following the same algorithm from Eq. (3.41), the action for the perturbations can be written as

$$\begin{aligned} \delta S = 2M^4 \sum_{m_1, m_2 \in \mathbb{I}} \int d^6 x e^{-4A} \sqrt{-\hat{g}} \left\{ -\frac{1}{4} \Phi_{m_1} \Phi_{m_2} \hat{\nabla}^\kappa (\tilde{\omega}_{m_1})^{\mu\nu} \hat{\nabla}_\kappa (\tilde{\omega}_{m_2})_{\mu\nu} \right. \\ \left. - \frac{1}{4} (\tilde{\omega}_{m_1})^{\mu\nu} (\tilde{\omega}_{m_2})_{\mu\nu} \hat{\nabla}^i \Phi_{m_1} \hat{\nabla}_i \Phi_{m_2} - \hat{\sigma}^{ij} \Phi_{m_1} (\tilde{\omega}_{m_1})^{\mu\nu} (\tilde{\omega}_{m_2})_{\mu\nu} \hat{\nabla}_j \Phi_{m_2} A_{,i} \right. \\ \left. + \Phi_{m_1} \Phi_{m_2} (\tilde{\omega}_{m_1})^{\mu\nu} (\tilde{\omega}_{m_2})_{\mu\nu} \left(2A^i A_{,i} - \frac{\Lambda}{6} - \frac{1}{2} \hat{\square} A \right) \right\}, \quad (3.47) \end{aligned}$$

where one has employed the fact that $\hat{\nabla}_i [\Phi_{m_j} (\tilde{\omega}_{m_j})^{\mu\nu}] = (\tilde{\omega}_{m_j})^{\mu\nu} \hat{\nabla}_i \Phi_{m_j}$, which is true because $\hat{\mathbf{g}}$ is factorisable and $\hat{\Gamma}_{j\mu}^\nu$ vanishes. After some straightforward simplifications, Eq. (3.47) can be reduced to

$$\begin{aligned} \delta S = 2M^4 \sum_{m, \tilde{m} \in \mathbb{I}} \int d^2 x \sqrt{\hat{\sigma}} e^{-4A} \Phi_{\tilde{m}} \Phi_m \int d^4 x \sqrt{-\omega} \left\{ -\frac{1}{4} \hat{\nabla}^\kappa (\tilde{\omega}_m)^{\mu\nu} \hat{\nabla}_\kappa (\tilde{\omega}_{\tilde{m}})_{\mu\nu} \right. \\ \left. - \frac{m^2}{4} (\tilde{\omega}_m)^{\mu\nu} (\tilde{\omega}_{\tilde{m}})_{\mu\nu} \right\}, \quad (3.48) \end{aligned}$$

and after rescaling the scalar field by $\Phi_m = e^{2A} \chi_m$, one finds

$$\delta S = -\frac{M^4}{2} \sum_{m, \tilde{m} \in \mathbb{I}} \int d^2 y \sqrt{\hat{\sigma}} \chi_{\tilde{m}} \chi_m \int d^4 x \sqrt{-\omega} \left(\hat{\nabla}^\kappa \tilde{\omega}_m^{\mu\nu} \hat{\nabla}_\kappa \tilde{\omega}_{\tilde{m}}^{\mu\nu} + m^2 \tilde{\omega}_m^{\mu\nu} \tilde{\omega}_{\tilde{m}}^{\mu\nu} \right), \quad (3.49)$$

which corresponds to the same problem driven by Eq. (3.42), if and only if the gravitational modes are

⁸ Similarly, the stability analysis for models *I* and *II* is more intricate, since the potential depends on both ϕ and ζ .

1. Normalizable, i.e. $0 < \int d^2y \sqrt{\hat{\sigma}} \chi_m^2 \neq \infty, \quad \forall m \in \mathbb{I};$
2. Orthogonal, i.e. $\int d^2y \sqrt{\hat{\sigma}} \chi_{\tilde{m}} \chi_m = 0$ if $m \neq \tilde{m}$.

When the above conditions are satisfied, for operators compatible with ω , the action reads

$$\delta S = -\frac{M^4}{2} \sum_{m \in \mathbb{I}} \int d^2y \sqrt{\hat{\sigma}} \chi_m^2 \int d^4x \sqrt{-\omega} \left(\Delta^\kappa \widetilde{\omega}_m^{\mu\nu} \Delta_\kappa \widetilde{\omega}_m^m + m^2 \widetilde{\omega}_m^{\mu\nu} \widetilde{\omega}_m^m \right), \quad (3.50)$$

which does not provide a coupling between the different states $\widetilde{\omega}_{m_i}$. In this scope, variations of action (3.50) lead to the Eq. (3.42). In particular, in higher-dimensional theories there should be as many massive gravitons as can be fit in the set \mathbb{I} , which contains the normalizable states of the Schrödinger equation (3.44) [69].

The requirement of normalizability again ratifies the quantum mechanical analogy. The gravitational modes χ_m must satisfy a Schrödinger-like equation and be normalized in the curved space $(\mathbb{B}^2, \hat{\sigma})$, and the localization of gravity at the vicinity of the brane now becomes contingent on the “quantum mechanical” problem described by Eqs. (3.44) and (3.50) [69]. The problem of locality is then reduced to solving the “quantum mechanical” problem described by Eq. (3.44) according to the normalization condition from Eq. (3.50) [69].

One can also note that the gravitational strength of the gravitation perturbation is directly related to such normalizability,

$$\frac{M^4}{2} \int d^2y \sqrt{\hat{\sigma}} \chi_m^2, \quad (3.51)$$

here this value is of no importance, what really matters is that $\int d^2x \sqrt{\hat{\sigma}} \chi_m^2$ is finite, or in other words, each of the states χ_m are normalizable in the curved space $(\mathbb{B}^2, \hat{\sigma})$. One can understand this condition as follows. If the χ_m were not normalizable the effective gravitational strength G , of such mode, would be zero, then no four-dimensional effective gravitational interaction would happen in the brane, since gravity would not couple to four-dimensional matter, gravity would not look four-dimensional and the graviton would not be “localized” in the brane.

3.1.6 The Newtonian Limit

Rigorously, for thick braneworlds, matter fields should be smeared over the bulk [69]. But, for the sake of simplicity, the gravitational potential will be generated by a point-like source of mass⁹ \mathcal{M} . From a general standpoint, one may write the action of matter fields as

$$S_{\mathcal{M}} = \int d^6x \sqrt{-\bar{g}} \mathcal{L}_{\mathcal{M}}(\Phi, \bar{g}), \quad (3.52)$$

⁹ This same strategy was employed by Ref. [71].

where Φ represents all matter fields. If $\bar{\mathbf{g}} = \mathbf{g} + \boldsymbol{\varpi}$, where $\boldsymbol{\varpi}$ is a perturbation, then the matter action to first order in $\boldsymbol{\varpi}$ takes the form

$$S_{\mathcal{M}} = \int d^6x \sqrt{-g} \mathcal{L}_{\mathcal{M}}(\Phi, \mathbf{g}) + \sum_{m \in \mathbb{I}} \int d^6x e^{-6A} \sqrt{-\hat{g}} \chi_m (\widetilde{\boldsymbol{\varpi}}_m)_{\mu\nu} \frac{T^{\mu\nu}}{2}, \quad (3.53)$$

where $T^{\mu\nu}$ is the stress energy tensor calculated out of $\mathcal{L}_{\mathcal{M}}(\Phi, \mathbf{g})$. On the other hand, if the matter is regarded as a point-like particle of mass \mathcal{M} , then the stress energy tensor is,

$$S_p = \mathcal{M} \int d\tau \sqrt{-g_{MN} \mathbf{v}^M \mathbf{v}^N} \implies T^{MN}(x^Q) = \frac{\mathcal{M} \delta(x^Q - x^P) \mathbf{v}^M(x^P) \mathbf{v}^N(x^P)}{\sqrt{-g}}. \quad (3.54)$$

Therefore, the action of a point-like particle, after substituting (3.54) into (3.53), up to the first order in $\boldsymbol{\varpi}$, is written as

$$\delta S_p = -\frac{\mathcal{M}}{2} \sum_{m \in \mathbb{I}} \int d^6x \chi_m \delta(x^Q - x^P) \widetilde{\boldsymbol{\varpi}}_{\mu\nu}^m \mathbf{v}^\mu \mathbf{v}^\nu. \quad (3.55)$$

where \mathbf{v} represents the velocity of the particle in space-time and x^P is the position in \mathbb{E}^6 . After a re-parameterization of the proper time so to satisfy $\omega_{\mu\nu} \mathbf{v}^\mu \mathbf{v}^\nu = -1$, for a particle at y_0^i , the total action, to the leading order in $\boldsymbol{\varpi}$, becomes

$$\delta S = - \sum_{m \in \mathbb{I}} \left[\frac{M^4}{2} \int d^2y \sqrt{\hat{\sigma}} \chi_m^2 \int d^4x \sqrt{-\omega} \left(\Delta^\kappa \widetilde{\boldsymbol{\varpi}}_m^{\mu\nu} \Delta_\kappa \widetilde{\boldsymbol{\varpi}}_{\mu\nu}^m + m^2 \widetilde{\boldsymbol{\varpi}}_m^{\mu\nu} \widetilde{\boldsymbol{\varpi}}_{\mu\nu}^m \right) + \frac{\mathcal{M}}{2} e^{2A(y_0^i)} \chi_m(y_0^i) \int dx^4 \delta(x^\mu - x^\alpha) \widetilde{\boldsymbol{\varpi}}_{\mu\nu}^m \mathbf{v}^\mu \mathbf{v}^\nu \right], \quad (3.56)$$

where x^α and y_0^i represent the position of the point-like particle in \mathbb{M}^4 and \mathbb{B}^2 , respectively. Varying with respect to $\boldsymbol{\varpi}$ leads to the equations of motion

$$\left(\Delta^2 - m^2 \right) \widetilde{\boldsymbol{\varpi}}_{\mu\nu}^m = \frac{\mathcal{M} e^{2A(y_0^i)} \chi_m(y_0^i) \mathbf{v}_\mu \mathbf{v}_\nu \delta(x^\mu - x^\alpha)}{2M^4 \int d^2y \sqrt{\hat{\sigma}} \chi_m^2 \sqrt{-\omega}}. \quad (3.57)$$

Hence, the Newtonian limit is obtained through the 00 component of Eq. (3.57), with $v^1 = v^2 = v^3 = 0$ and $v^0 = 1/\sqrt{-\omega_{00}}$, for a static particle [69]. Also supposing that the particle finds itself at the center of a system of coordinates ($\mathbf{r} = 0$), the configuration has been stabilized, *i.e.* with $\widetilde{\boldsymbol{\varpi}}$ independent of time, and the space displacements for identifying the Newtonian potential are not of cosmological scale ($\mathbf{r} \sim 1/\sqrt{\Lambda}$) [69]. It allows for setting the approximation $\boldsymbol{\omega} \approx \boldsymbol{\eta}$ so to simplify the equations of motion into the form of

$$\left(\nabla^2 - m^2 \right) \widetilde{\boldsymbol{\varpi}}_{00}^m = \frac{\mathcal{M} e^{2A(y_0^i)} \chi_m(y_0^i)}{2M^4 \int d^2y \sqrt{\hat{\sigma}} \chi_m^2} \delta(\mathbf{r}), \quad (3.58)$$

with the direct solution¹⁰

$$\widetilde{\boldsymbol{\varpi}}_{00}^m = \frac{\mathcal{M} e^{2A(y_0^i)} \chi_m(y_0^i)}{8\pi M^4 \int d^2y \sqrt{\hat{\sigma}} \chi_m^2} \frac{e^{-m\mathbf{r}}}{\mathbf{r}}, \quad (3.59)$$

¹⁰ The solution is true for as long as $m \in \mathbb{R}$, otherwise, *i.e.* $m \in \mathbb{C}$ ($Re(m) = 0$), one would find $\frac{\cos(m\mathbf{r})}{\mathbf{r}}$ instead of $\frac{e^{-m\mathbf{r}}}{\mathbf{r}}$.

so to obtain the Newtonian potential,

$$\phi_N(\mathbf{r}) = \frac{\varpi_{00}(y_0^i, \mathbf{r})}{4} = \sum_{m \in \mathbb{I}} \frac{\mathcal{M} e^{4A(y_0^i)} [\chi_m(y_0^i)]^2 e^{-mr}}{32\pi M^4 \int d^2y \sqrt{\hat{\sigma}} \chi_m^2} \frac{e^{-mr}}{r} \quad (3.60)$$

which can be considered in order to make the connection with the phenomenology of braneworlds [69].

3.2 The Quantum Analogue Problem for Separable Solutions

The prescription of the preceding subsections can be readily particularized to separable solutions. For the geometries described by Eq. (2.47), the quantum problem, Eq. (3.44), is characterized by the equation

$$\begin{aligned} & -e^{\tilde{f}-\tilde{h}} \left(e^{\tilde{f}-\tilde{h}} \chi_{m,u} \right)_{,u} - e^{\hat{h}-\hat{f}} \left(e^{\hat{h}-\hat{f}} \chi_{m,v} \right)_{,v} + 2 \left[2e^{2\tilde{f}-2\tilde{h}} \tilde{A}_{,u}^2 - e^{\tilde{f}-\tilde{h}} \left(e^{\tilde{f}-\tilde{h}} \tilde{A}_{,u} \right)_{,u} \right] \chi_m \\ & + 2 \left[2e^{2\hat{h}-2\hat{f}} \hat{A}_{,v}^2 - e^{\hat{h}-\hat{f}} \left(e^{\hat{h}-\hat{f}} \hat{A}_{,v} \right)_{,v} \right] \chi_m = e^{2\tilde{A}-2\tilde{h}} e^{2\hat{A}-2\hat{f}} \left(m^2 - \frac{2\Lambda}{3} \right) \chi_m. \end{aligned} \quad (3.61)$$

A separation of variables technique, with $\chi_m = e^{\frac{\tilde{f}-\tilde{h}}{2}} \sum_{k \in \mathbb{K}} \tilde{\chi}_k(u) \hat{\chi}_{km}(v)$, can be applied to Eq. (3.61) if:

1. $m = \sqrt{2\Lambda/3}$ (i.e. the zero mode);
2. $\tilde{h} = \tilde{A}$ or $\hat{f} = \hat{A}$.

If $\tilde{h} \neq \tilde{A}$ and $\hat{f} \neq \hat{A}$ the solutions of Eq. (3.61) are not separable unless $m = \sqrt{2\Lambda/3}$, which always has the solution $\chi_0 = be^{-2A}$, as can be seen from Eq. (3.43) [71]. On the other hand, whenever $\tilde{h} = \tilde{A}$ the variables are separable and Eq. (3.61) is reduced to two equations

$$-e^{\tilde{f}-\tilde{A}} \left(e^{\tilde{f}-\tilde{A}} \tilde{\chi}_{mk,u} \right)_{,u} + 2 \left[2e^{2\tilde{f}-2\tilde{A}} \tilde{A}_{,u}^2 - e^{\tilde{f}-\tilde{A}} \left(e^{\tilde{f}-\tilde{A}} \tilde{A}_{,u} \right)_{,u} \right] \tilde{\chi}_{mk} = k^2 \tilde{\chi}_{mk}, \quad (3.62)$$

and

$$\begin{aligned} -\hat{\chi}_{mk,vv} + \left[4\hat{A}_{,v}^2 - 2(\hat{h}-\hat{f})_{,v} \hat{A}_{,v} - 2\hat{A}_{,vv} - \frac{1}{2}(\hat{f}-\hat{h})_{,vv} \right. \\ \left. + \frac{1}{4}(\hat{f}_{,v}-\hat{h}_{,v})^2 + e^{2\hat{f}-2\hat{h}} k^2 \right] \hat{\chi}_{mk} = e^{2\hat{A}-2\hat{h}} \left(m^2 - \frac{2\Lambda}{3} \right) \hat{\chi}_{mk}. \end{aligned} \quad (3.63)$$

The normalization of the gravitational modes is fixed by

$$\int \sqrt{\hat{\sigma}} \chi_m^2 dudv = \sum_{k \in \mathbb{K}} \int e^{\tilde{A}-\tilde{f}} \tilde{\chi}_k^2 du \int e^{2\hat{A}-2\hat{h}} \hat{\chi}_{mk}^2 dv < \infty. \quad (3.64)$$

Eq. (3.62) and the normalization condition for $\tilde{\chi}_k$ are precisely the same as in five dimensions¹¹ [69]. However, Eq. (3.63) represents a distinct problem¹², as it shall be discussed in the following.

¹¹ Since coordinates can always be chosen such that $\tilde{f} = \tilde{A}$.

¹² Unless $\hat{f} = \hat{A}$, which is the case of trivial-like models.

3.2.1 Intersecting-like Models

Following the same procedure, a separation of variables technique can be applied to intersecting-like models if:

1. $m = \sqrt{2\Lambda/3}$ (i.e. the zero mode);
2. $p = 0$ (or $p = 1$) (i.e. for models *III*, *IV*, *V* and *VI*).

Models *I* and *II* will not present separable solutions, thus we will only be concerned with the zero modes for these models. On the other hand, the Schrödinger-like equation for models *III* to *VI* will be separable, but one will not always be able to solve the resulting equations. Solely model *IV* will have its full massive spectrum determined analytically.

3.2.1.1 Intesecting Branes: Models *I* and *II*

As argued before, for the $p \neq 0$ constructions, i.e. models *I* and *II*, one can merely determine the zero modes as, respectively,

$$\chi_0^I = B^I \sqrt{\cosh(2c_u u) \left| \cos\left(\frac{\varphi}{2}\right) \right|}, \quad (3.65)$$

and

$$\chi_0^{II} = B^{II} \sqrt{\left| \cos\left(\frac{\theta}{2}\right) \cos\left(\frac{\varphi}{2}\right) \right|}, \quad (3.66)$$

where B^I and B^{II} are normalization constants. Wave functions (3.65) and (3.66) are normalizable, since

$$\int \sqrt{\hat{\sigma}} (\chi_0^I)^2 dudv = \frac{r (B^I)^2}{2c_u} \frac{\pi \Gamma\left(\frac{p+3}{4}\right) \Gamma\left(\frac{p-2}{4}\right)}{\Gamma\left(\frac{p+5}{4}\right) \Gamma\left(\frac{p}{4}\right)}, \quad (3.67)$$

and

$$\int \sqrt{\hat{\sigma}} (\chi_0^{II})^2 dudv = r \rho (B^{II})^2 \frac{\pi \Gamma\left(\frac{4-p}{4}\right) \Gamma\left(\frac{p+3}{4}\right)}{\Gamma\left(\frac{6-p}{4}\right) \Gamma\left(\frac{p+5}{4}\right)}. \quad (3.68)$$

Additional massive modes are not straightforwardly obtained, thus the corrections to the Newtonian gravity cannot be evaluated. The associated Planck scale M_{pl} is depicted in Fig. 16.

Ordinarily, for brane models, the gravitational scale is controlled by the parameters c_u and c_v . In contrast, the strength of gravity for models *I* and *II* can be set by choosing the parameter p , which can take widely different values when $p \gtrsim 2$, for model *I*, or $p \lesssim 4$, for model *II* [69]. This is relevant when addressing the hierarchy problem, because a large Planck scale can be achieved for any value of c_u and c_v . Unfortunately, model *I* is plagued

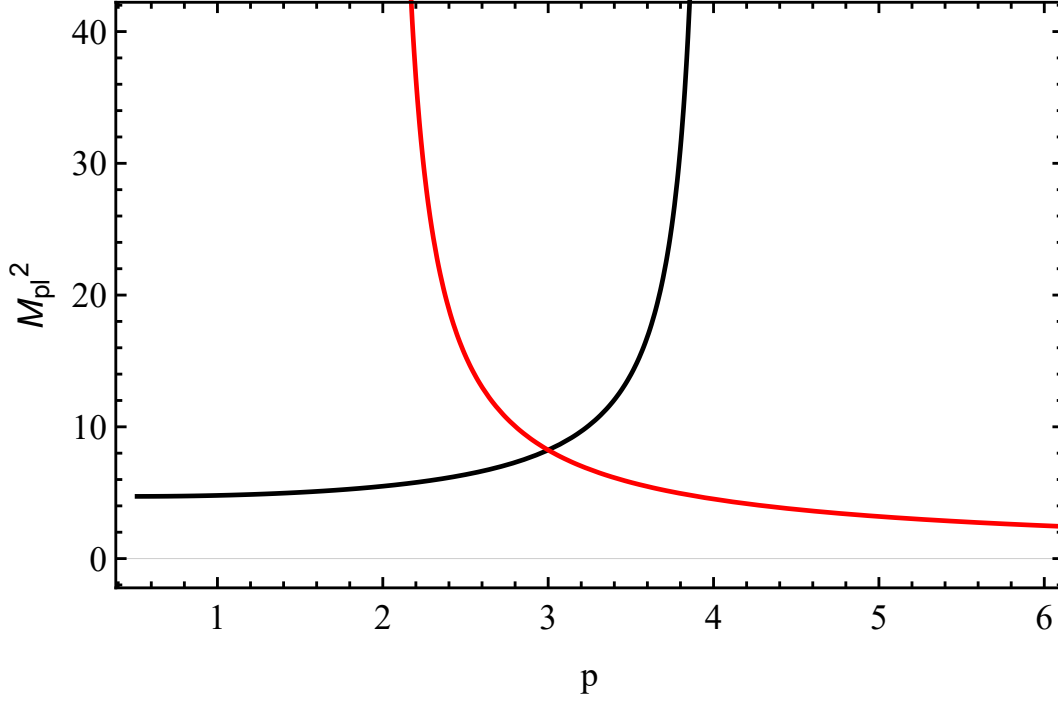


Figure 16 – The Planck scale $M_{pl}^* = 2M_{pl}\sqrt{c_u c_v}/M^2\sqrt{\pi}$ as a function of p . The plots are for model *I* (red line) and *II* (black line).

by several modeling issues: the stress energy tensor has singularities and the total defect energy formation is infinite. Model *II* on the other hand only presents singularities [69].

Even though models *I* and *II* are constructed from the same solution, the transition from one to the other involves redefining c_u from completely real, for model *I*, to completely imaginary, for model *II* [69]. This transition will imply in a discontinuous behavior for any physical constant, as exhibited by the discontinuity depicted in Fig. 16 at the boundary between models *I* and *II* [69]. Except for when $p = 3$, in this case the transition is not discontinuous.

3.2.1.2 Intesecting Branes: Model *III*

Eq. (3.63) for model *III* (represented by metric (2.90)) is expressed by

$$-\hat{\chi}_{mk,vv}^{III} - [C - k^2 + C \sec^2(2\sqrt{C}v)] \hat{\chi}_{mk}^{III} = \frac{m^2 \hat{\chi}_{mk}^{III}}{\sqrt{\cos(2\sqrt{C}v)}}. \quad (3.69)$$

For the general massive case, Eq. (3.69) cannot be straightforwardly integrated, and the unique immediate solution is the zero mode, which is proportional to the warp factor when $k = 0$ [69]. For any k , the zero mode can be written as

$$\hat{\chi}_{0k}^{III} = B_{0k}^{III} \sqrt{\cos(2\sqrt{C}v)} {}_2F_1 \left[\frac{1}{4} \left(1 - \sqrt{1 - \frac{k^2}{C}} \right), \frac{1}{4} \left(1 + \sqrt{1 - \frac{k^2}{C}} \right); 1; \cos^2(2\sqrt{C}v) \right]. \quad (3.70)$$

The hypergeometric component, ${}_2F_1(\alpha, \beta; \gamma; z)$, have arguments such that $\gamma - \alpha - \beta = 1/2$, thus a discontinuity of the first derivatives, at $v = 0$, is only avoidable if either α or β is a non-positive integer $-j$, $j \in \mathbb{N}$ (see Appendix B for further details) [69]. Otherwise, an unphysical discontinuity is identified for the stress energy tensor of the perturbations, since the latter depends on the first derivatives of (3.83) [69]. Therefore, the allowed values of l are given by $l = -j$ or $l = j + 1/2$, both implying into the same results. The first derivative of (3.70) is necessarily discontinuous at $v = 0$, unless the first or second argument of the hypergeometric function, ${}_2F_1$, is a non-positive integer $-j$, $j \in \mathbb{N}$, or $k^2 = -8Cj(2j + 1)$ [69]. This means that $k = 0$ should represent the zero mode for model III, since Eq. (3.62) is of similar structure to the quantum problem of five-dimensional models and thus be expected that $k^2 \geq 0$. Regardless, some of the “possible” degeneracies of the zero mode, for model III, are depicted in Fig. 17 [69].

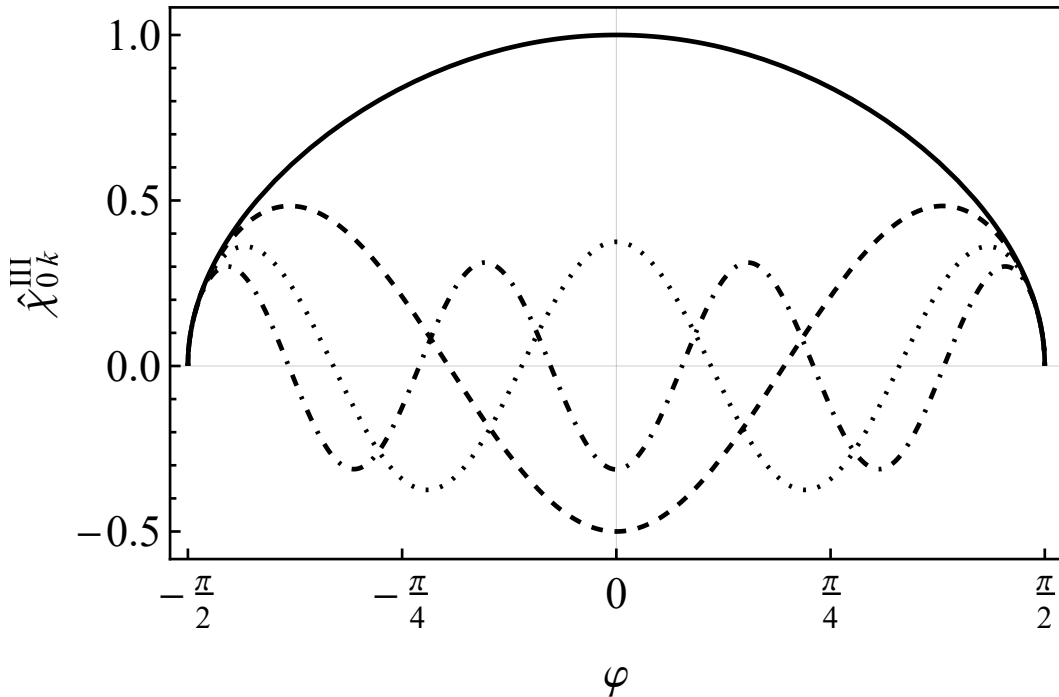


Figure 17 – The degeneracies of the zero mode of model III as functions of $\varphi = 2\sqrt{C}v$ for $j = 0$ (full line), $j = 1$ (dashed line), $j = 2$ (dotted line) and $j = 3$ (dot-dashed line).

Eq. (3.69) can be still more simplified if one makes $C = 0$ and $v = r\varphi$, leading to a trivial extension of five-dimensional models [1],

$$-\hat{\chi}_{mk,\varphi\varphi}^{III} = r^2 (m^2 - k^2) \hat{\chi}_{mk}, \quad (3.71)$$

which results into

$$\hat{\chi}_{mk}^{III} = B \cos(n\varphi), \quad (3.72)$$

where $m^2 = n^2/r^2 + k^2$, B is a normalization constant and one assumes boundary conditions¹³ such that $\hat{\chi}_{mk}^{III} = 0$ at $\varphi = \pm\pi$ [69]. This trivial solution will be important for the sphere models, where one will be able to compare trivial constructions with a more sophisticated configuration, namely that one engendered by model *IV* [69].

3.2.1.3 Intesecting Branes: Model *IV*

To simplify the analysis that follows, it is more convenient to work with coordinates such that

$$v = \frac{2}{\sqrt{C}} \arcsin \left[\tanh \left(\frac{\sqrt{C}y}{2} \right) \right], \quad (3.73)$$

which, from Eq. (2.104), implies into the metric *IV* recasted as

$$g^{IV} = \frac{4\Lambda}{3C} \operatorname{sech}^2 \left(\frac{\sqrt{C}y}{2} \right) e^{-2\tilde{A}} \omega_{\mu\nu} dx^\mu dx^\nu + e^{-2\tilde{A}} du^2 + e^{-2\tilde{A}} \operatorname{sech}^2 \left(\frac{\sqrt{C}y}{2} \right) dy^2. \quad (3.74)$$

and the Schrödinger-like equation (3.63) becomes a Pöschl-Teller equation [86],

$$-\hat{\chi}_{mk,zz}^{IV} - \lambda(\lambda - 1) \operatorname{sech}^2(z) \hat{\chi}_{mk}^{IV} = E \hat{\chi}_{mk}^{IV}, \quad (3.75)$$

where $\lambda = 2\sqrt{1 - \frac{k^2}{C}} + \frac{1}{2}$, $E = \frac{3m^2}{\Lambda} - \frac{17}{4}$ and $z = \sqrt{C}y/2$. The general solution of Eq. (3.75) is

$$\begin{aligned} \hat{\chi}_{mk}^{IV} = & B_1 \cosh^\lambda(z) {}_2F_1 \left[\alpha, \beta; \frac{1}{2}; -\sinh^2(z) \right] \\ & + B_2 \cosh^\lambda(z) \sinh(z) {}_2F_1 \left[\alpha + \frac{1}{2}, \beta + \frac{1}{2}; \frac{3}{2}; -\sinh^2(z) \right], \end{aligned} \quad (3.76)$$

with the parameters $\alpha = \frac{1}{2}(\lambda - \sqrt{-E})$ and $\beta = \frac{1}{2}(\lambda + \sqrt{-E})$. If $0 \leq \lambda \leq 1$ (i.e. $k^2 \geq 15C/16$) or $E > 0$ (i.e. $m^2 > \frac{17}{12}\Lambda$) the above solutions correspond to propagating modes [69]. The existence of singularities at the boundaries of model *IV* makes the propagating modes not unitary [82, 87, 69]. Otherwise, imposing unitary boundary conditions [82, 87, 69] suppresses all propagating modes. In this case, the unitary spectrum shall be composed uniquely of bound states¹⁴ [69].

The normalization condition for $\hat{\chi}_{mk}$, in terms of conformal coordinates (3.73), reads

$$0 < \int_{-\infty}^{\infty} \left(\hat{\chi}_{mk}^{IV} \right)^2 dy \neq \infty. \quad (3.77)$$

Therefore, normalizable modes will exist for $\lambda > 1$ and negative E , where

$$\hat{\chi}_{jk}^{IV+} = B_{jk}^+ \cosh^{2\sqrt{1 - \frac{k^2}{C}} + \frac{1}{2}}(z) {}_2F_1 \left[\frac{1}{2} + j, 2\sqrt{1 - \frac{k^2}{C}} - j; \frac{1}{2}; -\sinh^2(z) \right] \quad (3.78)$$

¹³ With the intent of discarding the $\sin(n\varphi)$ terms.

¹⁴ Because they do not generate any flux into the singularities at the boundaries of space.

represents normalizable even eigenstates, with mass eigenvalues

$$m_{jk}^{IV+} = \sqrt{\frac{\Lambda}{3} \left[\frac{17}{4} - \left(2\sqrt{1 - \frac{k^2}{C}} - \frac{1}{2} - 2j \right)^2 \right]}, \quad 0 \leq j < \sqrt{1 - \frac{k^2}{C}} - \frac{1}{4}; \quad (3.79)$$

and

$$\hat{\chi}_{lk}^{IV-} = B_{lk}^- \cosh^{2\sqrt{1 - \frac{k^2}{C}} + \frac{1}{2}}(z) \sinh(z) {}_2F_1 \left[\frac{3}{2} + l, 2\sqrt{1 - \frac{k^2}{C}} - l; \frac{3}{2}; -\sinh^2(z) \right] \quad (3.80)$$

represents normalizable odd eigenstates, with mass eigenvalues

$$m_{lk}^{IV-} = \sqrt{\frac{\Lambda}{3} \left[\frac{17}{4} - \left(2\sqrt{1 - \frac{k^2}{C}} - \frac{3}{2} - 2l \right)^2 \right]}, \quad 0 \leq l < \sqrt{1 - \frac{k^2}{C}} - \frac{3}{4}; \quad (3.81)$$

where j and l are natural numbers, and B_{jk}^\pm are normalization constants. Some normalizable modes are depicted in Fig. 18. The masses, as described by Eqs. (3.79) and (3.81), are strictly real valued as long as $0 \leq k^2 < 15C/16$, while for imaginary values of k some tachyonic states are allowed [69].

The constant k is defined out of the eigenvalue spectrum of Eq. (3.62), which is exactly the same Schrödinger-like equation, with energy k^2 , of the well known five-dimensional braneworld models [3, 4, 15, 16, 17, 18, 19, 20, 21, 22, 23, 24, 25, 26, 27, 28, 29, 30, 31, 32, 33, 34, 82]. If the warp factor \tilde{A} leads to a stable braneworld configuration, then the eigenvalues of Eq. (3.62) are positively valued, i.e. $k^2 \geq 0$, and model *IV* will be a stable configuration [69].

Interestingly, model *IV* does not have a singular Ricci scalar¹⁵, but it exhibits a mass gap between the zero and massive modes [69]. This is noteworthy because one would expect that a mass gap would imply in singularities of the Ricci scalar, which always happens for five-dimensional models [87]. Thus, one may conjecture that mass gaps and naked singularities are connected, but the singularity might be related with scalar invariants other than the Ricci scalar [69].

3.2.1.4 Intesectioning Branes: Model *V*

Finally, once applied to model *V*, Eq. (3.63) is cast into the form of

$$-\hat{\chi}_{mk,yy}^V + \left[-\frac{1}{4} \sec^2(y) + \cos^{\frac{2}{3}}(y) e^{-2\hat{A}} \frac{k^2}{3|\Lambda|} \right] \hat{\chi}_{mk}^V = \left(\frac{m^2}{3|\Lambda|} + \frac{17}{36} \right) \hat{\chi}_{mk}^V, \quad (3.82)$$

where $y = v\sqrt{3|\Lambda|}$. Fixing $k = 0$ transforms the above result, from Eq. (3.82), into a trigonometric Pöschl-Teller equation, with the straightforward solution identified by

$$\hat{\chi}_{m0}^V = c_1 \sqrt{\cos(y)} {}_2F_1 \left(\frac{1}{4} + \frac{\sqrt{12m^2 + 17|\Lambda|}}{12\sqrt{|\Lambda|}}, \frac{1}{4} - \frac{\sqrt{12m^2 + 17|\Lambda|}}{12\sqrt{|\Lambda|}}; 1; \cos^2(y) \right), \quad (3.83)$$

¹⁵ The singularities at the edges of space are associated with the Kretschmann scalar.

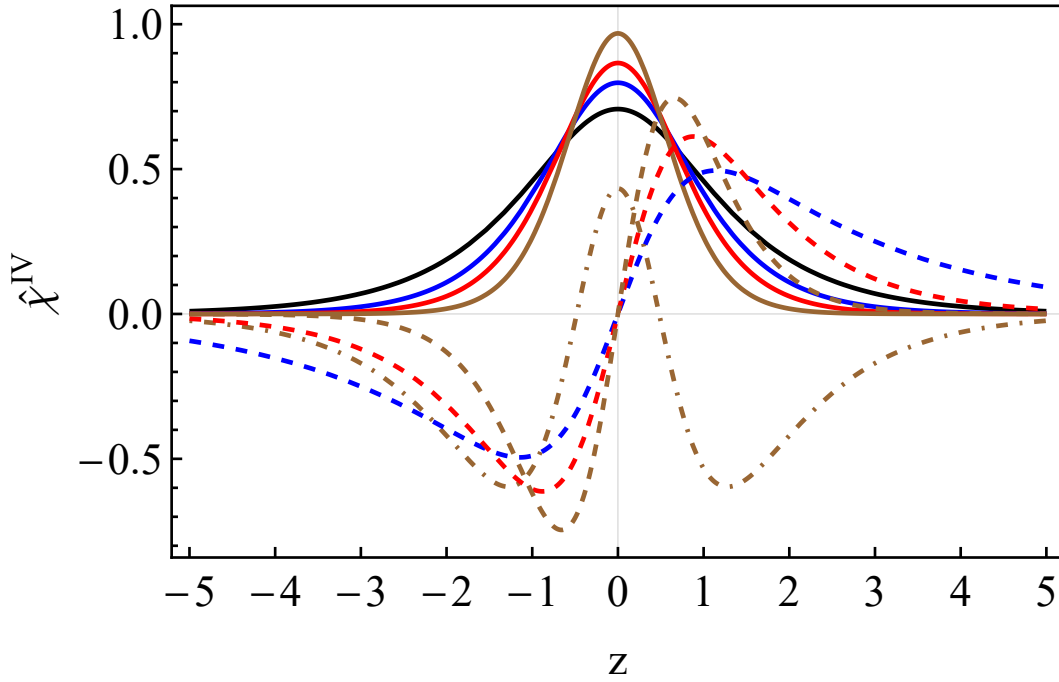


Figure 18 – Normalized gravitational wave functions $\hat{\chi}^{IV}$ for model *IV* as functions of $z = v\sqrt{C}/2$, for $k^2/C = 7/16$ (black lines), $k^2/C = 0$ (blue lines), $k^2/C = -9/16$ (red lines) and $k^2/C = -33/16$ (brown lines). The full, dashed and dot-dashed lines represent $j = 0$, $l = 0$ and $j = 1$, respectively.

The hypergeometric component, ${}_2F_1(\alpha, \beta; \gamma; z)$, have arguments such that $\gamma - \alpha - \beta = 1/2$, thus a discontinuity of the first derivatives, at $v = 0$, is only avoidable if either α or β is a non-positive integer $-j$, $j \in \mathbb{N}$ (see Appendix B for further details) [69]. Otherwise, an unphysical discontinuity is identified for the stress energy tensor of the perturbations, since the latter depends on the first derivatives of (3.83) [69]. Therefore, the allowed values of m are given by

$$m = \sqrt{\frac{2|\Lambda|}{3}} \sqrt{18j^2 + 9j - 1}, \quad (3.84)$$

The normalized profile of the wave function, Eq. (3.83), for several values of j is depicted in Fig. 19 [69]. The zero mode presents a negative eigenvalue, $m^2 = -\sqrt{\frac{2|\Lambda|}{3}}$, and therefore points to a possible instability of model *V*.

3.2.1.5 Intesecting Branes: Model *VI*

The last intersecting braneworld, model *VI*, presents a enhanced Schrödinger-like equation¹⁶,

$$-\chi_{mk,vv} + \left[\left(k^2 - \frac{15C}{16} \right) e^{-2\hat{A}} - \frac{3}{4} \left(\frac{3C}{4} - \Lambda \right) e^{6\hat{A}} \right] \chi_{mk} = \left(m^2 - \frac{17\Lambda}{12} \right) \chi_{mk}, \quad (3.85)$$

¹⁶ Coordinates are chosen such that $\hat{h} = \hat{A}$.

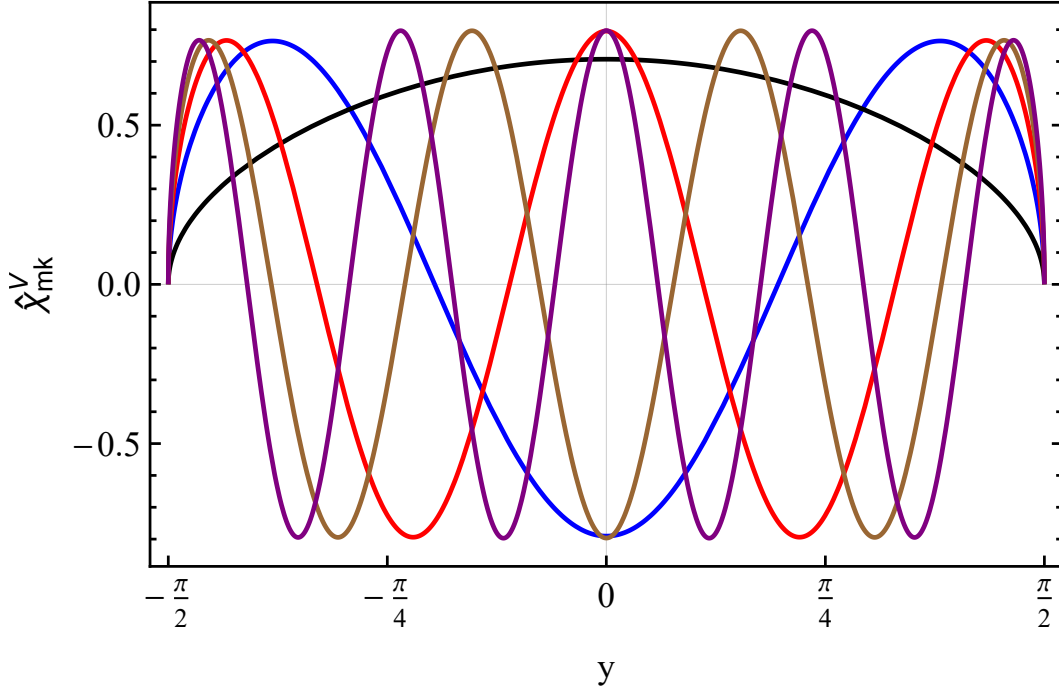


Figure 19 – Normalized gravitational wave functions $\hat{\chi}^V$ for model V as functions of $y = v\sqrt{3|\Lambda|}$, for $j = 0$ (black lines), $j = 1$ (blue lines), $j = 2$ (red lines), $j = 3$ (brown lines) and $j = 4$ (purple lines). The full, dashed and dot-dashed lines represent $j = 0, l = 0$ and $j = 1$, respectively.

which is not of straightforward integration. Yet, the zero mode $\chi_0^{VI} = B_{VI}e^{-2A}$ is a normalizable solution, since

$$\int \sqrt{\hat{\sigma}} (\chi_0^{VI})^2 dudv = B_{VI}^2 \int_0^\infty \frac{e^{-2\hat{A}} d\hat{A}}{\sqrt{\left(\frac{C}{4} - \frac{\Lambda}{3}\right) e^{8\hat{A}} + \frac{\Lambda}{3} e^{2\hat{A}} - \frac{C}{4}}} \int du e^{-\tilde{f}} e^{-3\hat{A}} \quad (3.86)$$

is finite, where B_{VI} is a normalization constant. Massive modes are not straightforwardly obtained, and the corrections to Newtonian theory cannot be determined. The associated Planck scale M_{pl} is depicted in Fig. 5.

3.2.2 The S^2 Models

The sphere models based on models *III* and *IV* [1] are achieved by assuming that $\tilde{A} = -\ln(\sin\theta)$, $\tilde{f} = 0$, $u = r\theta$ and $v = r\varphi$ [69]. Therefore, Eq. (3.62) can be written as

$$-\frac{\left[\sin(\theta) \tilde{\chi}_{k,\theta}^\zeta\right]_{,\theta}}{\sin(\theta)} + \left[\frac{4 + kr^2}{\sin^2(\theta)} - 6\right] \tilde{\chi}_k^\zeta = 0, \quad (3.87)$$

which has the solution

$$\tilde{\chi}_k^\zeta = B_{1k} P_2^{\sqrt{kr^2+4}}(\cos(\theta)) + B_{2k} Q_2^{\sqrt{kr^2+4}}(\cos(\theta)), \quad (3.88)$$

where B_{1k} and B_{2k} are normalization constants.

To avoid singularities and trivial null solutions (which would be non-normalizable), expression (3.88) restricts the possible values of k [69]. More precisely, normalizable modes are exclusively achieved for $k = -3/r^2$ or $k = 0$, which are both depicted in Fig. 20. However, the constant B_{2k} must be fixed to zero, since $Q_2^{\sqrt{kr^2+4}}$ is non-normalizable in this space for all k .

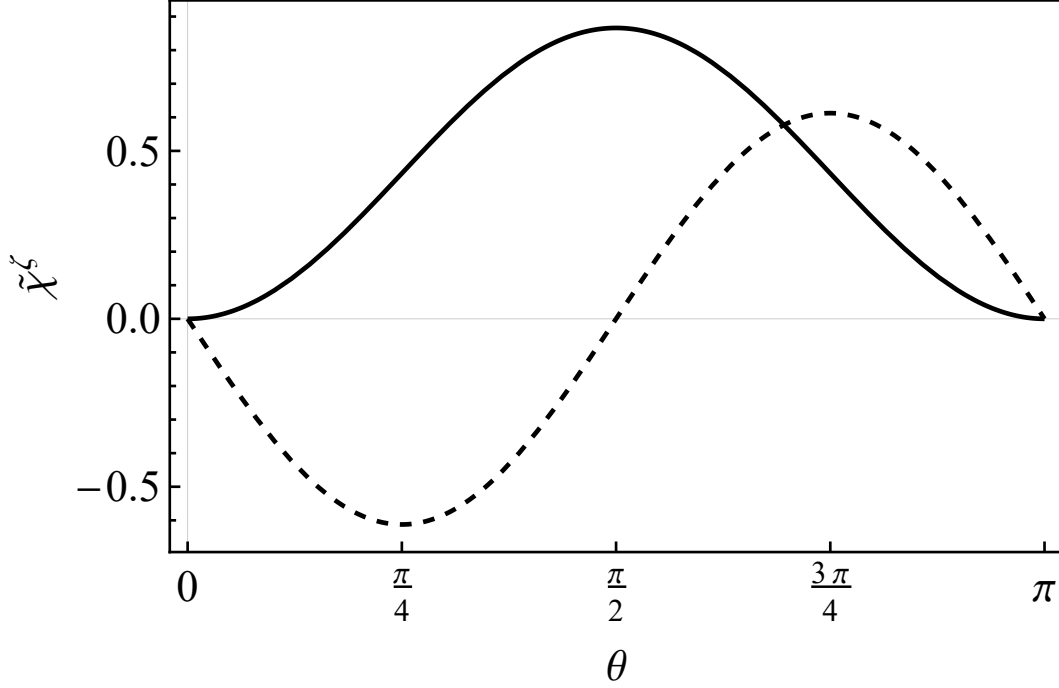


Figure 20 – Normalized gravitational wave functions $\tilde{\chi}_k^\zeta$ for the sphere models, for $k = 0$ (full black line) and $k = -3/r^2$ (black dashed line).

3.2.2.1 Model III ($C = 0$)

Let the sphere models be constructed out of model III, with $C = 0$, which is supported by the metric

$$\mathbf{g}_\zeta^{III} = \sin^2(\theta) \left(\eta_{\mu\nu} dx^\mu dx^\nu + r^2 d\varphi^2 \right) + r^2 d\theta^2. \quad (3.89)$$

The gravitational massive modes are then identified by

$$\chi_{\frac{\sqrt{n^2+3}}{r}}^{III} = B_{n1} \cos(n\varphi) \cos(\theta) \sin(\theta), \quad n \neq 1; \quad (3.90)$$

$$\chi_{\frac{n}{r}}^{III} = B_{n2} \cos(n\varphi) \sin^2(\theta), \quad n \neq 2; \quad (3.91)$$

and

$$\chi_{\frac{2}{r}}^{III} = B_{22} \cos(2\varphi) \sin^2(\theta) + B_{11} \cos(\varphi) \cos(\theta) \sin(\theta). \quad (3.92)$$

In this case, a point-like source, placed at $(\theta = \pi/2, \varphi = 0)$, produces a Newtonian potential¹⁷ of the form

$$\phi_N^{III}(\mathbf{r}) = \frac{3\mathcal{M}}{2^8\pi^2r^2M^4} \frac{1}{r} \left(1 + \frac{2}{e^{\frac{r}{r}} - 1}\right) \approx \begin{cases} \frac{3\mathcal{M}}{2^8\pi^2r^2M^4} \frac{1}{r}, & \text{if } r \gg r \\ \frac{3\mathcal{M}}{2^7\pi^2rM^4} \frac{1}{r^2}, & \text{if } r \ll r \end{cases}. \quad (3.93)$$

Thus, in the region $r \gg r$, the corrections to the Newtonian potential are exponentially suppressed, and one recovers the ordinary Newtonian theory [69]. Likewise, whenever $r \ll r$, the result from (3.93) is dominated by the higher-dimensional term, thus gravity behaves as if the universe was five-dimensional [69]. In summary, the Newtonian potential behaves exactly like in a five-dimensional ADD model [2, 69]. On the other hand, the Newtonian gravitational constant is

$$G_N^{III} = \frac{3}{2^8\pi^2r^2M^4}, \quad (3.94)$$

which is similar to the Newtonian constant as determined from a six-dimensional ADD model [2, 69].

3.2.2.2 Model IV

Model IV with a spherical internal space is characterized by the metric

$$\mathbf{g}_\zeta^{IV_n} = \frac{4r^2\Lambda}{3n^2} \cos^2\left(\frac{n\varphi}{2}\right) \sin^2(\theta) \omega_{\mu\nu}^+ dx^\mu dx^\nu + r^2 d\theta^2 + r^2 \sin^2(\theta) d\varphi^2, \quad (3.95)$$

where $n \in \{1, 2\}$ and represents two distinct configurations of spherical models, which shall be labeled IV_1 and IV_2 , for $n = 1$ and $n = 2$, respectively [69].

Correspondently, two normalizable graviton modes are identified,

$$\chi_{\frac{2\Lambda}{3}}^{IV_1} = B_1 \cos^2\left(\frac{\varphi}{2}\right) \sin^2(\theta), \quad (3.96)$$

and

$$\chi_{\frac{4\Lambda}{3}}^{IV_1} = B_2 \sin\left(\frac{\varphi}{2}\right) \cos^2\left(\frac{\varphi}{2}\right) \sin^2(\theta), \quad (3.97)$$

where B_1 and B_2 are normalization constants, and $\chi_{\frac{2\Lambda}{3}}^{IV_1}$ and $\chi_{\frac{4\Lambda}{3}}^{IV_1}$ represent gravitons of mass $m = \sqrt{2\Lambda/3}$ and $m = 2\sqrt{\Lambda/3}$, respectively. The Newtonian potential associated with model IV_1 is

$$\phi_N^{IV_1}(\mathbf{r}) = \frac{9\mathcal{M}}{2^9r^4\Lambda\pi^2M^4} \frac{e^{-\sqrt{\frac{2\Lambda}{3}}r}}{r} \approx \frac{9\mathcal{M}}{2^9r^4\Lambda\pi^2M^4} \frac{1}{r}, \quad (3.98)$$

¹⁷ Here one assumes that $B_{11} = 0$ for simpler equations.

where the last approximation reinforces our choice of displacements much smaller than the cosmological scale, i.e. $r \ll 1/\sqrt{\Lambda}$. Therefore, as far as the approximations here considered, model IV_1 implies, precisely, in Newton's theory, with the gravitational constant

$$G_N^{IV_1} = \frac{9}{2^9 r^4 \Lambda \pi^2 M^4}, \quad (3.99)$$

which is dependent upon the cosmological constant Λ and the radius r of \mathbb{S}^2 .

On the other hand, a spherical model with $n = 2$ (IV_2) implies into two normalizable gravitational modes:

$$\chi_{\frac{2\Lambda}{3}}^{IV_2} = B_1 \cos^2(\varphi) \sin^2(\theta), \quad (3.100)$$

and

$$\chi_{\frac{4\Lambda}{3}}^{IV_2} = B_2 \sin(\varphi) \cos^2(\varphi) \sin^2(\theta) + B_3 \cos(\varphi) \sin(\theta) \cos(\theta), \quad (3.101)$$

where B_1 , B_2 and B_3 are normalization constants.

The Newtonian potential for such a configuration is expressed by

$$\phi_N^{IV_2}(\mathbf{r}) = \frac{9\mathcal{M}}{2^7 \pi^2 M^4 r^4 \Lambda} \frac{e^{-\sqrt{\frac{2\Lambda}{3}}r}}{r} \approx \frac{9\mathcal{M}}{2^7 \pi^2 M^4 r^4 \Lambda} \frac{1}{r}, \quad (3.102)$$

where, once again, displacement are not of cosmological scale. Therefore model IV_2 also implies in Newtonian theory, with the gravitational constant

$$G_N^{IV_2} = \frac{9}{2^7 \pi^2 M^4 r^4 \Lambda}, \quad (3.103)$$

which is a similar result to that one from model IV_1 .

Had one proposed a more realistic model for matter¹⁸, then Eqs. (3.97) and (3.101) would have significant effects in both the gravitational constant and Newtonian potential, which could imply into significant phenomenological differences between models IV_1 and IV_2 [69]. The same is true for model III : in a more realistic description, Eq. (3.90) would modify Eqs. (3.93) and (3.94).

Just to conclude, considering that the grounds for the above discussed intersecting braneworld models have been established, the localization of scalar, gauge and spinor fields shall be in the core of the subsequent chapter.

¹⁸ Which is outside the scope of the present manuscript.

4 Matter Localization

For any braneworld model to be physically acceptable it ought to recover standard four dimensional physics, at least within reasonable limits [7], and all physical fields must thus be localized in a brane-like region of space. Considering that the grounds for both the classical and quantum gravitational analysis of separable braneworld models have been established, the localization of scalar, gauge and spinor fields shall be in the core of our investigations in this chapter.

Starting from an ordinary six-dimensional action for scalar, gauge and spinor fields, the problem of localization will be reduced to evaluating a quantum analogue problem; the physical fields will present co-dimensional profiles that are normalizable and are solutions of a Schrödinger-like equation, i.e. they constitute wave functions. From the perspective of an observer who believes the universe to be four-dimensional, the now so called four-dimensional observer, the action of six-dimensional fields must be minimized as if they were four-dimensional. Therefore the wave function of any physical field will only contribute to the coupling constants of this four-dimensional effective field theory.

If a physical field wave function is not normalizable, then the effective coupling, after canonical normalization, with other forms of matter would be zero and no coupling would happen in the brane. Since a non-normalizable field does not couple to four-dimensional matter, it would not look four-dimensional and be “localized” in the brane. This idea can be stated precisely by the subsequent definition:

Definition 1 *Let Ψ be a field on the space $(\mathbb{E}^6, \mathbf{g})$. We say that Ψ is “localized” in the 3-Brane (\mathbb{M}^4, ω) if it can be described by a four-dimensional effective field theory, i.e. the scale of Ψ in the 3-Brane is finite.*

In other words, if the setup predicts the scale of a field to be non-finite, i.e. non-normalizable, then it is not localized in the Brane and can not be described effectively in four dimensions. From a physical point of view, a four-dimensional observer will model six-dimensional fields by the localizable modes, and their physical scale determined by the normalization of its associated wave function. For the final objective of this manuscript, the leptons of the SM will be identified with the zero modes of Weyl spinors, and their masses will be determined from their wave functions.

For braneworld models in general, the inherited quantum problem for scalar fields will be of similar nature to the gravitational one, and every conclusion drawn in Ch. 3 can be extended to scalar fields. Gauge fields on the other hand are notoriously difficult to evaluate in a six-dimensional setup. The full massive spectrum is achievable if some

exceptional assumptions are to be made, with the exception of the zero mode which can be determined in more general terms.

Working with $(5 + 1)$ -dimensions indeed is not only constrained to model building, but also to localizing spin $1/2$ particles without introducing additional fields, i.e. through the same warp factor features that results into the gravity localization [64, 66, 67, 73]. In some sense, this is not admitted in $(4 + 1)$ -dimensions where some additional generating mass field mechanisms are required to achieve localization [15, 16, 24, 29, 88, 89, 90, 91, 92]. With the exception of string-like solutions, which are not our main concern, non-interacting Weyl spinors can not be localized in the vicinity of the braneworld. In particular, for Weyl spinors with a charge associated to a gauge field, model *IV* and trivial-like models are shown to give rise to localizable modes.

The chapter is thus organized as follows. In Sec. 4.1, the localization of scalar fields and their similarities to the gravitational field are discussed. Sec. 4.2 is devoted to the localization of gauge fields. Finally, in Sec. 4.3 the localization aspects of fermionic fields are described, and Weyl spinors are shown to be localizable, for intersecting-like braneworlds, if an interacting gauge field is included with a non-trivial co-dimensional profile.

4.1 Scalar Fields

The simplest form of matter is given by a scalar field, but the latter, as shall be argued as follows, satisfies the same equations for localization as the gravitational field. Starting from massless Klein-Gordon field, which is described by the action

$$S_{KG} = \frac{1}{2} \int d^6x \sqrt{-g} \Phi_{,M} \Phi_{,M}, \quad (4.1)$$

and satisfies the equation

$$\frac{1}{\sqrt{-g}} \left[\sqrt{-g} g^{MN} \Phi_{,N} \right]_{,M} = 0. \quad (4.2)$$

Eq. (4.2) can be readily refined by a rescaling by e^{2A} and applying a separation of variables algorithm,

$$\Phi(x^\mu, u, v) = e^{2A} \sum_{m \in \mathbb{I}} \phi_m(x^\mu) \xi_m(u, v), \quad (4.3)$$

which implies into two equations,

$$\frac{\left[\sqrt{-\omega} \omega^{\mu\nu} \phi_{, \mu} \right]_{, \nu}}{\sqrt{-\omega}} = m^2 \phi, \quad (4.4)$$

and

$$-\hat{\Delta}^2 \xi + \left(4\hat{\sigma}^{ij} A_{,i} A_{,j} - 2\hat{\Delta}^2 A \right) \xi = m^2 \xi. \quad (4.5)$$

where $\hat{\Delta}^2 = \hat{\sigma}^{ij} \hat{\nabla}_i \hat{\nabla}_j$ and m^2 is a separation constant. Following the same algorithm from Eq. (4.3), the Klein-Gordon action can be written as

$$S_{KG} = \frac{1}{2} \sum_{m_1, m_2 \in \mathbb{I}} \int d^2x \sqrt{\hat{\sigma}} \xi_{m_1} \xi_{m_2} \int d^4x \sqrt{-\omega} \left(\omega^{\mu\nu} \phi_{m_1, \mu} \phi_{m_2, \nu} + m^2 \phi_{m_1} \phi_{m_2} \right). \quad (4.6)$$

From Eqs. (4.5) and (4.6) it is clear that scalar fields satisfy the same quantum mechanical analogue problem, with the identification $m^2 - 2\Lambda/3 \rightarrow m^2$, as gravity. Therefore the results provided in Ch. 3 faithfully represent the localization aspects of massless Klein-Gordon fields¹, and no further analysis is needed.

4.2 Gauge Fields

The massive modes of gauge fields in six dimensional braneworlds are notoriously difficult to determine, unless some exceptional assumptions are made. On the other hand, the localization of zero modes is of straightforward analysis. Starting from the action of a $U(1)$ gauge field in six dimensions,

$$S_E = -\frac{1}{4} \int d^6x \sqrt{-g} F^2, \quad (4.7)$$

it follows the field equations

$$\nabla_M F^{MN} = 0, \quad (4.8)$$

where $F^2 = F_{MN} F^{MN}$, $F_{MN} = \nabla_{[M} B_{N]} = B_{N,M} - B_{M,N}$ and B_M is the electromagnetic potential. Eq. (4.8) can be broken into two equations, which after some manipulations are given by

$$\Delta_\nu F^{\nu\mu} + \frac{1}{\sqrt{\sigma}} \left[\sqrt{\sigma} \hat{\sigma}^{ji} \omega^{\mu\nu} F_{i\nu} \right]_{,j} = 0, \quad (4.9)$$

and

$$\frac{\hat{\sigma}^{ij}}{\sqrt{-\omega}} \left[\sqrt{-\omega} \omega^{\mu\nu} F_{\nu j} \right]_{,\mu} + \frac{1}{\sqrt{\sigma}} \left[\sqrt{\sigma} \hat{\sigma}^{lk} \hat{\sigma}^{ij} F_{kj} \right]_{,l} = 0. \quad (4.10)$$

The usual quantum mechanical analogy can be applied to gauge fields, but Eqs. (4.9) and (4.10) still lack some refinements that are specific to the type of mode one is describing.

4.2.1 The Zero Mode

A zero mode is thus defined by the solutions of Eqs. (4.9) and (4.10) that satisfies $\Delta_\nu F^{\nu\mu} = 0$ and $B_{i,\mu} = 0$, otherwise the zero mode would not describe an ordinary four dimensional gauge field. Therefore, by definition, the zero mode is described by the equations

$$\frac{1}{\sqrt{\sigma}} \left[\sqrt{\sigma} \hat{\sigma}^{ji} \omega^{\mu\nu} B_{\nu,i} \right]_{,j} = 0, \quad (4.11)$$

¹ Massive Klein-Gordon field could also be considered, but the results are similar to the massless case.

and

$$\frac{\hat{\sigma}^{ij}}{\sqrt{-\omega}} \left[\sqrt{-\omega} \omega^{\mu\nu} \mathbf{B}_{\nu,j} \right]_{,\mu} + \frac{1}{\sqrt{\sigma}} \left[\sqrt{\sigma} \hat{\sigma}^{lk} \hat{\sigma}^{ij} \mathbf{F}_{kj} \right]_{,l} = 0. \quad (4.12)$$

A straightforward solution of Eq. (4.11) is $\mathbf{B}_\nu = B_\nu(x^\mu)$. Finally, the zero mode of a gauge field is thus described by

$$\Delta_\nu F^{\nu\mu} = 0 \text{ and } \frac{1}{\sqrt{\sigma}} \left[\sqrt{\sigma} \hat{\sigma}^{lk} \hat{\sigma}^{ij} \mathbf{F}_{kj} \right]_{,l} = 0, \quad (4.13)$$

which is equivalent to two gauge fields each one living in a four and two dimensional spaces, respectively. One could also include currents J^N to the action, and the same would be true for zero modes.

The normalization of the zero mode is thus a trivial endeavor, since the space-time components of the gauge field \mathbf{B}_μ are independent from the co-dimensions, and the effective action is given by

$$S_E = -\frac{1}{4} \int d^2 y \sqrt{\hat{\sigma}} e^{-2A} \int d^4 x \sqrt{-\omega} F^2, \quad (4.14)$$

where $F^2 = \omega^{\mu\alpha} \omega^{\mu\beta} F_{\mu\nu} F_{\alpha\beta}$ and $F_{\mu\nu} = \Delta_\mu B_\nu - \Delta_\nu B_\mu$. For all braneworlds models build in Ch. 2, the co-dimensional portion of the integral in Eq. (4.14) converges, and the zero mode of gauge fields are localizable.

4.2.2 The Massive Modes

The spectrum of massive modes require an even large refinement: one must assume that the co-dimensional components of the gauge field vanish. Eqs. (4.9) and (4.10) can thus be written as

$$\Delta_\nu F^{\nu\mu} + \frac{1}{\sqrt{\sigma}} \left[\sqrt{\sigma} \hat{\sigma}^{ji} \omega^{\mu\nu} \mathbf{B}_{\mu,i} \right]_{,j} = 0, \quad (4.15)$$

and

$$-\frac{\hat{\sigma}^{ij}}{\sqrt{-\omega}} \left[\sqrt{-\omega} \omega^{\mu\nu} \mathbf{B}_{\nu,j} \right]_{,\mu} = 0. \quad (4.16)$$

Eq. (4.16) can be trivially satisfied by the gauge fixing $\nabla_M \mathbf{B}^M = 0$, and after a separation of variables technique,

$$\mathbf{B}_\mu = e^A \sum_m \phi_m B_\mu^m, \quad (4.17)$$

Eq. (4.15) is reduced to two equations,

$$\Delta_\nu F_m^{\nu\mu} = m^2 \omega^{\mu\nu} B_\nu^m, \quad (4.18)$$

and

$$-\hat{\Delta}^2 \phi_m + \left(\hat{\sigma}^{ji} A_{,j} A_{,i} - \hat{\Delta}^2 A \right) \phi_m = m^2 \phi_m, \quad (4.19)$$

which shall be identified with a time independent Schrödinger-like equation in curved space $(\mathbb{B}^2, \hat{\sigma})$, with the energy $E_{QM} = m^2$ and the “quantum mechanical” potential

$$V_{QM}(u, v) = \hat{\sigma}^{ji} A_{,j} A_{,i} - \hat{\Delta}^2 A. \quad (4.20)$$

On the other hand, the action for the gauge field, once the Eq. (4.17) is applied, can be written as

$$S_E = -\frac{1}{4} \int dy^2 \sqrt{\hat{\sigma}} \phi_m^2 \int d^4x \sqrt{-\omega} F^2 - \frac{1}{2} \int d^6x \sqrt{-g} F_{\mu i} F^{\mu i}, \quad (4.21)$$

thus the normalization is fixed by

$$\int dy^2 \sqrt{\hat{\sigma}} \phi_m^2 < \infty. \quad (4.22)$$

The localization of gauge fields now becomes contingent on the quantum mechanical problem described by Eqs. (4.19) and (4.22). This prescription can be readily particularized to separable solutions. The Schrödinger-like equation, Eq. (4.19), for the geometries described by Eq. (2.47) is characterized by the equation

$$\begin{aligned} & -e^{\tilde{f}-\tilde{h}} \left(e^{\tilde{f}-\tilde{h}} \phi_{m,u} \right)_{,u} - e^{\hat{h}-\hat{f}} \left(e^{\hat{h}-\hat{f}} \phi_{m,v} \right)_{,v} + \left[e^{2\tilde{f}-2\tilde{h}} \tilde{A}_{,u}^2 - e^{\tilde{f}-\tilde{h}} \left(e^{\tilde{f}-\tilde{h}} \tilde{A}_{,u} \right)_{,u} \right] \phi_m \\ & + \left[e^{2\hat{h}-2\hat{f}} \hat{A}_{,v}^2 - e^{\hat{h}-\hat{f}} \left(e^{\hat{h}-\hat{f}} \hat{A}_{,v} \right)_{,v} \right] \phi_m = e^{2\tilde{A}-2\tilde{h}} e^{2\hat{A}-2\hat{f}} m^2 \phi_m. \end{aligned} \quad (4.23)$$

A separation of variables technique, with $\phi_m = e^{\frac{\tilde{f}-\tilde{h}}{2}} \sum_{k \in \mathbb{K}} \tilde{\phi}_k(u) \hat{\phi}_{mk}(v)$, can be applied to Eq. (4.23) if $\tilde{h} = \tilde{A}$ or $\hat{f} = \hat{A}$. Whenever $\tilde{h} = \tilde{A}$ the variables are separable and Eq. (4.23) is reduced to two equations

$$-e^{\tilde{f}-\tilde{A}} \left(e^{\tilde{f}-\tilde{A}} \tilde{\phi}_{k,u} \right)_{,u} + \left[e^{2\tilde{f}-2\tilde{A}} \tilde{A}_{,u}^2 - e^{\tilde{f}-\tilde{A}} \left(e^{\tilde{f}-\tilde{A}} \tilde{A}_{,u} \right)_{,u} \right] \tilde{\phi}_k = k^2 \tilde{\phi}_k, \quad (4.24)$$

and

$$\begin{aligned} & -\hat{\phi}_{mk,vv} + \left[\hat{A}_{,v}^2 - \hat{A}_{,vv} - (\hat{h} - \hat{f})_{,v} \hat{A}_{,v} - \left(\frac{\hat{f} - \hat{h}}{2} \right)_{,vv} \right. \\ & \left. + \frac{1}{4} (\hat{f}_{,v} - \hat{h}_{,v})^2 + k^2 e^{2\hat{f}-2\hat{h}} \right] \hat{\phi}_{mk} = e^{2\hat{A}-2\hat{h}} m^2 \hat{\phi}_{mk}, \end{aligned} \quad (4.25)$$

where k^2 is a separation constant. On the other hand, the normalization is resolved by

$$\sum_{k \in \mathbb{K}} \int du e^{\tilde{A}-\tilde{f}} \tilde{\phi}_k^2 \int dv e^{2\hat{A}-2\hat{h}} \hat{\phi}_{mk}^2 < \infty. \quad (4.26)$$

Finally, the quantum mechanical problem, Eq. (4.25), for model² IV, with coordinate (3.73), is given by the Pöschl-Teller equation,

$$-\hat{\phi}_{mk,zz} - \lambda(\lambda - 1) \operatorname{sech}^2(z) \hat{\phi}_{mk} = \epsilon \hat{\phi}_{mk}. \quad (4.27)$$

where $z = \sqrt{C}y/2$, $\lambda = \sqrt{1 - \frac{4k^2}{C}} + \frac{1}{2}$ and $\epsilon = \frac{3m^2}{\Lambda} - \frac{1}{4}$. If $\epsilon > 0$ ($m^2 > \frac{\Lambda}{12}$) or $0 \leq \lambda \leq 1$ ($k^2 \geq \frac{3C}{16}$) then the solutions of Eq. (4.27) describe propagating modes. Otherwise, the solutions of Eq. (4.27) describe bound states, which are given by

$$\phi_{mk} = C_{mk} \operatorname{sech}^{\lambda-j-1}(y) {}_2F_1 \left(-j, 2\lambda - j - 1; \lambda - j; \frac{e^{-y} \operatorname{sech}(y)}{2} \right), \quad (4.28)$$

² We neglect other intersecting-like models because of their lesser physical appeal.

with the associated eigenvalues

$$m^2 = \frac{\Lambda}{3} \left[\frac{1}{4} - \left(\sqrt{1 - \frac{4k^2}{C}} - \frac{1}{2} - j \right)^2 \right]. \quad (4.29)$$

Therefore gauge fields in model IV possess a unique degenerate³ bound state, for $j = 0$, with mass $m = 0$, since $\lambda \leq 3/2$. A mass gap, $\Delta m^2 = \frac{\Lambda}{12}$, between the zero and massive modes is identified.

4.3 Fermionic Fields

The localization of bulk fermionic matter is usually investigated by considering that the D -dimensional Dirac algebra is realized by the objects $\Gamma^M = \mathbf{e}^M_{\bar{N}} \Gamma^{\bar{N}}$, where $\mathbf{e}^M_{\bar{N}}$ denotes a D -dimensional vielbein, Γ^M satisfy the Clifford relation $\{\Gamma^M, \Gamma^N\} = 2g^{MN} I^j$, I^j is the $j \times j$, with $j = 2^{D/2}$, unitary matrix, and $\Gamma^{\bar{N}}$ are the gamma matrices in D -dimensional flat space-time, i.e. they satisfy the Clifford relation $\{\Gamma^{\bar{M}}, \Gamma^{\bar{N}}\} = 2\eta^{\bar{M}\bar{N}} I^j$. Particularly, in a six dimensional space-time the Dirac matrices are 8×8 ($j = 8$), and the following representation is assumed⁴

$$\Gamma^{\bar{\mu}} = \begin{bmatrix} 0^4 & \gamma^\mu \\ \gamma^\mu & 0^4 \end{bmatrix}, \quad \Gamma^{\bar{4}} = - \begin{bmatrix} 0^4 & \gamma^5 \\ \gamma^5 & 0^4 \end{bmatrix}, \quad \text{and } \Gamma^{\bar{5}} = i \begin{bmatrix} 0^4 & -I^4 \\ I^4 & 0^4 \end{bmatrix}, \quad (4.30)$$

where γ^μ are the usual four dimensional Dirac matrices in the chiral representation, which in the signature $\{-, +, +, +\}$ satisfy $\{\gamma^\mu, \gamma^\nu\} = 2\eta^{\mu\nu} I^4$, and

$$\gamma^5 = i\gamma^0\gamma^1\gamma^2\gamma^3 = \begin{bmatrix} I^2 & 0^2 \\ 0^2 & -I^2 \end{bmatrix} \quad (4.31)$$

is the usual four dimensional chirality matrix. Here the γ^μ are associated with a metric of signature $\{-, +, +, +\}$, and thus are related to $\bar{\gamma}^\mu$, which are associated with a metric of signature $\{+, -, -, -\}$, by the relation $\gamma^\mu = i\bar{\gamma}^\mu$. Therefore, in the chiral representation, the gamma matrices are as follows

$$\gamma^0 = i \begin{bmatrix} 0^2 & I^2 \\ I^2 & 0^2 \end{bmatrix} \quad \text{and } \gamma^k = i \begin{bmatrix} 0^2 & \sigma^k \\ -\sigma^k & 0^2 \end{bmatrix} \quad (4.32)$$

In the (4.30) representation the six dimensional chirality matrix is diagonal

$$\Gamma^{\bar{7}} = \prod_M \Gamma^{\bar{M}} = \begin{bmatrix} I^4 & 0^4 \\ 0^4 & -I^4 \end{bmatrix}, \quad (4.33)$$

therefore the representation (4.30) is also a chiral representation.

³ The zero mode presents some degeneracies associated to the separation constant k .

⁴ The equations that follow are simpler in the representation (4.30).

To realize the Clifford relation in curved space time one defined $\Gamma^M = \mathbf{e}^M_{\bar{N}} \Gamma^{\bar{N}}$, for which $\{\Gamma^M, \Gamma^N\} = 2g^{MN} I^j$. Thus the gamma matrices in curved space time are written in terms of the frame basis, for which

$$g_{MN} = \mathbf{e}_M^{\bar{P}} \mathbf{e}_N^{\bar{Q}} \eta_{\bar{P}\bar{Q}}, \quad (4.34)$$

where the barred symbols, \bar{P} , refer to the frame basis, $\mathbf{e}^{\bar{P}}$, and the non-barred refer to the coordinate basis, ∂_P . The non-barred symbols are raised and lowered by the metric \mathbf{g} , while the barred symbols are raised and lowered by the Minkowski metric $\boldsymbol{\eta}$. For the metrics in the proposed classification, Eq. (2.1), one is able to also define the vielbein associated with a factorizable metric,

$$\hat{g} = \hat{\mathbf{e}}_M^{\bar{P}} \hat{\mathbf{e}}_N^{\bar{Q}} \eta_{\bar{P}\bar{Q}} \quad (4.35)$$

where $\mathbf{e}^{\bar{P}} = e^A \hat{\mathbf{e}}^{\bar{P}}$, such that $\mathbf{e}_M^{\bar{P}} = e^{-A} \hat{\mathbf{e}}_M^{\bar{P}}$ and $\mathbf{e}^{M\bar{P}} = e^A \hat{\mathbf{e}}^{M\bar{P}}$. Supposing that the only non-vanishing components of $\hat{\mathbf{e}}^{\bar{P}}$ are $\hat{\mathbf{e}}_{\mu}^{\bar{\nu}}$ and $\hat{\mathbf{e}}_j^{\bar{i}}$, which is allowed for a metric like Eq. (2.1), then one is able to define

$$\omega_{\mu\nu} = \mathbf{a}_{\mu}^{\bar{\mu}} \mathbf{a}_{\nu}^{\bar{\nu}} \eta_{\bar{\mu}\bar{\nu}} \quad (4.36)$$

$$\sigma_{ij} = \mathbf{b}_i^{\bar{i}} \mathbf{b}_j^{\bar{j}} \gamma_{\bar{i}\bar{j}} \quad (4.37)$$

where $\mathbf{a}_{\mu}^{\bar{\mu}} = \hat{\mathbf{e}}_{\mu}^{\bar{\nu}}$ and $\mathbf{b}_i^{\bar{i}} = e^{-A} \hat{\mathbf{b}}_i^{\bar{i}} = e^{-A} \hat{\mathbf{e}}_i^{\bar{i}} = \mathbf{e}_j^{\bar{i}}$ represent the frame basis vectors components in the coordinate basis ∂_{μ} and ∂_i , respectively, and $\boldsymbol{\gamma} = \text{diag}\{1, 1\}$.

4.3.1 Six-Dimensional Weyl Spinors

The action of a massless spinor in six dimensions can be expressed as

$$S_d = \int d^6x \sqrt{-g} \bar{\Psi}_{(6)} \Gamma^M \nabla_M \Psi_{(6)}, \quad (4.38)$$

where $\bar{\Psi}_{(6)} = \Psi_{(6)}^{\dagger} \Gamma^{\bar{0}}$. Here $\Psi_{(6)}$ is an eight component spinor and may be treated as,

$$\Psi_{(6)} = \begin{bmatrix} \Psi^+ \\ \Psi^- \end{bmatrix} = \Psi_{(6)}^+ + \Psi_{(6)}^-,$$

where $\Psi_{(6)}^{\pm}$ are six dimensional Weyl spinors of different chirality. Varying the action S_d with relation to $\bar{\Psi}_{(6)}$ implies in Dirac equation for 6-dimensional curved space-time,

$$\Gamma^M \nabla_M \Psi_{(6)} = 0. \quad (4.39)$$

The operator ∇_M is a covariant derivative and acts on spinors as

$$\nabla_M \Psi_{(6)} = (\partial_M + \mathbf{C}_M) \Psi_{(6)} \quad (4.40)$$

where \mathfrak{C}_M is the spinor connection of $(\mathbb{E}^6, \mathbf{g})$ and is determined by

$$\mathfrak{C}_M = \frac{1}{4} \mathfrak{C}_M^{\bar{M}\bar{N}} \Gamma_{\bar{M}} \Gamma_{\bar{N}} = \frac{1}{4} \left\{ -\frac{1}{2} \mathfrak{e}_M^{\bar{T}} \mathfrak{e}^{T\bar{R}} \mathfrak{e}^{Q\bar{S}} \partial_{[T} \mathfrak{e}_{Q]\bar{T}} + \frac{1}{2} \mathfrak{e}^{S[\bar{R}} \partial_{[M} \mathfrak{e}_{S]}^{\bar{S}]} \right\} \Gamma_{\bar{R}} \Gamma_{\bar{S}}, \quad (4.41)$$

one can now identify the different components of spin connections of \mathbb{E}^6 with the spin connection constructed from \mathbb{M}^4 and \mathbb{B}^2 , as follows,

$$\mathfrak{C}_\mu = \mathfrak{A}_\mu - \frac{1}{4} A_{,i} \hat{\mathfrak{e}}^{i\bar{j}} \hat{\mathfrak{e}}_\mu^{\bar{\nu}} \left(\Gamma_{\bar{\nu}} \Gamma_{\bar{j}} - \Gamma_{\bar{j}} \Gamma_{\bar{\nu}} \right), \quad (4.42)$$

and

$$\mathfrak{C}_i = \frac{1}{4} \Gamma_{\bar{\tau}} \Gamma_{\bar{s}} \left\{ -\frac{1}{2} \mathfrak{b}_i^{\bar{j}} \mathfrak{b}^{k\bar{r}} \mathfrak{b}^{l\bar{s}} \partial_{[k} \mathfrak{b}_{l]\bar{j}} + \frac{1}{2} \mathfrak{b}^{j[\bar{s}} \partial_{[j} \mathfrak{b}_{i]}^{\bar{r}]} \right\} = \mathfrak{B}_i, \quad (4.43)$$

where \mathfrak{A}_μ is the spin connection related to space-time $(\mathbb{M}^4, \boldsymbol{\omega})$,

$$\mathfrak{A}_\mu = \frac{1}{4} \left\{ -\frac{1}{2} \mathfrak{a}_\mu^{\bar{\tau}} \mathfrak{a}^{\tau\bar{\rho}} \mathfrak{a}^{\eta\bar{\kappa}} \partial_{[\tau} \mathfrak{a}_{\eta]\bar{\tau}} + \frac{1}{2} \mathfrak{a}^{\kappa[\bar{\rho}} \partial_{[\mu} \mathfrak{a}_{\kappa]}^{\bar{\kappa}]} \right\} \Gamma_{\bar{\rho}} \Gamma_{\bar{\kappa}}, \quad (4.44)$$

and \mathfrak{B}_i is the spin connection related to the internal space $(\mathbb{B}^2, \boldsymbol{\sigma})$. Substituting Eqs. (4.42) and (4.43) in to Eq. (4.39) implies in

$$\left(\hat{\mathfrak{e}}^\mu_{\bar{\nu}} \Gamma^{\bar{\nu}} \hat{\nabla}_\mu + \mathcal{D}^{\bar{i}} \Gamma_{\bar{i}} \right) \Psi_{(6)} = 0, \quad (4.45)$$

where one defines the operators

$$\mathcal{D}^{\bar{u}} = e^{-A} e^f \left(\partial_u - 2A_{,u} - \frac{1}{2} h_{,u} \right) \text{ and } \mathcal{D}^{\bar{v}} = e^{-A} e^h \left(\partial_v - 2A_{,v} - \frac{1}{2} f_{,v} \right). \quad (4.46)$$

Since Eq. (4.45) does not provide a mass for the spinors, then one can separate the equations in the different chiralities,

$$\left(\hat{\mathfrak{e}}^\mu_{\bar{\nu}} \gamma^{\bar{\nu}} \hat{\nabla}_\mu - \mathcal{D}^{\bar{u}} \gamma^5 + i\mathcal{D}^{\bar{v}} \right) \Psi^+ = 0, \quad (4.47)$$

and

$$\left(\hat{\mathfrak{e}}^\mu_{\bar{\nu}} \gamma^{\bar{\nu}} \hat{\nabla}_\mu - \mathcal{D}^{\bar{u}} \gamma^5 - i\mathcal{D}^{\bar{v}} \right) \Psi^- = 0. \quad (4.48)$$

One can apply chiral splitting and a separation of variable technique,

$$\Psi_\pm = \sum_m \left[\begin{array}{l} L_m^\pm(u, v) \psi_{m\pm}^L(x^\mu) \\ R_m^\pm(u, v) \psi_{m\pm}^R(x^\mu) \end{array} \right] = \sum_m \left[L_m^\pm(u, v) \Psi_{m\pm}^L(x^\mu) + R_m^\pm(u, v) \Psi_{m\pm}^R(x^\mu) \right], \quad (4.49)$$

to Eqs. (4.47) and (4.48), implying in

$$\hat{\gamma}^\mu \hat{\nabla}_\mu \Psi_{m\pm}^L = m_\pm \Psi_{m\pm}^R \text{ and } \hat{\gamma}^\mu \hat{\nabla}_\mu \Psi_{m\pm}^R = m_\pm \Psi_{m\pm}^L, \quad (4.50)$$

and for the co-dimensional components

$$m_\pm R_m^\pm - \mathcal{D}^{\bar{u}} L_m^\pm \pm i\mathcal{D}^{\bar{v}} L_m^\pm = 0, \quad (4.51)$$

and

$$m_\pm L_m^\pm + \mathcal{D}^{\bar{u}} R_m^\pm \pm i\mathcal{D}^{\bar{v}} R_m^\pm = 0. \quad (4.52)$$

The positive and negative expressions in Eqs. (4.51) and (4.52) are exactly the same, one just needs to identify $m = m_+ = m_-$, $R_m = R_m^+ = L_m^-$ and $L_m = L_m^+ = -R_m^-$. Therefore, one needs to solve either the positive or the negative version of Eqs. (4.51) and (4.52). A Schrödinger-like equation can be thus accomplished for the left and right-handed modes of spinors⁵, respectively, as

$$m^2 R_m + \mathcal{D}^{\bar{u}} \mathcal{D}^{\bar{u}} R_m + i [\mathcal{D}^{\bar{u}}, \mathcal{D}^{\bar{v}}] R_m + \mathcal{D}^{\bar{v}} \mathcal{D}^{\bar{v}} R_m = 0, \quad (4.53)$$

and

$$m^2 L_m + \mathcal{D}^{\bar{u}} \mathcal{D}^{\bar{u}} L_m - i [\mathcal{D}^{\bar{u}}, \mathcal{D}^{\bar{v}}] L_m + \mathcal{D}^{\bar{v}} \mathcal{D}^{\bar{v}} L_m = 0, \quad (4.54)$$

where $[\mathcal{D}^{\bar{u}}, \mathcal{D}^{\bar{v}}] = \mathcal{D}^{\bar{u}} \mathcal{D}^{\bar{v}} - \mathcal{D}^{\bar{v}} \mathcal{D}^{\bar{u}}$, which generally does not vanish.

On the other hand, the action for spinors is given by

$$\begin{aligned} S_d &= \int d^6 x \sqrt{-g} \bar{\Psi}_{(6)} \Gamma^M \nabla_M \Psi_{(6)} \\ &= \int d^6 x \sqrt{-\omega} \sqrt{\hat{\sigma}} e^{-5A} \Psi_-^\dagger \gamma^{\bar{0}} \left(\hat{\epsilon}^\mu_{\bar{\nu}} \hat{\nabla}_\mu \gamma^{\bar{\nu}} \Psi_- - \mathcal{D}^{\bar{4}} \gamma^{\bar{5}} \Psi_- - i \mathcal{D}^{\bar{5}} \Psi_- \right) \\ &\quad + \int d^6 x \sqrt{-\omega} \sqrt{\hat{\sigma}} e^{-5A} \Psi_+^\dagger \gamma^{\bar{0}} \left(\hat{\epsilon}^\mu_{\bar{\nu}} \hat{\nabla}_\mu \gamma^{\bar{\nu}} \Psi_+ - \mathcal{D}^{\bar{4}} \gamma^{\bar{5}} \Psi_+ + i \mathcal{D}^{\bar{5}} \Psi_+ \right). \end{aligned} \quad (4.55)$$

Applying chiral splitting, a separation of variables techniques, Eq. (4.49), and Eqs. (4.51) and (4.52) implies in

$$\begin{aligned} S_d &= \sum_{\bar{m}} \sum_m \int d^2 y \sqrt{\hat{\sigma}} e^{-5A} \bar{R}_{\bar{m}+} R_{m+} \int d^4 x \sqrt{-\omega} \bar{\Psi}_{\bar{m}+}^R \left(\hat{\gamma}^\mu \hat{\nabla}_\mu \Psi_{m+}^R - m_\pm \Psi_{m+}^L \right) \\ &\quad + \sum_{\bar{m}} \sum_m \int d^2 y \sqrt{\hat{\sigma}} e^{-5A} \bar{L}_{\bar{m}+} L_{m+} \int d^4 x \sqrt{-\omega} \bar{\Psi}_{\bar{m}+}^L \left(\hat{\gamma}^\mu \hat{\nabla}_\mu \Psi_{m+}^L - m_\pm \Psi_{m+}^R \right) \\ &\quad + \sum_{\bar{m}} \sum_m \int d^2 y \sqrt{\hat{\sigma}} e^{-5A} \bar{R}_{\bar{m}-} R_{m-} \int d^4 x \sqrt{-\omega} \bar{\Psi}_{\bar{m}-}^R \left(\hat{\gamma}^\mu \hat{\nabla}_\mu \Psi_{m-}^R - m_\pm \Psi_{m-}^L \right) \\ &\quad + \sum_{\bar{m}} \sum_m \int d^2 y \sqrt{\hat{\sigma}} e^{-5A} \bar{L}_{\bar{m}-} L_{m-} \int d^4 x \sqrt{-\omega} \bar{\Psi}_{\bar{m}-}^L \left(\hat{\gamma}^\mu \hat{\nabla}_\mu \Psi_{m-}^L - m_\pm \Psi_{m-}^R \right), \end{aligned} \quad (4.56)$$

where $\bar{\Psi} = \Psi^\dagger \gamma^{\bar{0}}$. Action (4.56) corresponds to the same problem driven by Eq. (4.50) if and only if the modes are orthonormal, i.e.

$$\int d^2 y \sqrt{\hat{\sigma}} e^{-5A} \bar{R}_{\bar{m}} R_m = \delta_{\bar{m}m} \quad \text{and} \quad \int d^2 y \sqrt{\hat{\sigma}} e^{-5A} \bar{L}_{\bar{m}} L_m = \delta_{\bar{m}m}, \quad (4.57)$$

with weight $\sqrt{\hat{\sigma}} e^{-5A}$. When the above condition is satisfied the effective action reads

$$S_d = \sum_{m \in \mathbb{I}} \int d^4 x \sqrt{-\omega} \left[\bar{\Psi}_m^+ \left(\hat{\gamma}^\mu \hat{\nabla}_\mu \Psi_m^+ - m \Psi_m^+ \right) + \bar{\Psi}_m^- \left(\hat{\gamma}^\mu \hat{\nabla}_\mu \Psi_m^- - m \Psi_m^- \right) \right]. \quad (4.58)$$

Therefore each one of the six dimensional Weyl spinors, $\Psi_{(6)}^\pm$, can be reduced to several four dimensional Dirac spinors with mass $m \in \mathbb{I}$. So far no charge with relation to some gauge field has been included to six dimensional spinors, therefore no difference between

⁵ For the zero modes one does not need any refinement, Eqs. (4.51) and (4.52) can be solved as presented.

the different chiral fermions have arisen. Eqs. (4.53), (4.54) and (4.57) establishes the quantum mechanical analogue problem for Weyl spinors. One now apply Eqs. (4.53), (4.54) and (4.57) to separable solutions, and to each one of the sets in the proposed classification of Ch. 2.

For separable solutions the quantum mechanical analogue problem, after a rescaling of the wave functions $R_m = e^{\frac{3}{2}A} e^{\frac{f+h}{2}} \mathcal{R}_m$ and $L_m = e^{\frac{3}{2}A} e^{\frac{f+h}{2}} \mathcal{L}_m$, and choosing coordinates such that $\tilde{f} = \tilde{A}$ and $\tilde{h} = \tilde{A}$, is summarized by the equations

$$m^2 \mathcal{R}_m + e^{2\tilde{f}-2\tilde{A}} \mathcal{R}_{m,uu} + e^{2\tilde{h}-2\tilde{A}} \mathcal{R}_{m,vv} + i \frac{(e^{\tilde{h}-\tilde{A}})_{,u}}{e^{\tilde{A}-\tilde{f}}} \mathcal{R}_{m,v} - i \frac{(e^{\tilde{f}-\tilde{A}})_{,v}}{e^{\tilde{A}-\tilde{h}}} \mathcal{R}_{m,u} = 0, \quad (4.59)$$

$$m^2 \mathcal{L}_m + e^{2\tilde{f}-2\tilde{A}} \mathcal{L}_{m,uu} + e^{2\tilde{h}-2\tilde{A}} \mathcal{L}_{m,vv} - i \frac{(e^{\tilde{h}-\tilde{A}})_{,u}}{e^{\tilde{A}-\tilde{f}}} \mathcal{L}_{m,v} + i \frac{(e^{\tilde{f}-\tilde{A}})_{,v}}{e^{\tilde{A}-\tilde{h}}} \mathcal{L}_{m,u} = 0, \quad (4.60)$$

and

$$\int d^2 y \bar{\mathcal{R}}_{\tilde{m}} \mathcal{R}_m = \delta_{\tilde{m}m} \text{ and } \int d^2 y \bar{\mathcal{L}}_{\tilde{m}} \mathcal{L}_m = \delta_{\tilde{m}m}. \quad (4.61)$$

A separation of variables technique can solely be applied to Eqs. (4.59) and (4.60) if either $\tilde{h} = \tilde{A}$ or $\tilde{f} = \tilde{A}$. Suppose a model for which $\tilde{h} = \tilde{A}$, which is true for most sets of the classification, then Eqs. (4.59) and (4.60) become

$$m^2 \mathcal{R}_m + e^{2\tilde{f}-2\tilde{A}} \mathcal{R}_{m,uu} + \mathcal{R}_{m,vv} - i (e^{\tilde{f}-\tilde{A}})_{,v} \mathcal{R}_{m,u} = 0, \quad (4.62)$$

and

$$m^2 \mathcal{L}_m + e^{2\tilde{f}-2\tilde{A}} \mathcal{L}_{m,uu} + \mathcal{L}_{m,vv} + i (e^{\tilde{f}-\tilde{A}})_{,v} \mathcal{L}_{m,u} = 0. \quad (4.63)$$

Clearly there is not potential to localize the wave functions in the u direction, therefore one must assume it to be compactified as a circle, such that $u = r\theta$, where $\theta \in \mathbb{S}^1$. Finally one can apply a separation of variables,

$$\mathcal{R}_m = \sum_k e^{ik\theta} \hat{\mathcal{R}}_{mk}(v), \quad (4.64)$$

and

$$\mathcal{L}_m = \sum_k e^{ik\theta} \hat{\mathcal{L}}_{mk}(v), \quad (4.65)$$

which after substitution in Eqs. (4.62) and (4.63) implies in the Schrödinger-like equations

$$-\hat{\mathcal{R}}_{mk,vv} + \left[e^{2\tilde{f}-2\tilde{A}} \frac{k^2}{r^2} - (e^{\tilde{f}-\tilde{A}})_{,v} \frac{k}{r} \right] \hat{\mathcal{R}}_{mk} = m^2 \hat{\mathcal{R}}_{mk}, \quad (4.66)$$

and

$$-\hat{\mathcal{L}}_{mk,vv} + \left[e^{2\tilde{f}-2\tilde{A}} \frac{k^2}{r^2} + (e^{\tilde{f}-\tilde{A}})_{,v} \frac{k}{r} \right] \hat{\mathcal{L}}_{mk} = m^2 \hat{\mathcal{L}}_{mk}. \quad (4.67)$$

The previous equations do not intrinsically have the needed structure to localize spinors, even if the space-time has the RS structure. None of the intersecting and trivial-like models

have the needed structure to localize spinors. String-like solutions could lead to localization, but will contradict with the localization of other fields. Model *IV* as an example leads to the equation

$$-\hat{\mathcal{R}}_{mk,vv} + \left[\frac{k^2}{r^2} \operatorname{sech}^2(y) - \operatorname{sech}(y) \tanh(y) \frac{k}{r} \right] \hat{\mathcal{R}}_{mk} = \frac{3m^2}{\Lambda} \hat{\mathcal{R}}_{mk}, \quad (4.68)$$

which does not have localizable solutions. But Weyl spinors are the simplest form of fermions and it is possible that massive or charged fermions could lead to a localization mechanism, the next subsection will propose that the inclusion of a gauge field leads to the localization of fermionic matter.

4.3.2 Six-Dimensional Charged Weyl Spinors

Weyl spinors fail to be localizable in intersecting-like models, thus additional interacting terms must be included if spinors ought to be localizable in the brane. Suppose that a Weyl spinor interacts with some $(0, q)$ -tensor field, with an associated interacting term

$$\mathcal{L}_{int} = \alpha \bar{\Psi} T_{M_1 M_2 \dots M_q} \Gamma^{M_1} \Gamma^{M_2} \dots \Gamma^{M_q} \Psi. \quad (4.69)$$

The equations of motion for Weyl spinors thus become

$$\left[\hat{\mathbf{e}}^\mu_{\bar{\nu}} \Gamma^{\bar{\nu}} \hat{\nabla}_\mu + \mathcal{D}^{\bar{i}} \Gamma_{\bar{i}} + \alpha T_{M_1 M_2 \dots M_q} \Gamma^{M_1} \Gamma^{M_2} \dots \Gamma^{M_q} \right] \Psi = 0,$$

Suppose that q is an even number or zero, thus the interacting term contributes necessarily as

$$\Gamma^{M_1} \Gamma^{M_2} \dots \Gamma^{M_q} \Psi = \Gamma^{M_1} \Gamma^{M_2} \dots \Gamma^{M_q} \begin{bmatrix} \Psi_+ \\ \Psi_- \end{bmatrix} = \begin{bmatrix} (\dots) \Psi_+ \\ (\dots) \Psi_- \end{bmatrix}. \quad (4.70)$$

On the other hand, the dynamical terms in the differential equation contributes as

$$\left(\hat{\mathbf{e}}^\mu_{\bar{\nu}} \Gamma^{\bar{\nu}} \hat{\nabla}_\mu + \mathcal{D}^{\bar{i}} \Gamma_{\bar{i}} \right) \Psi = \left(\hat{\mathbf{e}}^\mu_{\bar{\nu}} \Gamma^{\bar{\nu}} \hat{\nabla}_\mu + \mathcal{D}^{\bar{i}} \Gamma_{\bar{i}} \right) \begin{bmatrix} \Psi_+ \\ \Psi_- \end{bmatrix} = \begin{bmatrix} (\dots) \Psi_- \\ (\dots) \Psi_+ \end{bmatrix}. \quad (4.71)$$

Therefore there will be a coupling between Ψ_+ and Ψ_- , and, after chiral splitting, one finds four coupled differential equations for R^+ , R^- , L^+ and L^- , which will necessarily lead to fourth order differential equations. To avoid having to solve such an enhanced problem, one must restrict q to be odd, which necessarily decouples Ψ_+ and Ψ_- , thus leading to second order differential equations for R^+ , R^- , L^+ and L^- .

The simplest tensorial interaction, for odd q , is with a $U(1)$ gauge field \mathbf{B}_M . The gauge field can thus be interpreted as a curvature to which the fermions couple, exactly like the curvature of space-time. Suppose now a Weyl spinor coupled to a gauge field, \mathbf{B}_M , whose dynamics is governed by the action

$$S_d = \int d^6x \sqrt{-g} \bar{\Psi} \Gamma^M \mathbf{D}_M \Psi, \quad (4.72)$$

where $D_M = \nabla_M - iB_M$. If the gauge field finds itself in a zero mode, i.e. $B_\mu = B_\mu(x^\nu)$ and $B_i = B_i(y^j)$, the calculations to achieve the localization of charged Weyl spinors are similar to the ones performed in Subsec. 4.3.1, and, after applying a separation of variables technique and chiral splitting, one finds the equations

$$m_\pm R_m^\pm - \bar{\mathcal{D}}^{\bar{u}} L_m^\pm \pm i\bar{\mathcal{D}}^{\bar{v}} L_m^\pm = 0, \quad (4.73)$$

and

$$m_\pm L_m^\pm + \bar{\mathcal{D}}^{\bar{u}} R_m^\pm \pm i\bar{\mathcal{D}}^{\bar{v}} R_m^\pm = 0. \quad (4.74)$$

where it is defined

$$\bar{\mathcal{D}}^{\bar{u}} = e^{-A} e^f \left(\partial_u - 2A_{,u} - \frac{1}{2} h_{,u} - iB_u \right), \quad (4.75)$$

and

$$\bar{\mathcal{D}}^{\bar{v}} = e^{-A} e^h \left(\partial_v - 2A_{,v} - \frac{1}{2} f_{,v} - iB_v \right). \quad (4.76)$$

To solve Eqs. (4.73) and (4.74) a separation of variables technique will generally be necessary, which is only achievable if one assumes that $B_v = 0$ and $B_u = B_u(v)$. The zero modes can thus be straightforwardly determined from Eqs. (4.73) and (4.74) for any braneworld model. Take coordinates such that $f = h$ and apply a separation of variables technique to find

$$R_0^\pm = e^{2A} e^{\frac{f}{2}} \sum_k C_k^\pm e^{iku} e^{\mp kv} e^{\pm \int B_u dv} \quad (4.77)$$

and

$$L_0^\pm = e^{2A} e^{\frac{f}{2}} \sum_k D_k^\pm e^{iku} e^{\pm kv} e^{\mp \int B_u dv} \quad (4.78)$$

The normalization condition for the zero modes reads

$$\int d^2y \sqrt{\hat{\sigma}} e^{-5A} \bar{R}_0^\pm R_0^\pm = \sum_{k,l} \bar{C}_l^\pm C_k^\pm \int du \int dv e^{i(k-l)u} e^{A-f} e^{\pm(l+k)v} e^{\pm 2 \int B_u dv} = 1, \quad (4.79)$$

and

$$\int d^2y \sqrt{\hat{\sigma}} e^{-5A} \bar{L}_0^\pm L_0^\pm = \sum_{k,l} \bar{D}_l^\pm D_k^\pm \int du \int dv e^{i(k-l)u} e^{A-f} e^{\pm(l+k)v} e^{\mp 2 \int B_u dv} = 1, \quad (4.80)$$

which can be satisfied at the same time by either R_0^+ and L_0^- , or R_0^- and L_0^+ if the integral of B_u leads to a localized function. Therefore zero modes must take one of two forms,

$$\Psi_0 = \begin{bmatrix} L_0^+ \psi_{0+}^L \\ 0 \\ 0 \\ R_0^- \psi_{0-}^R \end{bmatrix} \quad \text{or} \quad \Psi_0 = \begin{bmatrix} 0 \\ R_0^+ \psi_{0+}^R \\ L_0^- \psi_{0-}^L \\ 0 \end{bmatrix}. \quad (4.81)$$

On the other hand, massive modes are not so straightforward and more assumptions will be necessary to achieve a separation of the co-dimensional variables for Eqs. (4.73)

and (4.74). Once applied the identification $m = m_+ = m_-$, $R_m = R_m^+ = L_m^-$ and $L_m = L_m^+ = -R_m^-$, Eqs. (4.73) and (4.74) can be combined to achieve two Schrödinger-like equations,

$$m^2 R_m + \overline{\mathcal{D}}^{\bar{u}} \overline{\mathcal{D}}^{\bar{u}} R_m + i [\overline{\mathcal{D}}^{\bar{u}}, \overline{\mathcal{D}}^{\bar{v}}] R_m + \overline{\mathcal{D}}^{\bar{v}} \overline{\mathcal{D}}^{\bar{v}} R_m = 0, \quad (4.82)$$

and

$$m^2 L_m + \overline{\mathcal{D}}^{\bar{u}} \overline{\mathcal{D}}^{\bar{u}} L_m - i [\overline{\mathcal{D}}^{\bar{u}}, \overline{\mathcal{D}}^{\bar{v}}] L_m + \overline{\mathcal{D}}^{\bar{v}} \overline{\mathcal{D}}^{\bar{v}} L_m = 0, \quad (4.83)$$

Informed by the previous results in Sec. 4.3.1, one chooses coordinates such that $\tilde{f} = \tilde{A}$ and $\tilde{h} = \tilde{A}$, and a separation of the co-dimensional variables is thus achievable if $\tilde{h} = \tilde{A}$ or $\tilde{f} = \tilde{A}$. Choosing the first, $\tilde{h} = \tilde{A}$, and applying a separation of variables technique,

$$\mathcal{R}_m = \sum_k e^{ik\theta} \hat{\mathcal{R}}_{mk}(v), \quad (4.84)$$

and

$$\mathcal{L}_m = \sum_k e^{ik\theta} \hat{\mathcal{L}}_{mk}(v), \quad (4.85)$$

leads to two Schrödinger-like equations,

$$-\hat{\mathcal{R}}_{mk,vv} + \left[e^{2\tilde{f}-2\tilde{A}} \left(\mathbf{B}_u - \frac{k}{r} \right)^2 - (e^{\tilde{f}-\tilde{A}})_{,v} \frac{k}{r} + (e^{\tilde{f}-\tilde{A}} \mathbf{B}_u)_{,v} \right] \hat{\mathcal{R}}_{mk} = m^2 \hat{\mathcal{R}}_{mk}, \quad (4.86)$$

and

$$-\hat{\mathcal{L}}_{mk,vv} + \left[e^{2\tilde{f}-2\tilde{A}} \left(\mathbf{B}_u - \frac{k}{r} \right)^2 + (e^{\tilde{f}-\tilde{A}})_{,v} \frac{k}{r} - (e^{\tilde{f}-\tilde{A}} \mathbf{B}_u)_{,v} \right] \hat{\mathcal{L}}_{mk} = m^2 \hat{\mathcal{L}}_{mk}, \quad (4.87)$$

where $u = r\theta$, and $\theta \in \mathbb{S}^1$. Eqs. (4.86) and (4.87) can finally be applied to the models previously categorized, with the exception of models *I* and *II* that do not satisfy the condition $\tilde{h} = \tilde{A}$.

4.3.2.1 Trivial-like Models

Once applied to trivial-like models, Eqs. (4.86) and (4.87) are cast as

$$-\hat{\mathcal{R}}_{mk,vv} + \left[\left(\mathbf{B}_u - \frac{k}{r} \right)^2 + \mathbf{B}_{u,v} \right] \hat{\mathcal{R}}_{mk} = m^2 \hat{\mathcal{R}}_{mk}, \quad (4.88)$$

and

$$-\hat{\mathcal{L}}_{mk,vv} + \left[\left(\mathbf{B}_u - \frac{k}{r} \right)^2 - \mathbf{B}_{u,v} \right] \hat{\mathcal{L}}_{mk} = m^2 \hat{\mathcal{L}}_{mk}. \quad (4.89)$$

To realize a simple quantum mechanical potential, the gauge field is assumed to be

$$\mathbf{B}_u = \mathbf{b} \tanh(Cv), \quad (4.90)$$

which once applied to Eqs. (4.88) and (4.89) implies in two Morse-Rosen equations,

$$-\mathbf{R}_{mk,yy} + \left[-\lambda(\lambda - 1) \operatorname{sech}^2(y) - ks \tanh(y) \right] \mathbf{R}_{mk} = \epsilon \mathbf{R}_{mk}, \quad (4.91)$$

and

$$-\mathbf{L}_{mk,yy} + \left[-\lambda(\lambda + 1) \operatorname{sech}^2(y) - ks \tanh(y) \right] \mathbf{L}_{mk} = \epsilon \mathbf{L}_{mk}, \quad (4.92)$$

where $y = Cv$, $\lambda = \frac{\mathbf{b}}{rC}$, $s = \frac{2\lambda}{rC}$, $\epsilon = \frac{m^2}{C^2} - \frac{k^2 s^2}{4\lambda^2} - \lambda^2$ and \mathbf{b} is a real valued constant. The quantum mechanical potential associated with left and right-handed spinors are, respectively,

$$U_R = \left[-\lambda(\lambda - 1) \operatorname{sech}^2(y) - ks \tanh(y) \right], \quad (4.93)$$

and

$$U_L = \left[-\lambda(\lambda + 1) \operatorname{sech}^2(y) - ks \tanh(y) \right]. \quad (4.94)$$

The potentials U_R and U_L , Eqs. (4.93) and (4.94), have an associated global minima⁶ if $\lambda > 1$ and $2\lambda(\lambda - 1) > s|k|$, and $\lambda > 0$ and $2\lambda(\lambda + 1) > s|k|$, respectively. Thus creating the conditions for producing bound states for all real valued s and integer k . The quantum mechanical potential, Eqs. (4.93) and (4.94), of the left and right-handed equations are depicted in Fig. 21.

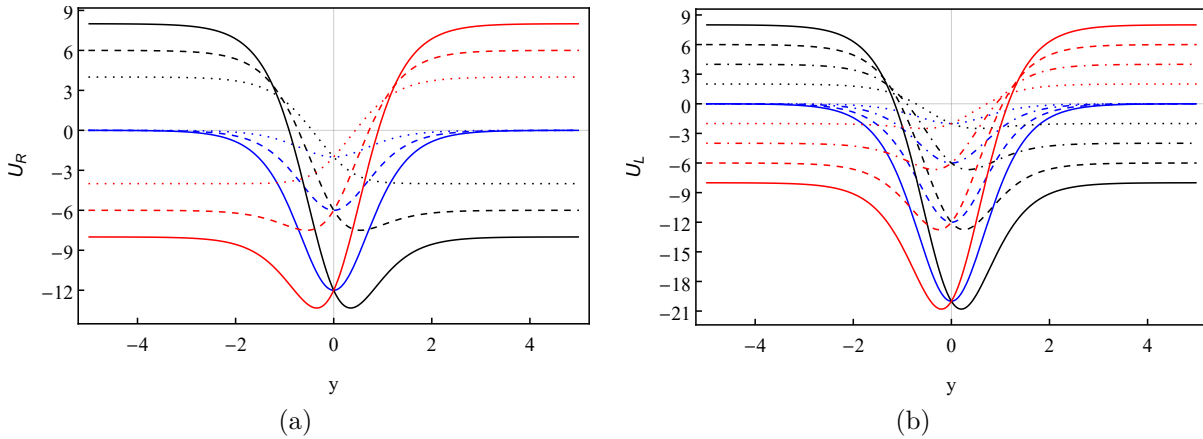


Figure 21 – (a) The quantum mechanical potential associated with right-handed spinors, U_R , for $\lambda = 4$ (solid lines), $\lambda = 3$ (dashed lines) and $\lambda = 2$ (dotted lines). (b) The quantum mechanical potential associated with left-handed spinors, U_L , for $\lambda = 4$ (solid lines), $\lambda = 3$ (dashed lines), $\lambda = 2$ (dot-dashed lines) and $\lambda = 1$ (dotted lines). The plots are for $k = 0$ (blue lines), $k = 1$ (black lines) and $k = -1$ (red lines), with $s = 2$.

The general solution of Eqs. (4.91) and (4.92) are, respectively,

$$\begin{aligned} \mathbf{R}_{mk} = & c_1 \operatorname{sech}^q(y) e^{py} {}_2F_1 \left(q + 1 - \lambda, \lambda + q; q - p + 1; \frac{e^{-y} \operatorname{sech}(y)}{2} \right) \\ & + c_2 \operatorname{sech}^p(y) e^{qy} {}_2F_1 \left(-\lambda + p + 1, \lambda + p; p - q + 1; \frac{e^{-y} \operatorname{sech}(y)}{2} \right), \quad (4.95) \end{aligned}$$

⁶ It is assumed that $\lambda > 0$.

and

$$\begin{aligned} \mathbf{L}_{mk} = & d_1 \operatorname{sech}^q(y) e^{py} {}_2F_1 \left(q - \lambda, \lambda + 1 + q; q - p + 1; \frac{e^{-y} \operatorname{sech}(y)}{2} \right) \\ & + d_2 \operatorname{sech}^p(y) e^{qy} {}_2F_1 \left(-\lambda + p, \lambda + 1 + p; p - q + 1; \frac{e^{-y} \operatorname{sech}(y)}{2} \right), \end{aligned} \quad (4.96)$$

where $q = \frac{\sqrt{\sqrt{\epsilon^2 - k^2 s^2} - \epsilon}}{\sqrt{2}}$ and $p = \operatorname{sign}(k) \frac{\sqrt{-\epsilon - \sqrt{\epsilon^2 - k^2 s^2}}}{\sqrt{2}}$. If $\epsilon \geq -|k|s$ or $m \geq \left| \lambda - \frac{|k|}{rC} \right|$ then Eqs. (4.95) and (4.96) correspond to the propagating modes. Otherwise, for $\epsilon < -|k|s$, the solutions (4.95) and (4.96) leads to the bound states

$$\mathbf{R}_{mk} = c_1 \operatorname{sech}^{\lambda-j-1}(y) e^{\frac{ksy}{2(\lambda-j-1)}} {}_2F_1 \left(-j, 2\lambda - j - 1; \lambda + \frac{ks}{2(\lambda-j-1)} - j; \frac{e^y \operatorname{sech}(y)}{2} \right), \quad (4.97)$$

and

$$\mathbf{L}_{mk} = d_1 \operatorname{sech}^{\lambda-j-1}(y) e^{\frac{ksy}{2(\lambda-j-1)}} {}_2F_1 \left(-j - 1, 2\lambda - j; \lambda + \frac{ks}{2(\lambda-j-1)} - j; \frac{e^y \operatorname{sech}(y)}{2} \right), \quad (4.98)$$

both associated with the mass eigenvalues

$$m = C \frac{\sqrt{(j+1)(2\lambda-j-1)}}{2\lambda(\lambda-j-1)} \sqrt{4\lambda^2(\lambda-j-1)^2 - k^2 s^2}, \quad (4.99)$$

where⁷ j is a natural number. In this way there is always a mass gap between the zero and massive modes, be it the discrete or continuous modes.

4.3.2.2 Intersecting-like Models: Model IV

To readily employ Eqs. (4.86) and (4.87) to model IV it is convenient to work with coordinates such that

$$v = \frac{2}{\sqrt{C}} \arcsin [\tanh(z)], \quad (4.100)$$

which, from Eq. (2.104), implies into the metric IV recasted as

$$g^{IV} = \frac{4\Lambda}{3C} \operatorname{sech}^2(z) e^{-2\tilde{A}} \omega_{\mu\nu} dx^\mu dx^\nu + e^{-2\tilde{A}} du^2 + \frac{4}{C} \operatorname{sech}^2(z) e^{-2\tilde{A}} dz^2. \quad (4.101)$$

A simple quantum mechanical potential is realized if

$$\mathbf{B}_z = B_0 \sinh(z), \quad (4.102)$$

and Eqs. (4.86) and (4.87) can thus be written as

$$\begin{aligned} -\mathbf{R}_{mk,zz} + \left\{ \left[k^2 b^2 - a(a-1) \right] \operatorname{sech}^2(z) \right. \\ \left. + kb(1-2a) \operatorname{sech}(z) \tanh(z) \right\} \mathbf{R}_{mk} = \left(\frac{3m^2}{\Lambda} - a^2 \right) \mathbf{R}_{mk}, \end{aligned} \quad (4.103)$$

⁷ With the exception of the zero mode that is constructed from Eq. (4.98) with $j = -1$.

and

$$-L_{mk,zz} + \left\{ \left[k^2 b^2 - a(a+1) \right] \operatorname{sech}^2(z) - kb(1+2a) \operatorname{sech}(z) \tanh(z) \right\} L_{mk} = \left(\frac{3m^2}{\Lambda} - a^2 \right) L_{mk}, \quad (4.104)$$

where $a = \frac{2eB_0}{\sqrt{C}}$ and $b = \frac{2}{e\sqrt{C}}$. The quantum mechanical potential associated with left and right-handed spinors are, respectively,

$$U_R = \left[kb(1-2a) \operatorname{sech}(z) \tanh(z) - a(a-1) \operatorname{sech}^2(z) + k^2 b^2 \operatorname{sech}^2(z) \right], \quad (4.105)$$

and

$$U_L = \left[-kb(1+2a) \operatorname{sech}(z) \tanh(z) - a(a+1) \operatorname{sech}^2(z) + k^2 b^2 \operatorname{sech}^2(z) \right]. \quad (4.106)$$

The potentials U_R and U_L have an associated global minima for $a > 1$ and $a > 0$, respectively, and they create the conditions for producing bound states for all real valued b and integer k . The quantum mechanical potential, Eqs. (4.105) and (4.106), of the left and right-handed equations are depicted in Fig. 22. If $3m^2 \geq a^2\Lambda$ the solutions of Eqs. (4.103)

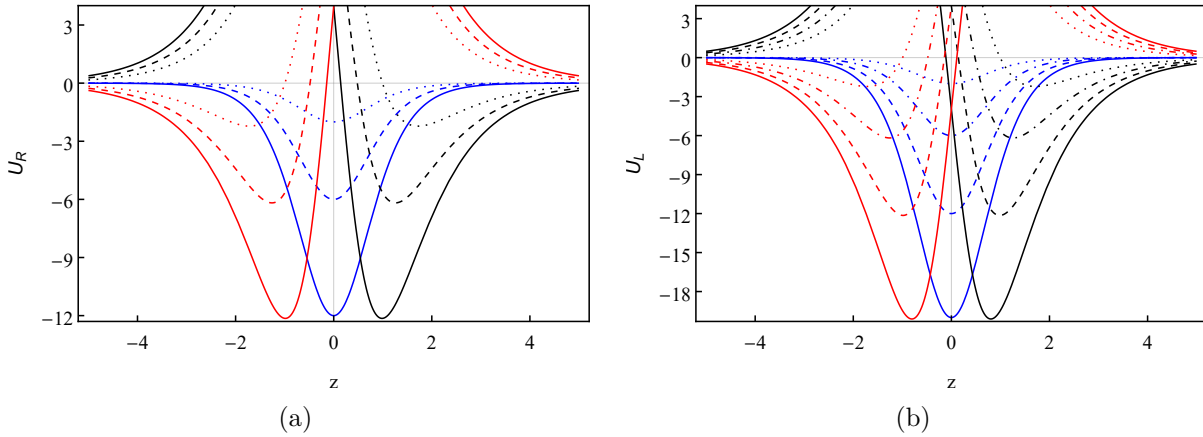


Figure 22 – (a) The quantum mechanical potential associated with right-handed spinors, U_R , for $a = 4$ (solid lines), $a = 3$ (dashed lines) and $a = 2$ (dotted lines). (b) The quantum mechanical potential associated with left-handed spinors, U_L , for $a = 4$ (solid lines), $a = 3$ (dashed lines), $a = 2$ (dot-dashed lines) and $a = 1$ (dotted lines). The plots are for $k = 0$ (blue lines), $k = 1$ (black lines) and $k = -1$ (red lines), with $b = 4$.

and (4.104) correspond to propagating modes, otherwise they are described by bound states. For $k = 0$, Eqs. (4.103) and (4.104) become a Posch-Teller equation, and the bound states can be straightforwardly determined. The general case requires a more intricate analysis. After returning to the departure coordinate v , from Eq. (4.100), thus recasting the metric as (2.104), and rescaling the wavefunctions, $R_{mk} = e^{\frac{\hat{A}}{2}} \hat{\mathcal{R}}_{km}$ and $L_{mk} = e^{\frac{\hat{A}}{2}} \hat{\mathcal{L}}_{km}$, the Schrödinger-like equations, Eqs. (4.103) and (4.104), become a trigonometric Morse-Rosen

equation,

$$-\hat{\mathcal{R}}_{km,yy} + \left\{ \frac{l(l-1)}{4 \cos^2\left(\frac{y}{2}\right)} - kb \left(a - \frac{1}{2}\right) \tan\left(\frac{y}{2}\right) + k^2 b^2 - \frac{1}{4} \left(a - \frac{1}{2}\right)^2 \right\} \hat{\mathcal{R}}_{km} = 0, \quad (4.107)$$

and

$$-\hat{\mathcal{L}}_{km,yy} + \left\{ \frac{l(l-1)}{4 \cos^2\left(\frac{y}{2}\right)} - kb \left(a + \frac{1}{2}\right) \tan\left(\frac{y}{2}\right) + k^2 b^2 - \frac{1}{4} \left(a + \frac{1}{2}\right)^2 \right\} \hat{\mathcal{L}}_{km} = 0, \quad (4.108)$$

where $l = \sqrt{a^2 - \frac{3m^2}{\Lambda}} + \frac{1}{2}$ (or $m = \sqrt{\frac{\Lambda}{3}} \sqrt{a^2 - \left(l - \frac{1}{2}\right)^2}$) and $y = \sqrt{C}v$. The general solution of Eqs. (4.107) and (4.108) are, respectively,

$$\begin{aligned} \hat{\mathcal{R}}_k = & c_1 \left(e^{i\frac{y}{2}}\right)^{a+2ikb-\frac{1}{2}+l} \cos^l\left(\frac{y}{2}\right) {}_2F_1\left(a+l-\frac{1}{2}, l+2ikb; a+2ikb+\frac{1}{2}; -e^{iy}\right) \\ & + c_2 \left(e^{i\frac{y}{2}}\right)^{l-a-2ikb+\frac{1}{2}} \cos^l\left(\frac{y}{2}\right) {}_2F_1\left(l+\frac{1}{2}-a, l-2ikb; \frac{3}{2}-a-2ikb; -e^{iy}\right), \end{aligned} \quad (4.109)$$

and

$$\begin{aligned} \hat{\mathcal{L}}_k = & d_1 \left(e^{i\frac{y}{2}}\right)^{-a-2ikb-\frac{1}{2}+l} \cos^l\left(\frac{y}{2}\right) {}_2F_1\left(l-\frac{1}{2}-a, l-2ikb; \frac{1}{2}-a-2ikb; -e^{iy}\right) \\ & + d_2 \left(e^{i\frac{y}{2}}\right)^{a+2ikb+\frac{1}{2}+l} \cos^l\left(\frac{y}{2}\right) {}_2F_1\left(a+l+\frac{1}{2}, 2ikb+l; a+2kbi+\frac{3}{2}; -e^{iy}\right). \end{aligned} \quad (4.110)$$

The asymptotic behavior of expressions (4.109) and (4.110) at y approaching $\pm\pi$ can be cast as

$$\begin{aligned} \hat{\mathcal{R}}_k \rightarrow & c_1 \left(e^{i\frac{y}{2}}\right)^{a+2ikb-\frac{1}{2}+l} \left[\frac{\cos^l\left(\frac{y}{2}\right) \Gamma(1-2l) \Gamma(2l)}{\Gamma(2ikb+1-l) \Gamma\left(a+\frac{1}{2}-l\right)} \right. \\ & \left. - \left(e^{i\frac{y}{2}}\right)^{1-2l} \frac{2^{1-2l} \cos^{1-l}\left(\frac{y}{2}\right) \Gamma(1-2l) \Gamma(2l)}{\Gamma\left(a+l-\frac{1}{2}\right) \Gamma(l+2ikb)} \right] \\ & + c_2 \left(e^{i\frac{y}{2}}\right)^{-a-2ikb+\frac{1}{2}+l} \left[\frac{\cos^l\left(\frac{y}{2}\right) \Gamma(1-2l) \Gamma(2l)}{\Gamma(1-2ikb-l) \Gamma\left(\frac{3}{2}-a-l\right)} \right. \\ & \left. - \left(e^{i\frac{y}{2}}\right)^{1-2l} \frac{2^{1-2l} \cos^{1-l}\left(\frac{y}{2}\right) \Gamma(1-2l) \Gamma(2l)}{\Gamma\left(l+\frac{1}{2}-a\right) \Gamma(l-2ikb)} \right], \end{aligned} \quad (4.111)$$

and

$$\begin{aligned} \hat{\mathcal{L}}_k \rightarrow & \mathbf{d}_1 \left(e^{i\frac{y}{2}} \right)^{-\mathbf{a}-2ikb-\frac{1}{2}+l} \left[\frac{\cos^l \left(\frac{y}{2} \right) \Gamma(1-2l) \Gamma(2l)}{\Gamma(1-l-2ikb) \Gamma\left(\frac{1}{2}-\mathbf{a}-l\right)} \right. \\ & \left. - \left(e^{i\frac{y}{2}} \right)^{1-2l} \frac{2^{1-2l} \cos^{1-l} \left(\frac{y}{2} \right) \Gamma(1-2l) \Gamma(2l)}{\Gamma\left(l-\frac{1}{2}-\mathbf{a}\right) \Gamma(l-2ikb)} \right] \\ & + \mathbf{d}_2 \left(e^{i\frac{y}{2}} \right)^{\mathbf{a}+2ikb+\frac{1}{2}+l} \left[\frac{\cos^l \left(\frac{y}{2} \right) \Gamma(1-2l) \Gamma(2l)}{\Gamma(1+2ikb-l) \Gamma\left(\mathbf{a}+\frac{3}{2}-l\right)} \right. \\ & \left. - \left(e^{i\frac{y}{2}} \right)^{1-2l} \frac{2^{1-2l} \cos^{1-l} \left(\frac{y}{2} \right) \Gamma(1-2l) \Gamma(2l)}{\Gamma\left(\mathbf{a}+l+\frac{1}{2}\right) \Gamma(2ikb+l)} \right], \quad (4.112) \end{aligned}$$

respectively. Thus, the bound states of Eqs. (4.107) and (4.108) are, respectively, the ones for which⁸ $l = \mathbf{a} - j - \frac{1}{2}$ and $\mathbf{c}_1 = 0$, and $l = \frac{1}{2} + \mathbf{a} - j$ and $\mathbf{d}_2 = 0$, where $j \in \mathbb{N}$. Otherwise, expressions (4.109) and (4.110) will not be normalizable, since the components with $\cos^{1-l} \left(\frac{y}{2} \right)$ of expressions (4.111) and (4.112) will always imply in divergent integrands⁹ for the normalization. Explicitly, the eigenstates of Eqs. (4.107) and (4.108) are, respectively,

$$\hat{\mathcal{R}}_{kj} = \mathbf{c}_{kj} e^{kby-ij\frac{y}{2}} \cos^{\mathbf{a}-j-\frac{1}{2}} \left(\frac{y}{2} \right) {}_2F_1 \left(-j, \mathbf{a} - j - \frac{1}{2} - 2ikb; \frac{3}{2} - \mathbf{a} - 2ikb; -e^{iy} \right), \quad (4.113)$$

and

$$\hat{\mathcal{L}}_{kj} = \mathbf{d}_{kj} e^{[kb-\frac{i(j+1)}{2}]y} \cos^{\mathbf{a}-j-\frac{1}{2}} \left(\frac{y}{2} \right) {}_2F_1 \left(-j-1, \mathbf{a} - j - \frac{1}{2} - 2ikb; \frac{1}{2} - \mathbf{a} - 2ikb; -e^{iy} \right), \quad (4.114)$$

with mass eigenvalues

$$m = \sqrt{\frac{\Lambda}{3}} \sqrt{j+1} \sqrt{2\mathbf{a}-j-1}. \quad (4.115)$$

where $\mathbf{a} > j+1$. A normalizable zero mode is solely achieved for the left-handed expression, from Eq. (4.114) with¹⁰ $j = -1$. Notice that there are left and right-handed normalizable zero modes, because $L_m = L_m^+ = -R_m^-$. Thus, a zero mode can be localized for the positive left-handed spinors, while the right-handed can only be localized for negative ones¹¹.

Finally, returning to the coordinate z , from Eq. (4.100), and rescaling the wave functions, one achieves the bound states of Eqs. (4.103) and (4.104):

$$\begin{aligned} \mathbf{R}_{kj} = & \mathbf{c}_{kj} e^{2kb \arcsin[\tanh(z)]} [\operatorname{sech}(z) - i \tanh(z)]^j \operatorname{sech}^{\mathbf{a}-j-1}(z) \times \\ & \times {}_2F_1 \left(-j, \mathbf{a} - j - \frac{1}{2} - 2ikb; 2\mathbf{a} - 2j - 1; 1 + [\operatorname{sech}(z) + i \tanh(z)]^2 \right), \quad (4.116) \end{aligned}$$

⁸ It is assumed that $\mathbf{a} > 0$.

⁹ This is true because the normalization in this coordinates involve $\cos^{-2} \left(\frac{y}{2} \right)$ as an integration weight.

¹⁰ To achieve Eq. (4.114) the integer j was redefined to include -1 in its spectrum, thus $j \in \{-1, 0, 1, 2, \dots\}$.

¹¹ The zero modes can be expressed by $\Psi = \begin{bmatrix} L\psi_L^+ \\ 0 \\ 0 \\ 0 \end{bmatrix}$ or $\Psi = \begin{bmatrix} 0 \\ 0 \\ 0 \\ L\psi_R^- \end{bmatrix}$.

and

$$\begin{aligned} L_{kj} = & d_{kj} e^{2kb \arcsin[\tanh(z)]} [\operatorname{sech}(z) - i \tanh(z)]^{j+1} \operatorname{sech}^{a-j-1}(z) \times \\ & \times {}_2F_1\left(-j-1, a-j-\frac{1}{2}-2ikb; 2a-2j-1; 1 + [\operatorname{sech}(z) + i \tanh(z)]^2\right). \end{aligned} \quad (4.117)$$

Some of the normalizable modes, from Eqs. (4.116) and (4.117), are depicted in Figs. 23, 24, 25 and 26. The eigenvalues of Eqs. (4.103) and (4.104) are the same as a Posch-Teller system, however the eigenstates are not symmetrical with respect to the center of the configuration, which is justified by the shape and depth of the potentials U_R and U_L , as presented in Fig. 22.

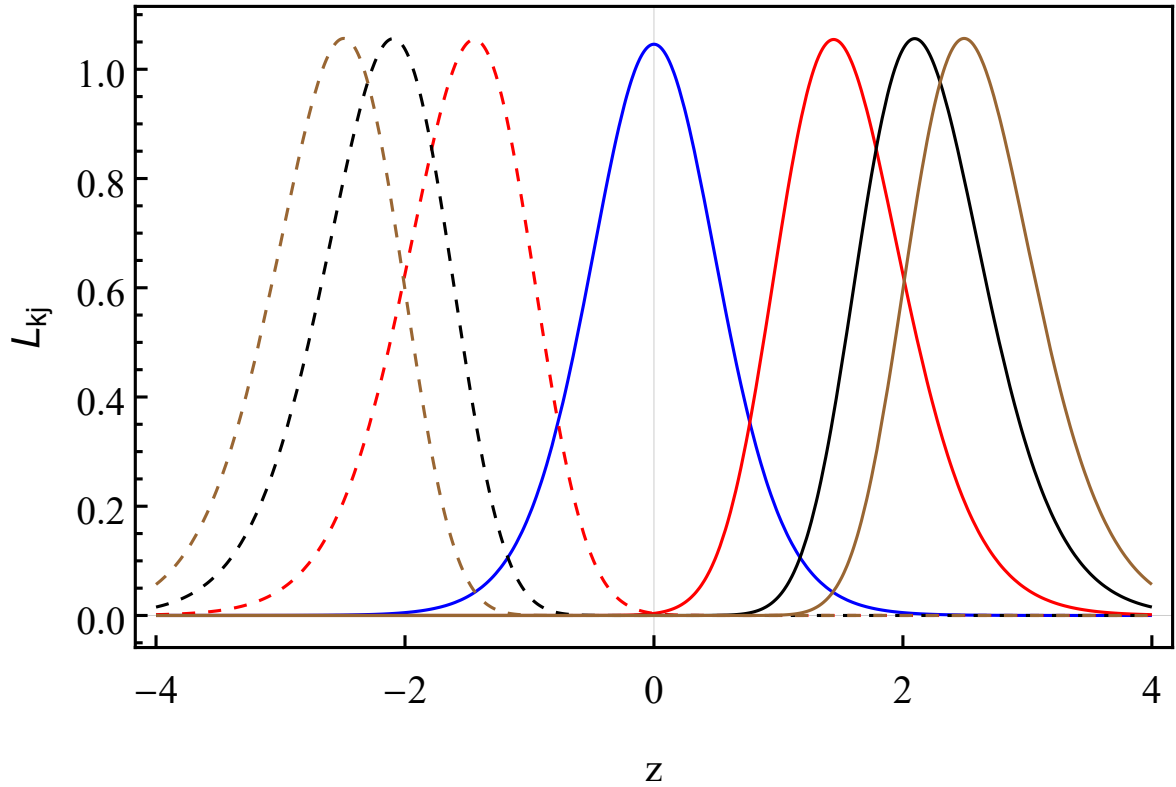


Figure 23 – The normalized zero modes with $a = b = 4$, for $k = 0$ (solid blue line), $k = 1$ (solid red line), $k = 2$ (solid black line), $k = 3$ (solid brown line), $k = -1$ (dashed red line), $k = -2$ (dashed black line) and $k = -3$ (dashed brown line).

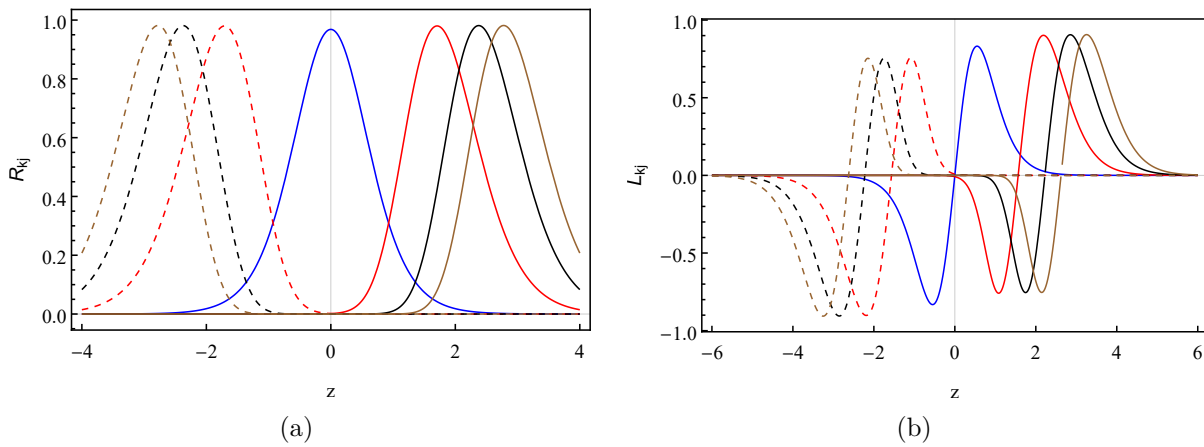


Figure 24 – (a) The normalized right-handed bound states. (b) The normalized left-handed bound states. The plots are for $k = 0$ (solid blue line), $k = 1$ (solid red line), $k = 2$ (solid black line), $k = 3$ (solid brown line), $k = -1$ (dashed red line), $k = -2$ (dashed black line) and $k = -3$ (dashed brown line), with $a = b = 4$ and $j = 0$.

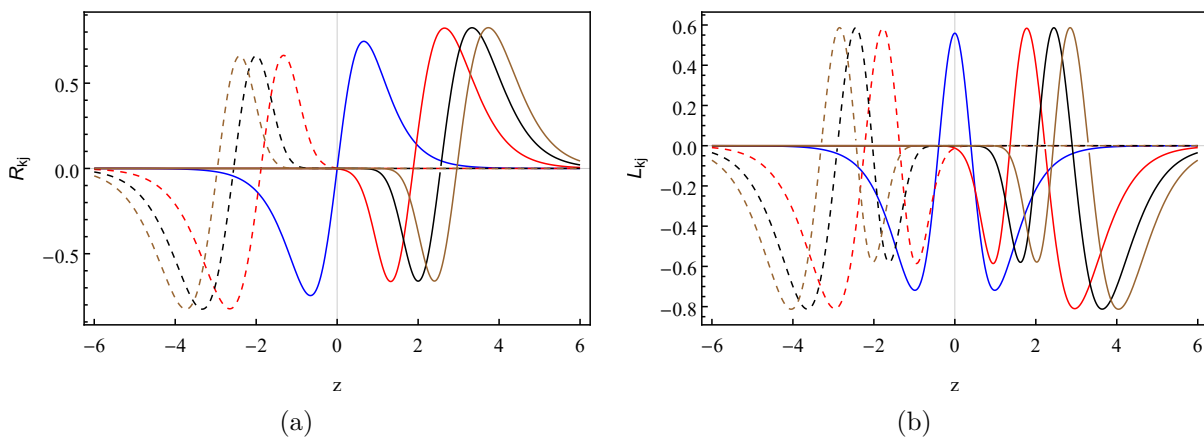


Figure 25 – (a) The normalized right-handed bound states. (b) The normalized left-handed bound states. The plots are for $k = 0$ (solid blue line), $k = 1$ (solid red line), $k = 2$ (solid black line), $k = 3$ (solid brown line), $k = -1$ (dashed red line), $k = -2$ (dashed black line) and $k = -3$ (dashed brown line), with $a = b = 4$ and $j = 1$.

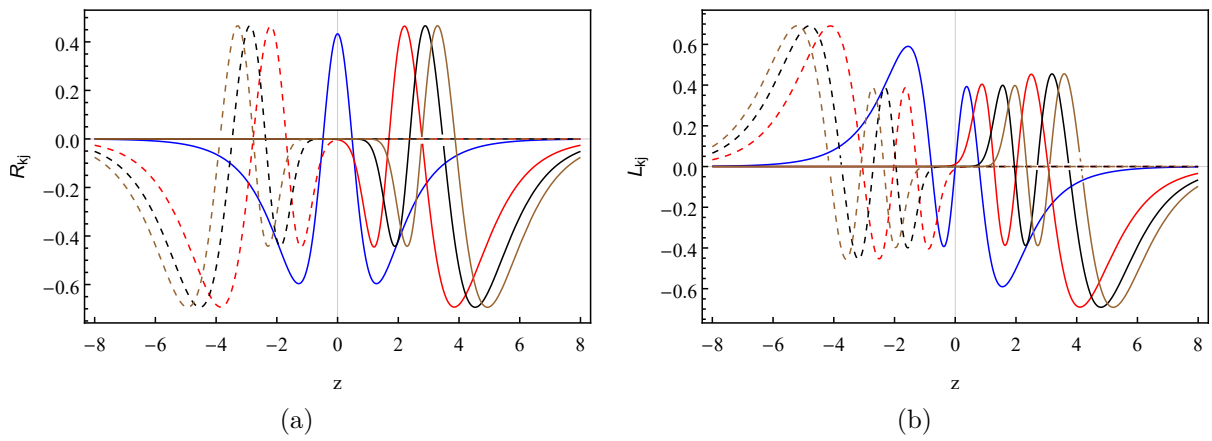


Figure 26 – (a) The normalized right-handed bound states. (b) The normalized left-handed bound states. The plots are for $k = 0$ (solid blue line), $k = 1$ (solid red line), $k = 2$ (solid black line), $k = 3$ (solid brown line), $k = -1$ (dashed red line), $k = -2$ (dashed black line) and $k = -3$ (dashed brown line), with $\mathbf{a} = \mathbf{b} = 4$ and $j = 2$.

5 Asymmetrical Branes and the Charged Lepton Spectrum

Within the Standard Model (SM), the masses and mixings of the quarks and leptons originates from their interactions with the Higgs field. Even though such interactions have been experimentally confirmed, the interaction coupling constants are free parameters and the generating mechanism of the relations between them is still unveiled. Notwithstanding the well-defined mass spectrum exhibited by the three families of charged leptons, an explanation for the mass values and their relative gaps is indeed an open problem. Phenomenological approaches [93, 94] have been proposed through empirical relations among the fermion masses, as an attempt of uncovering some of its underlying physics¹.

In a parallel context, extra dimensions have played a prominent role in our understanding of the hierarchy between the Planck and weak scales [2, 3]. Thus, it is natural to assume that other properties of the SM could also be understood from such paradigm. The mass spectrum of fermions should be no different. The most promising higher-dimensional scenarios are based on braneworld models with non-factorizable geometries [3, 4, 15, 16, 17, 18, 19, 20, 21, 22, 23, 24, 25, 26, 27, 28, 29, 30, 31, 32, 33, 34, 1, 69, 95], where a \mathbb{Z}_2 -symmetric brane is mostly assumed². Nevertheless, generalization of these models are obtained by relaxing the mirror symmetry across the brane [33, 51, 55, 98, 99, 100, 101, 102, 103, 104, 105, 106, 107, 108, 109, 110]. The term “asymmetric” brane refers to any braneworld model for which the mirror symmetry is not required. Here, an asymmetric brane model will be an essential feature for realizing the spectrum of the fermions.

In this chapter, a braneworld mechanism for explaining the charged lepton mass spectrum is evaluated. Modeling the fermion spectrum through extra dimensions is indeed not a new idea. It has been addressed in the literature through different contexts [111, 112, 113, 114, 115, 116, 117, 118, 119, 120, 121]. However, instead of either considering that the distinct chiralities are differently placed over the extra dimensions [111, 112] or relying on a non-trivial higher-dimensional Higgs and several other fields [113, 114, 115,

¹ For instance, the so-called Koide’s mass formula [93, 94],

$$\mathcal{K} = \frac{m_e + m_\mu + m_\tau}{(\sqrt{m_e} + \sqrt{m_\mu} + \sqrt{m_\tau})^2} = \frac{2}{3}, \quad (5.1)$$

provides such a speculative relation which can be translated as a weaker condition for the fractions $m_\mu/m_e \approx 207$ and $m_\tau/m_\mu \approx 17$, here m_e , m_μ and m_τ .

² Since they are generally motivated by the Horava-Witten model [96, 97].

116, 117, 118, 119, 120, 121], a simpler mechanism shall be here admitted. By considering a six-dimensional braneworld constructed from an asymmetric conformally flat metric, a non-trivial bulk profile for the gauge boson and a dark³ scalar field, a single six-dimensional charged spinorial field, whose dynamic is driven by an ordinary $SU(2) \times U(1)$ action, is shown to give rise to several massive four-dimensional spinors. In particular, for the right choice of the parameters, the number of massive spinors becomes exactly three, and their mass spectrum shall coincide with that for the charged leptons.

Without a supporting action, i.e. without knowing the equations of motion, to drive the dynamics of the leptons, one can construct some general ideas of how the leptons masses might be realized for higher-dimensional models. First, assume a six-dimensional model, be it a braneworld model or not, for which one of the additional dimensions is compactified in a circle. Secondly, assume that a zero mode of leptons can be localized, taking the form

$$\Psi_0^{(6)} = \sum_k \begin{bmatrix} L_{0k}^+(\theta, y) \psi_{0k}^{L+}(x^\mu) \\ 0 \\ 0 \\ R_{0k}^-(\theta, y) \psi_{0k}^{R-}(x^\mu) \end{bmatrix}, \quad (5.2)$$

where $\theta \in S^1$, y is the other additional dimension and $k \in \mathbb{Z}$. Thirdly, suppose that the masses of the leptons is driven by an interaction with the Higgs field, i.e.

$$S_m = m_0 \int dx^6 \sqrt{-g} \bar{\Psi}^{(6)} \mathbf{H} \Psi^{(6)}, \quad (5.3)$$

where $\mathbf{H} = \phi(\theta, y) H(x^\mu)$ is a zero mode of the Higgs.

The mass term is determined by substituting Eq. (5.2) in action (5.3) and employing canonical normalization, leading to

$$\begin{aligned} S_m &= m_0 \int dx^6 \sqrt{-g} \bar{\Psi}^{(6)} \mathbf{H} \Psi^{(6)} \\ &= m_0 \sum_{k,l} \int dx^6 \sqrt{-g} \begin{bmatrix} \overline{L_{0k}^+} \psi_{0k}^{L+\dagger} & 0 & 0 & \overline{R_{0k}^-} \psi_{0k}^{R-\dagger} \end{bmatrix} \begin{bmatrix} 0 & \gamma^0 \\ \gamma^0 & 0 \end{bmatrix} \mathbf{H} \begin{bmatrix} L_{0l}^+ \psi_{0l}^{L+} \\ 0 \\ 0 \\ R_{0l}^- \psi_{0l}^{R-} \end{bmatrix} \\ &= m_0 \sum_{k,l} \frac{\int dy^2 e^{-4A} e^{-2B} \overline{L_{0k}^+} R_{0l}^- \phi \int dx^4 \sqrt{-\omega} \bar{\psi}_k H \psi_l}{\sqrt{\int dy^2 e^{-3A} e^{-2B} |L_{0k}^+|^2} \sqrt{\int dy^2 e^{-3A} e^{-2B} |R_{0l}^-|^2}}, \end{aligned} \quad (5.4)$$

where $\bar{\psi}_k = \psi_k^\dagger \gamma^0$, $\psi_k = \begin{bmatrix} \psi_{0k}^{L+} \\ \psi_{0k}^{R-} \end{bmatrix}$ and it is assumed that the right and left-handed mass terms are the same.

³ Dark is used here to describe physical fields that only exist in the bulk, and are not perceived directly by four dimensional observers.

After breaking the gauge symmetry, the Higgs field acquires a vacuum expectation value v , and the mass matrix observed by a four-dimensional observer becomes

$$m_{kl} = \frac{m_0 v}{\sqrt{2}} \sum_{k,l} \frac{\int dy^2 e^{-4A} e^{-2B} \overline{L_{0k}^+} R_{0l}^- \phi}{\sqrt{\int dy^2 e^{-3A} e^{-2B} |L_{0k}^+|^2} \sqrt{\int dy^2 e^{-3A} e^{-2B} |R_{0l}^-|^2}}. \quad (5.5)$$

Note that the inclusion of the interacting term (5.3) is assumed to be irrelevant when determining the wave functions of zero modes, for this reason one is able substitute Eq. (5.2) in action (5.3) and realize Eq. (5.5). One can justify this in two ways:

1. One just assumes that the interacting term, Eq. (5.3), is a perturbation, therefore not affecting the wave functions, and that the SM leptons are the zero modes;
2. One does not assume the interacting term to be a perturbation, but still defines that the SM particles are the consequence of zero modes.

For the conclusions we wish to draw from this manuscript both of the previous options are equivalent. We shall generally refer back to the first, since from it the massive modes can be determined. Any other solution, besides the zero modes, should account for beyond SM physics.

From Eq. (5.5) there are thus three approaches one can follow to achieve the masses of the fermions of the SM, which here shall be referred by:

1. The left/right-handed chiral approach;
2. The non-trivial bulk Higgs approach;
3. Or the non-trivial curvature approach.

The first technique, the left/right-handed chiral approach, constructs the spectrum of the fermions by assuming that the left and right handed bulk components, L_{0k}^+ and R_{0l}^- , are localized at distinct positions, and their overlap generates the different masses of the SM. An illustration of this method is shown in Fig. 27a.

The second one relies on the existence of a non-trivial bulk profile for the Higgs, i.e. one assumes that ϕ is some complicated function of θ and y , and its overlap with the wave functions of the fermions leads to their masses. An illustration of this method is shown in Fig. 27b.

The third and last method relies on a non-trivial profile for the warp, A , and conformal, B , factors, which after overlapping with the wave functions of the fermions leads to their masses. This shall be explored further, but some asymmetry on the metric

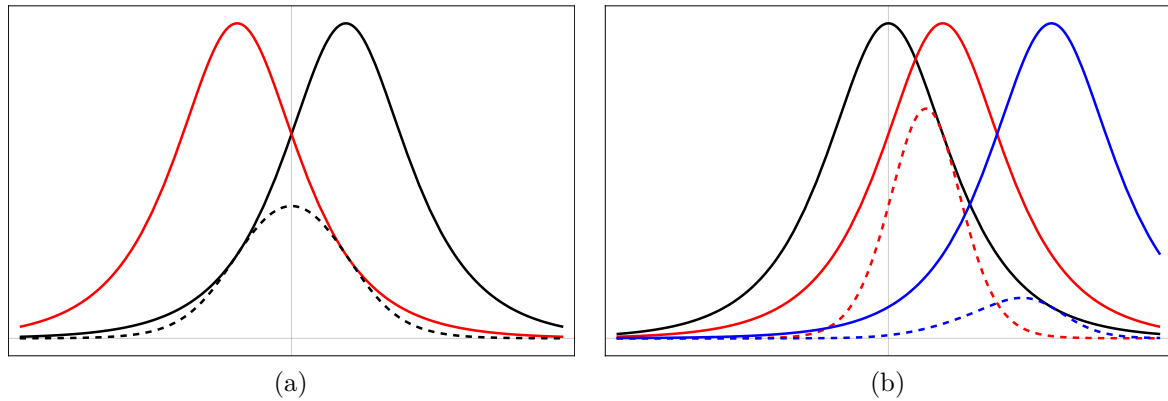


Figure 27 – (a) The left/right-handed chiral approach. The solid red and black lines represent the left, right-handed wave functions, while the dashed black line represents the overlap between them. (b) The non-trivial bulk Higgs approach.

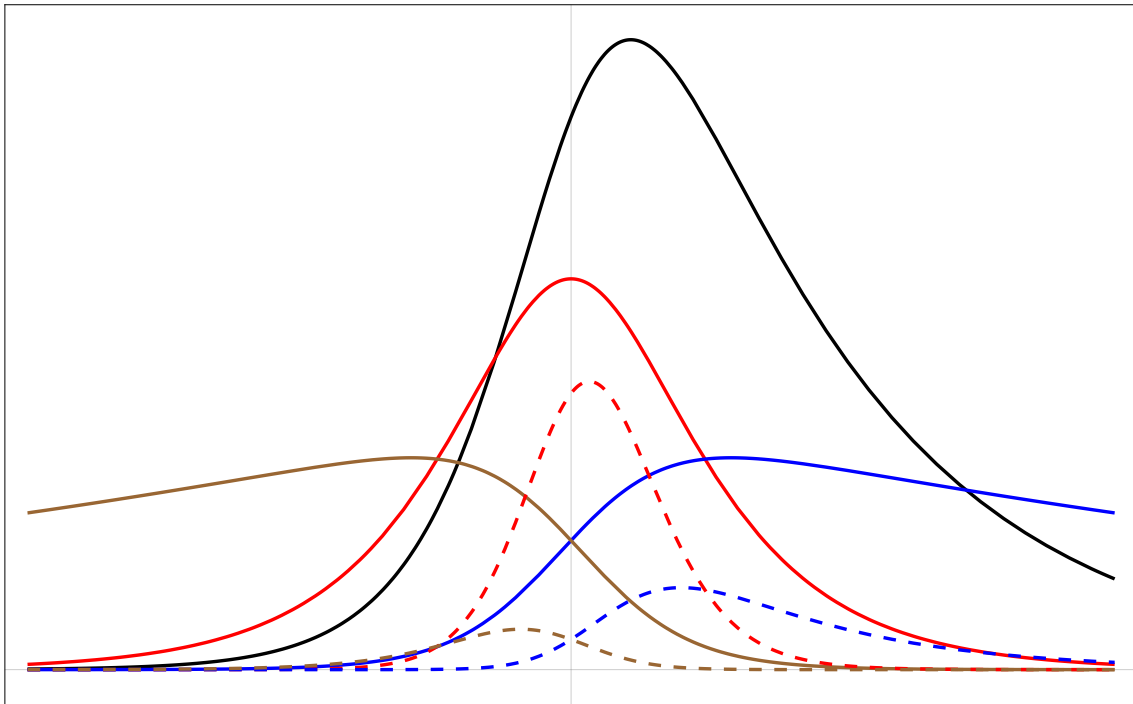


Figure 28 – The non-trivial curvature approach. The solid black line represents the warp factor A (here $A \equiv B$). The solid red, blue and brown represent the normalized wave functions of the tauon, muon and electron, respectively. The dashed red, blue and brown lines represent the overlap between the wave functions of tauon, muon and electron with the warp factor, respectively.

shall be an essential feature of this method. An illustration of this method is shown in Fig. 28.

The first two techniques were investigated by [111, 112, 113, 114, 115, 116, 117, 118, 119, 120, 121], while the third is a novel approach proposed by this manuscript, which will shall label the asymmetrical mechanism. There are two main advantages of this novel approach: the three charged leptons are a consequence of single six-dimensional spinorial

field, and their masses can be analytically determined.

5.1 The Asymmetrical Mechanism

The setup for the proposed mechanism comes from a six-dimensional braneworld \mathbb{E}^6 that is, as a set, equivalent to the product space $\mathbb{M}^4 \times \mathbb{R} \times \mathbb{S}^1$, where \mathbb{M}^4 is some four-dimensional pseudo-Riemannian manifold, \mathbb{R} is the real line and \mathbb{S}^1 is the circle. The following ansatz is assumed for the metric of \mathbb{E}^6 ,

$$\mathbf{g} = e^{-2A(y)} \left(\eta_{\mu\nu} dx^\mu dx^\nu + r^2 d\theta^2 + \rho^2 dy^2 \right), \quad (5.6)$$

where A is the warp factor, $\eta_{\mu\nu}$ is the Minkowski metric⁴ of the space-time \mathbb{M}^4 , $\theta \in \mathbb{S}^1$, r is the radius of \mathbb{S}^1 , $y \in \mathbb{R}$ and ρ is the brane model scale. An asymmetry of the braneworld is achieved by imposing that $e^{-A} = f_+ + f_-$, where f_+ and f_- are even and odd non-null functions, respectively, and $f_+ \geq |f_-|$ for all y .

5.1.1 The Mechanism for a $U(1)$ Model

To illustrate the mechanism we consider first a $U(1)$ abelian gauge theory, and present the basic features necessary for the charged lepton spectrum. In a later section, the mechanism shall be extended to a $SU(2)_L \times U(1)_Y$ theory.

In conformally flat metrics, like (5.6), fermionic fields can not be localized at the vicinity of the brane. Thus the proposal will also rely on the existence of an abelian gauge field⁵ $\mathbf{B} = \mathbf{B}_M dx^M$, defined by the zero mode

$$\mathbf{B}_\mu = \mathbf{B}_\mu(x^\nu), \mathbf{B}_\theta(y) = -\frac{r}{2\rho e} \frac{F_{,y}}{F} \text{ and } \mathbf{B}_y = 0, \quad (5.7)$$

where F is some positive even function of y , e is the electronic charge, and the subscript index “,” stands for partial derivatives. The gauge field (5.7) drives the localization of fermionic modes [73]. The fermions are thus represented by the action

$$\bar{S}_d = \int d^6x \sqrt{-g} \bar{\Psi}^{(6)} \Gamma^M \mathbf{D}_M \Psi^{(6)} - m_0 \int d^6x \sqrt{-g} \bar{\Psi}^{(6)} \Psi^{(6)}, \quad (5.8)$$

where $\mathbf{D}_M := \partial_M + \mathfrak{C}_M - ie\mathbf{B}_M$ is the covariant derivative and \mathfrak{C}_M is the spin connection of $(\mathbb{E}^6, \mathbf{g})$. The parameter m_0 sets the scale of the charged lepton masses, which is much smaller than the brane model scale $1/\rho$, and is treated as a perturbation of the system. Therefore the m_0 scale does not affect the co-dimensional wave functions, which are

⁴ Clarifying the notation, Greek indices (μ, ν, \dots) are valued in the set $\{0, 1, 2, 3\}$, uppercase Latin indices (M, N, \dots) are valued in $\{0, 1, 2, 3, 4, 5\}$, lowercase Latin indices (m, n, i, j, \dots) are valued in $\{4, 5\}$ (and represent the bulk co-dimensions) and the labels $x^4 = \theta$ and $x^5 = y$, represent the choice of coordinates for the co-dimensions (\mathbb{B}^2); finally, tensors when being referred to its (abstract) entirety will be in boldface, as \mathbf{g} , but its components will be cast in regular font, as $g_{\mu\nu}$.

⁵ Alternatively, one could also consider a scalar field $\phi = \phi(y)$ as the localization mechanism [122].

determined as if the fermions were massless. The zero modes are thus described by the equation

$$\Gamma^i D_i \Psi_0^{(6)} = 0. \quad (5.9)$$

Following a separation of variables technique, Eq. (5.9) is reduced to a Schrödinger-like equation and the fermionic zero modes are described by⁶

$$\Psi_0^{(6)} = e^{\frac{5A}{2}} \begin{bmatrix} \sum_k L_{0k}^+(\theta, y) \psi_{0k}^{L+}(x^\mu) \\ 0 \\ 0 \\ \sum_k R_{0k}^-(\theta, y) \psi_{0k}^{R-}(x^\mu) \end{bmatrix}, \quad (5.10)$$

where

$$R_{0k}^- = L_{0k}^+ = C_k e^{ik\theta} e^{\frac{k\rho y}{r}} F^{\frac{1}{2}} \quad (5.11)$$

represent the fermionic co-dimensional wave functions, $k \in \mathbb{Z}$ and the C_k are integration constants. The existence of the perturbation m_0 breaks the degeneracy of the zero modes, implying in a tower of spinors with varying masses driven by integer values, k .

The SM leptons are thus represented by the localizable zero modes and a four-dimensional observer will model them by an effective action, which follows from substituting Eq. (5.10) into Eq. (5.8),

$$S_{eff} = \sum_k \int d^4x \left(\bar{\Psi}_k \gamma^\mu D_\mu \Psi_k - m_k \bar{\Psi}_k \Psi_k \right), \quad (5.12)$$

where⁷ $\Psi_k = \begin{bmatrix} \psi_{0k}^{L+} \\ \psi_{0k}^{R-} \end{bmatrix}$ and

$$m_k = \frac{m_0 \int dy e^{-A} \bar{L}_{0k}^+ R_{0k}^+}{\sqrt{\int dy |L_{0k}^+|^2} \sqrt{\int dy |R_{0k}^+|^2}} = \frac{m_0 \int_{-\infty}^{\infty} dy (f_+ + f_-) F e^{\frac{2\rho k}{r} y}}{\int_{-\infty}^{\infty} dy F e^{\frac{2\rho k}{r} y}}. \quad (5.13)$$

Eq. (5.13) gives the effective masses as perceived by a four-dimensional observer. The mechanism to achieve the charged leptons masses can finally be explained. By assuming $F = \text{sech}^a(y)$, which is concomitant to

$$\mathbf{B}_\theta = \frac{ar}{2\rho e} \tanh(y), \quad (5.14)$$

⁶ The components $\Psi_0^{(6)} = \sum_k \begin{bmatrix} R_{0k}^+(\theta, y) \psi_{0k}^{L+}(x^\mu) \\ L_{0k}^-(\theta, y) \psi_{0k}^{R-}(x^\mu) \\ 0 \end{bmatrix}$ are non-normalizable, since $R_{0k}^+ = L_{0k}^- =$

$B_k e^{-ik\theta} e^{\frac{5A}{2}} e^{\frac{k\rho y}{r}} e^{\frac{\rho y}{r}} \int B_\theta dy$.

⁷ In a six-dimensional notation $\Psi_k^{(6)} = \begin{bmatrix} \psi_{0(k)}^{L+} \\ 0 \\ 0 \\ \psi_{0(k)}^{R-} \end{bmatrix}$.

and that $a/2 \leq 2\rho/r < a$, solely three normalizable fermionic zero modes can be identified, each of them associated with $k = -1$, $k = 0$ and $k = 1$, which are now to be labeled, respectively, as the electron, tauon and muon, i.e. $\mathbf{m}_{-1} = m_e$, $\mathbf{m}_0 = m_\tau$ and $\mathbf{m}_1 = m_\mu$. After some straightforward manipulations one finds

$$\frac{m_\mu}{m_e} = \frac{\int_{-\infty}^{\infty} dy \operatorname{sech}^a(y) e^{2\frac{\rho}{r}y} (f_+ + f_-)}{\int_{-\infty}^{\infty} dy \operatorname{sech}^a(y) e^{-2\frac{\rho}{r}y} (f_+ + f_-)}, \quad (5.15)$$

and

$$m_\tau = (m_\mu + m_e) \frac{\Gamma\left(\frac{a-2\rho}{2}\right) \Gamma\left(\frac{a+2\rho}{2}\right) \int_{-\infty}^{\infty} dy \operatorname{sech}^a(y) f_+}{2\Gamma\left(\frac{a}{2}\right)^2 \int_{-\infty}^{\infty} dy \operatorname{sech}^a(y) \cosh\left(2\frac{\rho}{r}y\right) f_+}. \quad (5.16)$$

The largeness of the tauonic mass is an effect of canonical normalization and it is independent from the space-time asymmetry. If a is larger but of similar value to $2\rho/r$, then the wave functions of the electron and muon, which are not localized at the center, become spread out, while the wave function of the tauon gets localized at the center of the system of coordinates. After canonical normalization, the electronic and muonic masses pickup a very small term when compared with the tauonic term, thus explaining the largeness of the tauon mass. In this way, charged lepton mass constraints can be straightforwardly attained regardless of the asymmetry, since the tauon mass can be made as large as necessary, albeit not correctly valued. On the other hand, the relation between the electron and muon masses relies on the asymmetry of the warp factor. The wave functions of the electron and muon are a mirror of one each other, and the overlap between each and an asymmetric warp factor leads to different masses. Yet, not all asymmetric warp factors can conclude the correct masses, since a very light electron is only realized when $f_+ - f_-$ goes to zero much faster than $f_+ + f_-$ for positive y . It is noteworthy that the co-dimensional wave functions that represent the fermionic fields are not gauge invariant, but the normalization condition and the masses as calculated here are gauge invariant. This is clear since the latter are calculated directly from the action, which is gauge invariant.

In a following section a choice for the metric will be made to exemplify the mechanism in a more explicit, and parametrized, way.

5.1.2 The Complete Lepton Sector

The complete lepton sector can be constructed from the action, following the notation of [123],

$$S_{SU(2)_L \times U_1} = \int d^6x \sqrt{-g} \left\{ \bar{L}^{(6)} \Gamma^M \left(\nabla_M - ig\tau_a W_M^a + \frac{i}{2} \mathbf{g}' B_M \right) L^{(6)} \right. \\ \left. + \bar{e}_-^{(6)} \Gamma^M \left(\nabla_M + ig' B_M + \zeta_{,M} \right) e_-^{(6)} + \bar{\nu}_-^{(6)} \Gamma^M \left(\nabla_M - \mathbf{b} \zeta_{,M} \right) \nu_-^{(6)} \right. \\ \left. - m_0 \left(\bar{L}^{(6)} \mathbf{H} e_-^{(6)} + \bar{e}_-^{(6)} \mathbf{H}^\dagger L^{(6)} \right) \right\}, \quad (5.17)$$

where $\nabla_M := \partial_M + \mathfrak{C}_M$, \mathfrak{C}_M is the spin connection of $(\mathbb{E}^6, \mathbf{g})$, ζ is some dark scalar field, B_M is the hypercharge gauge boson, W_M^a are the $SU(2)$ gauge bosons, \mathbf{g} and \mathbf{g}' are the $SU(2)$ and $U(1)$ couplings, $\tau_a = \sigma_a/2$ are the $SU(2)$ generators, $\mathbf{H} = \begin{Bmatrix} H_+ \\ H_0 \end{Bmatrix}$ is the Higgs doublet, \mathbf{b} is a real constant, and m_0 is the coupling constant with the Higgs field. The left-handed leptons pair up to transform under $SU(2)$,

$$L^{(6)} = \begin{Bmatrix} \nu_+^{(6)} \\ e_+^{(6)} \end{Bmatrix}, \quad (5.18)$$

where

$$\nu_+^{(6)} = \begin{bmatrix} \Psi_\nu^{L+} \\ \Psi_\nu^{R+} \\ 0 \\ 0 \end{bmatrix} \quad \text{and} \quad e_+^{(6)} = \begin{bmatrix} \Psi_e^{L+} \\ \Psi_e^{R+} \\ 0 \\ 0 \end{bmatrix} \quad (5.19)$$

represent the left-handed charged leptons and neutrinos, respectively. While

$$e_-^{(6)} = \begin{bmatrix} 0 \\ 0 \\ \Psi_e^{L-} \\ \Psi_e^{R-} \end{bmatrix} \quad \text{and} \quad \nu_-^{(6)} = \begin{bmatrix} 0 \\ 0 \\ \Psi_\nu^{L-} \\ \Psi_\nu^{R-} \end{bmatrix} \quad (5.20)$$

represent the right-handed charged leptons and neutrinos, which are uncharged under $SU(2)$.

The charged lepton masses are a consequence of the existence of a Higgs field, which is driven by the action

$$S_H = \int dx^6 \sqrt{-g} \left\{ \left[\left(\nabla_M - ig\tau_a W_M^a - \frac{i}{2} \mathbf{g}' B_M \right) \mathbf{H} \right]^\dagger \left(\nabla^M - ig\tau^b W_b^M - \frac{i}{2} \mathbf{g}' B^M \right) \mathbf{H} \right. \\ \left. - \zeta^{,M} \zeta_{,M} \mathbf{H}^\dagger \mathbf{H} + V(\mathbf{H}) \right\}, \quad (5.21)$$

where $V(\mathbf{H}) = \mu^2 \mathbf{H}^\dagger \mathbf{H} - \lambda (\mathbf{H}^\dagger \mathbf{H})^2$.

For conformally flat metrics (cf. (5.6)), fermionic fields can not be localized at the vicinity of the brane. Hence, the proposal thus relies on the existence of a non-trivial bulk profile for the hypercharge gauge boson $\mathbf{B} = B_M dx^M$ and the scalar field⁸ ζ , each defined by

$$B_\mu = B_\mu(x^\nu), W_\mu^a = W_\mu^a(x^\nu), B_y = W_i^a = 0, B_\theta = \frac{r}{\rho g'} \frac{F_{,y}}{F} \text{ and } \zeta = \frac{1}{2} \ln(F), \quad (5.22)$$

where F is some positive even function of y and the subscript index “,” stands for partial derivatives. Gauge and scalar fields defined in Eq. (5.22) drive the localization of fermionic modes⁹ [73, 122], and can be interpreted as background fields.

The parameters μ^2 , λ and m_0 set the scale of the charged lepton masses, which are much smaller than the brane model scale $1/\rho$ or $1/r$, and are treated as a perturbation of the system. This can be justified directly from the action

$$S = \int d^6x \sqrt{-g} \left[\bar{\mathbf{L}}^{(6)} \left(\Gamma^\mu \mathbf{D}_\mu + \frac{1}{\rho} \Gamma^y \mathbf{D}_y + \frac{1}{r} \Gamma^\theta \mathbf{D}_\theta \right) \mathbf{L}^{(6)} + \bar{\mathbf{e}}_-^{(6)} \left(\Gamma^\mu \mathbf{D}_\mu + \frac{1}{\rho} \Gamma^y \mathbf{D}_y + \frac{1}{r} \Gamma^\theta \mathbf{D}_\theta \right) \mathbf{e}_-^{(6)} - m_0 \left(\bar{\mathbf{L}}^{(6)} H \mathbf{e}_-^{(6)} + \bar{\mathbf{e}}_-^{(6)} H^\dagger \mathbf{L}^{(6)} \right) \right], \quad (5.23)$$

which implies that the co-dimensional portion of the action is of the order of $1/r$ or $1/\rho$, while the rest is of the order of m_0 . Therefore the terms μ^2 , λ and m_0 do not affect the co-dimensional wave functions, which are determined as if the fermions were massless and $V(H)$ vanished. The zero modes of leptons are thus described by the equations

$$\Gamma^i \left(\nabla_i + i g' \frac{1}{2} \mathbf{B}_i \right) \mathbf{L}_0^{(6)} = 0, \quad (5.24)$$

$$\Gamma^i (\nabla_i + i g' \mathbf{B}_i + \zeta_{,i}) \mathbf{e}_{-0}^{(6)} = 0, \quad (5.25)$$

and

$$\Gamma^i (\nabla_i - \mathbf{b} \zeta_{,i}) \nu_{-0}^{(6)} = 0. \quad (5.26)$$

Following a separation of variables technique, Eqs. (5.24), (5.25) and (5.26) are reduced to a Schrödinger-like equations and the localizable leptonic zero modes are described by¹⁰

$$\mathbf{L}_0^{(6)} = \begin{Bmatrix} \nu_{+0}^{(6)} \\ \mathbf{e}_{+0}^{(6)} \end{Bmatrix}, \nu_{+0}^{(6)} = e^{\frac{5A}{2}} \sum_k L_{0k}^+ \begin{bmatrix} \psi_{\nu 0k}^{L+}(x^\mu) \\ 0 \\ 0 \\ 0 \end{bmatrix}, \mathbf{e}_{+0}^{(6)} = e^{\frac{5A}{2}} \sum_k L_{0k}^+ \begin{bmatrix} \psi_{\mathbf{e} 0k}^{L+}(x^\mu) \\ 0 \\ 0 \\ 0 \end{bmatrix}, \quad (5.27)$$

⁸ The scalar field is not essential for the mechanism, however, simpler expressions and more elegant properties are obtained for the reduced resulting effective four-dimensional action in that case.

⁹ With the exception of $\zeta_{,M} \zeta_{,M} \mathbf{H}^\dagger \mathbf{H}$, which serves the purpose of achieving a trivial bulk profile for the Higgs, as shall be presented later.

¹⁰ The components $\Psi_0^{(6)} = e^{\frac{5A}{2}} \sum_k \begin{bmatrix} 0 \\ R_{0k}^+(\theta, y) \psi_{0k}^{L+}(x^\mu) \\ L_{0k}^-(\theta, y) \psi_{0k}^{R-}(x^\mu) \\ 0 \end{bmatrix}$ are non-normalizable, since $L_{0k}^- = A_k e^{-ik\theta} e^{\frac{k\rho y}{r}} F^{-\frac{3}{2}}$ and $R_{0k}^+ = B_k e^{-ik\theta} e^{\frac{k\rho y}{r}} F^{-\frac{1}{2}}$.

$$\mathbf{e}_{-0}^{(6)} = e^{\frac{5A}{2}} \sum_k R_{0k}^- \begin{bmatrix} 0 \\ 0 \\ 0 \\ \psi_{\mathbf{e}0k}^{R-}(x^\mu) \end{bmatrix} \text{ and } \nu_{-0}^{(6)} = e^{\frac{5A}{2}} F^{\frac{b-1}{2}} \sum_k R_{0k}^- \begin{bmatrix} 0 \\ 0 \\ \psi_{\nu0k}^{L-}(x^\mu) \\ \psi_{\nu0k}^{R-}(x^\mu) \end{bmatrix}, \quad (5.28)$$

where

$$L_{0k}^+ = C_k e^{ik\theta} e^{\frac{k\rho y}{r}} F^{\frac{1}{2}} \text{ and } R_{0k}^- = D_k e^{ik\theta} e^{\frac{k\rho y}{r}} F^{\frac{1}{2}}, \quad (5.29)$$

represent the fermionic co-dimensional wave functions, $k \in \mathbb{Z}$, C_k and D_k are integration constants.

On the other hand, the zero mode of the Higgs field satisfies the equation

$$\nabla^i \nabla_i \mathbf{H} - i \frac{\mathbf{g}'}{r^2} \mathbf{B}_\theta \mathbf{H}_\theta = 0, \quad (5.30)$$

which after a rescaling and a separation of variables technique, with $\mathbf{H} = \sum_k e^{ik\theta} e^{2A} \hat{\phi}_k H_k(x^\mu)$, reduces to

$$\hat{\phi}_{k,vv} + 2(A_{,vv} - 2A_{,v^2}) \hat{\phi}_k + k \frac{\mathbf{g}'}{r^2} \mathbf{B}_\theta \hat{\phi}_k = \frac{k^2}{r^2} \hat{\phi}_k. \quad (5.31)$$

The zero mode of scalar fields are generally like $\hat{\phi}_0 = c e^{-2A}$, which is the solution of Eq. (5.31) for¹¹ $k = 0$, implying in a trivial bulk profile for the Higgs field,

$$\mathbf{H} = c H_0(x^\mu) = c \begin{Bmatrix} \phi_+(x^\mu) \\ \phi_0(x^\mu) \end{Bmatrix}, \quad (5.32)$$

where c is an integration constant. The existence of the perturbation m_0 breaks the degeneracy of the zero modes, implying in a tower of spinors with varying masses driven by integer values, k . The SM leptons are thus represented by the localizable zero modes and a four-dimensional observer will model them by an effective action, which follows from substituting Eqs. (5.27), (5.28) and (5.32) into Eq. (5.17) and canonically normalizing,

$$S_{Eff} = \sum_k \int d^4x \left[\bar{\mathbf{L}}_k \gamma^\mu \left(\nabla_\mu - ig\tau_a \mathbf{W}_\mu^a + \frac{i}{2} \mathbf{g}' \mathbf{B}_\mu \right) \mathbf{L}_k + \bar{\mathbf{e}}_{Rk} \gamma^\mu \left(\nabla_\mu + ig' \mathbf{B}_\mu \right) \mathbf{e}_{Rk} \right. \\ \left. + \bar{\nu}_k^- \gamma^\mu \nabla_\mu \nu_k^- - m_k \left(\bar{\mathbf{L}}_k H_0 \mathbf{e}_{Rk} + \bar{\mathbf{e}}_{Rk} H_0^\dagger \mathbf{L}_k \right) \right], \quad (5.33)$$

where

$$\mathbf{L}_k = \begin{Bmatrix} \nu_{Lk} \\ \mathbf{e}_{Lk} \end{Bmatrix}, \nu_{Lk} = \begin{bmatrix} \psi_{\nu0k}^{L+} \\ 0 \end{bmatrix}, \mathbf{e}_{Lk} = \begin{bmatrix} \psi_{\mathbf{e}0k}^{L+} \\ 0 \end{bmatrix}, \nu_k^- = \begin{bmatrix} \psi_{\nu0k}^{L-} \\ \psi_{\nu0k}^{R-} \end{bmatrix}, \mathbf{e}_{Rk} = \begin{bmatrix} 0 \\ \psi_{\mathbf{e}0k}^{R-} \end{bmatrix} \quad (5.34)$$

and

$$m_k = \frac{m_0 \int dy e^{-A} \bar{L}_{0k}^+ R_{0k}^+}{\sqrt{\int dy |L_{0k}^+|^2} \sqrt{\int dy |R_{0k}^+|^2} \sqrt{\int dy \hat{\phi}_0^2}} = \frac{m_0 \int_{-\infty}^{\infty} dy (f_+ + f_-) F e^{\frac{2\rho k}{r} y}}{\int_{-\infty}^{\infty} dy F e^{\frac{2\rho k}{r} y} \sqrt{\int_{-\infty}^{\infty} dy (f_+ + f_-)^4}}. \quad (5.35)$$

¹¹ Other values of k necessarily imply in a massive mode.

Analogously, a four-dimensional observer will model the Higgs field by an effective action, which follows from substituting Eq. (5.32) into Eq. (5.21),

$$S_H^{(4)} = \int dx^4 \left\{ \left[\left(\nabla^\mu - ig\tau^a W_a^\mu - \frac{i}{2}g'B^\mu \right) H_0 \right]^\dagger \left(\nabla_\mu - ig\tau_b W_\mu^b - \frac{i}{2}g'B_\mu \right) H_0 + V_{eff}(H_0) \right\}, \quad (5.36)$$

where $V_{eff}(H_0) = \mu_{eff}^2 H_0^\dagger H_0 - \lambda_{eff} (H_0^\dagger H_0)^2$, with

$$\mu_{eff}^2 = \mu^2 \frac{\int_{-\infty}^{\infty} dy e^{-6A}}{\int_{-\infty}^{\infty} dy e^{-4A}} \quad \text{and} \quad \lambda_{eff} = \lambda \frac{\int_{-\infty}^{\infty} dy e^{-6A}}{\left(\int_{-\infty}^{\infty} dy e^{-4A} \right)^2}. \quad (5.37)$$

After breaking the gauge symmetry, the Higgs field acquires a vacuum expectation value (v.e.v), driven by μ_{eff} and λ_{eff} , as

$$v = \frac{\mu_{eff}}{\sqrt{\lambda_{eff}}} = \frac{\mu}{\sqrt{\lambda}} \sqrt{\int_{-\infty}^{\infty} dy (f_+ + f_-)^4}, \quad (5.38)$$

and $m_k = m_k v / \sqrt{2}$, from Eqs. (5.35) and (5.38), gives the effective masses as measured by a four-dimensional observer,

$$m_k = \frac{\mu m_0}{\sqrt{2\lambda}} \frac{\int_{-\infty}^{\infty} dy (f_+ + f_-) F e^{\frac{2\rho k}{r} y}}{\int_{-\infty}^{\infty} dy F e^{\frac{2\rho k}{r} y}}. \quad (5.39)$$

Eq. (5.39) is exactly the same as Eq. (5.13), with the substitution $m_0 \rightarrow \mu m_0 / \sqrt{2\lambda}$. Therefore, Eq. (5.39) leads to the same mechanism, for a $SU(2)_L \times U(1)$ model, that was discussed previously for an $U(1)$ model.

5.1.3 The Asymmetry Parametrized

To exemplify the mechanism in effect we propose a model for which $f_+ = \text{sech}^l(y) \cosh(oy)$ and $f_- = \text{sech}^l(y) \sinh(oy)$, which, after substitution into Eq. (5.6), leads to

$$\mathbf{g} = \text{sech}^{2l}(y) e^{2oy} \left(\eta_{\mu\nu} dx^\mu dx^\nu + r^2 d\theta^2 + \rho^2 dy^2 \right). \quad (5.40)$$

The fractions of the charged lepton masses associated with the metric (5.40), calculated from Eqs. (5.15) and (5.16), become

$$\frac{m_\mu}{m_e} = \frac{\Gamma\left(\frac{l-o+a-\frac{2\rho}{r}}{2}\right) \Gamma\left(\frac{l+o+a+\frac{2\rho}{r}}{2}\right)}{\Gamma\left(\frac{l+o+a-\frac{2\rho}{r}}{2}\right) \Gamma\left(\frac{l-o+a+\frac{2\rho}{r}}{2}\right)}, \quad (5.41)$$

and

$$\frac{m_\tau}{m_\mu} = \frac{\Gamma\left(\frac{a-2\rho}{2}\right) \Gamma\left(\frac{a+2\rho}{2}\right) \Gamma\left(\frac{l+a-o}{2}\right) \Gamma\left(\frac{l+a+o}{2}\right)}{\Gamma\left(\frac{a}{2}\right)^2 \Gamma\left(\frac{l+a-2\rho-o}{2}\right) \Gamma\left(\frac{l+a+2\rho+o}{2}\right)}. \quad (5.42)$$

If o is an integer and $l - o$ is an even integer, then Eqs. (5.41) and (5.42) become polynomial equations. Particularly, for $o = 2$ and $l = 4$ one can solve Eqs. (5.41) and (5.42) analytically to find $a = 34.9562$ and $a - 2\rho/r = 0.28488$. In fact, there are many combinations of o and l for which the lepton spectrum is achievable. Fig. 29 depicts the values of l , a and $a - 2\rho/r$ with fixed $l - o$ for which the proper fractions of the masses and Koide's formula are realized for the metric Eq. (5.40). Correspondently, Fig. 30 depicts the values of l , $l - o$ and $a - 2\rho/r$ with fixed a for which the proper fractions of the masses and Koide's formula are realized for the metric Eq. (5.40). The intersection of the curves in both Figs. 29 and 30 are identified according to the parameter values that lead to the charged lepton mass spectrum.

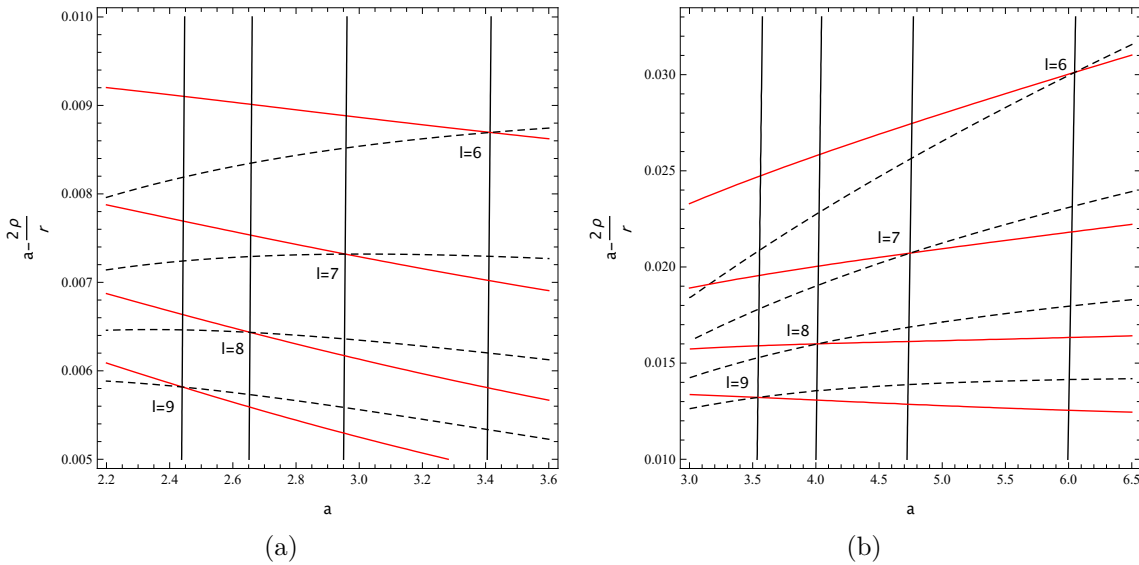


Figure 29 – (a) The charged lepton mass spectrum associated with the metric (5.40) for $l - o = 1$. (b) The charged lepton mass spectrum associated with the metric (5.40) for $l - o = 2$. The solid black, solid red and dashed black lines represent the equations $m_\mu/m_e = 206.768$, $m_\tau/m_\mu = 16.817$ and $\mathcal{K} = 2/3$, respectively. Results are for triple intersecting points at $l = 6, 7, 8$, and 9 .

5.1.4 Beyond The Standard Model

The last important aspect to realizing realistic models is achieving a mass gap between the zero and massive modes. Being the SM particles represented by the zero modes, the massive modes are thus associated with beyond SM physics. From a phenomenological point of view, it is important to realize models that allow for the existence of a mass gap

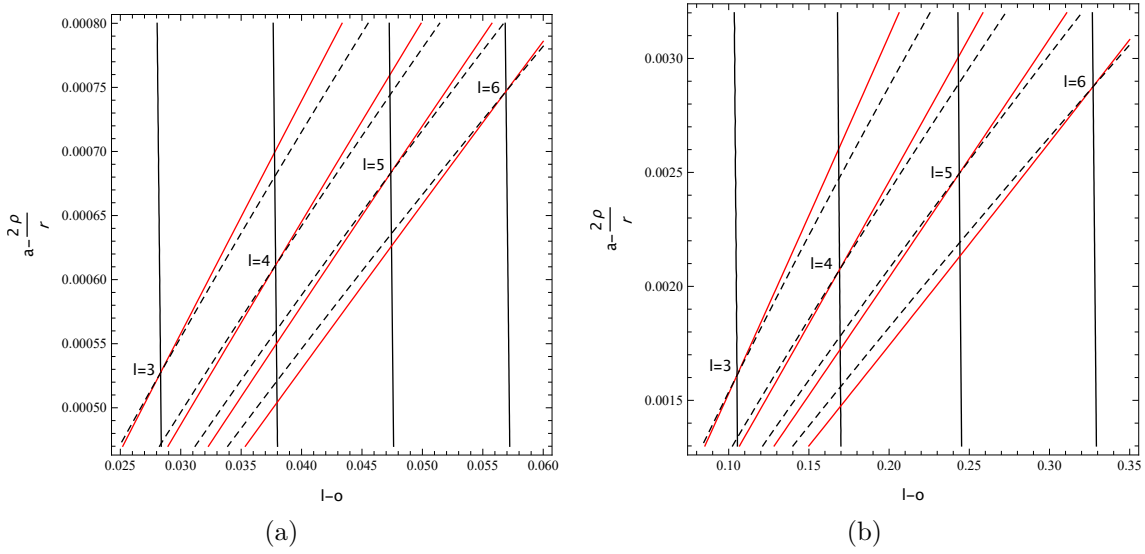


Figure 30 – (a) The charged lepton mass spectrum associated with the metric (5.40) for $\mathbf{a} = 1$. (b) The charged lepton mass spectrum associated with the metric (5.40) for $\mathbf{a} = 2$. The solid black, solid red and dashed black lines represent the equations $m_\mu/m_e = 206.768$, $m_\tau/m_\mu = 16.817$ and $\mathcal{K} = 2/3$, respectively. Results are for triple intersecting points at $l = 3, 4, 5$, and 6 .

[87], between the zero and massive modes, in the spectrum of leptons. Then the energy scale at which the massive modes can be excited is fixed by this gap, and its existence is relevant for distinguishing the footprints of the massless modes, identified with stable four-dimensional SM particles, from those coming from the massive modes, either discrete or continuous. When no mass gap is present, then there exist several massive modes with masses small to the point of being indistinguishable from the massless ones.

5.1.4.1 Massive Modes: The Charged Leptons

To realize the massive modes of the charged leptons, the six-dimensional braneworlds Dirac equation must be evaluated, which is given by

$$\left(\hat{\Gamma}^\mu \mathcal{D}_\mu + \mathcal{D}^{\bar{i}} \Gamma_{\bar{i}}\right) \Psi^{(6)} = 0, \quad (5.43)$$

Following the same arguments as outline in Subsecs. 4.3.1 and 4.3.2, one finds four equations

$$m^2 L_m^+ + \mathcal{D}_+^{\bar{4}} \mathcal{D}_+^{\bar{4}} L_m^+ - i \left[\mathcal{D}_+^{\bar{4}}, \mathcal{D}_+^{\bar{5}}\right] L_m^+ + \mathcal{D}_+^{\bar{5}} \mathcal{D}_+^{\bar{5}} L_m^+ = 0, \quad (5.44)$$

$$m^2 R_m^+ + \mathcal{D}_+^{\bar{4}} \mathcal{D}_+^{\bar{4}} R_m^+ + i \left[\mathcal{D}_+^{\bar{4}}, \mathcal{D}_+^{\bar{5}}\right] R_m^+ + \mathcal{D}_+^{\bar{5}} \mathcal{D}_+^{\bar{5}} R_m^+ = 0, \quad (5.45)$$

$$m^2 L_m^- + \mathcal{D}_-^{\bar{4}} \mathcal{D}_-^{\bar{4}} L_m^- + i \left[\mathcal{D}_-^{\bar{4}}, \mathcal{D}_-^{\bar{5}}\right] L_m^- + \mathcal{D}_-^{\bar{5}} \mathcal{D}_-^{\bar{5}} L_m^- = 0, \quad (5.46)$$

and

$$m^2 R_m^- + \mathcal{D}_-^{\bar{4}} \mathcal{D}_-^{\bar{4}} R_m^- - i \left[\mathcal{D}_-^{\bar{4}}, \mathcal{D}_-^{\bar{5}}\right] R_m^- + \mathcal{D}_-^{\bar{5}} \mathcal{D}_-^{\bar{5}} R_m^- = 0, \quad (5.47)$$

that define the massive modes of the leptons, where it is defined

$$\mathcal{D}_+^{\bar{5}} = \frac{1}{\rho} \left[\partial_y - \frac{5}{2} A_{,y} + \frac{i}{2} \mathbf{g}' \mathbf{B}_y \right], \quad \mathcal{D}_-^{\bar{5}} = \frac{1}{\rho} \left[\partial_y + \zeta_{,y} - \frac{5}{2} A_{,y} + i \mathbf{g}' \mathbf{B}_y \right], \quad (5.48)$$

$$\mathcal{D}_+^{\bar{4}} = \frac{1}{r} \left[\partial_\theta - \frac{5}{2} A_{,\theta} + \frac{i}{2} \mathbf{g}' \mathbf{B}_\theta \right] \quad \text{and} \quad \mathcal{D}_-^{\bar{4}} = \frac{1}{r} \left[\partial_\theta + \zeta_{,\theta} - \frac{5}{2} A_{,\theta} + i \mathbf{g}' \mathbf{B}_\theta \right]. \quad (5.49)$$

Substituting Eqs. (5.14) and (5.22) into Eqs. (5.44), (5.45), (5.46) and (5.47), after a rescaling of the wave functions $L_m^+ = e^{5A/2} \sum_k e^{ik\theta} \mathbf{L}_{mk}^+$ and $L_m^- = e^{5A/2} e^{-\zeta} \sum_k e^{ik\theta} \mathbf{L}_{mk}^-$ (the same is true for R_m^+ and R_m^-), implies in four Morse-Rosen equations,

$$-\mathbf{L}_{mk,yy}^+ + \left[-\frac{\lambda}{2} \left(\frac{\lambda}{2} + 1 \right) \text{sech}^2(y) - ks \tanh(y) \right] \mathbf{L}_{mk}^+ = \epsilon_+ \mathbf{L}_{mk}^+, \quad (5.50)$$

$$-\mathbf{R}_{mk,yy}^+ + \left[-\frac{\lambda}{2} \left(\frac{\lambda}{2} - 1 \right) \text{sech}^2(y) - ks \tanh(y) \right] \mathbf{R}_{mk}^+ = \epsilon_+ \mathbf{R}_{mk}^+, \quad (5.51)$$

$$-\mathbf{L}_{mk,yy}^- + \left[-\lambda(\lambda - 1) \text{sech}^2(y) - 2ks \tanh(y) \right] \mathbf{L}_{mk}^- = \epsilon_- \mathbf{L}_{mk}^-, \quad (5.52)$$

and

$$-\mathbf{R}_{mk,yy}^- + \left[-\lambda(\lambda + 1) \text{sech}^2(y) - 2ks \tanh(y) \right] \mathbf{R}_{mk}^- = \epsilon_- \mathbf{R}_{mk}^-. \quad (5.53)$$

where $\lambda = \frac{\mathbf{g}' \rho \mathbf{q}}{r}$, $s = \frac{\rho \lambda}{r}$, $\epsilon_+ = m^2 \rho^2 - \frac{k^2 s^2}{\lambda^2} - \frac{\lambda^2}{4}$, $\epsilon_- = m^2 \rho^2 - \frac{k^2 s^2}{\lambda^2} - \lambda^2$ and \mathbf{q} is a real valued constant. Eqs. (5.50), (5.51), (5.52) and (5.53) are equivalent to Eqs. (4.91) and (4.92), therefore their eigenvalue spectrum follows from Eq. (4.99). In this way there is always a mass gap between the zero and massive modes, be it the discrete or continuous modes.

In conclusion, for configurations with a non-trivial profile for the gauge and scalar field, like Eq. (5.14), the fermionic massive modes are solutions of Morse-Rosen equations, for which a discrete set of eigenstates can be identified, each associated with the mass eigenvalues

$$m_{jk}^+ = \frac{2}{\rho} \frac{\sqrt{(j+1)(\mathbf{a}-j-1)}}{|\mathbf{a}-2j-2|} \sqrt{\left(\frac{\mathbf{a}}{2} - j - 1 \right)^2 - \frac{k^2 \rho^2}{r^2}}, \quad (5.54)$$

and

$$m_{jk}^- = \frac{1}{\rho} \frac{\sqrt{(j+1)(2\mathbf{a}-j-1)}}{|\mathbf{a}-j-1|} \sqrt{(\mathbf{a}-j-1)^2 - \frac{k^2 \rho^2}{r^2}}, \quad (5.55)$$

where j is an integer, $0 \leq j < \mathbf{a}/2 - 1$ and m_{jk}^\pm references the discrete masses of positive and negative components of spinors, respectively. While continuous modes are related to masses

$$m^+ \geq \frac{1}{2\rho} \left| \mathbf{a} - \frac{2\rho |k|}{r} \right| \quad \text{and} \quad m^- \geq \frac{1}{\rho} \left| \mathbf{a} - \frac{\rho |k|}{r} \right|, \quad (5.56)$$

therefore, a mass gap between the zero and massive modes is found whenever the zero modes are normalizable.

For metric (5.40) the lepton mass gap, between the continuous and massless modes, is $m \sim 10^{-2}/\rho$. A realistic mass gap, for small values of l , is thus achievable for

$\rho \ll 10^{-18}$ m, since $m_0 v / \sqrt{2} \approx m_\tau = 1.7$ GeV. On the other hand, for large values of l , tiny values of $1 - o/l$ and a of the order of unity, a realistic mass gap is achievable for $\rho \ll 2^l \Gamma(a) / [l^{a/2} \Gamma(a/2)] 10^{-16}$ m, since $m_0 v / \sqrt{2} \approx l^{a/2} \Gamma(a/2) / [2^l \Gamma(a)]$ GeV. Therefore, for $l \sim 50$ the mass gap is achievable for $\rho \ll 1$ m.

5.1.4.2 Massive Modes: The Higgs Field

In the same line of reasoning, the Higgs field must also have a mass gap between the zero and massive modes. But the massive modes of the Higgs depends upon the choice of metric. Particularly, for the metric considered in this manuscript,

$$\mathbf{g} = \text{sech}^{2l}(y) e^{2oy} \left(\eta_{\mu\nu} dx^\mu dx^\nu + r^2 d\theta^2 + \rho^2 dy^2 \right). \quad (5.57)$$

and the gauge boson is once again

$$\mathbf{B}_\theta = -\mathbf{q} \tanh(y), \quad (5.58)$$

the bulk profile of the Higgs field follows from the equation

$$-\phi_{,yy} + \left[-2l(2l+1) \text{sech}^2(y) - (8ol - ks) \tanh(y) + 4l^2 + 4o^2 + \frac{k^2 s^2}{\lambda^2} \right] \phi = m^2 \rho^2 \phi, \quad (5.59)$$

where $\lambda = \frac{\mathbf{g}'_{\rho\mathbf{q}}}{r}$ and $s = \frac{\lambda\rho}{r}$. The general solution of Eq. (5.59) takes the form

$$\begin{aligned} \phi_{kj} = & c_1 \text{sech}^q(y) e^{py} {}_2F_1 \left(q - 2l, 2l + 1 + q; q - p + 1; \frac{e^{-y} \text{sech}(y)}{2} \right) \\ & + c_2 \text{sech}^p(y) e^{qy} {}_2F_1 \left(p - 2l, 2l + 1 + p; p - q + 1; \frac{e^{-y} \text{sech}(y)}{2} \right), \end{aligned} \quad (5.60)$$

where $q = \frac{\sqrt{\epsilon^2 - (8ol - ks)^2 - \epsilon}}{\sqrt{2}}$, $p = \frac{|8ol - ks|}{2q}$ and $\epsilon = m^2 \rho^2 - 4l^2 - 4o^2 - \frac{k^2 s^2}{\lambda^2}$. If $\epsilon \geq -|8ol - ks|$ then Eq. (5.60) corresponds to the propagating modes. Otherwise, for $\epsilon < -|8ol + ks|$, the solution (5.60) leads to the bound states

$$\phi_{kj}(y) = c e^{\frac{|8ol - ks|}{2(2l-j)} y} \text{sech}^{2l-j}(y) {}_2F_1 \left(-j, 4l + 1 - j; 2l + 1 - j - \frac{|4ol - ks|}{2l - j}; \frac{e^{-y} \text{sech}(y)}{2} \right). \quad (5.61)$$

both associated with the mass eigenvalues

$$m^2 \rho^2 = 4l^2 + 4o^2 + \frac{k^2 s^2}{\lambda^2} - (2l - j)^2 - \frac{(8ol - ks)^2}{4(2l - j)^2}, \quad (5.62)$$

where j is a natural number. In this way there is always a mass gap between the zero and massive modes, be it a discrete or continuous mode. The mass gap for the Higgs field follows similar patterns to the ones found for the leptons.

5.1.5 Neutrino Masses

So far only the charged leptons have been included in the mass generation mechanism, but neutrinos should also present a mass. In this subsection, a speculation of how the neutrinos may acquire mass is postulated in this six-dimensional setup. First assume that the neutrinos interact with the Higgs as follows,

$$S_\nu = - \int d^6x \sqrt{-g} m_\nu \phi \left[\bar{L}^{(6)} \tilde{H} \nu_-^{(6)} + \bar{\nu}_-^{(6)} \tilde{H}^\dagger L^{(6)} \right], \quad (5.63)$$

where $\tilde{H} = i\sigma_2 H^*$, m_ν is the neutral lepton coupling constant with the Higgs field and ϕ is some dark real scalar field that is a function of only θ . The scalar field ϕ is important to establish the interaction between the different flavors of neutrinos. Secondly, take ϕ to be the most general scalar field one can fit in S^1 , i.e.

$$\phi(\theta) = \sum_j c_j e^{ij\theta}. \quad (5.64)$$

A four-dimensional observer will thus model the neutrino interaction with the Higgs, which follows from substituting Eqs. (5.27), (5.28), (5.32) and (5.64) in Eq. (5.63) and canonically normalizing, by an effective term

$$S_\nu = - \sum_{k,j} m_{kj} \int d^4x \left(\bar{L}_k \tilde{H}_0 \nu_j^- + \bar{\nu}_k^- \tilde{H}_0^\dagger L_j \right), \quad (5.65)$$

where

$$m_{kj} = \frac{\mu m_\nu}{\sqrt{2\lambda}} \frac{c_{k-j} 2^l \sqrt{\Gamma(\mathbf{a}) \Gamma(\mathbf{b}\mathbf{a})} \Gamma\left(\frac{l + \frac{\mathbf{a}\mathbf{b} + \mathbf{a}}{2} - o - \frac{(k+j)\rho}{r}}{2}\right) \Gamma\left(\frac{l + \frac{\mathbf{a}\mathbf{b} + \mathbf{a}}{2} + \left[o + \frac{(k+j)\rho}{r}\right]}{2}\right)}{\Gamma\left(l + \frac{\mathbf{a}\mathbf{b} + \mathbf{a}}{2}\right) \sqrt{\Gamma\left(\frac{\mathbf{a} - \frac{2j\rho y}{r}}{2}\right) \Gamma\left(\frac{\mathbf{a} + \frac{2j\rho y}{r}}{2}\right)} \sqrt{\Gamma\left(\frac{\mathbf{b}\mathbf{a} - \frac{2k\rho y}{r}}{2}\right) \Gamma\left(\frac{\mathbf{b}\mathbf{a} + \frac{2k\rho y}{r}}{2}\right)}}. \quad (5.66)$$

The full asymmetrical lepton model has nine parameters: c_{-2}/c_0 , c_{-1}/c_0 , c_1/c_0 , c_2/c_0 , \mathbf{a} , ρ/r , \mathbf{b} , m_ν and m_0 . If metric (5.40) is to be assumed then there are two parameters defining the braneworld model: l and o . While the SM with the Pontecorvo–Maki–Nakagawa–Sakata (PMNS) matrix has ten parameters¹² [123]: θ_{12} , θ_{13} , θ_{23} , δ , m_1 , m_2 , m_3 , m_e , m_μ and m_τ . The correct mass matrix for the neutrinos could be achievable with (5.66). Considering that the parameters \mathbf{a} and ρ/r are fixed by the charged lepton mass fractions, then one can choose the c_j such that the mixing angles, θ_{12} , θ_{13} and θ_{23} , and Dirac phase, δ , of the PMNS matrix are exactly like the experimentally verified. The parameters m_ν , \mathbf{b} , l and o that are left should be enough to fix the neutrino masses m_1 , m_2 and m_3 , such that they satisfy the constrictions imposed by Solar and atmospheric neutrino oscillations. The complete analysis of the values of the parameters that fix the correct PMNS matrix is outside the scope of the present work, and is left for future work.

¹² It is assumed that the neutrinos masses do not contain a Majorana term.

5.2 For Other Sets of the Classification

So far the proposed mechanism has been presented for trivial-like solutions, thus this section is dedicated to exploring the mechanism along the other sets in the classification. It is straightforward to extend the proposed mechanism to string-like solutions. From action (5.17), and the same assumptions about the gauge and scalar fields, one can achieve the following expression for the masses, after the Higgs field has broken the gauge symmetry and acquired a v.e.v,

$$m_k = \frac{\mu m_0}{\sqrt{2\lambda}} \frac{\int dy e^{-B} \overline{L_{0k}^+} R_{0k}^+}{\sqrt{\int dy e^{A-B} |L_{0k}^+|^2} \sqrt{\int dy e^{A-B} |R_{0k}^+|^2}}. \quad (5.67)$$

Thus, assuming that

$$\mathbf{g} = (f_+ + f_-)^2 \eta_{\mu\nu} dx^\mu dx^\nu + Q^2 (f_+ + f_-)^2 (\rho^2 dy^2 + r^2 d\theta^2), \quad (5.68)$$

which is equivalent to

$$e^{-B} = Q (f_+ + f_-) \quad \text{and} \quad e^{A-B} = Q(y), \quad (5.69)$$

where Q is some even function of y , implies in the masses

$$m_k = \frac{\mu m_0}{\sqrt{2\lambda}} \frac{\int dy (f_+ + f_-) Q F e^{2k\frac{\rho}{r}}}{\sqrt{\int dy Q F e^{2k\frac{\rho}{r}}} \sqrt{\int dy Q F e^{2k\frac{\rho}{r}}}}. \quad (5.70)$$

Therefore, Eq. (5.70) is equivalent to Eq. (5.35), if one substitutes $F \rightarrow QF$, and the same conclusions drawn in Secs. 5.1.1, 5.1.2 and 5.1.3 are also valid for string-like solutions¹³.

For the intersecting-like models, solely the ones for which $p = 0$ (or $p = 1$) can comport the mechanism, i.e. models *III*, *IV*, *V* and *VI*. The other two models, I and II, do not possess the possibility of an asymmetry in the warp factor, since it is symmetrical with respect to the center of the configuration. For models *III*, *IV*, *V* and *VI* one can achieve an asymmetry by imposing that \tilde{A} be asymmetrical. Regardless, this section shall only address the mechanism for model *IV*, since it has been confirmed in previous chapters to correspond to the most physically significant one.

To realize the mechanism for model *IV*, a new dark scalar field must be introduced to the formalism, this is to achieve the localization of spinors not only in the direction of

¹³ A brief caveat is needed here: It is important that while QF is a “localized” function, QF^{-1} must diverge at infinity, which guarantees that the internal components of the six-dimensional spinors, i.e. R_+ and L_- , are not-localized.

y , but also of φ . To this end, one specifies the action for spinors as

$$S_{SU(2)_L \times U_1} = \int d^6x \sqrt{-g} \left\{ \bar{\mathbf{L}}^{(6)} \Gamma^M \left[\nabla_M - i\mathbf{g}\tau_a \mathbf{W}_M^a + \frac{i}{2} \mathbf{g}' \mathbf{B}_M + \phi_{,M} \right] \mathbf{L}^{(6)} \right. \\ \left. + \bar{\mathbf{e}}_-^{(6)} \Gamma^M \left[\nabla_M + i\mathbf{g}' \mathbf{B}_M + \zeta_{,M} + \phi_{,M} \right] \mathbf{e}_-^{(6)} - m_0 \left[\bar{\mathbf{L}}^{(6)} \mathbf{H} \mathbf{e}_-^{(6)} + \bar{\mathbf{e}}_-^{(6)} \mathbf{H}^\dagger \mathbf{L}^{(6)} \right] \right\}, \quad (5.71)$$

where the scalar field $\phi = \phi(\varphi)$ has been included to guarantee that the zero modes of spinors are localized, all other fields will be equivalent to the ones previously introduced in Subsec. 5.1.2. The zero modes of the leptons are similar to the ones at Subsec. 5.1.2, but the inclusion of the scalar leads to

$$\mathbf{L}_0^{(6)} = \begin{Bmatrix} \nu_{+0}^{(6)} \\ \mathbf{e}_{+0}^{(6)} \end{Bmatrix}, \nu_{+0}^{(6)} = e^{\frac{5A}{2}} \sum_k L_{0k}^+ \begin{bmatrix} \psi_{\nu 0k}^{L+}(x^\mu) \\ 0 \\ 0 \\ 0 \end{bmatrix}, \mathbf{e}_{+0}^{(6)} = e^{\frac{5A}{2}} \sum_k L_{0k}^+ \begin{bmatrix} \psi_{\mathbf{e} 0k}^{L+}(x^\mu) \\ 0 \\ 0 \\ 0 \end{bmatrix}, \quad (5.72)$$

and

$$\mathbf{e}_{-0}^{(6)} = e^{\frac{5A}{2}} \sum_k R_{0k}^- \begin{bmatrix} 0 \\ 0 \\ 0 \\ \psi_{\mathbf{e} 0k}^{R-}(x^\mu) \end{bmatrix}, \quad (5.73)$$

where

$$L_{0k}^+ = C_k e^{ik\varphi} e^{-\phi} e^{\frac{k\rho y}{r}} F^{\frac{1}{2}} \text{ and } R_{0k}^- = D_k e^{ik\varphi} e^{-\phi} e^{\frac{k\rho y}{r}} F^{\frac{1}{2}}. \quad (5.74)$$

Relevant to the leptons masses is the normalization of the lepton wave functions, which are given by

$$\int dy^2 e^{A-B} \bar{L}_{0l}^+ L_{0k}^+ = \int_{-\pi}^{\pi} d\varphi e^{\hat{A}} e^{i(k-l)\varphi} e^{-2\phi} \int_{-\infty}^{\infty} dy e^{\frac{(l+k)\rho y}{r}} F, \quad (5.75)$$

the right-handed wave function also follows the same integration. The simplest way for integral (5.75) to be finite is when ϕ coincides with $\hat{A}/2$, therefore implying in

$$\int dy^2 e^{A-B} \bar{L}_{0l}^+ L_{0k}^+ = \delta_{lk} \int_{-\infty}^{\infty} dy e^{\frac{(l+k)\rho y}{r}} F. \quad (5.76)$$

which is finite within this formalism. Essentially the scalar field for model *IV* satisfies

$$e^{-2\phi} = \cos\left(\frac{n\varphi}{2}\right). \quad (5.77)$$

To finally find the masses one must now look into the Higgs field. To achieve the correct masses one must impose the action for the Higgs as

$$S_H = \int dx^6 \sqrt{-g} \left\{ \left[\left(\nabla_M - i g \tau_a \mathbf{W}_M^a - \frac{i}{2} \mathbf{g}' \mathbf{B}_M + 2\phi_{,M} \right) \mathbf{H} \right]^\dagger \right. \\ \left. \times \left(\nabla^M - i g \tau^b \mathbf{W}_b^M - \frac{i}{2} \mathbf{g}' \mathbf{B}^M + 2\phi_{,M} \right) \mathbf{H} \right. \\ \left. - \zeta^{,M} \zeta_{,M} \mathbf{H}^\dagger \mathbf{H} + V(\mathbf{H}) \right\}, \quad (5.78)$$

where the Higgs also couples to the scalar field ϕ . The zero modes of the Higgs with the inclusion of the scalar field ϕ are simply

$$\mathbf{H} = c e^{-2\phi} H(x^\mu) = c \cos\left(\frac{n\varphi}{2}\right) H(x^\mu). \quad (5.79)$$

Finally, the mass matrix of the leptons is given by the equation

$$m_{kl} = \frac{\mu m_0}{\sqrt{2\lambda}} \frac{\int dy^2 e^{-B} \cos\left(\frac{n\varphi}{2}\right) \overline{L_{0k}^+} R_{0l}^+}{\sqrt{\int dy^2 e^{A-B} |L_{0k}^+|^2} \sqrt{\int dy^2 e^{A-B} |R_{0k}^+|^2}} \\ = \frac{\mu m_0}{\sqrt{2\lambda}} \frac{2r}{n} \sqrt{\frac{\Lambda}{3}} \frac{\int_{-\pi}^{\pi} d\varphi \cos^2\left(\frac{n\varphi}{2}\right) e^{i(k-l)\varphi} \int_{-\infty}^{\infty} dy e^{-\tilde{A}} e^{\frac{(l+k)\rho y}{r}} F}{\sqrt{\int_{-\infty}^{\infty} dy e^{\frac{k\rho y}{r}} F} \sqrt{\int_{-\infty}^{\infty} dy e^{\frac{l\rho y}{r}} F}}, \quad (5.80)$$

The mass matrix (5.80) is not always diagonal, and therefore does not in general lead to the charged lepton mass spectrum. In fact, as long as $n > 2$, $n \in \mathbb{N}^+$, the mass matrix is diagonal and leads to the same conclusions derived in Sec. 5.1. Thus the asymmetrical mechanism, as described in Sec. 5.1, can be trivially extended to model *IV* if $n > 2$.

One could attempt to further extend the mechanism for model *IV* to include $n = 1$ or $n = 2$ by changing the coupling constant of the Higgs with the scalar field ϕ from 2 to some real α . But, it is straightforward to conclude that the mass matrix is diagonal if and only if $n > 2$ and α is some even natural positive number, which excludes model *IV* when $n = 1$ or $n = 2$ independently on the choice of α .

A similar procedure could be employed for models *III* and *V*, but one would have to fine tune the choice of α , i.e. the coupling between the Higgs and the scalar field ϕ , to achieve a diagonal mass matrix for the charged leptons. Aside from this fine tuning problem, the asymmetrical mechanism can be straightforwardly achieved for these models.

6 Conclusion

Some old and novel solutions of braneworld models in $(5 + 1)$ -dimensions were classified and explored. Such braneworld models were thus employed in a mechanism for explaining the masses of the charged leptons. In the following, a specialized summary and discussion of the main results is presented.

6.1 On the Six-dimensional Braneworld Models

As a preliminary proposal, braneworlds generated by two scalar fields were obtained as solutions depending solely on a single coordinate of the co-dimensions, therefore constituting an intersection of two thick branes, where the adopted procedure involved constraining the metric components to be separable functions of the co-dimensions. Braneworlds on top of two different geometries of \mathbb{S}^2 , the sphere and spheroid, were also constructed, and trivial and non-trivial extensions of the well known $(4 + 1)$ -dimensional brane-world models were identified. All the results implied into six different models, where two of them were strictly defined (models *I* and *II*) up to some constant p , and the other four (models *III*, *IV*, *V* and *VI*) have maintained some degree freedom not specified by the field equations.

In the first subset, models *I* and *II* constituted strictly defined models, determined from a flat brane where the separation constant p was set different from 1 (or 0) so as to strictly determine all the involved quantities from the Einstein field equations. The intrinsic difference between such models emerges from the choice of a constant parameter c_u : for real c_u one finds model *I*, and imaginary c_u one finds model *II*. For model *I* one identifies a metric with a non-RS-like warp factor, but still noticing that the effective finite volume of the bulk allows for localizing fields in the brane. The biggest complication of model *I* is its requirement of an infinite amount of energy to achieve the localized gravity configuration, which induces one to regard it as unphysical. Model *II* is significantly more interesting in the sense that where several singularities may be identified, its total defect formation energy is finite. Nevertheless, due to the singularities in the stress energy tensor, one may regard model *II* also as an unphysical configuration.

In the second subset, models *III*, *IV*, *V* and *VI* consisted in braneworld configurations with some degree of freedom not strictly specified by Einstein field equations. They were constructed by assuming that the auxiliary constant is set $p = 0$ such that one is able to obtaining solutions for the whole range of possible values of the cosmological constant Λ ($= 0, > 0$ or < 0). All the solutions contain extensions of some well-known five-dimensional braneworlds when the separation constant introduced for solving the coupled Einstein equations is set as $C = 0$, being it either a trivial or non-trivial extension. More relevantly,

some solutions for the sphere and spheroid geometries, where model *IV* seems to be of particular interest to physics, have been scrutinized.

In particular, model *III* was constructed upon a flat brane model with two scalar fields, for which the solution implies into some singularities where the warp factor exhibits cusped profile. Overall, the fields that constitute model *III* have similar behavior to the ones in model *II*. The above-mentioned model *IV* seems to be the most relevant solution here depicted. This model consists in a de Sitter brane with a single scalar field with a consistently and smoothly well behaved warp factor. No cusps are found in the warp factor and the so ingrained singularities in the stress energy tensor, which emerge with other models, are avoided. Regardless, after evaluating the Kretschmann scalar, for model *IV*, curvature singularities are still encountered. Model *IV* also eventually discards the role of the scalar field ϕ , since one could assume any generic form for the stress energy tensor as long as $T^u{}_u(u)$, $T^\mu{}_\nu(u) = \delta^\mu{}_\nu T^v{}_v(u)$ and $T_{uv} = 0$. Thus model *IV* may be found into other applications other than those for thick branes generated by scalar fields. For completeness, considering the whole spectrum of possible values for the cosmological-like constant Λ , model *V* was considered upon an anti-de Sitter brane with two scalar fields, where the separation constant has been set as $C = 0$. It resulted into model *V* possessing similar features to model *III*, which essentially exhibits the same singularities and cusps of the latter.

It is also worth to mention that, for models *III*, *IV*, *V* and *VI*, from the second subset, the Einstein equations do not define all fields. The scalar field ϕ , the warp factor \tilde{A} and the potential \mathcal{V} of are not strictly defined from field equations and one thus still has some freedom in choosing such quantities. This opened the possibility for considering predetermined geometries for the internal space. By choosing \tilde{A} and \tilde{f} with predetermined geometry, one is able to achieve two setups that allow for the integration of the corresponding metric Eq. (2.85). From such choices of \tilde{A} and \tilde{f} , one is able to accomplish a solution over the sphere and spheroid for models *III* and *IV*. For the sphere models, two solutions for model *IV* and nine solutions for model *III* were achieved, one for each possible value of a discrete degree of freedom n . In particular, for model *IV*, for $n = 1$, one has found a solution for which the stress energy tensor is smoothly well-behaved, even if the scalar ϕ exhibit some singularities. On the other hand, the $n = 2$ model depicts a dS^6 space, since there are no scalar fields, only the vacuum. Likewise, the spheroid seems to enjoy the most interesting features of the S^2 models. Constructed for model *IV*, with $n = 2$, one is able to achieve several interesting configurations for the warp factor and the scalar field, which guarantees the localization of gravity. Also, the spheroid solution pointed to a new solution for $(4 + 1)$ -dimensional models, represented by metric (2.146), where the actual localization parameter are given in terms of an arbitrary constant, κ .

The gravitational fluctuations and phenomenological implications of intersecting-

like braneworlds have also been explored. For the so-called models *I*, *II*, *III* and *VI*, zero modes have been computed, for model *IV*, the entire spectrum of graviton modes were analytically identified, and for model *V*, only some could be computed. In addition, the implications of spherical internal spaces have been investigated for models *III* and *IV*.

Generically, in contrast to ordinary five-dimensional models, six-dimensional models rely on a more intricate quantum mechanical two-dimensional analogue problem, where the assessment of the localization of gravity is driven by the curved space co-dimensional variables, $(\mathbb{B}^2, \hat{\sigma})$, rendering a Schrödinger-like equation for each co-dimension, from which localization modes have been identified.

Despite the reiterated physical appealing limitations of models *I* and *II* (cf. Ref. [1]), the profile of the gravitational constant G_N has been obtained, at least, as a pedagogical exercise. Results from models *I* and *II* attest that the gravitational strength may be as small as one wishes by setting the parameter p close to 2 or 4, instead of reflecting some usual brane “radius” (parameters c_u and c_v) tuning effect. -

More problematically, model *III* implied into a Schrödinger-like equation whose massive states are not straightforwardly determined, with the exception for a trivial extension of five-dimensional models ($C = 0$), for which massive states are similar to flat compactified models.

The most physically appealing intersecting braneworld, model *IV*, revealed a Schrödinger-like equation with a Pösch-Teller potential, admitting a finite and discrete number of gravitons, whose masses are bounded from above by an interplay between the separation constant k and the cosmological constant¹ Λ . Any propagating mode was summarily discarded after imposing unitary boundary conditions, thus rendering the singularities at the boundaries of space harmless. It is also noteworthy that model *IV* presents a mass gap between the zero and massive modes, all the while retaining a smooth Ricci scalar but a singular Kretschmann scalar. This is in contrast to five-dimensional models, where mass gaps and a singular Ricci scalar are directly connected [87]. Thus we conjectured that the existence of a mass gap in higher-dimensional braneworlds, other than five, may be connected to naked singularities of other scalar invariants besides the Ricci scalar.

The unique model constructed out of an anti-de Sitter brane, model *V*, has alluded to a Schrödinger-like equation with a trigonometric Pösch-Teller potential and a discrete set of gravitational modes. Unfortunately, model *V* presents a tachyonic graviton mode, which points to an instability of the configuration.

Finally, concerning some technicalities pointed out in Sec. 2.4.6, through models *III* and *IV*, one could also construct braneworld models whose internal space are spheres.

¹ For instance, if k is non-positive one can find at most two massive gravitons.

The spherical models constructed out of model *III*, but with $C = 0$, rely on a trivial extension of five-dimensional braneworlds. Remarkably, such trivial extensions imply into a gravitational interaction that behaves like a five-dimensional ADD model, while the gravitational constant behaves like a six-dimensional one. On the other hand, sphere models constructed out of model *IV* implied in two normalizable modes and the usual Newtonian interaction, with the gravitational constant being determined by a combination of the cosmological constant (Λ) and the radius of \mathbb{S}^2 (r).

The localization of matter fields have also been investigated. Scalar fields generally follow the same quantum mechanical problem as the gravitational one, and every conclusion for gravity could be extended to them. Gauge fields are more complicated, their zero modes localization follow straightforwardly from the equations of motion, but the massive modes required some extraordinary assumptions. Concerning strictly model *IV*, the full spectrum of massive gauge modes was determined, with a unique mode being localized, the zero mode.

Differing from gauge and scalar fields, fermionic matter required a more intricate analysis. Contrasting to the results of other matter fields, Weyl spinors can not be localized for the intersecting-like branes. Thus the localization of spinorial fields supported by a gauge field was investigated. In the trivial-like case, the localization becomes independent from warp factor, being solely determined from the gauge. In particular, fixing the co-dimensional components of the gauge field to be $B_y = 0$ and $B_\theta = b \tanh(y)$, transformed the Schrödinger-like into a Morse-Rosen equation, and its entire spectrum of modes was evaluated.

At last, for what concerns model *IV*, a new Schrödinger-like equation, that is dual to a trigonometric Morse-Rosen equation, was introduced after a special choice for the gauge field. The eigenvalues are exactly the same as a Posch-Teller system, for which the deepness of the potential well is controlled by the gauge field strength, but the eigenstates differ considerably. It is shown that there are finitely many, but degenerate, localized states, being the continuous modes separated from the bound states by a mass gap.

6.2 On the Lepton Masses

From a classical perspective, fermions are localized at the vicinity of an asymmetric conformally flat brane by the inclusion of a non-trivial bulk profile for the hypercharge gauge boson and a dark scalar field; and the proper mass fractions are a consequence of canonical normalization and the overlap between the fermionic wave functions with the asymmetric warp factor. A mechanism for explaining the spectrum of the charged lepton masses was therefore build for both a $U(1)$ and $SU(2)_L \times U(1)$ models, and upon two parameters: the gauge field strength, \mathbf{a} , and the ratio between the co-dimensional sizes,

ρ/r .

In particular, from a model represented by metric Eq. (5.40), which was proposed for the sole reason of achieving analytical expressions, the proper fractions between the electron, muon and tauon masses were obtained, solely requiring that $\mathbf{a} - 2\rho/r$ be tiny. Even when \mathbf{a} is of the order of unity, the correct fractions for the masses can be realized when the warp factor presents a large asymmetry, which for Eq. (5.40) is achievable when $1 - o/l$ is tiny.

Furthermore, other asymmetric warp factors, in principle, also have the necessary structure to realize the needed mass spectrum, but an adjustment of the parameter values would be necessary. Even if surprising simple integrals have emerged when one assumed the metric as Eq. (5.40), other setups may not be so treatable as for finding analytical values for the masses. These results can also be trivially extended to other elements of the proposed classification, i.e. for string and intersecting-like braneworlds.

In this matter, relevant for next investigations, the same mechanism could also be employed for describing neutrino and quark mass hierarchy problems, since their diagonal masses should satisfy a similar spectra. Of course, specific features related to neutrino and quark interactions, and their implications for the mass generation mechanism, turn the problem sufficiently more complex for such a preliminary analysis. In particular, the neutrino mass matrix can be straightforwardly determined, but evaluating the individual neutrino masses and their mixing angles is an intricate problem.

Bibliography

- 1 GAUY, H. M.; BERNARDINI, A. E. (5+1)-dimensional analytical braneworld models: Intersecting thick branes. *Phys. Rev. D*, American Physical Society (APS), v. 105, n. 2, p. 024068, jan 2022. Citado 43 vezes nas páginas [17](#), [19](#), [20](#), [21](#), [22](#), [23](#), [24](#), [25](#), [26](#), [27](#), [28](#), [29](#), [30](#), [31](#), [32](#), [33](#), [35](#), [36](#), [37](#), [38](#), [39](#), [40](#), [41](#), [42](#), [43](#), [44](#), [47](#), [48](#), [49](#), [51](#), [53](#), [54](#), [55](#), [56](#), [57](#), [58](#), [65](#), [70](#), [71](#), [77](#), [81](#), [107](#), and [129](#).
- 2 ARKANI-HAMED, N.; DIMOPOULOS, S.; DVALI, G. The hierarchy problem and new dimensions at a millimeter. *Phys. Lett. B*, v. 429, n. 3, p. 263–272, 1998. ISSN 0370-2693. Citado 4 vezes nas páginas [17](#), [19](#), [83](#), and [107](#).
- 3 RANDALL, L.; SUNDRUM, R. Large mass hierarchy from a small extra dimension. *Phys. Rev. Lett.*, American Physical Society, v. 83, p. 3370–3373, Oct 1999. Citado 6 vezes nas páginas [17](#), [19](#), [61](#), [62](#), [79](#), and [107](#).
- 4 RANDALL, L.; SUNDRUM, R. An alternative to compactification. *Phys. Rev. Lett.*, American Physical Society, v. 83, p. 4690–4693, Dec 1999. Citado 5 vezes nas páginas [17](#), [61](#), [62](#), [79](#), and [107](#).
- 5 RUBAKOV, V. A.; SHAPOSHNIKOV, M. E. Do we live inside a domain wall? *Phys. Lett. B*, v. 125, n. 2, p. 136–138, 1983. ISSN 0370-2693. Citado na página [19](#).
- 6 SUNDRUM, R. Effective field theory for a three-brane universe. *Phys. Rev. D*, American Physical Society, v. 59, p. 085009, Mar 1999. Citado na página [19](#).
- 7 ANTONIADIS, I. et al. New dimensions at a millimeter to a fermi and superstrings at a tev. *Phys. Lett. B*, v. 436, n. 3, p. 257–263, 1998. ISSN 0370-2693. Citado 3 vezes nas páginas [19](#), [61](#), and [85](#).
- 8 KAKUSHADZE, Z.; Henry Tye, S.-H. Brane world. *Nucl. Phys. B*, v. 548, n. 1, p. 180–204, 1999. ISSN 0550-3213. Citado na página [19](#).
- 9 NUSSINOV, S.; SHROCK, R. Some remarks on theories with large compact dimensions and tev-scale quantum gravity. *Phys. Rev. D*, American Physical Society, v. 59, p. 105002, Mar 1999. Citado na página [19](#).
- 10 SHIU, G.; TYE, S.-H. H. Tev scale superstring and extra dimensions. *Phys. Rev. D*, American Physical Society, v. 58, p. 106007, Oct 1998. Citado na página [19](#).
- 11 DONINI, A.; RIGOLIN, S. Anisotropic type i string compactification, winding modes and large extra dimensions. *Nucl. Phys. B*, v. 550, n. 1, p. 59–76, 1999. ISSN 0550-3213. Citado na página [19](#).
- 12 ARKANI-HAMED, N.; DIMOPOULOS, S.; DVALI, G. Phenomenology, astrophysics, and cosmology of theories with submillimeter dimensions and tev scale quantum gravity. *Phys. Rev. D*, American Physical Society, v. 59, p. 086004, Mar 1999. Citado na página [19](#).

- 13 CULLEN, S.; PERELSTEIN, M. Sn 1987a constraints on large compact dimensions. *Phys. Rev. Lett.*, American Physical Society, v. 83, p. 268–271, Jul 1999. Citado na página 19.
- 14 LUKAS, A. et al. Universe as a domain wall. *Phys. Rev. D*, American Physical Society, v. 59, p. 086001, Mar 1999. Citado na página 19.
- 15 BERNARDINI, A. E.; ROCHA, R. da. Matter localization on brane-worlds generated by deformed defects. *Adv. High Energy Phys.*, Hindawi Limited, v. 2016, p. 3650632, 2016. Citado 5 vezes nas páginas 19, 39, 79, 86, and 107.
- 16 ALMEIDA, C. A. S. et al. Fermion localization and resonances on two-field thick branes. *Phys. Rev. D*, American Physical Society, v. 79, p. 125022, Jun 2009. Citado 5 vezes nas páginas 19, 39, 79, 86, and 107.
- 17 BAZEIA, D.; FURTADO, C.; GOMES, A. R. Brane structure from a scalar field in warped spacetime. *J. Cosmol. Astropart. Phys.*, IOP Publishing, v. 2004, n. 02, p. 002–002, feb 2004. Citado 4 vezes nas páginas 19, 39, 79, and 107.
- 18 DZHUNUSHALIEV, V.; FOLOMEEV, V.; MINAMITSUJI, M. Thick brane solutions. *Rep. Prog. Phys.*, IOP Publishing, v. 73, n. 6, p. 066901, may 2010. Citado 4 vezes nas páginas 19, 39, 79, and 107.
- 19 BAZEIA, D.; LOSANO, L.; MALBOUISSON, J. M. C. Deformed defects. *Phys. Rev. D*, American Physical Society, v. 66, p. 101701, Nov 2002. Citado 4 vezes nas páginas 19, 39, 79, and 107.
- 20 DEWOLFE, O. et al. Modeling the fifth dimension with scalars and gravity. *Phys. Rev. D*, American Physical Society, v. 62, p. 046008, Jul 2000. Citado 4 vezes nas páginas 19, 39, 79, and 107.
- 21 AHMED, A.; GRZADKOWSKI, B. Brane modeling in warped extra-dimension. *J. High Energy Phys.*, Springer Science and Business Media LLC, v. 2013, n. 1, jan 2013. Citado 4 vezes nas páginas 19, 39, 79, and 107.
- 22 GREMM, M. Four-dimensional gravity on a thick domain wall. *Phys. Lett. B*, Elsevier BV, v. 478, n. 4, p. 434–438, apr 2000. Citado 6 vezes nas páginas 19, 39, 61, 62, 79, and 107.
- 23 CHINAGLIA, M.; BERNARDINI, A. E.; ROCHA, R. da. Braneworld scenarios from deformed defect chains. *Int. J. Theor. Phys.*, Springer Science and Business Media LLC, v. 55, n. 10, p. 4605–4619, jun 2016. Citado 4 vezes nas páginas 19, 39, 79, and 107.
- 24 KEHAGIAS, A.; TAMVAKIS, K. Localized gravitons, gauge bosons and chiral fermions in smooth spaces generated by a bounce. *Phys. Lett. B*, Elsevier BV, v. 504, n. 1-2, p. 38–46, apr 2001. Citado 5 vezes nas páginas 19, 39, 79, 86, and 107.
- 25 KOBAYASHI, S.; KOYAMA, K.; SODA, J. Thick brane worlds and their stability. *Phys. Rev. D*, American Physical Society, v. 65, p. 064014, Feb 2002. Citado 4 vezes nas páginas 19, 39, 79, and 107.
- 26 BRONNIKOV, K. A.; MEIEROVICH, B. E. A General thick brane supported by a scalar field. *Gravitation Cosmol.*, v. 9, p. 313–318, 2003. Citado 4 vezes nas páginas 19, 39, 79, and 107.

- 27 BAZEIA, D.; GOMES, A. R.; LOSANO, L. Gravity localization on thick branes: a numerical approach. *Int. J. Mod. Phys. A*, World Scientific Pub Co Pte Lt, v. 24, n. 06, p. 1135–1160, mar 2009. Citado 4 vezes nas páginas [19](#), [39](#), [79](#), and [107](#).
- 28 BARBOSA-CENDEJAS, N. et al. Mass hierarchy, mass gap and corrections to newton’s law on thick branes with poincaré symmetry. *Gen. Relativ. Gravit.*, Springer Science and Business Media LLC, v. 46, n. 1, dec 2013. Citado 4 vezes nas páginas [19](#), [39](#), [79](#), and [107](#).
- 29 ZHANG, X.-H.; LIU, Y.-X.; DUAN, Y.-S. Localization of fermionic fields on braneworlds with bulk tachyon matter. *Mod. Phys. Lett. A*, World Scientific Pub Co Pte Lt, v. 23, n. 25, p. 2093–2101, aug 2008. Citado 4 vezes nas páginas [19](#), [79](#), [86](#), and [107](#).
- 30 MELFO, A.; PANTOJA, N.; SKIRZEWSKI, A. Thick domain wall spacetimes with and without reflection symmetry. *Phys. Rev. D*, American Physical Society, v. 67, p. 105003, May 2003. Citado 3 vezes nas páginas [19](#), [79](#), and [107](#).
- 31 BAZEIA, D. et al. Braneworld models of scalar fields with generalized dynamics. *Phys. Lett. B*, Elsevier BV, v. 671, n. 3, p. 402–410, jan 2009. Citado 3 vezes nas páginas [19](#), [79](#), and [107](#).
- 32 KOLEY, R.; KAR, S. A novel braneworld model with a bulk scalar field. *Phys. Lett. B*, Elsevier BV, v. 623, n. 3-4, p. 244–250, sep 2005. Citado 3 vezes nas páginas [19](#), [79](#), and [107](#).
- 33 BAZEIA, D.; MENEZES, R.; ROCHA, R. da. A note on asymmetric thick branes. *Adv. High Energy Phys.*, Hindawi Limited, v. 2014, p. 276729, 2014. Citado 3 vezes nas páginas [19](#), [79](#), and [107](#).
- 34 BERNARDINI, A. E.; BERTOLAMI, O. Equivalence between born–infeld tachyon and effective real scalar field theories for brane structures in warped geometry. *Phys. Lett. B*, Elsevier BV, v. 726, n. 1-3, p. 512–517, oct 2013. Citado 3 vezes nas páginas [19](#), [79](#), and [107](#).
- 35 HALL, L. J.; SMITH, D. Cosmological constraints on theories with large extra dimensions. *Phys. Rev. D*, American Physical Society, v. 60, p. 085008, Sep 1999. Citado na página [19](#).
- 36 AHMED, A.; GRZADKOWSKI, B.; WUDKA, J. Thick-brane cosmology. *J. High Energy Phys.*, Springer Science and Business Media LLC, v. 2014, n. 4, apr 2014. Citado 2 vezes nas páginas [19](#) and [27](#).
- 37 CSÁKI, C. et al. General properties of the self-tuning domain wall approach to the cosmological constant problem. *Nucl. Phys. B*, Elsevier BV, v. 584, n. 1-2, p. 359–386, sep 2000. Citado na página [19](#).
- 38 RUBAKOV, V.; SHAPOSHNIKOV, M. Extra space-time dimensions: Towards a solution to the cosmological constant problem. *Phys. Lett. B*, Elsevier BV, v. 125, n. 2-3, p. 139–143, may 1983. Citado na página [19](#).
- 39 BINÉTRUY, P. et al. Brane cosmological evolution in a bulk with cosmological constant. *Phys. Lett. B*, Elsevier BV, v. 477, n. 1-3, p. 285–291, mar 2000. Citado na página [19](#).

- 40 BINÉTRUY, P.; DEFFAYET, C.; LANGLOIS, D. Non-conventional cosmology from a brane universe. *Nucl. Phys. B*, Elsevier BV, v. 565, n. 1-2, p. 269–287, jan 2000. Citado na página 19.
- 41 CLINE, J. M.; GROJEAN, C.; SERVANT, G. Cosmological expansion in the presence of an extra dimension. *Phys. Rev. Lett.*, American Physical Society, v. 83, p. 4245–4248, Nov 1999. Citado na página 19.
- 42 CSÁKI, C. et al. Cosmology of one extra dimension with localized gravity. *Phys. Lett. B*, Elsevier BV, v. 462, n. 1-2, p. 34–40, sep 1999. Citado na página 19.
- 43 CSÁKI, C. et al. Cosmology of brane models with radion stabilization. *Phys. Rev. D*, American Physical Society, v. 62, p. 045015, Jul 2000. Citado na página 19.
- 44 FLANAGAN, E. E.; TYE, S.-H. H.; WASSERMAN, I. Cosmological expansion in the randall-sundrum brane world scenario. *Phys. Rev. D*, American Physical Society, v. 62, p. 044039, Jul 2000. Citado na página 19.
- 45 KANTI, P. et al. Single-brane cosmological solutions with a stable compact extra dimension. *Phys. Rev. D*, American Physical Society, v. 61, p. 106004, Apr 2000. Citado na página 19.
- 46 KANTI, P. et al. Cosmological 3-brane solutions. *Phys. Lett. B*, Elsevier BV, v. 468, n. 1-2, p. 31–39, nov 1999. Citado na página 19.
- 47 BAZEIA, D.; BRITO, F. A.; COSTA, F. G. First-order framework and domain-wall/brane-cosmology correspondence. *Phys. Lett. B*, Elsevier BV, v. 661, n. 2-3, p. 179–185, mar 2008. Citado na página 19.
- 48 GEORGE, D. P.; TRODDEN, M.; VOLKAS, R. R. Extra-dimensional cosmology with domain-wall branes. *J. High Energy Phys.*, Springer Science and Business Media LLC, v. 2009, n. 02, p. 035–035, feb 2009. Citado na página 19.
- 49 KADOSH, A.; DAVIDSON, A.; PALLANTE, E. Slinky evolution of domain wall brane cosmology. *Phys. Rev. D*, American Physical Society, v. 86, p. 124015, Dec 2012. Citado na página 19.
- 50 KIM, H. B.; KIM, H. D. Inflation and gauge hierarchy in randall-sundrum compactification. *Phys. Rev. D*, American Physical Society, v. 61, p. 064003, Feb 2000. Citado na página 19.
- 51 BOWCOCK, P.; CHARMOUSIS, C.; GREGORY, R. General brane cosmologies and their global spacetime structure. *Classical Quantum Gravity*, IOP Publishing, v. 17, n. 22, p. 4745–4763, oct 2000. Citado 2 vezes nas páginas 19 and 107.
- 52 GUHA, S.; BHATTACHARYA, P. Five-dimensional warped product space-time with time-dependent warping and a scalar field in the bulk. *Gravitation Cosmol.*, Pleiades Publishing Ltd, v. 24, n. 3, p. 274–284, jul 2018. Citado na página 19.
- 53 MUKOHYAMA, S.; SHIROMIZU, T.; MAEDA, K.-i. Global structure of exact cosmological solutions in the brane world. *Phys. Rev. D*, American Physical Society, v. 62, p. 024028, Jun 2000. Citado na página 19.

- 54 CHUNG, D. J. H.; FREESE, K. Cosmological challenges in theories with extra dimensions and remarks on the horizon problem. *Phys. Rev. D*, American Physical Society, v. 61, p. 023511, Dec 1999. Citado na página 19.
- 55 IDA, D. Brane-world cosmology. *J. High Energy Phys.*, Springer Science and Business Media LLC, v. 2000, n. 09, p. 014–014, sep 2000. Citado 2 vezes nas páginas 19 and 107.
- 56 CHUNG, D. J. H.; FREESE, K. Can geodesics in extra dimensions solve the cosmological horizon problem? *Phys. Rev. D*, American Physical Society, v. 62, p. 063513, Aug 2000. Citado na página 19.
- 57 MUKOHYAMA, S. Brane-world solutions, standard cosmology, and dark radiation. *Phys. Lett. B*, v. 473, n. 3, p. 241–245, 2000. ISSN 0370-2693. Citado na página 19.
- 58 MERSINI, L. RADION POTENTIAL AND BRANE DYNAMICS. *Mod. Phys. Lett. A*, World Scientific Pub Co Pte Lt, v. 16, n. 24, p. 1583–1595, aug 2001. Citado na página 19.
- 59 BERNARDINI, A. E.; CAVALCANTI, R. T.; ROCHA, R. da. Spherically symmetric thick branes cosmological evolution. *Gen. Relativ. Gravit.*, Springer Science and Business Media LLC, v. 47, n. 1, p. 1840, dec 2014. Citado na página 19.
- 60 CASADIO, R.; OVALLE, J.; ROCHA, R. da. Black strings from minimal geometric deformation in a variable tension brane-world. *Classical Quantum Gravity*, IOP Publishing, v. 31, n. 4, p. 045016, feb 2014. Citado na página 19.
- 61 MALDACENA, J.; MILEKHIN, A. Humanly traversable wormholes. *Phys. Rev. D*, American Physical Society, v. 103, p. 066007, Mar 2021. Citado na página 19.
- 62 DUFF, M. J. *Kaluza-Klein Theory in Perspective*. [S.l.]: arXiv, 1994. Citado na página 19.
- 63 KOLEY, R.; KAR, S. Braneworlds in six dimensions: new models with bulk scalars. *Classical Quantum Gravity*, IOP Publishing, v. 24, n. 1, p. 79–94, nov 2006. Citado 3 vezes nas páginas 20, 21, and 30.
- 64 GHERGHETTA, T.; SHAPOSHNIKOV, M. Localizing gravity on a stringlike defect in six dimensions. *Phys. Rev. Lett.*, American Physical Society, v. 85, p. 240–243, Jul 2000. Citado 4 vezes nas páginas 20, 21, 30, and 86.
- 65 PARK, D. K.; KIM, H. Single 3-brane brane-world in six dimension. *Nucl. Phys. B*, Elsevier BV, v. 650, n. 1-2, p. 114–124, feb 2003. Citado 3 vezes nas páginas 20, 21, and 30.
- 66 PARAMESWARAN, S. L.; RANDJBAR-DAEMI, S.; SALVIO, A. Gauge fields, fermions and mass gaps in 6d brane worlds. *Nucl. Phys. B*, v. 767, n. 1, p. 54–81, 2007. ISSN 0550-3213. Citado 4 vezes nas páginas 20, 21, 30, and 86.
- 67 SINGLETON, D. Gravitational trapping potential with arbitrary extra dimensions. *Phys. Rev. D*, American Physical Society, v. 70, p. 065013, Sep 2004. Citado 4 vezes nas páginas 20, 21, 30, and 86.

- 68 MULTAMAKI, T.; VILJA, I. Warped and compact extra dimensions: 5d branes in 6d models. *Phys. Lett. B*, Elsevier BV, v. 545, n. 3-4, p. 389–402, oct 2002. Citado 3 vezes nas páginas 20, 21, and 30.
- 69 GAUY, H. M.; BERNARDINI, A. E. Gravity localization on intersecting thick braneworlds. *Physical Review D*, American Physical Society (APS), v. 106, n. 8, p. 084003, oct 2022. Citado 24 vezes nas páginas 20, 61, 62, 63, 64, 65, 66, 67, 70, 71, 72, 73, 74, 75, 76, 77, 78, 79, 80, 81, 82, 83, 84, and 107.
- 70 GAUY, H. M.; BERNARDINI, A. E. Asymmetrical braneworlds and the charged lepton mass spectrum. *Physics Letters B*, Elsevier BV, v. 846, p. 138205, nov 2023. Citado na página 20.
- 71 CSÁKI, C. et al. Universal aspects of gravity localized on thick branes. *Nucl. Phys. B*, v. 581, n. 1, p. 309–338, 2000. ISSN 0550-3213. Citado 9 vezes nas páginas 21, 61, 62, 63, 64, 66, 67, 72, and 74.
- 72 ARKANI-HAMED, N. et al. Infinitely large new dimensions. *Phys. Rev. Lett.*, American Physical Society, v. 84, p. 586–589, Jan 2000. Citado na página 21.
- 73 LIU, Y.-X.; ZHAO, L.; DUAN, Y.-S. Localization of fermions on a string-like defect. *J. High Energy Phys.*, Springer Science and Business Media LLC, v. 2007, n. 04, p. 097–097, apr 2007. Citado 4 vezes nas páginas 21, 86, 111, and 115.
- 74 DZHUNUSHALIEV, V. et al. Thick brane in 7d and 8d spacetimes. *Gen. Relativ. Gravit.*, Springer Science and Business Media LLC, v. 41, n. 1, p. 131–146, jun 2008. Citado na página 21.
- 75 DZHUNUSHALIEV, V.; FOLOMEEV, V.; MINAMITSUJI, M. Thick de sitter brane solutions in higher dimensions. *Phys. Rev. D*, American Physical Society, v. 79, p. 024001, Jan 2009. Citado na página 21.
- 76 GREGORY, R. Nonsingular global string compactifications. *Phys. Rev. Lett.*, American Physical Society, v. 84, p. 2564–2567, Mar 2000. Citado na página 21.
- 77 COHEN, A. G.; KAPLAN, D. B. Solving the hierarchy problem with noncompact extra dimensions. *Phys. Lett. B*, Elsevier BV, v. 470, n. 1-4, p. 52–58, dec 1999. Citado na página 21.
- 78 D'INVERNO, R. *Introducing Einstein's Relativity*. [S.l.]: Oxford University Press, 1992. ISBN 0198596863. Citado 2 vezes nas páginas 21 and 28.
- 79 GIBBONS, G. W.; KALLOSH, R.; LINDE, A. D. Brane world sum rules. *J. High Energy Phys.*, v. 01, p. 022, 2001. Citado na página 29.
- 80 LEBLOND, F.; MYERS, R. C.; WINTERS, D. J. Consistency conditions for brane worlds in arbitrary dimensions. *J. High Energy Phys.*, Springer Science and Business Media LLC, v. 2001, n. 07, p. 031–031, jul 2001. Citado na página 29.
- 81 AFONSO, V. I.; BAZEIA, D.; LOSANO, L. First-order formalism for bent brane. *Phys. Lett. B*, v. 634, n. 5, p. 526–530, 2006. ISSN 0370-2693. Disponível em: <<https://www.sciencedirect.com/science/article/pii/S0370269306001808>>. Citado 3 vezes nas páginas 47, 48, and 71.

- 82 GREMM, M. Thick domain walls and singular spaces. *Phys. Rev. D*, American Physical Society, v. 62, p. 044017, Jul 2000. Citado 6 vezes nas páginas 48, 61, 62, 71, 78, and 79.
- 83 SASAKURA, N. A de-sitter thick domain wall solution by elliptic functions. *J. High Energy Phys.*, Springer Science and Business Media LLC, v. 2002, n. 02, p. 026–026, feb 2002. Citado 2 vezes nas páginas 48 and 71.
- 84 BRANDHUBER, A.; SFETSOS, K. Non-standard compactifications with mass gaps and newton's law. *J. High Energy Phys.*, Springer Science and Business Media LLC, v. 1999, n. 10, p. 013–013, oct 1999. Citado na página 62.
- 85 ISAACSON, R. A. Gravitational radiation in the limit of high frequency. i. the linear approximation and geometrical optics. *Phys. Rev.*, American Physical Society (APS), v. 166, n. 5, p. 1263–1271, feb 1968. Citado na página 63.
- 86 FLÜGGE, S. *Practical Quantum Mechanics*. [S.l.]: Springer Berlin Heidelberg, 1998. ISBN 3540650350. Citado 2 vezes nas páginas 78 and 151.
- 87 HERRERA-AGUILAR, A. et al. ASPECTS OF THICK BRANE WORLDS: 4d GRAVITY LOCALIZATION, SMOOTHNESS, AND MASS GAP. *Mod. Phys. Lett. A*, World Scientific Pub Co Pte Lt, v. 25, n. 24, p. 2089–2097, aug 2010. Citado 4 vezes nas páginas 78, 79, 119, and 129.
- 88 PAL, S.; KAR, S. de sitter branes with a bulk scalar. *Gen. Relativ. Gravit.*, Springer Science and Business Media LLC, v. 41, n. 5, p. 1165–1179, oct 2008. Citado na página 86.
- 89 MENDES, W. M.; ALENCAR, G.; LANDIM, R. R. Spinors fields in co-dimension one braneworlds. *J. High Energy Phys.*, Springer Science and Business Media LLC, v. 2018, n. 2, feb 2018. Citado na página 86.
- 90 LIU, Y.-X. et al. Fermions on thick branes in the background of sine-gordon kinks. *Phys. Rev. D*, American Physical Society, v. 78, p. 065025, Sep 2008. Citado na página 86.
- 91 LIU, Y.-X. et al. Localization and mass spectra of fermions on symmetric and asymmetric thick branes. *Phys. Rev. D*, American Physical Society, v. 80, p. 065020, Sep 2009. Citado na página 86.
- 92 LIU, Y.-X. et al. Localization of gravity and bulk matters on a thick anti-de sitter brane. *Phys. Rev. D*, American Physical Society, v. 84, p. 044033, Aug 2011. Citado na página 86.
- 93 KOIDE, Y. Fermion-boson two-body model of quarks and leptons and cabibbo mixing. *Lettere al Nuovo Cimento*, Springer Science and Business Media LLC, v. 34, n. 8, p. 201–205, jun 1982. Citado na página 107.
- 94 SUMINO, Y. Family gauge symmetry and koide's mass formula. *Physics Letters B*, Elsevier BV, v. 671, n. 4-5, p. 477–480, feb 2009. Citado na página 107.

- 95 ROSA, J. L.; BAZEIA, D.; LOBÃO, A. S. Effects of cuscuton dynamics on braneworld configurations in the scalar–tensor representation of $\left(r, t \right)$ gravity. *The European Physical Journal C*, Springer Science and Business Media LLC, v. 82, n. 3, mar 2022. Citado na página 107.
- 96 HORAVA, P.; WITTEN, E. Heterotic and type i string dynamics from eleven dimensions. *Nuclear Physics B*, v. 460, n. 3, p. 506–524, 1996. ISSN 0550-3213. Citado na página 107.
- 97 HORAVA, P.; WITTEN, E. Eleven-dimensional supergravity on a manifold with boundary. *Nuclear Physics B*, v. 475, n. 1, p. 94–114, 1996. ISSN 0550-3213. Citado na página 107.
- 98 KRAUS, P. Dynamics of anti-de sitter domain walls. *Journal of High Energy Physics*, v. 1999, p. 011–011, 1999. Citado na página 107.
- 99 DERUELLE, N.; DOLEŽEL, T. Brane versus shell cosmologies in einstein and einstein-gauss-bonnet theories. *Physical Review D*, American Physical Society (APS), v. 62, n. 10, p. 103502, oct 2000. Citado na página 107.
- 100 PERKINS, W. B. Colliding bubble worlds. *Physics Letters B*, v. 504, p. 28–32, 2001. Citado na página 107.
- 101 CARTER, B. et al. Simulated gravity without true gravity in asymmetric brane-world scenarios. *Classical and Quantum Gravity*, IOP Publishing, v. 18, n. 22, p. 4871–4895, nov 2001. Citado na página 107.
- 102 GERGELY, L. A. Generalized friedmann branes. *Physical Review D*, v. 68, p. 124011, 2003. Citado na página 107.
- 103 APPLEBY, S. A.; BATTYE, R. A. Regularized braneworlds of arbitrary codimension. *Phys. Rev. D*, American Physical Society, v. 76, p. 124009, Dec 2007. Citado na página 107.
- 104 SHTANOV, Y.; VIZNYUK, A.; GRANDA, L. N. ASYMMETRIC EMBEDDING IN BRANE COSMOLOGY. *Modern Physics Letters A*, World Scientific Pub Co Pte Lt, v. 23, n. 12, p. 869–878, apr 2008. Citado na página 107.
- 105 CHARMOUSIS, C.; GREGORY, R.; PADILLA, A. Stealth acceleration and modified gravity. *Journal of Cosmology and Astroparticle Physics*, IOP Publishing, v. 2007, n. 10, p. 006–006, oct 2007. Citado na página 107.
- 106 KOYAMA, K.; PADILLA, A.; SILVA, F. P. Ghosts in asymmetric brane gravity and the decoupled stealth limit. *Journal of High Energy Physics*, Springer Science and Business Media LLC, v. 2009, n. 03, p. 134–134, mar 2009. Citado na página 107.
- 107 GUERRERO, R.; RODRIGUEZ, R. O.; TORREALBA, R. de sitter and double asymmetric brane worlds. *Physical Review D*, American Physical Society (APS), v. 72, n. 12, p. 124012, dec 2005. Citado na página 107.
- 108 GERGELY, L. A.; MAARTENS, R. Asymmetric brane-worlds with induced gravity. *Phys. Rev. D*, American Physical Society, v. 71, p. 024032, Jan 2005. Citado na página 107.

- 109 PADILLA, A. Cosmic acceleration from asymmetric branes. *Classical and Quantum Gravity*, IOP Publishing, v. 22, n. 4, p. 681–694, jan 2005. Citado na página 107.
- 110 PADILLA, A. Infra-red modification of gravity from asymmetric branes. *Classical and Quantum Gravity*, IOP Publishing, v. 22, n. 6, p. 1087–1104, mar 2005. Citado na página 107.
- 111 ARKANI-HAMED, N.; SCHMALTZ, M. Hierarchies without symmetries from extra dimensions. *Physical Review D*, American Physical Society (APS), v. 61, n. 3, p. 033005, jan 2000. Citado 2 vezes nas páginas 107 and 110.
- 112 ARKANI-HAMED, N. et al. Neutrino masses from large extra dimensions. *Physical Review D*, American Physical Society (APS), v. 65, n. 2, p. 024032, dec 2001. Citado 2 vezes nas páginas 107 and 110.
- 113 DVALI, G.; SHIFMAN, M. Families as neighbors in extra dimension. *Physics Letters B*, Elsevier BV, v. 475, n. 3-4, p. 295–302, mar 2000. Citado 2 vezes nas páginas 107 and 110.
- 114 KAPLAN, D. E.; TAIT, T. M. Supersymmetry breaking, fermion masses and a small extra dimension. *Journal of High Energy Physics*, Springer Science and Business Media LLC, v. 2000, n. 06, p. 020–020, jun 2000. Citado 2 vezes nas páginas 107 and 110.
- 115 HUBER, S. J.; SHAFI, Q. Fermion masses, mixings and proton decay in a randall–sundrum model. *Physics Letters B*, Elsevier BV, v. 498, n. 3-4, p. 256–262, jan 2001. Citado 2 vezes nas páginas 107 and 110.
- 116 FRÈRE, J.-M.; LIBANOV, M. V.; TROITSKY, S. V. Neutrino masses with a single generation in the bulk. *Journal of High Energy Physics*, Springer Science and Business Media LLC, v. 2001, n. 11, p. 025–025, nov 2001. Citado 2 vezes nas páginas 107 and 110.
- 117 FRÈRE, J.-M.; LIBANOV, M.; TROITSKY, S. Three generations on a local vortex in extra dimensions. *Physics Letters B*, Elsevier BV, v. 512, n. 1-2, p. 169–173, jul 2001. Citado 2 vezes nas páginas 107 and 110.
- 118 FRÈRE, J.-M. et al. Fermions in the vortex background on a sphere. *Journal of High Energy Physics*, Springer Science and Business Media LLC, v. 2003, n. 06, p. 009–009, jun 2003. Citado 2 vezes nas páginas 107 and 110.
- 119 FRÈRE, J.-M. et al. Neutrino hierarchy and fermion spectrum from a single family in six dimensions: realistic predictions. *Journal of High Energy Physics*, Springer Science and Business Media LLC, v. 2013, n. 8, aug 2013. Citado 2 vezes nas páginas 107 and 110.
- 120 LIBANOV, M.; TROITSKY, S. Three fermionic generations on a topological defect in extra dimensions. *Nuclear Physics B*, Elsevier BV, v. 599, n. 1-2, p. 319–333, apr 2001. Citado 2 vezes nas páginas 107 and 110.
- 121 LIBANOV, M.; NOUGAEV, E. Towards the realistic fermion masses with a single family in extra dimensions. *Journal of High Energy Physics*, Springer Science and Business Media LLC, v. 2002, n. 04, p. 055–055, apr 2002. Citado 2 vezes nas páginas 107 and 110.

122 LIU, Y.-X. et al. New localization mechanism of fermions on braneworlds. *Phys. Rev. D*, American Physical Society (APS), v. 89, n. 8, p. 086001, apr 2014. Citado 2 vezes nas páginas [111](#) and [115](#).

123 SCHWARTZ, M. D. *Quantum field theory and the standard model*. [S.l.]: Cambridge University Press, 2013. Citado 2 vezes nas páginas [114](#) and [122](#).

Appendix

APPENDIX A – Details of models *I* and *II*

From solutions (2.66) and (2.67), one is able to write the metric in the form

$$\mathbf{g} = \sqrt{\cosh [2c_u(u + u_0)] \cosh [2c_v(v + v_0)]} \eta_{\mu\nu} dx^\mu dx^\nu + \sqrt{\frac{\cosh^p [2c_v(v + v_0)]}{\cosh^{p-1} [2c_u(u + u_0)]}} (du^2 + dv^2), \quad (\text{A.1})$$

from which it is indeed not so clear whether gravity is localized in the brane. One should notice that if $Re(c_v) \neq 0$, since $p \geq 1/2$, there would be no way of “localizing” fields in the “direction of v ”, since both conformal factors which multiply $\eta_{\mu\nu} dx^\mu \otimes dx^\nu$ and $dv \otimes dv$ “increase with v ”. Thus one is constrained to assume $Re(c_v) = 0$ to achieve an acceptable physical solutions, which means that the v coordinate can be compactified into a circle \mathbb{S}^1 , or in some other words, $v = r\varphi$, where r is the radius of \mathbb{S}^1 and $\varphi \in \mathbb{S}^1$. Since the metric must be continuous in \mathbb{S}^1 , the $e^{-2\hat{A}}$ factor must be continuous in \mathbb{S}^1 , i.e.

$$|\cos(2|c_v|r2\pi)| = |\cos(0)| = 1 \implies |c_v| = \frac{n}{4r}, \quad n \in \mathbb{N}.$$

Likewise, one still needs to verify the localization along the “direction of u ”, which can be achieved in two different ways.

For instance, when $Im(c_u) = 0$, if one sets p large enough (i.e. at least $p \geq 3$), the effective volume associated with \mathbb{B}^2 becomes finite. Even though the warp factor does not have a RS-like profile, because the volume of \mathbb{B}^2 is finite, one can still possibly “localize” gravity and other fields. Otherwise, when $Re(c_u) = 0$, in a similar fashion to the content discussed for coordinate v , the space coordinate u can be compactified as a circle \mathbb{S}^1 . In this case, one must impose $1/2 \leq p \leq 3$, otherwise the effective volume is not finite (this is clearer when observing the metric from (A.1) for $p < 3$). Therefore, it is imperative to choose either $Im(c_u) = 0$ for models with $p \geq 3$ or $Re(c_u) = 0$ for models with $p \leq 3$ in order to obtain consistent solutions with localized gravity.

Even if one is able to localize fields in the brane, the configuration may still not be physical. If the total energy associated with the configuration is infinite, then one can argue that the solutions are not physical ones. Therefore, to realize the total energy of the system one thus writes the stress energy tensor as

$$T_{\mu\nu} = -\eta_{\mu\nu} \sqrt{\frac{\cosh^p(2c_u u)}{\left|\cos\left(\frac{n\varphi}{2}\right)\right|^{p-1}}} \left[\frac{(\phi_{,u})^2}{2} + \frac{(\zeta_{,\varphi})^2}{2r^2} + \mathcal{V} \right]. \quad (\text{A.2})$$

As claimed above, the energy density which is computed from $\sqrt{-g}T_{\mu\nu}$ must be finite, otherwise the total energy in this configuration will not be finite. One thus has

$$T_{\mu\nu}\sqrt{-g} = -\frac{r}{2}\eta_{\mu\nu} \left[(\phi_{,u})^2 + \frac{(\zeta_{,\varphi})^2}{r^2} + 2\mathcal{V} \right] \left| \cos\left(\frac{n\varphi}{2}\right) \right|^{3/2} \cosh^{3/2}(2c_u u), \quad (\text{A.3})$$

from which it can be noticed that, if $Im(c_u) = 0$, since $\zeta = \zeta(v)$, the integration of Eq. (A.3) throughout space will necessarily be infinite. Therefore one may claim that the $Im(c_u) = 0$ configurations requires an unphysical infinite amount of energy to be realized. Following a similar analysis, from Eq. (A.3), no conclusive assertion about the choice of $Re(c_u) = 0$ instead of $Im(c_u) = 0$ can be performed. However, as a matter of completeness, the calculations will be carried out for both configurations.

A.1 Model I

Model I is resumed by expressions (2.69), (2.70), (2.71) and (2.72) and the dependence on φ for the warp and conformal factors are depicted in Figs. 31a and 31b.

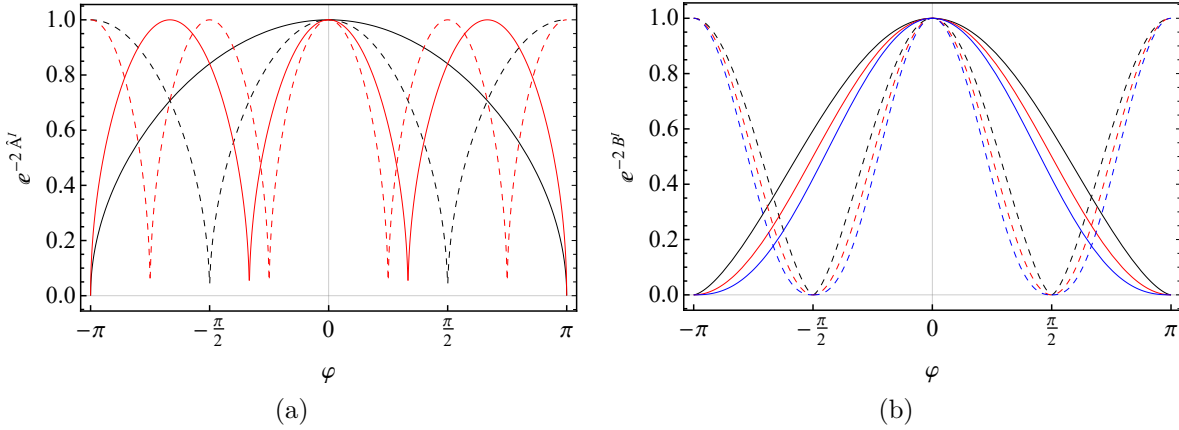


Figure 31 – (a) Warp factor $e^{-2\hat{A}}$ of model I as a function of φ , for $n = 1$ (solid black line), $n = 2$ (dashed black line), $n = 3$ (solid red line) and $n = 4$ (dashed red line). (b) Conformal factor e^{-2B^I} of model I as a function of φ , for $p = 3$ (black), $p = 4$ (red) and $p = 5$ (blue), the solid and dashed lines correspond to $n = 1$ and $n = 2$, respectively.

In particular, for $b_\phi = b_\zeta = -1$, one has $c_u = |c_v| = n/4r$. In this case, since $a_\phi \geq 0$ one realizes that $p \geq 5/2$, which is a tautology since $p \geq 3$. For this choice, one finds the scalar fields and potential in the following form,

$$\mathcal{V}^I = 0, \quad (\text{A.4})$$

$$\phi^I = \pm \sqrt{2p - 5} M^2 \arcsin \left[\tanh \left(\frac{nu}{2r} \right) \right], \quad (\text{A.5})$$

$$\zeta^I = \pm \sqrt{3 + 2p} M^2 \operatorname{arctanh} \left[\sin \left(\frac{n\varphi}{2} \right) \right]. \quad (\text{A.6})$$

The scalar fields are depicted in Fig. 32. The structure of the scalar field ζ^I , as given by (A.6), shall recurrently appear as a driver for $(5 + 1)$ -dimensional thick brane-worlds. As it shall be noticed in the following models, the scalar field dependence on the angular-like variables in much sense reproduce the behavior depicted in Fig. 32. Interestingly, the scalar field ϕ^I is zero when $p = 5/2$, implying into a singular configuration with a single scalar field ζ^I , with $\mathcal{V}^I = 0$.

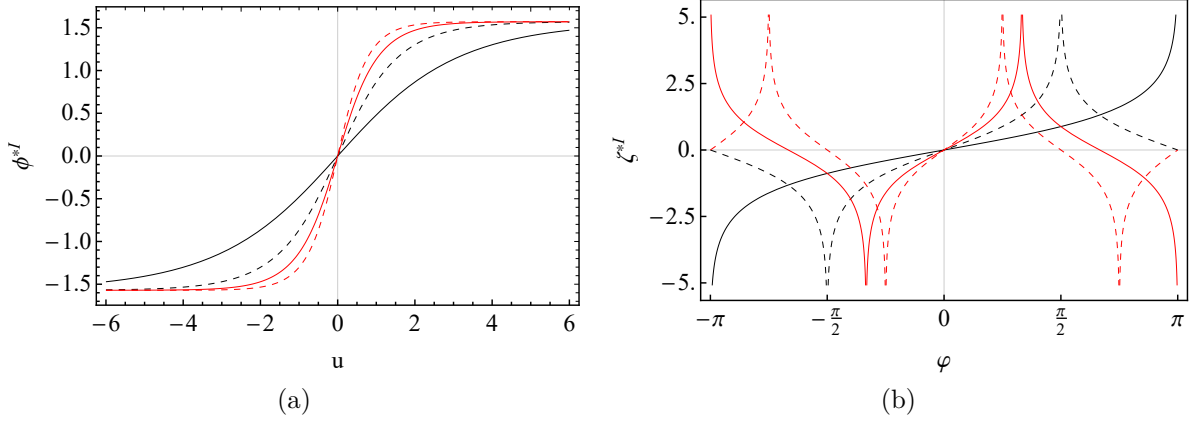


Figure 32 – The scalar fields of model *I*: (a) $\phi^{*I} = \phi^I / \sqrt{2p - 5} M^2$; (b) $\zeta^{*I} = \zeta^I / \sqrt{3 + 2p} M^2$. The plots are for $n = 1$ (solid black line), $n = 2$ (dashed black line), $n = 3$ (solid red line) and $n = 4$ (dashed red line).

Finally, the stress energy tensor for model *I* is simply written as

$$T_{\mu\nu} = \frac{M^4 n^2 \eta_{\mu\nu}}{8r^2} \frac{(5 - 2p) \operatorname{sech}^2\left(\frac{nu}{2r}\right) - (2p + 3) \sec^2\left(\frac{n\varphi}{2}\right)}{\sqrt{\operatorname{sech}^p\left(\frac{nu}{2r}\right) \left|\cos\left(\frac{n\varphi}{2}\right)\right|^{p-1}}}, \quad (\text{A.7})$$

where its several singularities are consistent with the numerous cusps exhibited by the warp factor. Also, an infinite amount of energy is necessary to achieve such configuration, as one can check after integrating the previous expression throughout space coordinates.

A.2 Model II

Model *II* can be summarized by expressions (2.76), (2.77), (2.78) and (2.79). The soft shortcoming of model *II* is concerned with not being possible to rewrite \mathcal{V} as function of ϕ and ζ , since the expressions for (2.78) and (2.79) are not invertible. It would be advisable since one had started with the assumption that $\mathcal{V} = \mathcal{V}(\phi, \zeta)$. The shape of the scalar fields, ϕ and ζ , and of the potential \mathcal{V} are presented in Figs. 33 and 34, respectively.

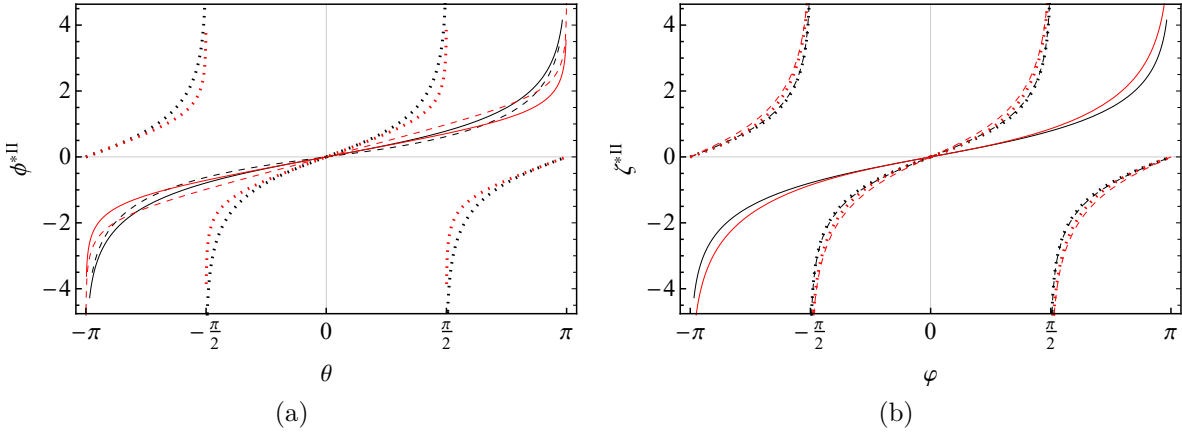


Figure 33 – Scalar fields of model *II* for $p = 1/2$ (black) and $p = 2$ (red): (a) $\phi^{*II} = \phi^{II}/M^2$ as a function of θ ; (b) $\zeta^{*II} = \zeta^{II}/M^2$ as a function of φ . The plots are for $n = l = 1$ (solid lines), $n = 2, l = 1$ (dashed lines) and $n = l = 2$ (dotted lines).

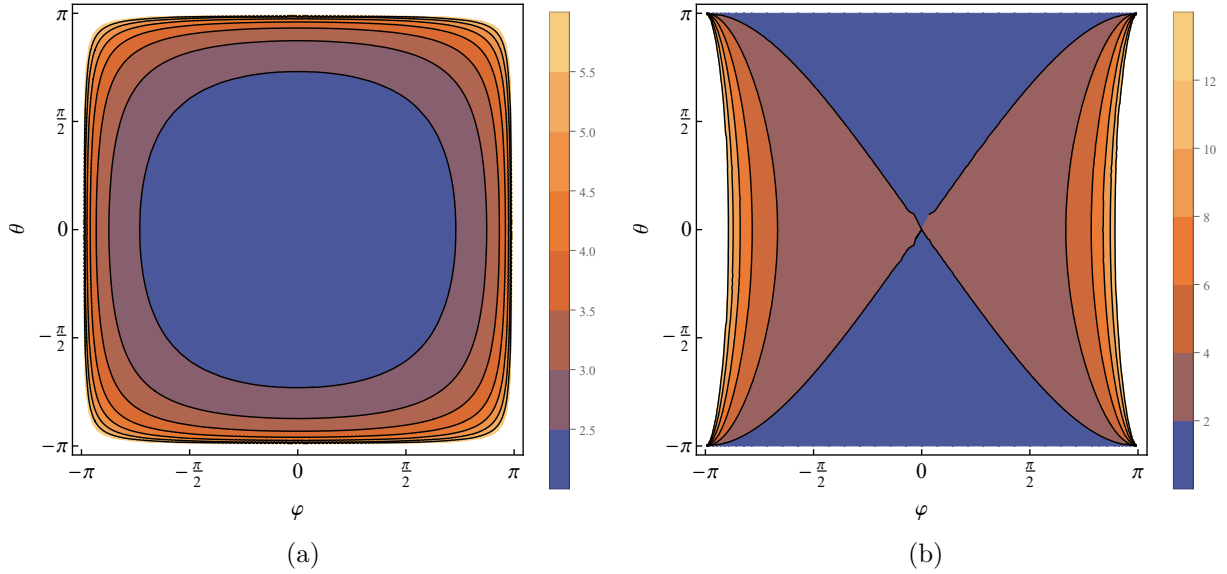


Figure 34 – Potential \mathcal{V}^{II} of model *II* as a function of (θ, φ) , for $p = 1/2$ (a) and $p = 2$ (b).

Analogously, the stress energy tensor is expressed by

$$T_{\mu\nu}^{II} = -2M^4\eta_{\mu\nu}\sqrt{\frac{|\cos(\frac{l\theta}{2})|^p}{|\cos(\frac{n\varphi}{2})|^{p-1}}}\left\{a_\phi\left[1-b_\phi\tan^2\left(\frac{l\theta}{2}\right)\right]+a_\zeta\left[1-b_\zeta\tan^2\left(\frac{n\varphi}{2}\right)\right]+\sqrt{\frac{|\cos(\frac{l\theta}{2})|^{p-1}}{|\cos(\frac{n\varphi}{2})|^p}}\left(\frac{l^2}{4\rho^2}+\frac{n^2}{4r^2}\right)\right\}. \quad (\text{A.8})$$

which exhibits several singularities, depending on the values for n and l . In fact, for $n = 1$ and $l = 1$ it has 2 singularities, one at $\varphi = \pi$ (or $-\pi$) and another one at $\theta = \pi$ (or $-\pi$).

These singularities explain the number of cusps in the warp factor. In order to realize physically consistent solutions, the required energy to achieve their internal structure must be finite. From the perspective of the bulk, such a required energy is given by

$$E_{\mu\nu}^{II} = \int_{\mathbb{E}^6} T_{\mu\nu}^{II} \sqrt{-g} d^6x$$

$$\propto \int_{-\pi}^{\pi} \int_{-\pi}^{\pi} \frac{a_{\phi} \left[1 - b_{\phi} \tan^2\left(\frac{l\theta}{2}\right)\right] + a_{\zeta} \left[1 - b_{\zeta} \tan^2\left(\frac{n\varphi}{2}\right)\right] + \sqrt{\frac{|\cos(\frac{l\theta}{2})|^{p-1}}{|\cos(\frac{n\varphi}{2})|^p} \left(\frac{l^2}{4\rho^2} + \frac{n^2}{4r^2}\right)}}{|\sec(\frac{l\theta}{2})|^{3/2} |\sec(\frac{n\varphi}{2})|^{3/2}} d\theta d\varphi, \quad (\text{A.9})$$

with last integral converging for several values of n , l and p ¹. Therefore, even though model II exhibits several singularities as depicted by the stress energy tensor, the total energy necessary to accomplish model II is finite. This is an evinced advantage with respect to the model I. The form of the energy density for model II ($T_{\mu\nu}^{II} \sqrt{-g}^{II}$) is depicted in Fig. 35. Although model II has finite total energy, one may still argue against its physical significance, due to its recurrent singularities, a shortcoming that must be considered in the following model issues.

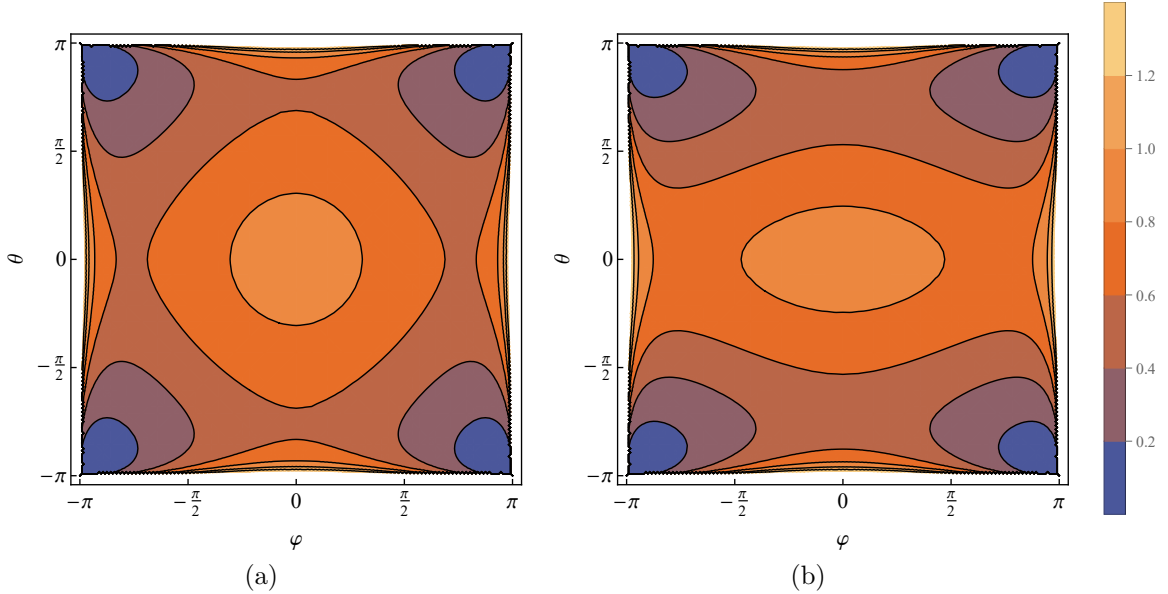


Figure 35 – Energy density $-T_{\mu\nu}^{II} \sqrt{-g}$ of model II as a function of (θ, φ) , for $p = 1/2$ (a) and $p = 2$ (b).

¹ For instance, when $n = l = 1$ and $p = 1/2$, it integrates to

$$\frac{2\pi\Gamma\left(\frac{9}{8}\right)^2}{\Gamma\left(\frac{13}{8}\right)^2} + \frac{33\pi^3}{2^8\Gamma\left(\frac{7}{4}\right)^4}.$$

APPENDIX B – On the Smoothness of Hypergeometric Functions

Assume a general wave function of the form

$$\chi = \cos^l(y) {}_2F_1[\alpha, \beta; \gamma; \cos^2(y)], \quad (\text{B.1})$$

its first derivative is simply

$$\chi_{,y} = -l \cos^{l-1}(y) \sin(y) {}_2F_1[\alpha, \beta; \gamma; \cos^2(y)] - 2 \sin(y) \cos^{l+1}(y) {}_2F_1'[\alpha, \beta; \gamma; \cos^2(y)]. \quad (\text{B.2})$$

The derivatives of hypergeometric functions follow the rule

$${}_2F_1'[\alpha, \beta; \gamma; z] = \frac{d {}_2F_1[\alpha, \beta; \gamma; z]}{dz} = \frac{\alpha\beta}{\gamma} {}_2F_1[\alpha + 1, \beta + 1; \gamma + 1; z]. \quad (\text{B.3})$$

Substituting into $\chi_{,y}$ one finds

$$\chi_{,y} = \cos^{l-1}(y) \sin(y) \left\{ -l {}_2F_1[\alpha, \beta; \gamma; \cos^2(y)] - 2 \cos^2(y) \frac{\alpha\beta}{\gamma} {}_2F_1[\alpha + 1, \beta + 1; \gamma + 1; \cos^2(y)] \right\}. \quad (\text{B.4})$$

Let the parameters α , β and γ satisfy $\gamma - \alpha - \beta = 1/2$, then ${}_2F_1[\alpha + 1, \beta + 1; \gamma + 1; \cos^2(y)]$ will not converge at $\cos^2(y) = 1$. To analyze this divergence further one uses the following property of hypergeometric functions [86]:

$$\begin{aligned} {}_2F_1(\alpha, \beta; \gamma; z) &= \frac{\Gamma(\gamma)\Gamma(\gamma - \alpha - \beta)}{\Gamma(\gamma - \alpha)\Gamma(\gamma - \beta)} {}_2F_1(\alpha, \beta; \alpha + \beta - \gamma + 1; 1 - z) \\ &+ \frac{\Gamma(\gamma)\Gamma(\alpha + \beta - \gamma)}{\Gamma(\alpha)\Gamma(\beta)} (1 - z)^{\gamma - \alpha - \beta} {}_2F_1(\gamma - \alpha, \gamma - \beta; \gamma - \alpha - \beta + 1; 1 - z), \end{aligned} \quad (\text{B.5})$$

thus the first derivative satisfy

$$\begin{aligned} \chi_{,y} &= -l \cos^{l-1}(y) \sin(y) {}_2F_1[\alpha, \beta; \gamma; \cos^2(y)] \\ &- 2 \cos^{l+1}(y) \sin(y) \frac{\alpha\beta}{\gamma} \frac{\Gamma(\gamma + 1)\Gamma(-1/2)}{\Gamma(\gamma - \alpha)\Gamma(\gamma - \beta)} {}_2F_1[\alpha + 1; \beta + 1, 3/2; \sin^2(y)] \\ &- 2 \cos^{l+1}(y) \text{sign}[\sin(y)] \frac{\alpha\beta}{\gamma} \frac{\Gamma(\gamma + 1)\Gamma(1/2)}{\Gamma(\alpha + 1)\Gamma(\beta + 1)} {}_2F_1[\gamma - \alpha, \gamma - \beta; 1/2; \sin^2(y)], \end{aligned} \quad (\text{B.6})$$

and at the vicinity of $y = 0$ it behaves like

$$\chi_{,y} \Big|_{y \rightarrow 0} = -2 \text{sign}[\sin(y)] \frac{\alpha\beta}{\gamma} \frac{\Gamma(\gamma + 1)\Gamma(1/2)}{\Gamma(\alpha + 1)\Gamma(\beta + 1)}, \quad (\text{B.7})$$

leading to a discontinuity unless α or β is a non-positive integer $-j$, $j \in \mathbb{N}$.